FINAL REPORT
PHASE II
LUNAR PHOTO STUDY

Contract NAS 9-3826

1 November 1965 - 1 November 1966

Z3841

Prepared by

EASTMAN KODAK COMPANY
Apparatus and Optical Division
Rochester, New York 14650

For

NASA Manned Spacecraft Center
Lunar Surface Technology Branch/EF321
Space Science Division
2101 Webster-Seabrook Road
Houston, Texas 77058

Prepared by: Edgar D. Seymour

Approved by: C. Spacely

1 November 1966

FOREWORD

This work represents the Final Report on the Lunar Photo Study, Phase II, for the National Aeronautics and Space Administration, Manned Spacecraft Center, Houston, Texas, Under Contract NAS9-3826 to the Eastman Kodak Company, Rochester, New York.

The phase I Lunar Photo Study was completed in October 1965. Phase II of the contract authorized a one year continuation of this work beginning 1 November 1965 to study Contour Mapping by Photoclinometry, Detection and Enhancement of Lunar Photo Details, and Methods of Rating the Quality of Lunar Pictures. The study was conducted under the cognizance of the Space Science Division, with Mr. Robert L. Jones of the Lunar Surface Technology Branch serving as Technical Representative.

TABLE OF CONTENTS (Continued)

LIST OF ILLUSTRATIONS

LIST OF TABLES

SUMMARY

This final report covers the work performed from 1 November 1965 through 1 November 1966 under Phase II of the Lunar Photo Study of Simulated Lunar Surfaces. The report is divided into three sections: (A) Contour Mapping by Photoclinometry, (B) Detection and Enhancement of Lunar Photo Details, (C) Methods of Rating Lunar Picture Quality.

A. Photoclinometry

Fifteen photoclinometric experiments were performed starting with simple geometric shapes showing no shadows and proceeding to KLM6-65, a simulated lunar surface with low slopes, craters, geometric shapes, boulders and shadows. These objects, photographed at a nominal sun elevation of 15°, were models dusted with copper oxide, a material that has a photometric function similar to the photometric function of the moon.

Three photo systems were studied. Experiments No. 3 through No. 12 investigated, at a scale of 1:2448, the effects of microdensitometer spot size and spot spacing on a single photograph in which the object size was very large compared to the resolution capability of the lens-film system. Experiments No. 13 and No. 15 photographed simple geometric shapes and low slopes with photo system A, a positive photo record at a scale of 1:10,000 simulating the Lunar Orbiter record. At a sun elevation of 15° system A could map a level surface and slopes of ± 3 1/2° and detect an 8-foot crater. It was difficult to find evidence of 4-foot craters and the 4-foot, 26° cones were enlarged and flattened. Experiments No. 14, No. 16, and No. 18 photographed simple geometric shapes, low slopes and a simulated lunar surface with photo system B, a negative photo record with a scale of 1:30,000. At a sun elevation of 15°, system B could easily map level surfaces, slopes of ± 3 1/2°, craters 8 and 4 feet in diameter and 26° cones, 4 feet in diameter.

An error analysis shows that 2-sigma uncertainties of ± 2.4° tau angle in the laboratory and + 7.8°, - 15° tau angle in the LOP System can be expected. The major contributing factors to these uncertainties in the laboratory are:

processing (2.0°), albedo (1.3°), and illumination (1.0°) while in the LOP System the major factor is uncertainty in the lunar photometric function. Two-sigma uncertainty in tau angle from film grain is about ± 1.2° in photo system A and about ± 3.3° in photo system B. The errors in calculated height after a scan of 100 feet are:

	2-sigma error in height after 100-feet scan, feet
Photo System A - Lab	± 0.5
Photo System A - Mission	± 2.0
Photo System B - Lab	± 0.4

Contour maps made of an area 8 feet x 80 feet using photoclinometry and stereo methods were compared to a contour map made from physical measurements of the same area of the model. A contour map made by photoclinometry from a single photograph with photo system B parameters compares favorably with a contour map made by stereo methods from a pair of photographs with photo system B parameters. The 2-sigma value for the difference in height between the elevations calculated by photoclinometry and the model dimensions is ± .1306 meter (± 5.1 inches) over the 8-x 80-foot mapped section based upon 4290 calculated height values.

B. Detection and Enhancement of Lunar Photo Details

Three methods were studied for the detection and enhancement of photographic details. Multiple printing of the same lunar scene from photographs taken from the same position permits detail to be observed that would be lost in the grain of a single photograph. An example of this technique for grain suppressions is shown in the report, as is an example of the enhancement of detail by high contrast printing of a very low contrast scene.

Motion picture simulations of the landing LEM with four different sun elevations are described. These motion pictures were forwarded to NASA during August, 1966

A study was made of the appearance of Surveyor as photographed by the 24-inch lens on Lunar Orbiter at several sun elevations, at several scales and with two lunar backgrounds. A report and a set of photographs were sent to NASA in April, 1966.

C. Methods of Rating Lunar Picture Quality

Two methods are described for rating the quality of lunar pictures. The first method describes edge trace analysis which can be used in photography where no tri-bars are present in the scene. A count of traceable edges in simulated lunar scenes indicates that there is a selection of edges that is satisfactory for this type of analysis at sun elevations of interest. For a sun elevation of 20° there are at least 80 edges, 30 microns long and at least 5 edges, 100 microns long for each 3000 square meters of lunar surface that appear suitable for tracing. An analysis at three quality levels of one of these simulated lunar edges, along with an artificial edge indicates that this method can be successfully used with lunar photography. Based upon a very preliminary AIM curve derived for the LOP system the 2-sigma variation in the resolution predicted using the MTF curve calculated from an edge trace is ± 3 lines/mm at a quality level of 13.6 lines per millimeter on the GRE film.

A comparison picture file was made for photo system A by varying the following six parameters: scale, sun elevation, radiation fog, exposure, image smear and lens aperture. These photographs were sent through the LOP read-out system, then copied and mounted in cardboard mounts, labeled, and assembled into sets. Ten sets of this scene file and a comparison viewer were delivered to NASA in November 1966.

SECTION A

PHOTOCLINOMETRY

A.1 CONTOUR MAPPING BY PHOTOCLINOMETRY

Photometric Considerations

A short introduction to lunar mapping is well described in an article by L. J. Kosofsky and G. C. Broome in the September 1965 Journal of the SMPTE, Vol. 74, page 773. The following paragraphs have been adapted from that paper.

Plans to photograph the moon, as well as plans for using the photographs, must take into account its peculiar properties as a reflective surface. Far from being a uniformly diffusing surface (a Lambert reflector), the moon is a highly directional backscatterer of incident light. This effect is seen in the observation that a full moon reflects 12 times as much sunlight to the earth as does a half moon. In addition, the moon is a very poor reflector whose normal albedo averages about 7 percent. The normal albedo is measured where the angles of incidence and emittance to the surface normal are zero, and it is the ratio of the measured luminance to that of an ideal white surface. The photometric function expresses the variation in luminance with the geometry of the illumination and viewing situation.

The photometric function at a point can most usefully be described in terms of two variables, alpha and tau, where alpha is the phase angle (the angle between the line of sight and the sun line) and tau is the angle between the surface normal, projected into the phase plane, and the line of sight. These angles are shown in the upper part of Figure A1-1.

These relationships are simplified when the camera is vertical and has a small angular coverage. For these conditions the phase angle, alpha, is the same as the sun's zenith distance (the complement of the solar altitude), and tau is the component of the ground slope in the direction of the sun.

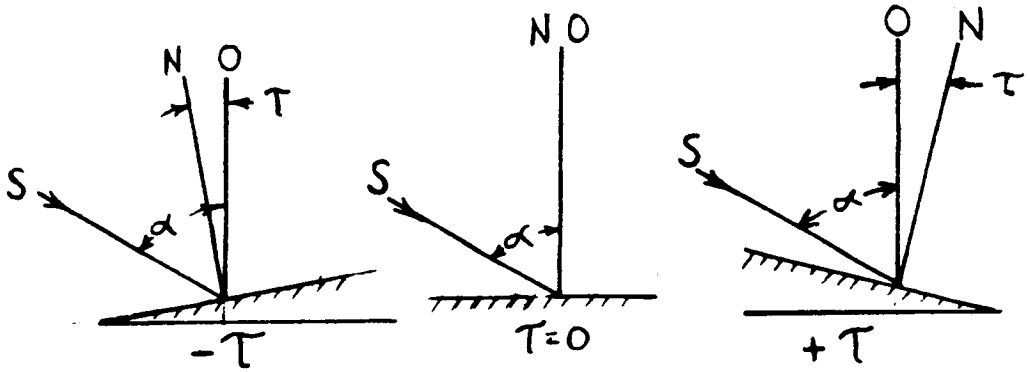

O = OBSERVER OR CAMERA
S = SUN
N = PROJECTION OF THE NORMAL INTO THE PHASE PLANE

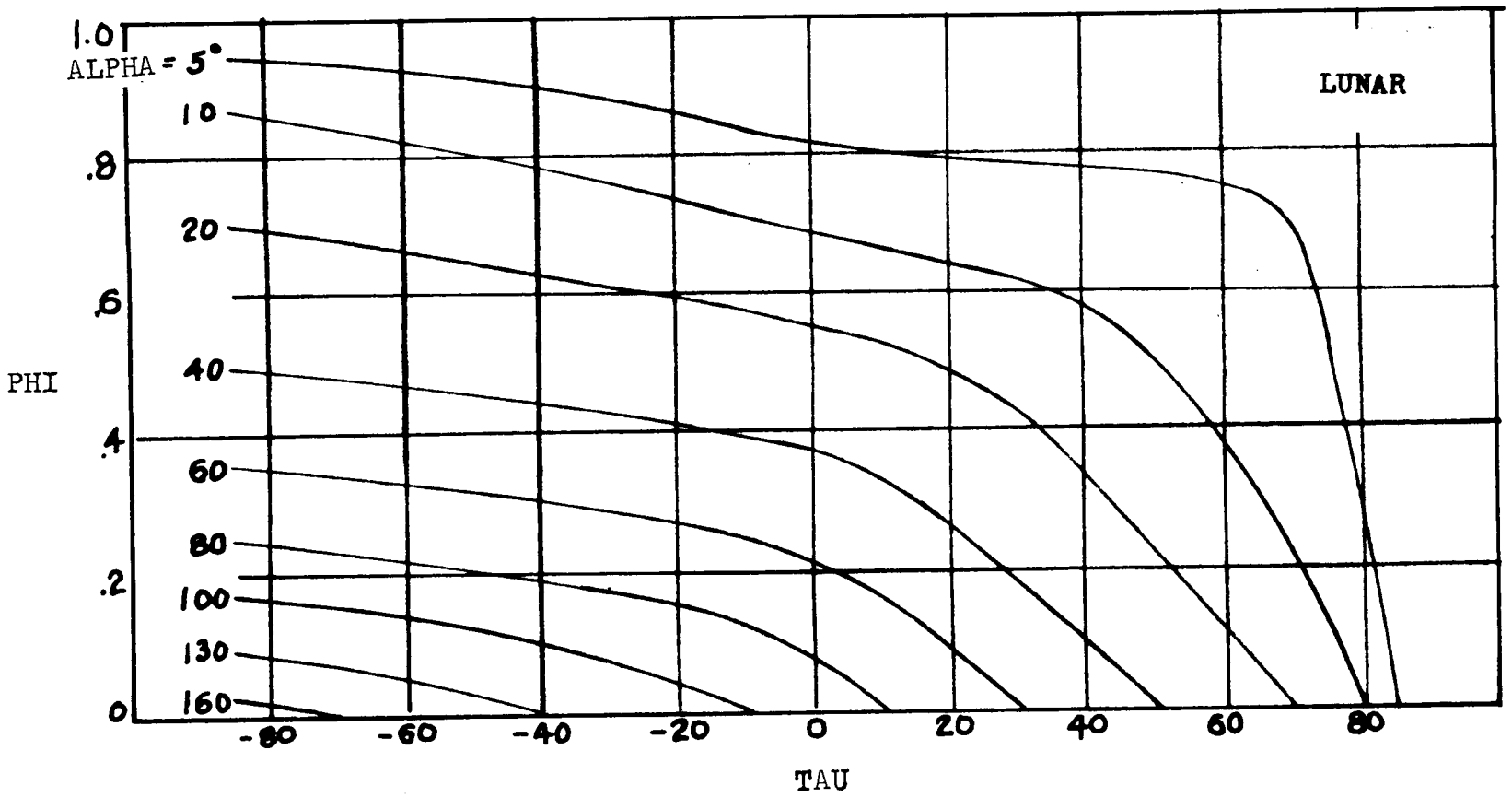

Figure A1-1. PHOTOMETRIC FUNCTION PHI VERSUS ANGLE TAU FOR SEVERAL PHASE ANGLES ALPHA

In order to enhance our ability to detect changes in surface slope, we chose a range of phase angles over which the photometric function is most sensitive to departures of tau from zero. The lower portion of Figure A1-1 is a plot of the photometric function vs tau for constant values of alpha. A practical operating range corresponds to solar altitudes between 15° and 30°.

Mapping the moon from orbital photography involves the complementary use of wide-angle and high-resolution coverage of the same area. The accuracy of stereoscopic height and slope measurements on wide-angle photographs depends primarily on the geometry (the base/height ratio), provided fine details on the ground are shown in sufficient contrast. Without the latter, stereoscopic vision is difficult or even impossible. On the other hand, slope determination from the high-resolution photographs depends on the faithful reproduction of luminance values in the scene.

To determine these values, the photograph is scanned with a microdensitometer in lines along the direction of the illuminant. Since the solar altitude and camera orientation are known, the phase angle can be calculated for each portion of the scan. For near-vertical, narrow-field photography, the photometric function then is a function of the single variable tau, the ground slope in the sun-line direction.

Unfortunately, the calculated luminance at a point is always ambiguous, since it varies as the product of the normal albedo and the photometric function. When mapping small landing sites about 100 to 200 feet in diameter, it is necessary to assume that the normal albedo is the same all over the area.

In this case, stereoscopic, wide-angle photographs will complement the high-resolution photographs. Wherever a slope has sufficient horizontal extent to be clearly seen at lower ground resolution, its inclination can be measured stereoscopically. This measurement will permit the determination of the normal albedo at many places on each wide-angle photograph, giving reference points for interpretation of the photometry from the narrow angle pictures.

At this stage, it is possible to integrate the slopes over the length of a scan to produce a ground profile. Since the photometric method can provide no information about slope components perpendicular to the sun line, adjacent profiles cannot be precisely tied together to form a surface without recourse to stereoscopic information. To produce a large-scale map showing fine details, the elevations at the ends of each photometrically derived profile should be adjusted to fit the contours of the base maps determined stereoscopically.

Procedure For Photometric Mapping

The purpose of the first part of the study was to determine the accuracy and precision with which contour maps can be made by photoclinometry and by stereo techniques from photographs of lunar scenes. The procedure for studying lunar map making by photoclinometry was as follows:

1. Realistic lunar models which have the correct lunar photometric function as established in Phase I of this study were constructed.
2. These models were photographed at appropriate scales and sun elevations, using careful photometric controls.

3. The resulting photographs were analysed with a microdensitometer to determine the tau angle.

4. Microdensitometer measurements were converted to lunar profiles and the profiles adjusted to make a lunar map.

Three models with increasingly complex detail were analyzed:

a. A simple geometric shape on a plane background.

b. Several geometric shapes with three different slopes as a background.

c. A complex lunar landscape (KLM 6-65).

These models were dusted with copper oxide to produce a surface whose photometric function closely matched that of the moon. The reflectance of this surface for a vertical view has been carefully measured as a function of both surface slope angle and solar elevation. From the densities measured on a photograph of the models, and using a computer program, the slope of the dusted surface at many points on the model was calculated. Assuming constant albedo and a uniform surface slope between adjacent points, it was possible to make a contour map from a single photograph.

Fundamental Equations

There are four fundamental equations which must be solved to photometrically derive a lunar profile from a lunar photograph. These equations, described below, relate density on the film to slopes and elevations on the moon.

EQ.1 $D = f(E)$, see Figure A1-2

Where D = Density

E = exposure (meter - candle - seconds)

The density obtained on the film also depends upon the sensitometric material and the processing of this material. In this study, a characteristic curve for each photograph was obtained and this curve used in the analysis of the photograph. For accurate work, the exposure time should be the same for both the picture and the sensitometric gray scale.

EQ.2 $$E = \frac{10.76 I \rho \Phi T t}{4N^2}$$

where E = exposure (meter - candle - seconds)

I = Illuminance on the scene, ft - candles

ρ = Albedo

Φ = Photometric function, a function of alpha and tau (Figure A1-1)

T = Transmission of the lens

t = Exposure time (seconds)

N = F aperture

This equation relates the camera exposure to the optical parameters and the scene illuminance. All of the terms are multipliers which are easily handled by a computer. For a single vertical photograph showing a lunar scene of constant albedo, all of these parameters are constant except Φ which varies only with tau under these conditions.

The ratio Φ/E is used frequently in future computations where the exposure can be calculated from measured densities over an area of known slopes. This ratio is defined as follows:

$$A = \Phi/E = \frac{4N^2}{10.76\ I\rho T t}$$

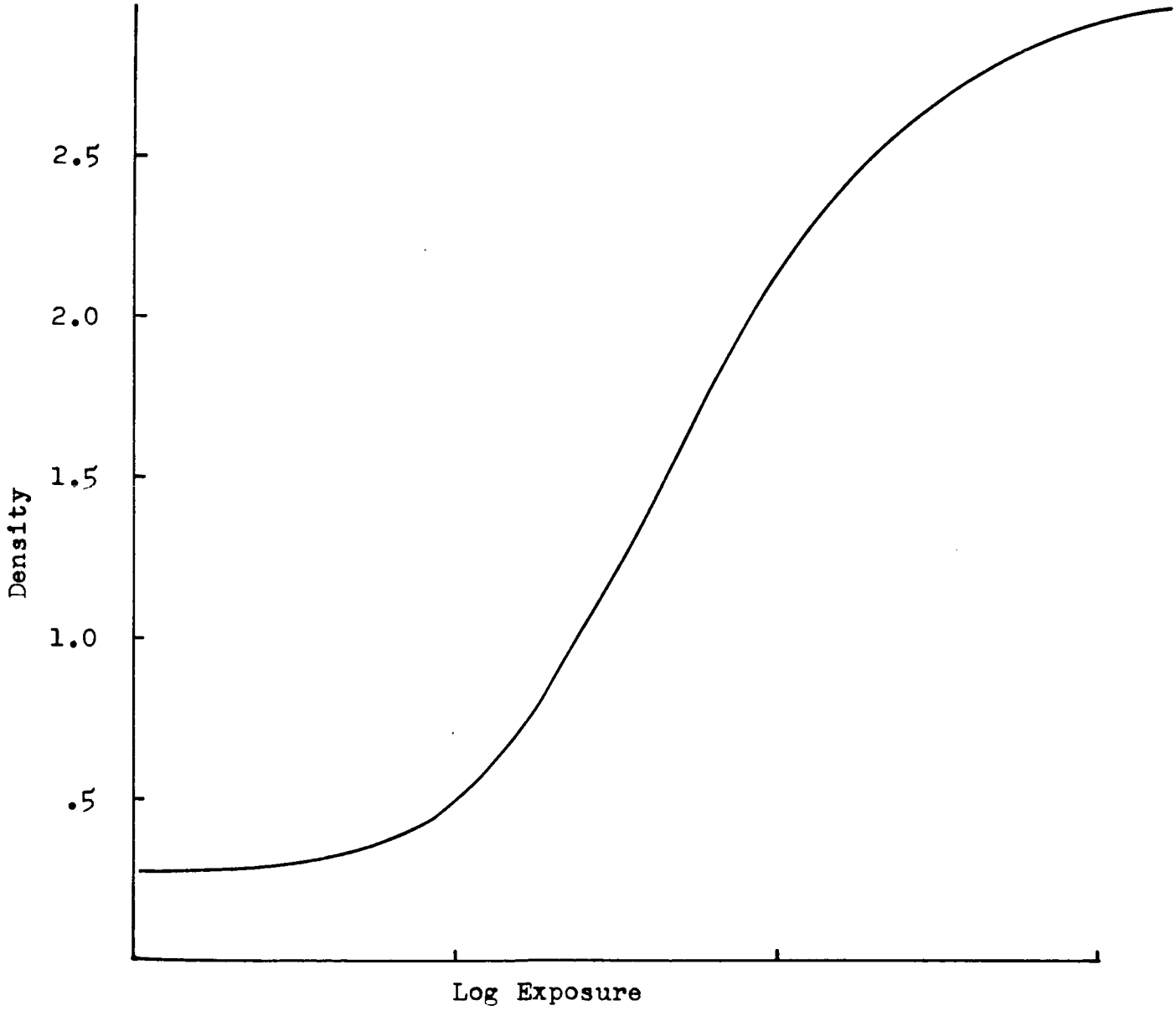

Figure A1-2. DENSITY VERSUS LOG EXPOSURE

EQ-3 phi = (alpha, tau)

Phi is a function of alpha and tau as indicated in Figure A1-1. This function has been established by astronomers and has been supplied by NASA based upon Fedoretz' data. In phase I of this study, it was shown that copper oxide dust can be easily applied to lunar models and has reflection properties that closely resemble the lunar photometric function at tau = 0°. In order to apply this photometric function to the lunar models of the phase II study, the photometric function of copper oxide dust was measured for many values of alpha and tau. The results of these measurements are shown in Figure A1-3. A comparison of the lunar photometric function with the copper oxide photometric function is shown in Figure A1-4 for alpha = 75° and alpha = 60° which correspond to sun elevations of 15° and 30° respectively. It should be noticed that the agreement is very good in the region tau = ±15°. This region is of interest since these values of tau will reveal likely landing areas with slopes less than 10°. As tau changes from -20° to -90°, the copper oxide photometric function becomes increasingly greater than the lunar photometric function.

From the data in Figure A1-3 for the two phase angles 60° and 75°, best fit polynomial equations were generated. These equations relating tau to the photometric function of copper oxide dust for the two phase angles are as follows:[1]

1 The computed coefficients in these equations have been rounded to the nearest third significant figure.

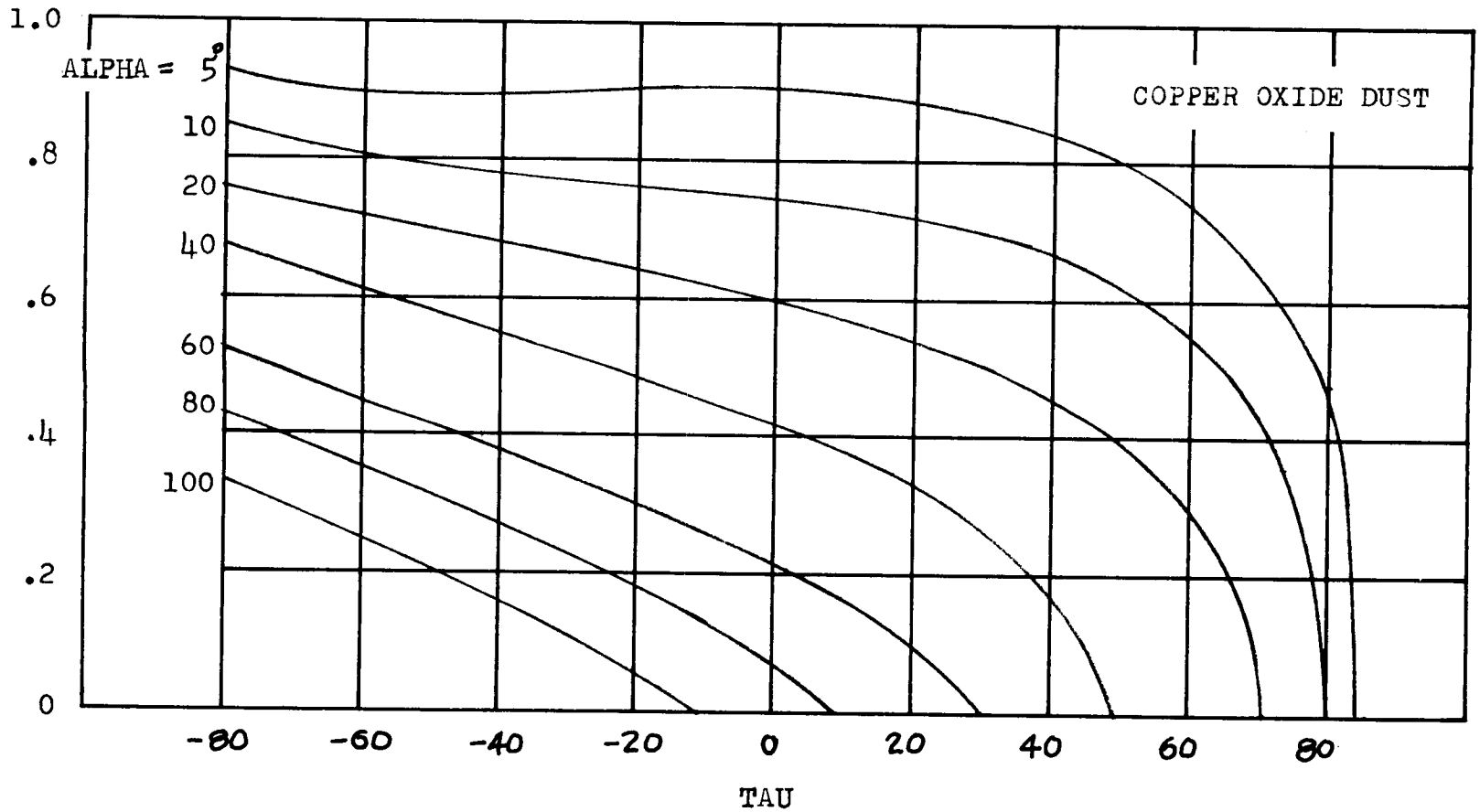

Figure A1-3. PHOTOMETRIC FUNCTION PHI FOR COPPER OXIDE DUST VERSUS ANGLE TAU FOR SEVERAL PHASE ANGLES ALPHA

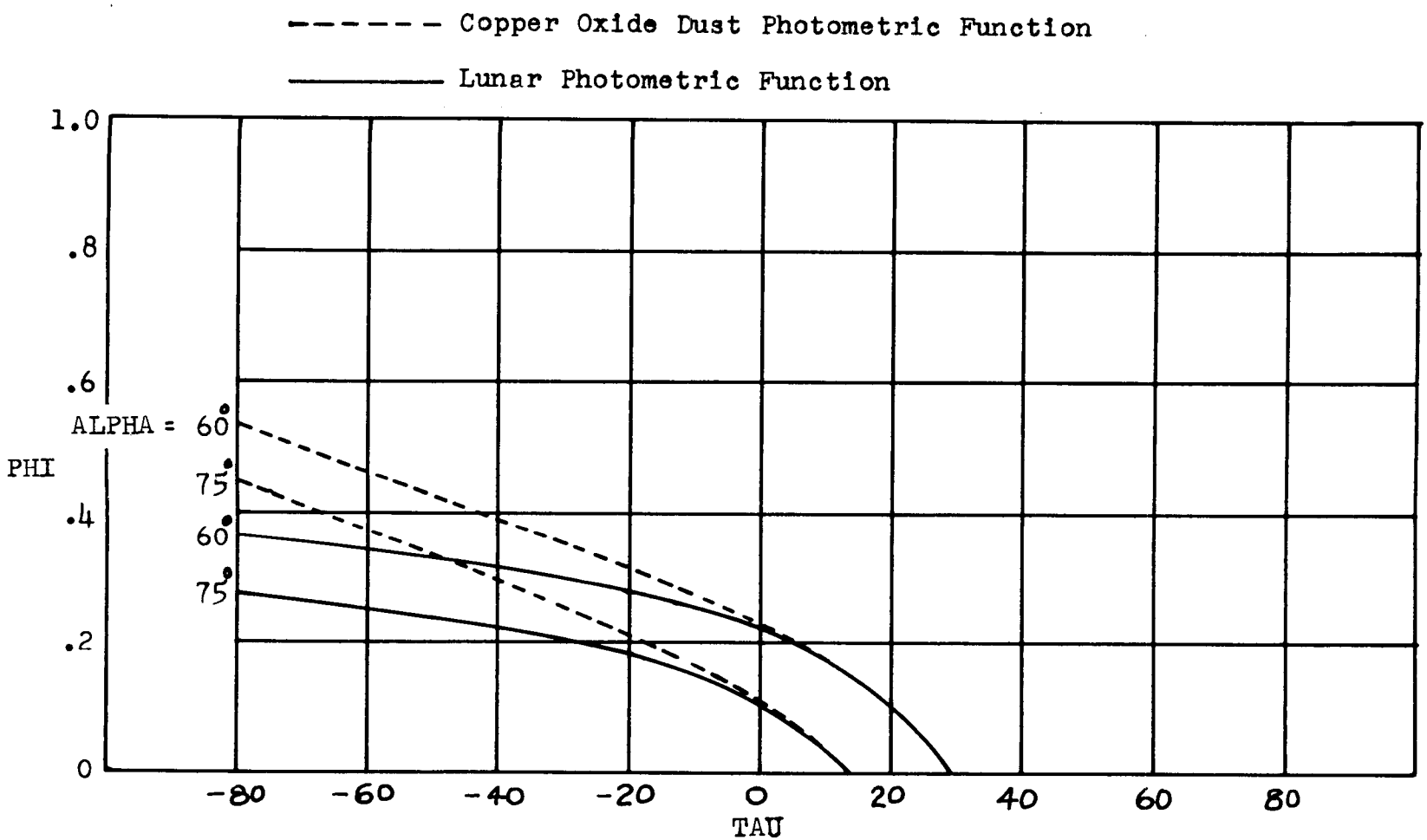

Figure A1-4. PHOTOMETRIC FUNCTION PHI OF THE LUNAR SURFACE AND COPPER OXIDE DUST VERSUS ANGLE TAU FOR PHASE ANGLES OF 60° AND 75°

For 75° phase angle (15° sun elevation)

$$\text{EQ-3a} \quad \text{Tau} = 14.0 - 32.3\Phi - 1510.\Phi^2 + .822 \times 10^4\Phi^3 - .150 \times 10^5\Phi^4 - .474 \times 10^5\Phi^5 + .122 \times 10^6\Phi^6 + .237 \times 10^6\Phi^7 + .290 \times 10^6\Phi^8 - .158 \times 10^7\Phi^9 + .221 \times 10^7\Phi^{10}$$

and for 60° phase angle (30° sun elevation)

$$\text{EQ-3b} \quad \text{Tau} = 31.6 - 168\ \Phi + .141 \times 10^4\Phi^2 - .109 \times 10^5\Phi^3 + .293 \times 10^5\Phi^4 - .397 \times 10^5\Phi^5 + .122 \times 10^6\Phi^6 - .428 \times 10^6\Phi^7 + .391 \times 10^6\Phi^8 + .556 \times 10^6\Phi^9 - .797 \times 10^6\Phi^{10}$$

Fortran Subprogram CURFIT was developed at Kodak to obtain these equations from the measured data. Figure A1-5 shows excellent agreement between the observed points and the points calculated from the above equations. *

Collectively equations 1, 2, and 3 relate angle tau with density. For negatives exposed in vertical photography, density converted to a tau angle gives the component of ground slope parallel to the phase plane. Since a density measurement covers a finite area on the film, a tau angle calculated from this density is related to the <u>average</u> slope of the corresponding area on the moon. From a series of closely spaced density measurements, an approximate ground profile can be constructed by assuming the calculated tau to

---

* Three Phi Tau equations were used in the 18 experiments. The above was used in experiments 3 and 4. A refined Phi Tau equation is described in the error investigation after experiment 4, and was used for experiments 5 through 16. A third Phi Tau equation was derived for experiment 18. All three equations were obtained from the same observed data.

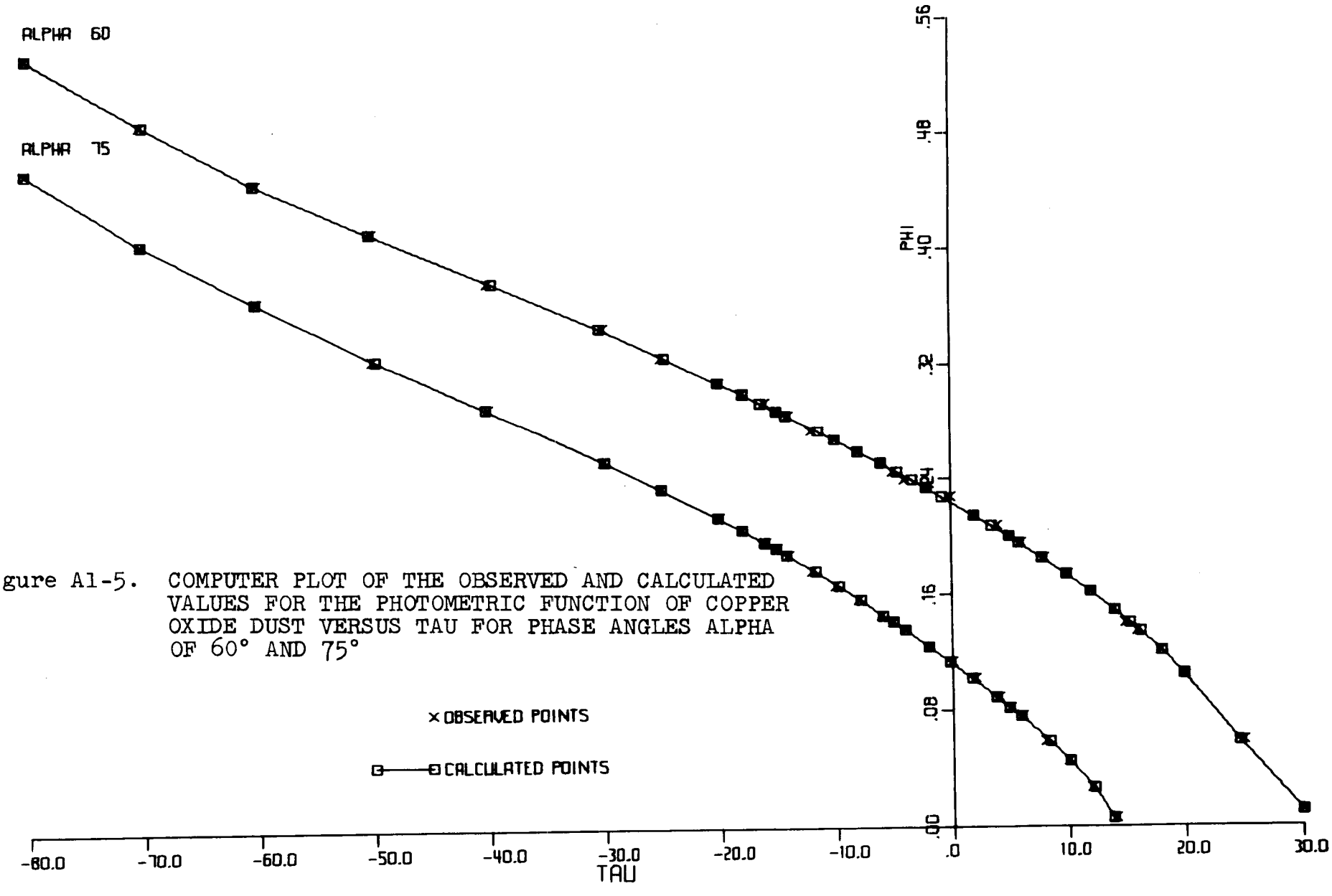

Figure A1-5. COMPUTER PLOT OF THE OBSERVED AND CALCULATED VALUES FOR THE PHOTOMETRIC FUNCTION OF COPPER OXIDE DUST VERSUS TAU FOR PHASE ANGLES ALPHA OF 60° AND 75°

be the average slope between measurements and then calculating the change in elevation over this distance:

$$\Delta h = \tan \text{tau}. \quad \Delta x$$

After n steps the elevation will be given by:

EQ-4 $$h_{x_n} = \sum_{i=o}^{n} \tan \text{tau } i \ \Delta x_i$$

Where h_{x_n} is the elevation at the position x_n of the nth density measurement on a scan, measured relative to the elevation at position x_o of the first density measurement of the scan. See Figure A1-6.

A graphical solution to equations 1 to 3b is shown in Figure A1-7. In setting up these curves, it is necessary to note the density obtained for a known value of tau and alpha while using specific values for I, ρ, T, t and N. The correct value of log A is positioned opposite the appropriate point of the log Phi scale and also aligned with the value of log E which gives the observed density. An index mark at the bottom of the D-log E curve is used to reposition the two graphs when a change is made in one or more of the photometric parameters.

Once the graphs are positioned for a particular set of conditions, changes in microdensitometer voltage may be read out as changes in tau angle.

The graphical solution helps to visualize the effect of small changes in the variables. It also aids in determining an exposure yielding densities that are most sensitive to changes in tau.

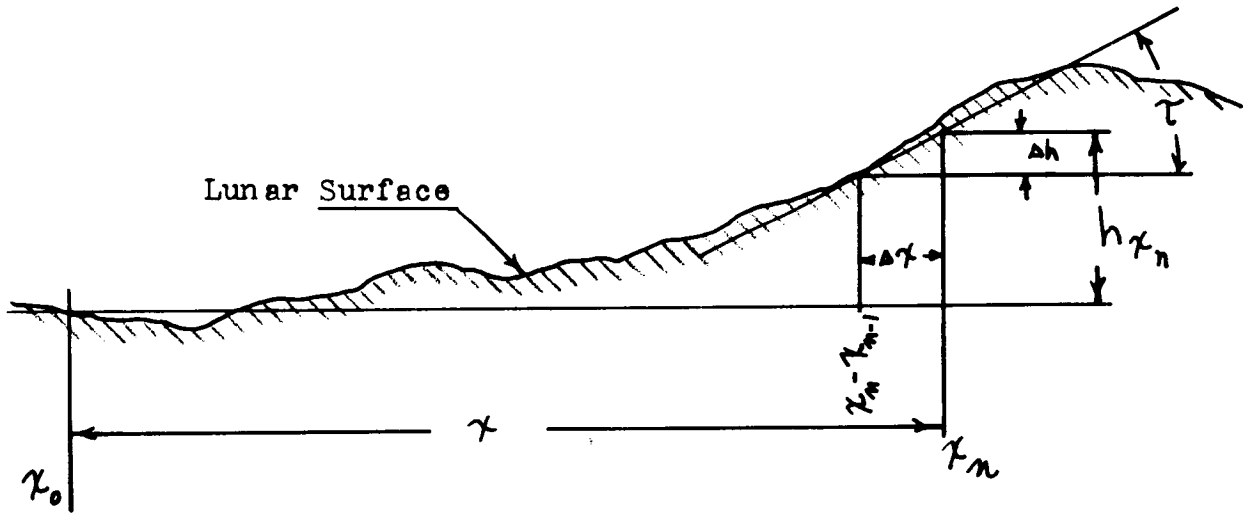

$$\Delta h = \tan \tau \ \Delta x$$

$$h_{x_n} = \sum_{i=0}^{n} \tan \tau_i \ \Delta x_i$$

Figure A1-6. METHOD OF SUMMING CALCULATED INCREMENTS OF Δh TO OBTAIN A LUNAR PROFILE.

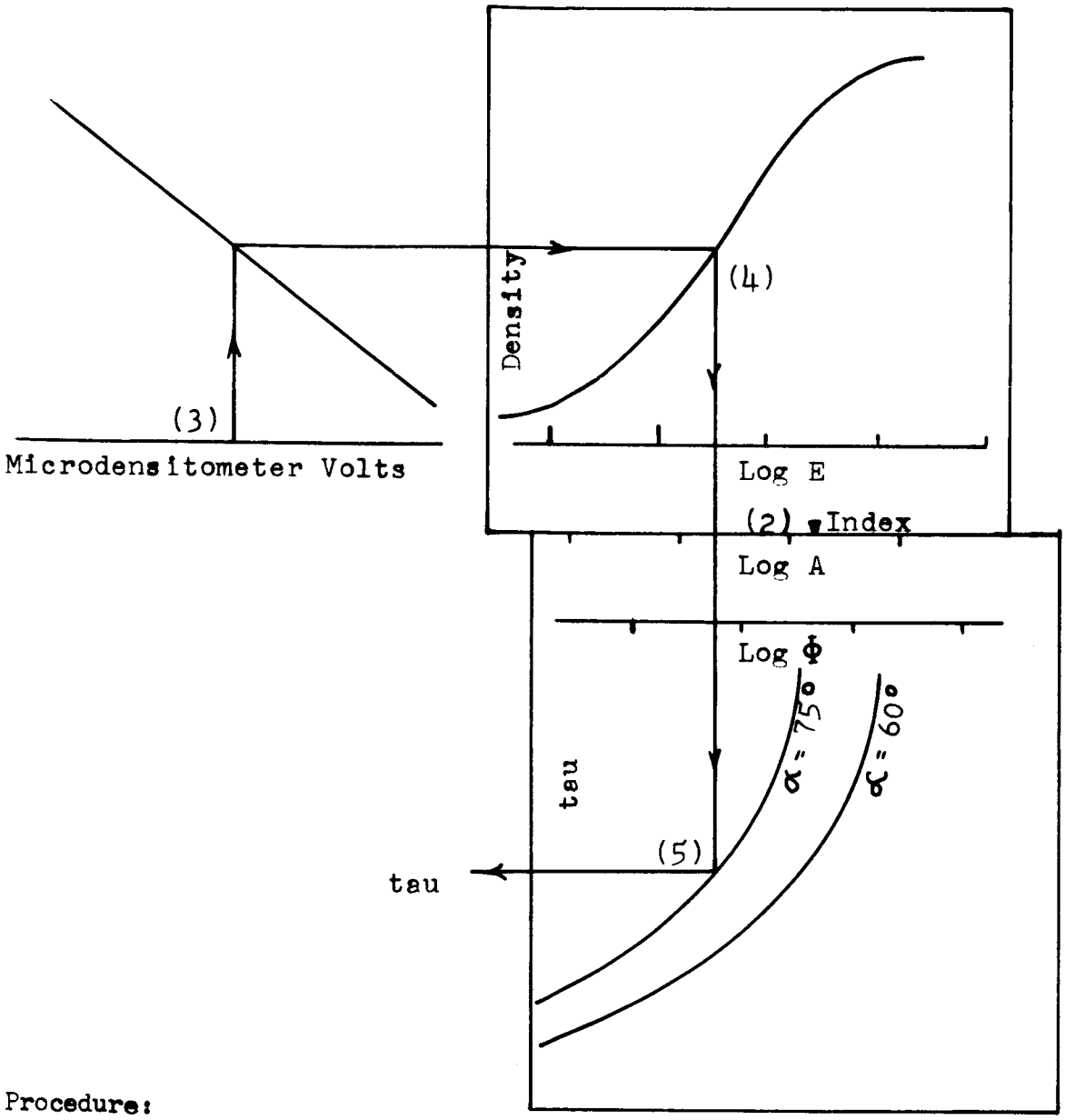

Procedure:

1 Obtain value for Log $\frac{4\ N^2}{10.76\ I\ \rho\ T\ t}$ = Log A = Log $\frac{\Phi}{E}$

(2) Align Value of Log A with Index on D-Log E Curve

(3) Enter with Microdensitometer Volts and obtain Density

(4) From Density obtain Log E

(5) Drop down to the correct alpha and obtain tau

Figure A1-7. GRAPHICAL SOLUTION FOR OBTAINING TAU FROM MICRODENSITOMETER VOLTS

Computer Solution For Lunar Profiles

A computer can readily handle the large quantities of data from photoclinometry as well as the multiplication involved in the fundamental equations. In fact, it is easy to combine the calibration curve of the microdensitometer with the characteristic curve of the film using the computer CURFIT program so as to go directly from the microdensitometer voltage to film exposure. Figure A1-8 shows this conversion curve drawn by the computer from processing and density data obtained in recording model LM-3. The computer equation for this curve is:

$$E = -3.03 + 1.69V - .300V^2 + .0195V^3$$

where E = exposure in meter - candle - seconds

V = microdensitometer voltage

For the analysis of target LM-3 shown in Figure A1-9 the slope of the background was considered to be zero degrees. The density of the background on the film negative was measured, and the relationship between E and Φ was computed from the multiplier, A, required to convert E into Φ for a known microdensitometer voltage and for tau equal to zero. Variations in microdensitometer voltage then become variations in tau which are obtained by solving equations 1 to 3b.

Profiles of the model were made using equation 4 for each microdensitometer scan. The microdensitometer voltage was measured at uniform increments of distance (ΔX) along the scan and placed on IBM cards. The computer program multiplies the calculated slope angle (tau) by the ΔX-interval to arrive at an increment in elevation Δh. The distances along the scan are the x-dimension of the lunar map, and the computed altitudes form the lunar profile. The separation between scan lines determines the separation between profiles and becomes the y-dimension of the lunar map.

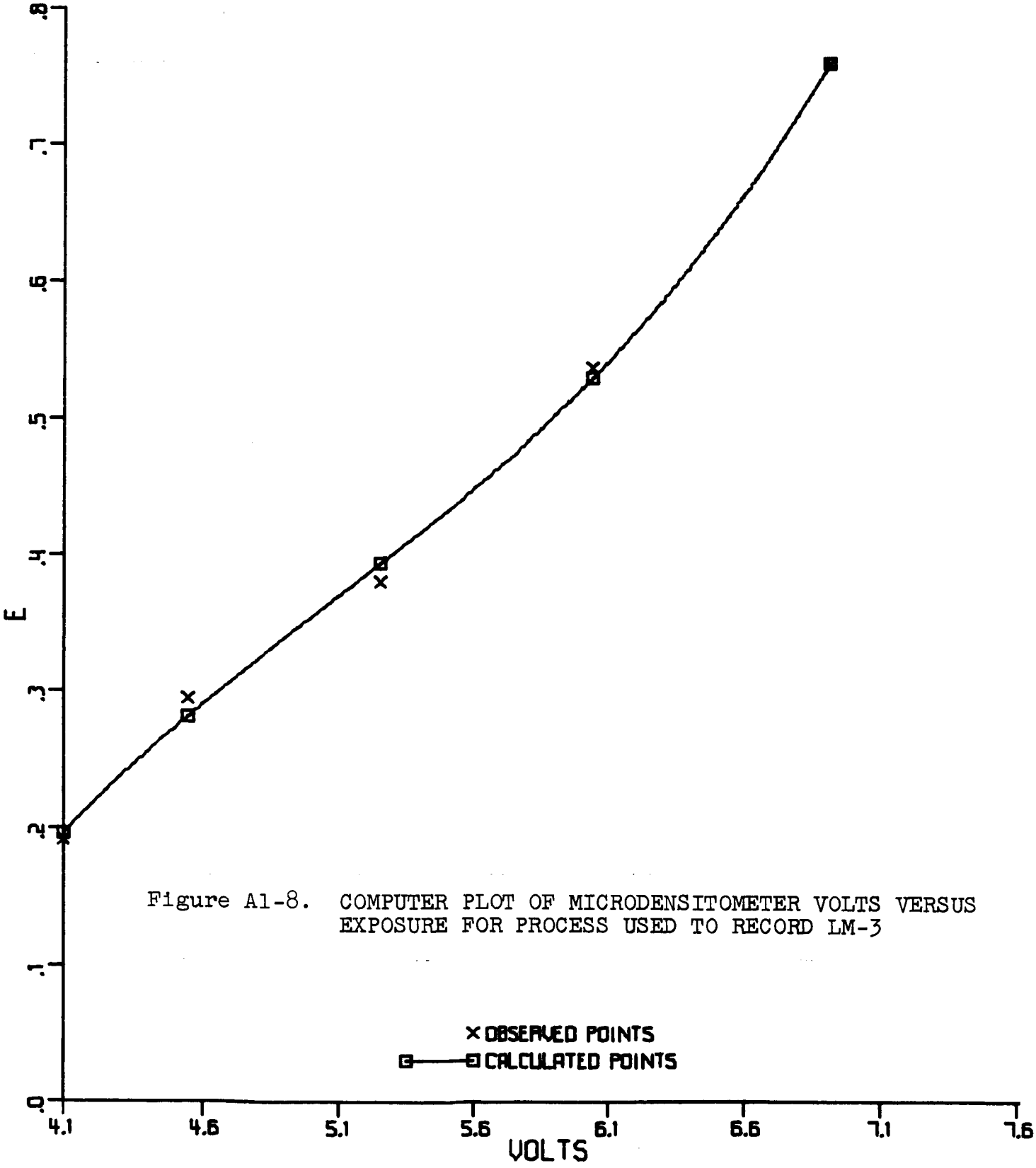

Figure A1-8. COMPUTER PLOT OF MICRODENSITOMETER VOLTS VERSUS EXPOSURE FOR PROCESS USED TO RECORD LM-3

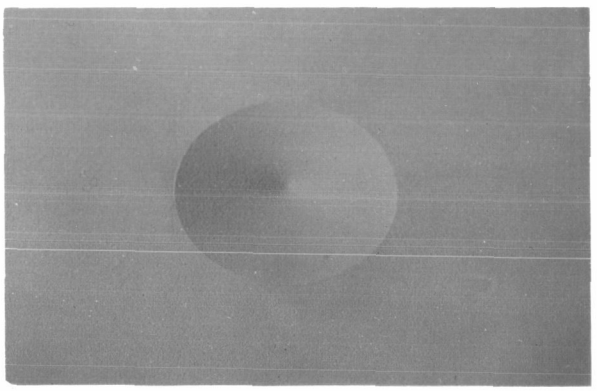

L M-3 7° CONE

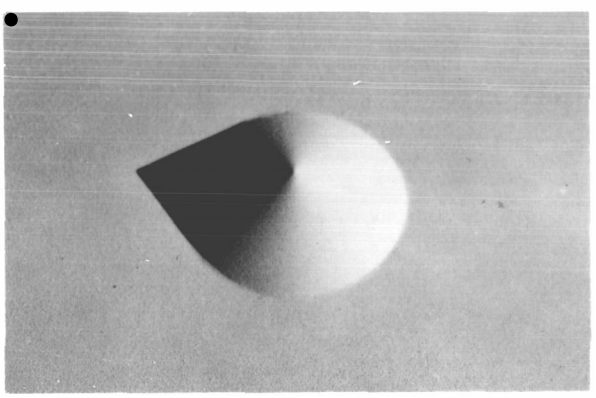

L M-4 26° CONE

Figure A1-9. GEOMETRIC SHAPES USED IN LUNAR MAPPING STUDY

Mapping A Geometric Shape

Experiments No. 1 and No. 2 using hemispheres were photographed and traced but not analyzed, as it was felt that we could obtain more useful information by analyzing the cone shapes of Experiment No. 3 and No. 4, since the elements of the cones are straight lines.

Experiment No. 3 Run No. 1

To demonstrate the methods used in photoclinometry, a map was made of a 4-inch diameter cone of base angle 6.8° (LM-3, see Figure A1-9). This plastic model was dusted with copper oxide and photographed at a scale of 1:51 at a phase angle of 75° (sun elevation 15°). A Cannon 85mm F.L. lens with an axis transmission of 89 percent and set at f/4 formed the image on SO-243 film. Exposure time was 20 seconds. Perpendicularity of target plane and camera axis was assured to ±1/2° or better by adjusting the target plane to cause an incident beam of light along the camera axis to be reflected back on itself towards the source by a mirror in the target plane. The negative was scanned in the direction of the sun with a microdensitometer equipped with a circular scanning spot of 53-microns diameter. Eighty readings were taken per scan, and 20 scans each separated by 150 microns were made across the image. This spacing of readings, with separation in one direction equaling three times the separation in the other direction, is sufficient for mapping a known geometric shape, but was not used for analyzing more complex surfaces. Appendix I shows the relative sizes of scanning spot, cone, and limiting tri-bar resolution projected onto the model and to the lunar surface assuming a model scale of 1:48.

The diameter of the microdensitometer spot was selected as 53 microns, six times larger than the pitch of the limiting high contrast tri-bar chart. This factor insures that the noise caused by film grain will not appreciably effect mapping accuracy.

The IBM cards with the voltage readings obtained from the microdensitometer were run through the 7044 computer along with the other optical and photographic data and the computer program. For each scan the computer printed out the following values: microdensitometer volts, exposure, A, phi, tau, x, y and height. Then an automatic curve plotter drew the profiles shown in Figure A1-10 from the x and height data. Next the computer examined the x, y, and height data, grouping heights in predetermined cells according to the contour interval desired. Finally, the elevation map shown in Figure A1-11 was drawn. In this map the contour interval is 0.1 foot; e.g., the computer plotted 0.2 for all height values between 0.15 and 0.25.

Discussion

Measurements on the model are compared with the values obtained by photoclinometry in Table A1-I. The model has a flat background (tau = 0°) for which the range of calculated elevations was from + .067 to - .154 foot. Errors in elevation accumulate across the eighty points in a scan, as the starting point is assumed to be zero elevation and the height at each succeeding point is the sum of all the previous heights and their associated errors.

Near the end of this study, Experiment No. 3 run No. 2 was computed with all the improved techniques found in the later experiments. Elevation map, Figure A1-12, was made with this Run No. 2 data. Table A1-I shows the measurements that were made on LM-3 compared to the values obtained by photoclinometry in Experiment No. 3, Run No. 1 and Experiment No. 3, Run No. 2.

In both Run No. 1 and Run No. 2 the errors contributed by the lens aperture, lens transmission, exposure time, illuminance and albedo were minimized by setting the known zero tau angle equal to the measured density at zero slope for each value of X across the model. This procedure is possible only when the slopes in the photograph are known; it is not possible for a lunar scene of unknown shape and orientation where the brightness of the image on the film

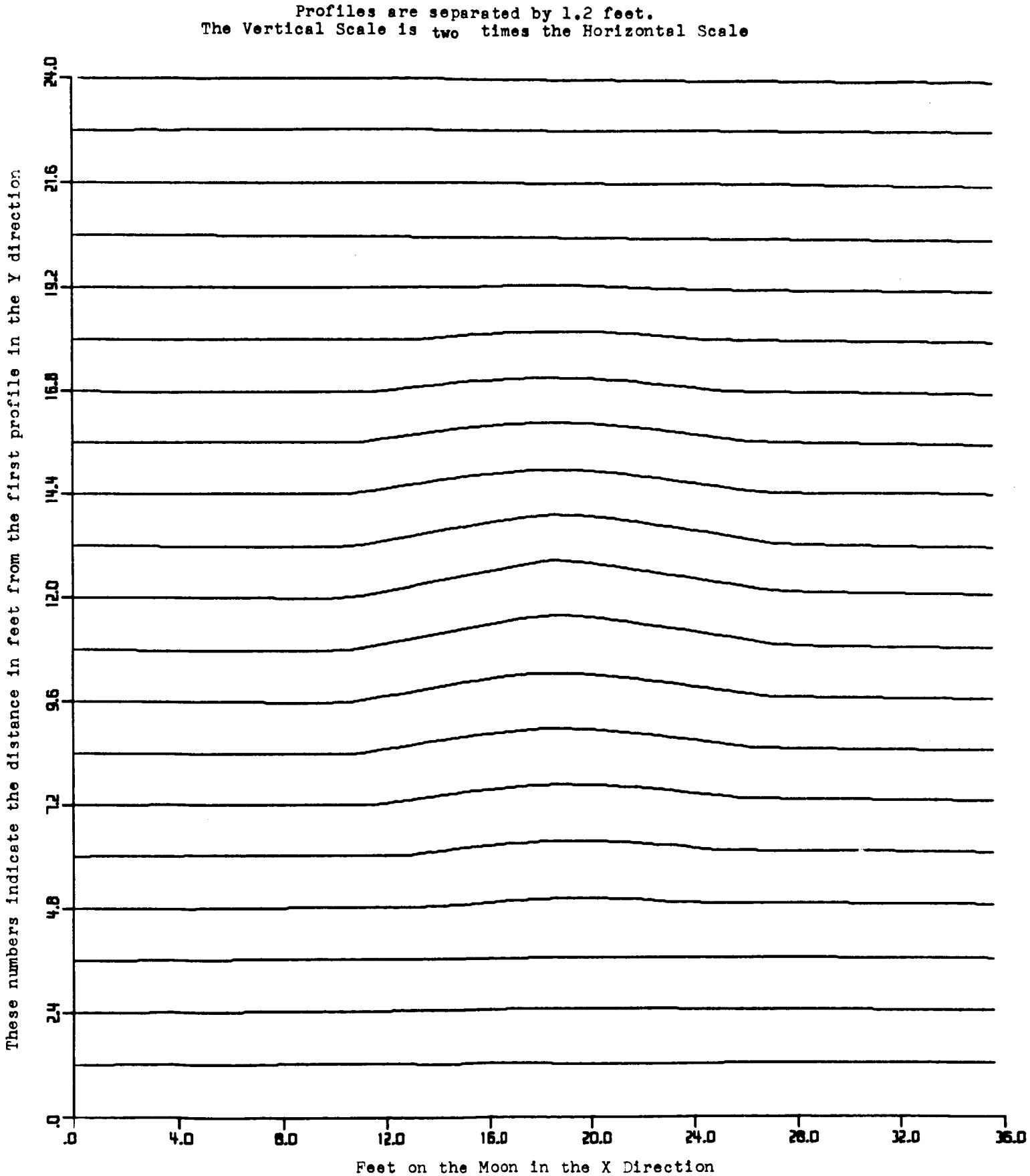

Figure A1-10. COMPUTER PLOT OF THE 20 PROFILES MADE FROM MICRODENSITOMETER SCANS OF LM-3

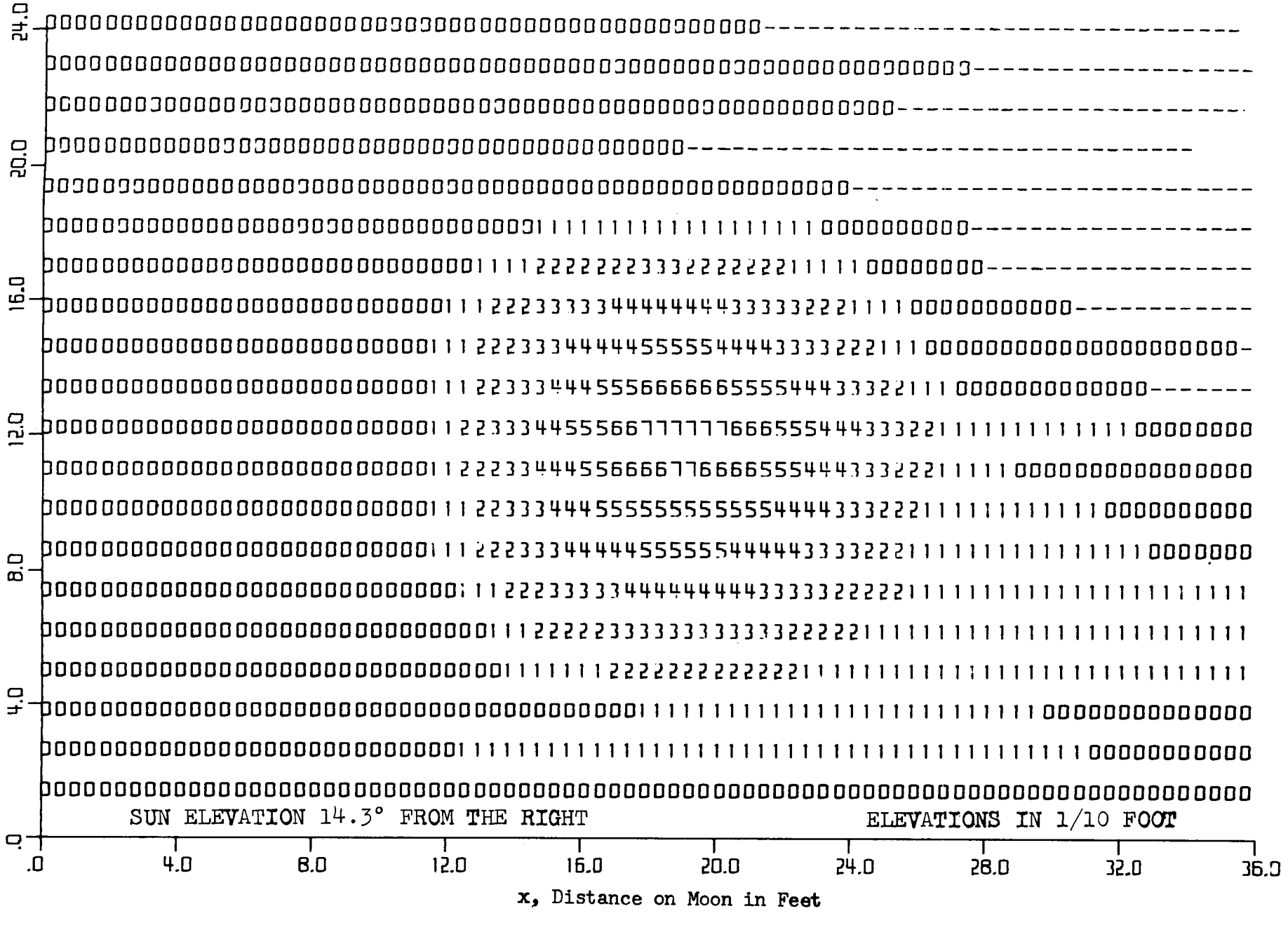

Figure A1-11. ELEVATION MAP FOR LM-3, RUN 1 NUMBERS PLOTTED GIVE ELEVATIONS IN TENTHS OF A FOOT.

TABLE A1-I

COMPARISON OF DIMENSIONS ON MODEL LM-3
WITH THOSE CALCULATED BY PHOTOCLINOMETRY

	Model Dimension	Scaled Lunar Dimension	EXPERIMENT 3			
			RUN 1		RUN 2	
			Photo Mapped Dimension	% Error	Photo Mapped Dimension	% Error
Base Angle	6.8°	6.8°	5.3° shadow side 4.4° sun side	22. 35.	7.0° 7.0°	3.0 3.0
Diameter	4.013 in.	16 ft.	16.8 ft.	5.	16.4	2.5
Peak Elevation	0.24 in.	0.96 ft.	0.71 ft.	26.	1.01	5.0
Background Elevation	zero	zero	+ .067 ft. - .154 ft.	—	Less than ± .05 ft.	—

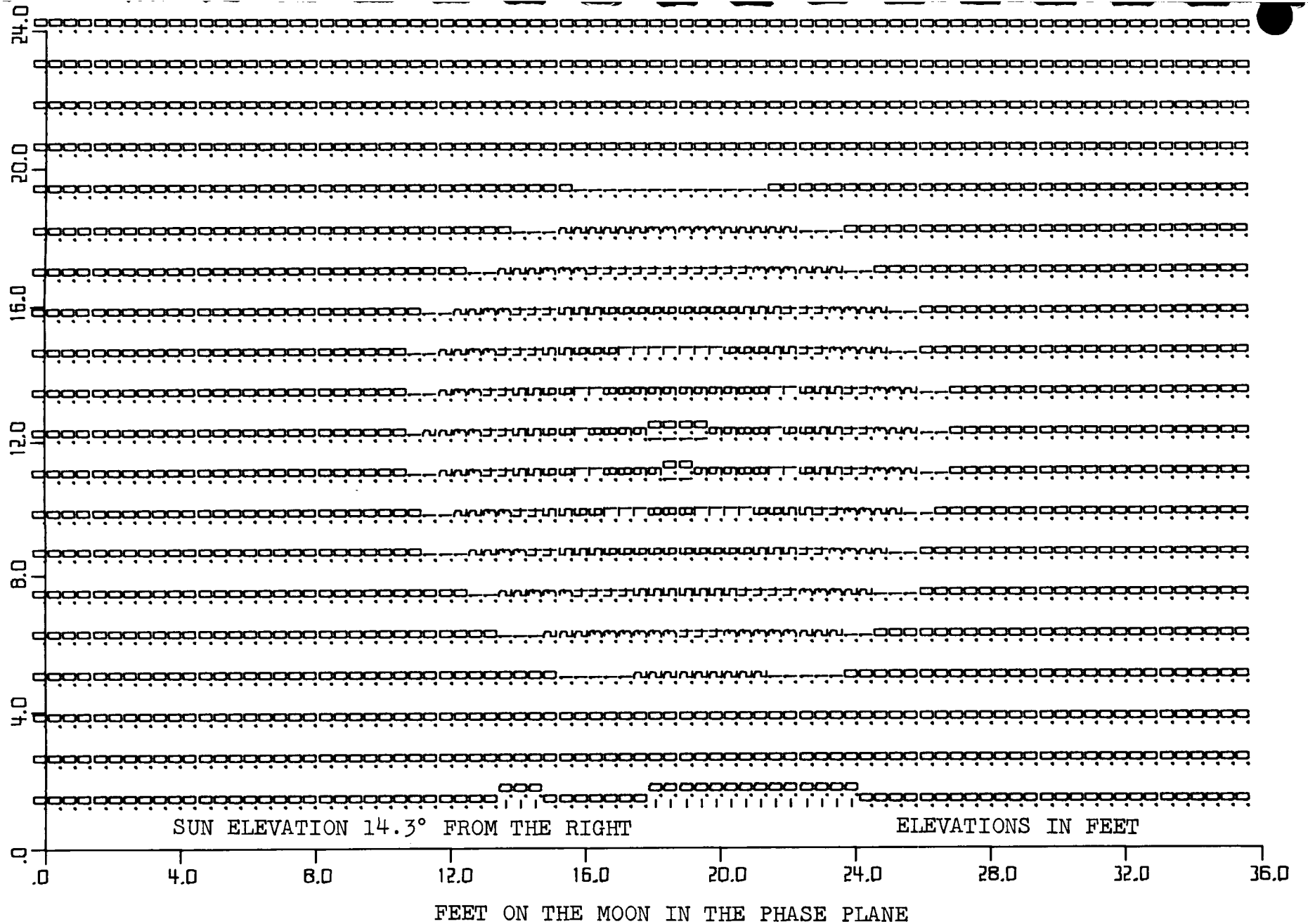

Figure A1-12. ELEVATION MAP FOR LM-3, RUN 2

must be calculated for assumed slope of unknown albedo.

The calculated values of elevation plotted in Figure A1-12 were made using adjusted sensitometry, the error of closure method on each scan, and a single phi-tau equation. The plotted elevation numbers are rounded by adding 0.05 foot to each computed value and plotting the first figure only (except for the 6 values above 0.95 foot where two significant figures were plotted). All of these techniques are described later in this report. Figure A1-12 is included as a check on these techniques.

Mapping LM-4 Experiment No. 4

The second geometric shape to be mapped was LM-4, a 4-inch diameter 26° cone. This model was used to investigate the problems associated with making a contour map when shadows and steep elements are present. The procedure for mapping this model is the same as for LM-3 which is reviewed in the next paragraphs.

This plastic model was dusted with copper oxide and photographed at a scale of 1:51 at a phase angle of 75° (sun elevation 15°). A Cannon 85mm F.L. lens with an axial transmission of 89 percent formed the image on the SO-243 film. Exposure time was 20 seconds at f/4. Perpendicularity of target plane and camera axis was assured to ± 1/2° by adjusting the target plane to cause an incident light beam along the camera axis to be reflected back upon itself towards the source by a mirror in the target plane. The negative was scanned in the direction of the sun with a microdensitometer equipped with a circular scanning spot of 53-microns diameter. Eighty readings were taken per scan, and 20 scans, each separated by 150 microns, were made across the image. Appendix I shows the relative sizes of scanning spot, cone, limiting tri-bar resolution projected onto the model and onto the lunar surface, assuming a model scale of 1:48.

The diameter of the microdensitometer scanning spot was selected as 53 microns, about six times larger than the pitch of the limiting high contrast tri-bar chart. This insures that the noise caused by film grain will not appreciably effect mapping accuracy.

For LM-4, the computer program was given the microdensitometer voltage corresponding to tau equal zero. Both exposure (E) and the photometric function (Φ) have been used to calculate $A = \frac{\Phi}{E}$, eliminating the uncertainty of:

T, Lens transmission

t, Exposure time

I, Illumination

N, F/aperture

For each scan the computer printed out the following values: microdensitometer volts, exposure, phi, tau, x, y and height. Then an automatic curve plotter drew the profiles shown in Figure A1-13 from the x and height data. Because of the errors discussed in the following paragraphs, no elevation map based on these data was compiled.

In LM-4 the 26° cone photographed at a sun elevation of 15° causes a shadow area which requires special consideration, since there are lunar surfaces of unknown slope within this shadow. This condition has been accounted for in the computer program in two ways. Whenever a very low density occurs (base plus fog) the computer assumed (1) a slope corresponding to the sun elevation, and (2) commanded the printer to print an asterisk rather than an elevation value at that value of x in the elevation plot.

The profiles plotted in Figure A1-13 show considerable error on the side of the cone facing the sun. Profiles that cut the cone parallel to the axis of the cone but do not pass over the peak of the cone will be hyperbolas if no shadow is encountered by the scanning spot. Profiles on the sun side of LM-4 should and do show a hyperbolic shape, but the hyperbolas are too shallow. Also, the profiles equidistant from the central profile should be similar to each other. The computer makes all profiles in the shadow have a slope equal to the sun elevation.

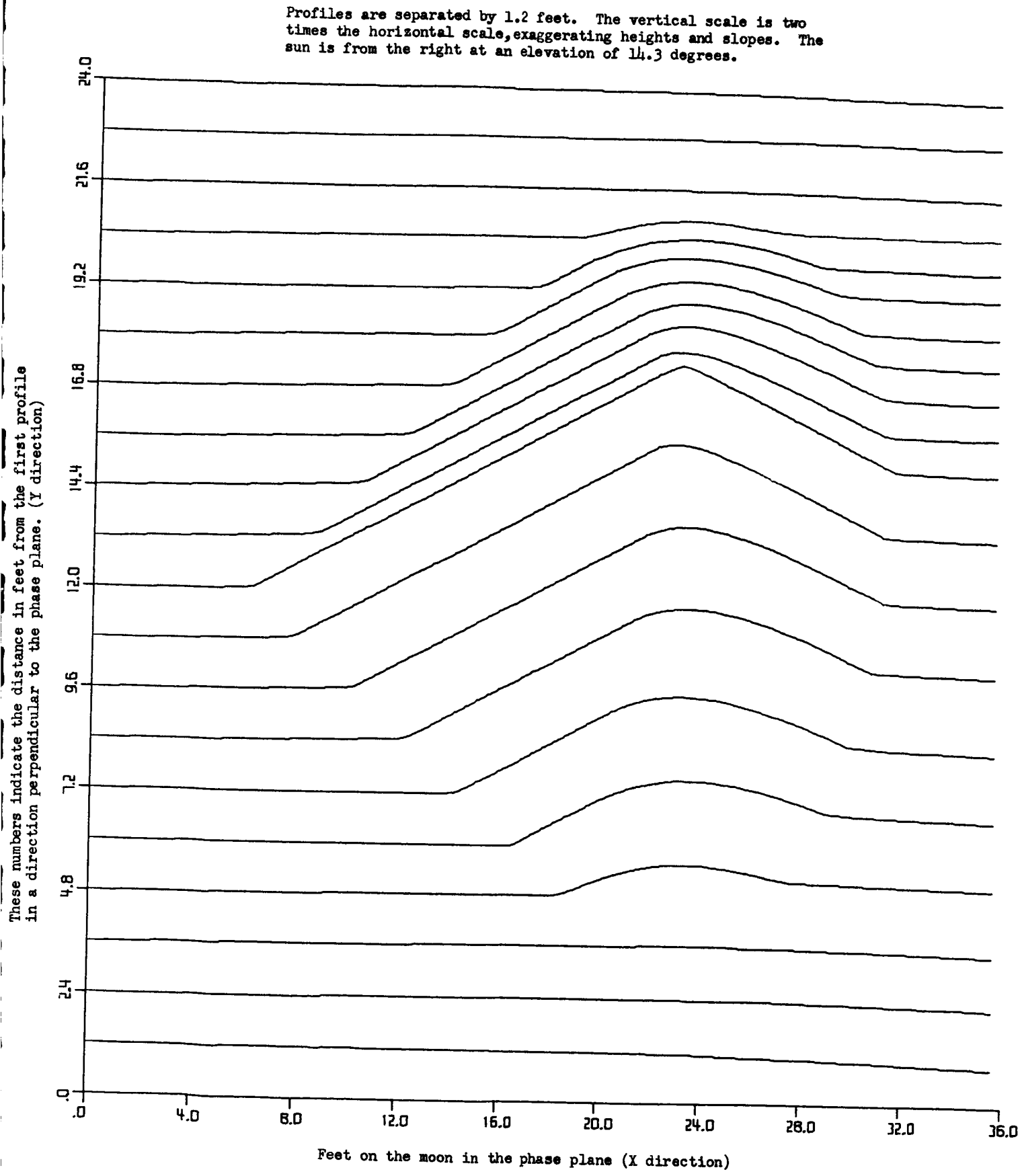

Figure A1-13. LM-4 PROFILES COMPUTED FROM MICRODENSITOMETER SCANS

The profile that passes over the peak of the cone should be composed of straight lines - the shadow side should have a slope equal to the sun elevation and the sun side should have a slope equal to the cone base angle. To examine the errors in this profile, note Figure A1-14, where a 26° cone has been drawn to scale in its correct location.

Several errors are immediately evident:

1. The shadow is too long; either the profile begins too far from the peak of the cone or the shadow angle is too steep, making the profile too high.
2. The slope of the sun side is not steep enough but it does cover the correct distance along the x axis.
3. The profile does not return to the zero base line.

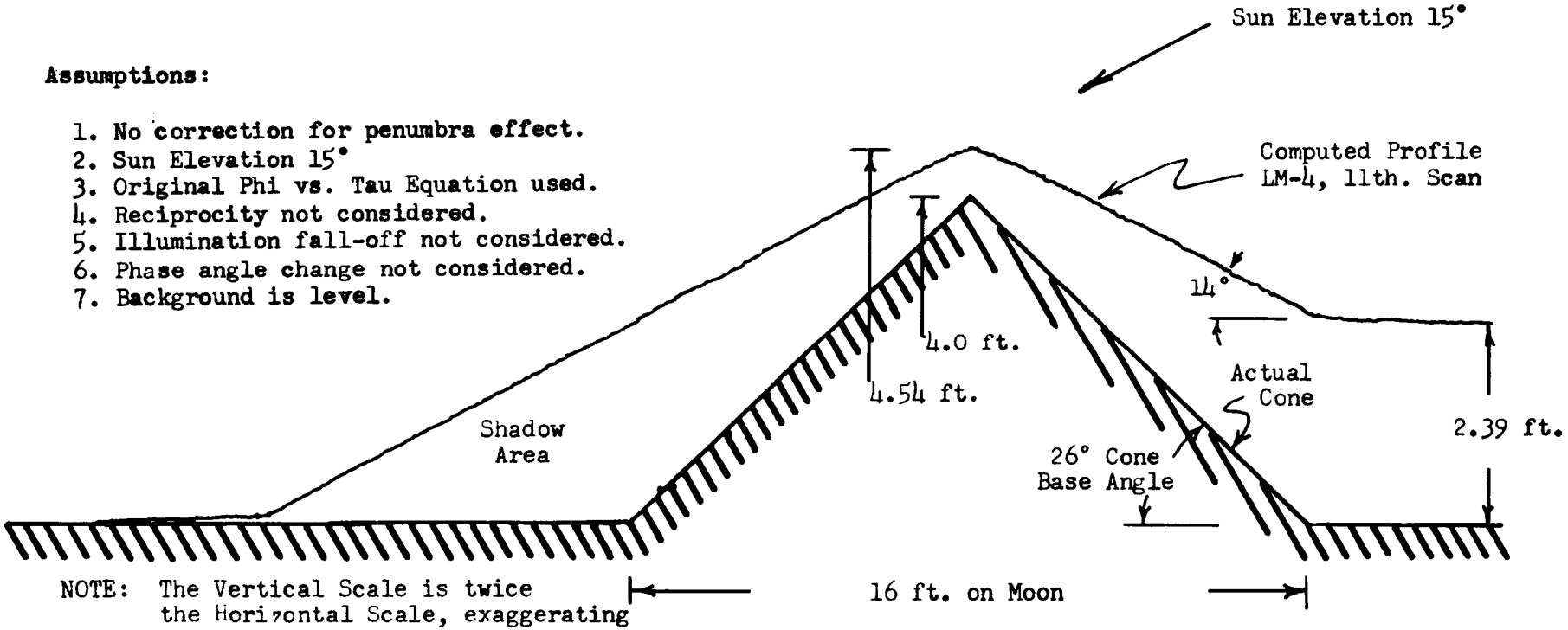

Figure A1-14. LM-4 COMPUTED PROFILE FOR THE CENTRAL SCAN COMPARED WITH ACTUAL PROFILE.

ERROR INVESTIGATION

The following items were investigated to discover the reason for the discrepancies in the profiles of LM-4 shown in Figure A1-14.

1. Penumbra effects
2. More accurate measure of sun elevation
3. Refined Phi-Tau equation
4. Film reciprocity
5. Illumination fall-off across the model
6. Phase angle change across the model

Penumbra Effects

The equations upon which the slope analysis is based apply when the illumination is uniform or when we know how the illumination changes within the scene. Figure A1-15 shows details of the penumbra caused by the finite diameter of the sun. When the microdensitometer is tracing toward the sun, the illumination will start to decrease 1/4 degree before the sun elevation angle has been reached. The effect when tracing in this direction is to give an upward slope to the profile at the edge of the penumbra, the magnitude of this slope change will depend upon the length of the shadow, the sun elevation, the spot diameter of the microdensitometer, and the distance between readings.

For LM-4, with the peak of the cone at 4 feet and the sun at 14.3° elevation, the projected length of the shadow at the lunar plane would be 188 inches with the penumbra about 7 inches across (± 3 1/2").

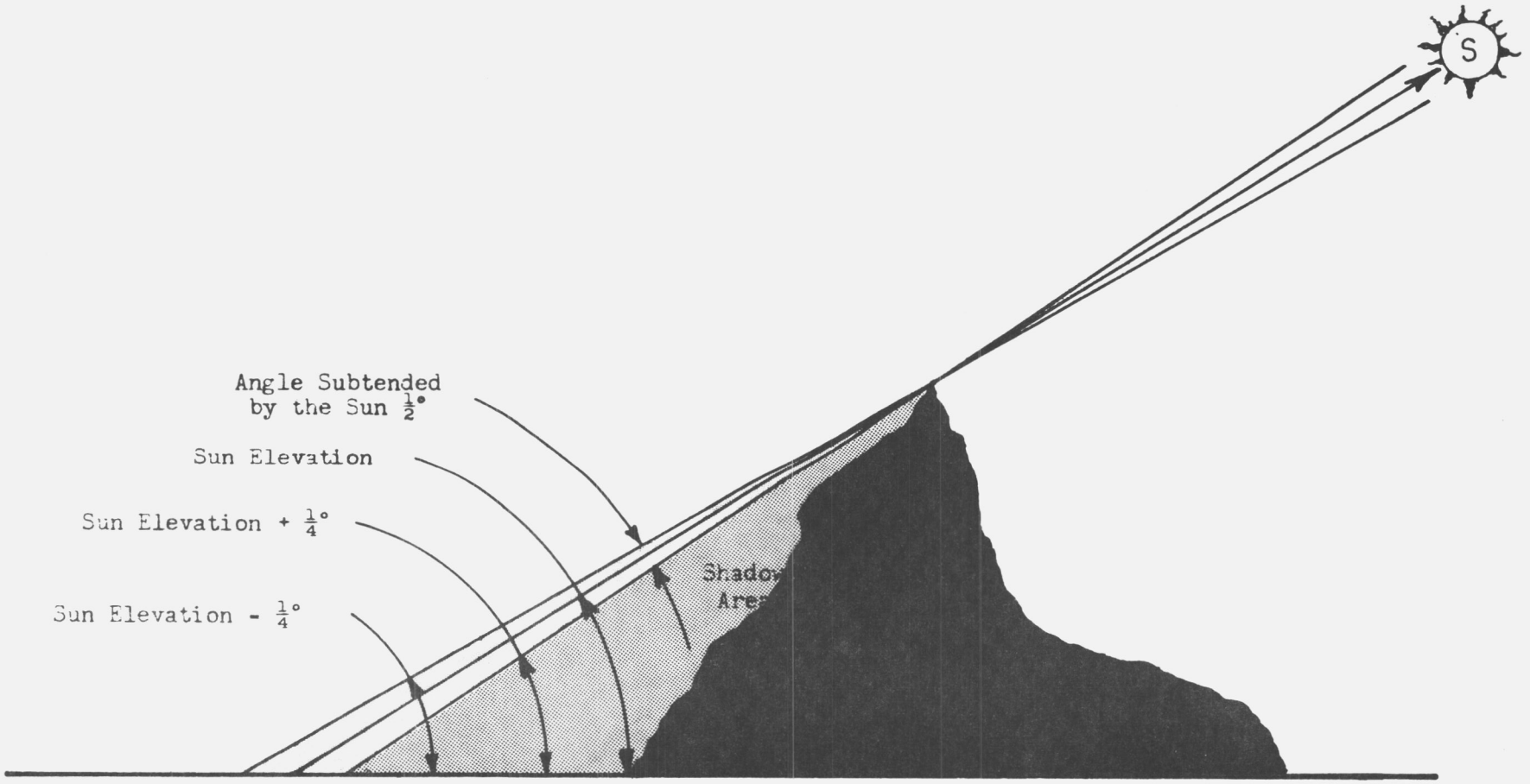

Figure A1-15. DETAILS OF PENUMBRA

For microdensitometer spots 5.1 inches in diameter and 5.3 inches apart, two or three readings will be influenced by the shadow.

A reading computed at 14 degrees for a distance of 5.3 inches would cause an error in elevation of about + .11 foot for the remainder of the trace.

If the microdensitometer scanning spot were reduced in size and spacing to 1/2 the pitch of the limiting tri-bar (0.9 inch), then 8 or 9 density readings will be in the penumbra with 1/2 of them reduced in value and 1/2 increased in value from the readings obtained using a point source.

It is possible by examining the original photograph or the trace to decide on the position of the center of the shadow and reduce this elevation error provided it is certain that the background is flat. If it is not flat, then the uncertainty in the location of the shadow caused by the penumbra will cause an error in the profile elevation along the remainder of the trace.

It has been suggested that the computer recognize the first change in microdensity voltage caused by the penumbra; then using the sun elevation minus 1/4°, the computer would plot the upper edge of the shadow until the sun-lit edge is reached. This would be satisfactory provided the shadow edge were always on a plane level surface. It is probable that the shadow will fall on a surface of changing slope, in which case the correction for the penumbra could cause as much error as we are trying to eliminate.

For the remainder of this study, a value of 0.7° less than the measured sun elevation was used. This empirical value is exactly correct only for projected shadow lengths of 17 feet, with sun elevations of 15° and with the penumbra falling on a level plane. This height calculation is a function of three factors: projected shadow length, sun elevation, and slope on which the penumbra falls. However, experiments Nos. 5, 7, 9 and 11 will show that a correction of - 0.7° can be used for a wide range of spot sizes and spot spacings over the peak of LM-4.

More Accurate Measure of Sun Elevation

The nominal 15° sun elevation was checked for LM-3 and LM-4 with a transit, and found to be 14.3°. The lower actual sun elevations helps to explain some of the error in the profile of LM-4, since a smaller sun elevation will lower the profile and make a better match with the peak of the cone. When the projected shadow length is 188 inches, a change of 0.7° from 14.3° to 15° will make a change of + .21 foot in the elevation of the peak of the cone and the profile.

Refined Phi vs Tau Equation

A refined equation has been generated by the computer from the original data taken for phi vs tau at a nominal phase angle 75° (sun elevation nominal 15°, actual 14.3°). This curve has been considered in two sections as follows:

For phi between 0 and .1881 inclusive, use

$$\tau = 14.48 - .77 \times 10^{2}\,\Phi - .78 \times 10^{3}\,\Phi^{2} + .74 \times 10^{4}\,\Phi^{3} - .55 \times 10^{5}\,\Phi^{4} + .14 \times 10^{6}\,\Phi^{5}$$

and for phi between .1881 and .3267 inclusive, use

$$\tau = 118 - 1630\,\Phi + .57 \times 10^{4}\,\Phi^{2} + .84 \times 10^{4}\,\Phi^{3} - .52 \times 10^{5}\,\Phi^{4} - .32 \times 10^{6}\,\Phi^{5} + .17 \times 10^{7}\,\Phi^{6} - .21 \times 10^{7}\,\Phi^{7}$$

These curves were made from the original observations by a modified least squares method as described in the 5th Bi-Monthly Report. By fitting the curve in two parts, the maximum difference between the observed values and the computed curves is reduced from 0.40 degree with a single equation (page 14, equation 3a) to 0.23 degree using the two equations given above. Figure A1-16 shows the observed and computed values for phi vs tau obtained using these equations.

For phi between 0 and .1881 inclusive, use

$$\tau = 14.48 - .77 \times 10^{2}\,\Phi - .78 \times 10^{3}\,\Phi^{2} + .74 \times 10^{4}\,\Phi^{3} - .55 \times 10^{5}\,\Phi^{4} + .14 \times 10^{6}\,\Phi^{5}$$

and for phi between .1881 and .3267 inclusive, use

$$\tau = 118 - 1630\,\Phi + .57 \times 10^{4}\,\Phi^{2} + .84 \times 10^{4}\,\Phi^{3} - .52 \times 10^{5}\,\Phi^{4} - .32 \times 10^{6}\,\Phi^{5} + .17 \times 10^{7}\,\Phi^{6} - .21 \times 10^{7}\,\Phi^{7}$$

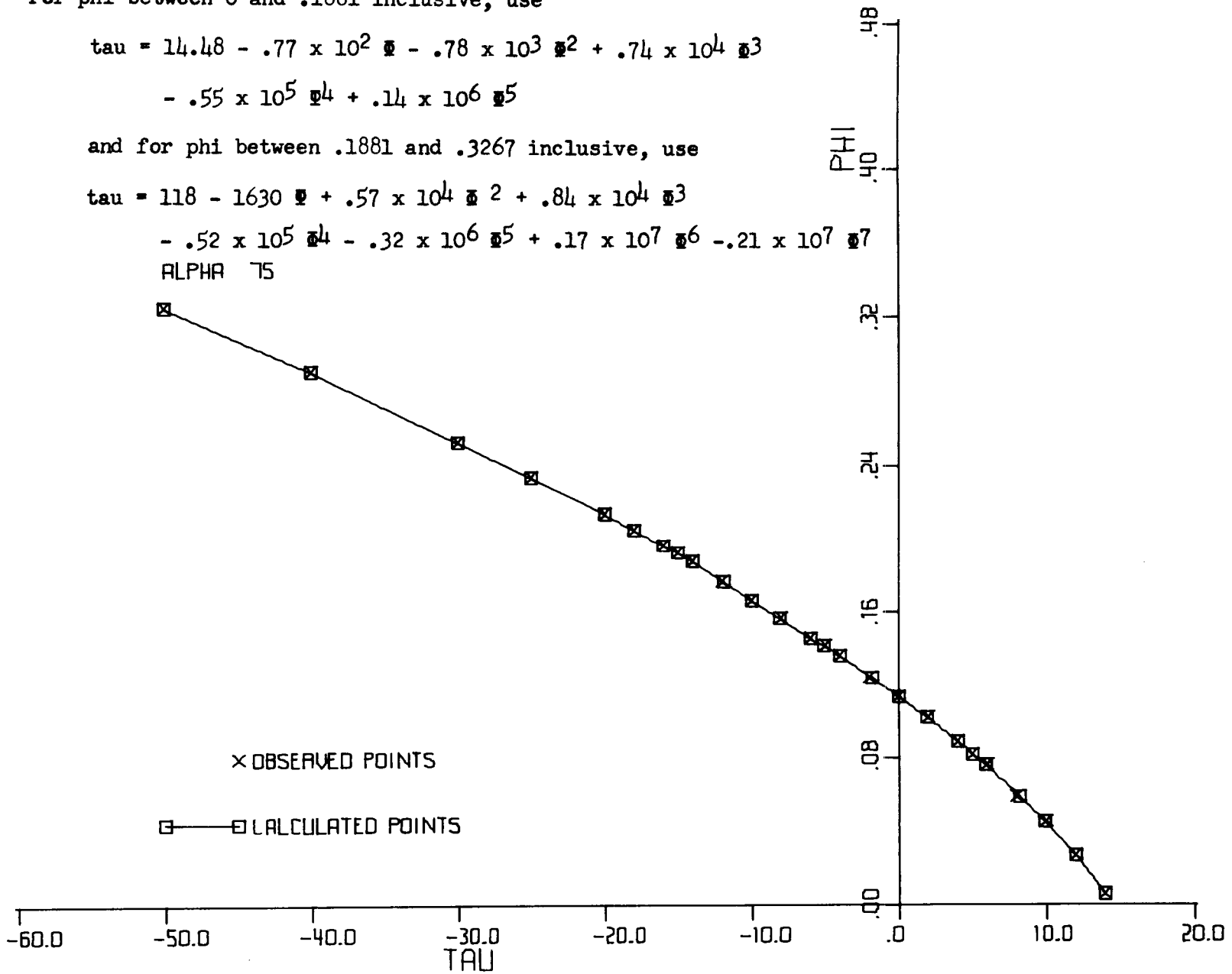

Figure A1-16. COMPUTER PLOT OF OBSERVED AND CALCULATED VALUES FOR THE PHOTOMETRIC FUNCTION OF COPPER OXIDE DUST VERSUS TAU FOR A PHASE ANGLE ALPHA OF 75°

Film Reciprocity

For careful photometric work, the failure of the reciprocity law makes it necessary that gray scale exposures be made at the same exposure time used for the picture exposure.

When mapping LM-3 and LM-4, the sensitometric strips were made with a Kodak Model 60 sensitometer at 1/10 second, while the picture exposures were made at 20 seconds. To check the effect of this difference in exposure time on the photometry, characteristic curves for SO-243 were made at 1/10 second in the Kodak Model 60 sensitometer and at 20 seconds in the Kodak 1B sensitometer; both curves are shown in Figure A1-17. The curve for 20 seconds in considerably slower and has a gamma of 1.4 compared to 1.9 for the 1/10 second curve. The result of this lower gamma is increased lunar slopes for a given density (microdensitometer volts) as shown in Figure A1-18.

As an example of the improvement in mapping accuracy caused by proper allowance for reciprocity failure, the following data compare values derived for LM-3:

	Scaled Lunar Dimension on Model	A		B	
		Mapped Dimension	% Error	Mapped Dimension	% Error
Base Angle					
Shadow Side	6.8°	5.3°	22.	7.0°	3.
Sun Side	6.8°	4.4°	35.	6.6°	3.
Peak Elevation	0.96 ft.	0.71 ft.	26.	0.95 ft.	1.

A - Derived without allowance for reciprocity effect.

B - Derived with proper allowance for reciprocity effect.

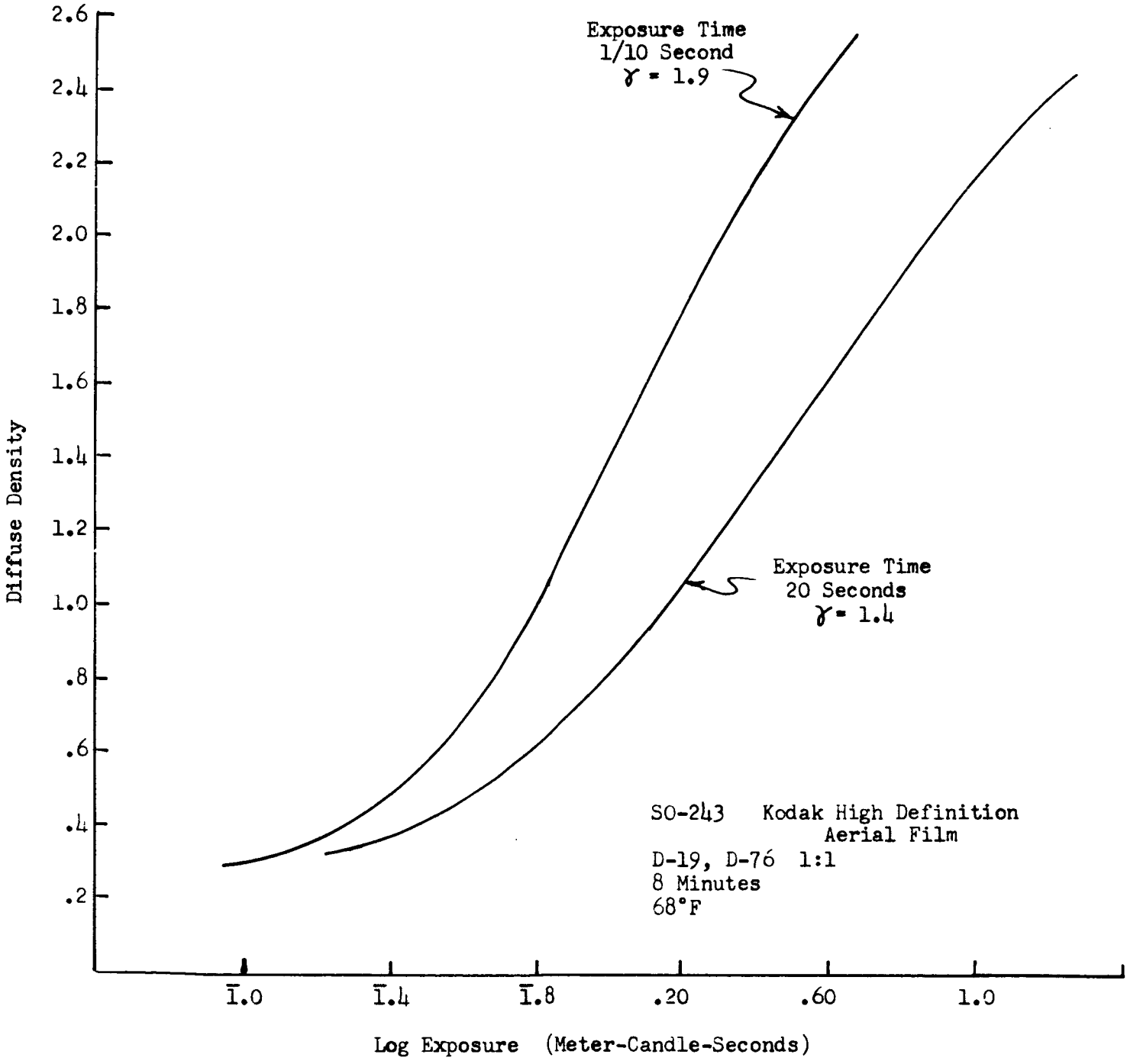

Figure A1-17. CHARACTERISTIC CURVES FOR SO-243 EXPOSED AT 1/10 SECOND AND 20 SECONDS.

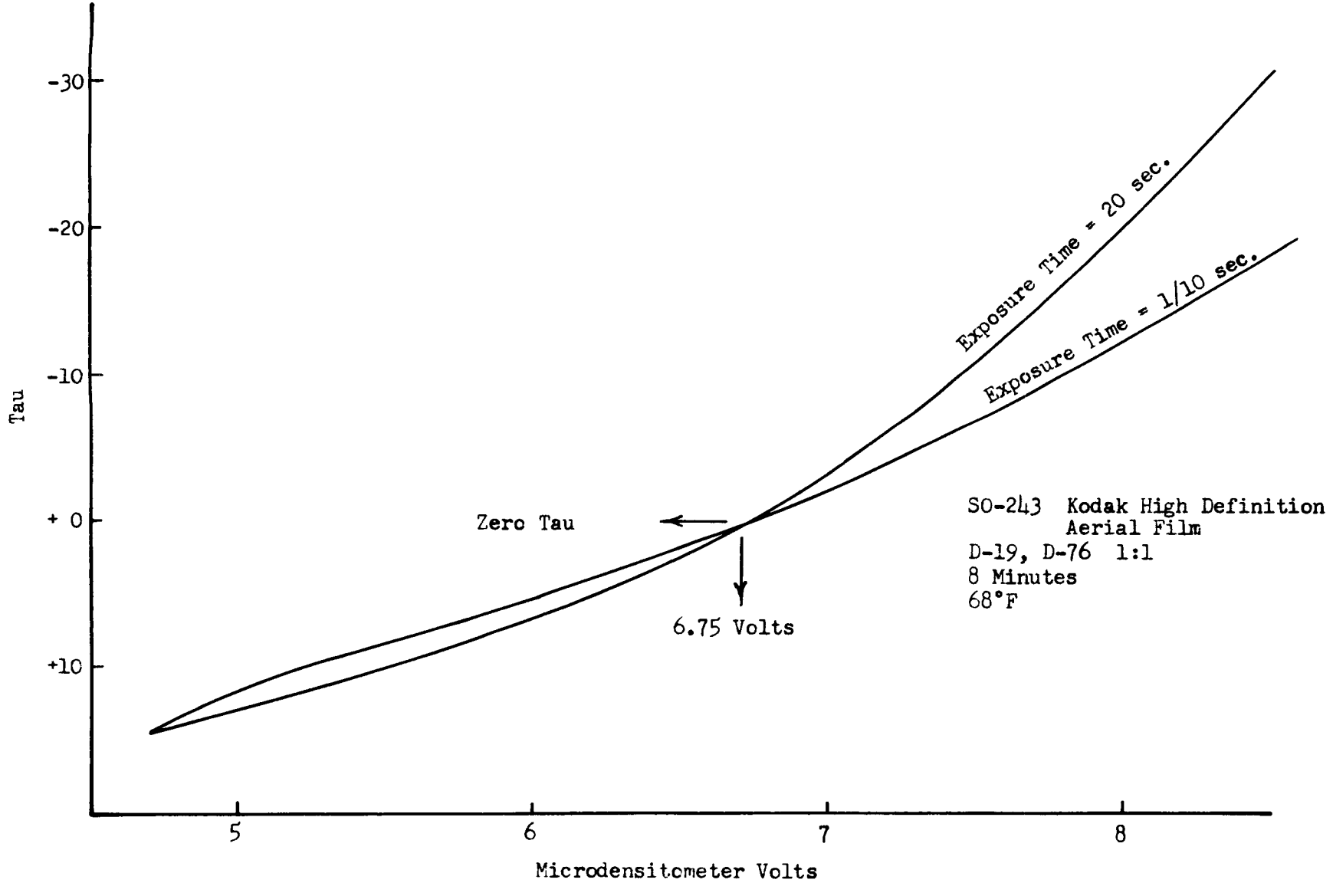

Figure A1-18. MICRODENSITOMETER VOLTS VERSUS TAU CURVE WITH 6.75 MICRODENSITOMETER VOLTS EQUAL TO ZERO TAU FOR SO-243.

The large reduction in error for test B emphasizes the need for careful sensitometry in photoclinometry. However, it is likely that errors as low as 1 to 3 percent may be obtained only when the ground resolution is substantially smaller than the object being measured.

Illumination Fall-Off Across The Model

The light source for photography of LM-3 and LM-4 is placed 18 feet from the center of the model to insure that the 1.9-inch diameter lens will subtend 1/2 degree at the model and simulate the lunar conditions. In contrast to the real lunar situation where the sun can be considered at infinity, in the model when the phase angle becomes large (sun elevation small) the area of the model nearest the light source will receive higher illumination than the center, and the areas further away from the light source will receive less illumination.

The amount of this illumination change can be calculated by determining the ratio of the square of the distance from the point in question to the square of the distance to the center of the model. If we consider only the points in the phase plane containing the center of the model during vertical photography, then the amount of this illumination can be calculated from the following formulas:

$$\frac{I_x}{I_c} = \left[\frac{s_c}{s_x}\right]^2 = \left[\frac{s_c}{s_c - x \cos (90^\circ - \alpha)}\right]^2$$

Where I_x = illumination at the point x

I_c = illumination at the center of the model

x = the distance of the point in question from the center of the model

Plus x is in the direction of the light source

Minus x is in the direction away from the light source

α = Phase angle, the angle between the observer and the light source measured at the center of the model

s_c = Distance from the light source to the center of the model

s_x = Distance from the light source to the point x in the model

This relationship is shown in Figure A1-19 for objects in the phase plane. The illumination of points in phase planes not containing the center of the model can be calculated by taking into account the square of the relative distances as mentioned above.

For the LM-4 model where x is a maximum of ± 4.45 inches, the illumination near the light source is 1.04 times the illumination in the center, and the illumination on the far side of the model is 0.96 times the illumination in

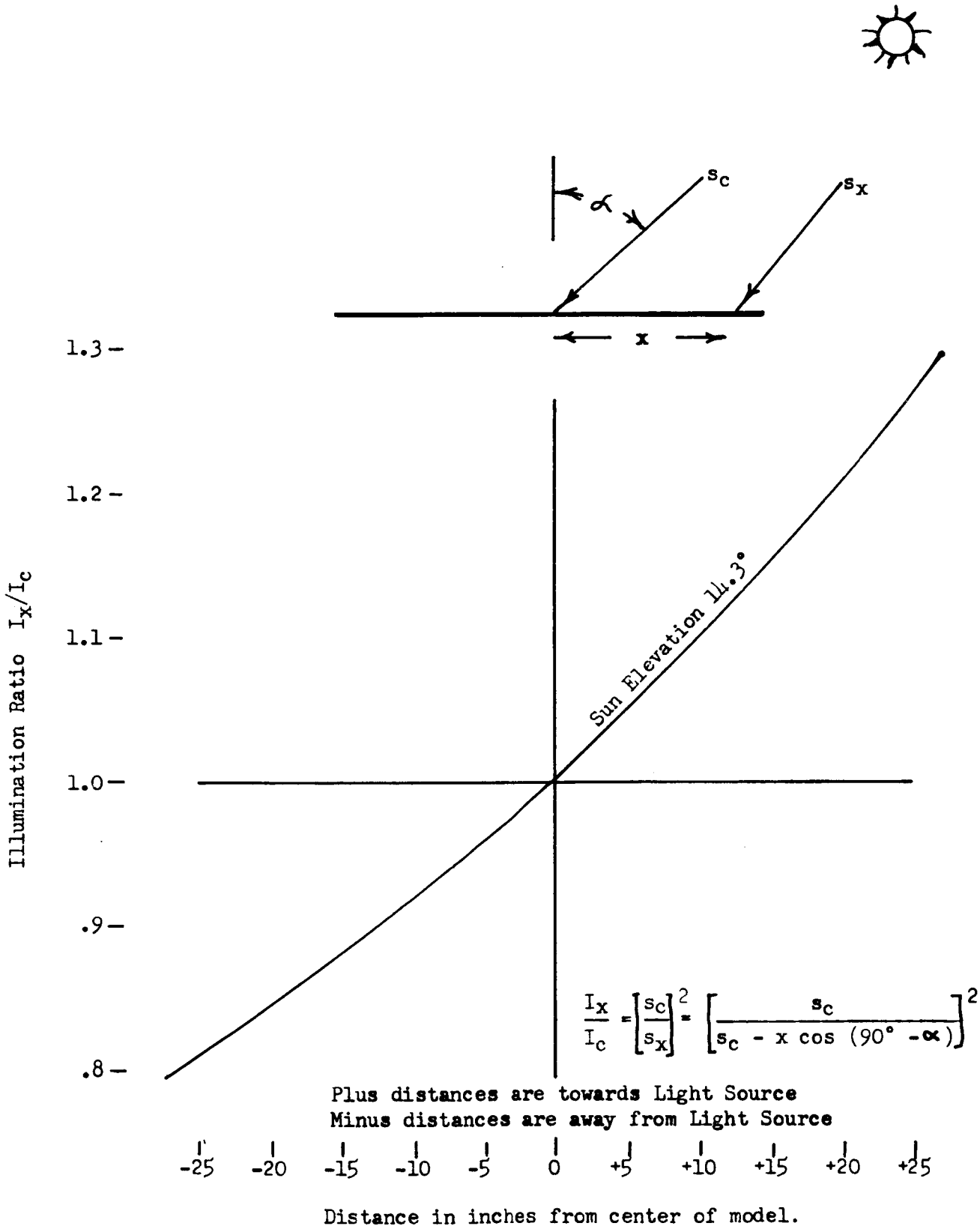

igure A1-19. THEORETICAL ILLUMINATION RATIO FOR DISTANCES FROM CENTER OF MODEL IN THE PHASE PLANE WITH SUN ELEVATION AT 14.3 DEGREES.

the center of the model. This amounts to an illumination change of ± 2 foot-candles from a nominal 44 foot-candles. This corresponds to a Δ log E of nearly ± .02 which will cause a change in slope of about 2° across the background of LM-4. If no correction for illumination fall-off were made, then a flat level surface would appear to be a continuously curved convex surface with a change in slope between the ends of about 2°. An average slope error of 1° would account for about - 0.6 foot in elevation across the 36 feet of mapped surface on LM-4.

An examination of the microdensitometer traces for the background of LM-4 shows an average change in level of about 0.19 volt across the model. This value is equivalent to a change in slope of about 2° in the background area and agrees with the calculated values above.

To account for this illumination fall-off, the computer program has been modified to calculate a new value of A for each microdensitometer reading, depending upon the position of the reading in the trace. In the graphical solution to LM-4 profiles, this is equivalent to sliding the phi-tau curve an amount corresponding to a change in microdensitometer voltage of 0.19/80 for each reading, thereby causing the average background slope to remain level.

Phase Angle Change Across the Model

The phase angle change across LM-4 is + 0.8° in the direction of the sun which amounts to a change in tau of about + 0.8° and has the effect of making the background appear concave. Similarly, the phase angle change away from the sun amounts to - 0.8° and will change the tau angle by - 0.9°, making an over-all error in the background slope of LM-4 of about 1.7° across the model. This change will be included in the light fall-off equation for zero tau angle if it is derived from observed microdensitometer voltage change across a known level slope.

TABLE A1-II SUMMARY OF INVESTIGATED ITEMS

Item	Effect of Profile	Compensation
1. Penumbra Effect	High profile at peak of cone. + 1/2 ft. at 2 ft.	Empirically it was found that a sun elevation .7° lower than the measured sun elevation gave more nearly the correct change in height across shadow area in experiment 4 through 12
2. Sun Elevation Measurement	Shadow too long for assumed sun elevation	Remeasured sun elevation. 14.3° sun elevation was used for both photometric function determination and experiments 3 through 18 (nominal 15°)
3. Refined Phi-Tau equation	Small errors in tau	Improved Phi-Tau curve with 2 sigma error in tau = ± .15°
4. Film Reciprocity	High gamma obtained with incorrect exposure time makes a slope of 7° look like a slope of about 5° in Experiment 3, and a slope of 26 1/2° look like a slope of 18° in Experiment 4.	Use correct exposure times in sensitometer to obtain correct gamma.
5. Illumination fall-off*	Level surface will appear convex unless corrected. Tau angle errors will be less than 2° with parameters used in Experiment 3 through 18. This will cause height errors of about - 1.5 feet in 80 ft. across the model.	Use empirical light fall-off equation to correct for uneven illumination. (This will include correction for phase angle change across the model).

* These errors effect the analysis when utilizing models, but are not factors when analyzing lunar photography of limited angular coverage. Analysis of wide angle lunar photography will need to account for phase angle changes across the scene.

Table Cont'd on Next Page.

TABLE A1-II SUMMARY OF INVESTIGATED ITEMS (Cont'd)

Item	Effect of Profile	Compensation
6. Phase angle change across Model*	Level surface will appear concave unless corrected. Tau angle errors less than ± 1.7° in Experiments 3 through 12, 14, 16 and 18. In Experiments 13, 15 and 17 the tau error will be less than .2°	This error can be neglected if empirical light fall-off equation is used for item 5.

* These errors effect the analysis when utilizing models, but are not factors when analyzing lunar photography of limited angular coverage. Analysis of wide angle lunar photography will need to account for phase angle changes across the scene.

REVISED COMPUTER PROGRAM

The computer program was modified, based upon the above investigation to include these corrections and the LM-4 readings used to make another set of profiles. These are shown in Figure A1-20. The profile made from central trace number 11 is shown in Figure A1-21 with the 26° cone drawn in the proper location and to the correct scale. The error at the right side of the profile is +0.92 foot.

Notice in Figure A1-21 that the length and slope of the shadow bring the peak of the profile to an elevation of 4.27 feet when the actual elevation is 4 feet. Also, the slope of the profile on the sun side is 22.5° where it should be 26.8°, making an additional error in elevation over the 8-foot radius of the cone of +0.7 feet. The difference between 26.8° and 22.5° corresponds to a Δ log E of 0.03 on the camera film. These two errors total +1.0-foot at the end of the profile and explain the major error in elevation. The errors at the end of other profiles in Figure A1-20 are all positive and are proportional to both the amount of shadow traced by the profile and to the steepness of the slopes of the elements encountered.

One possible source of residual error is placement of the model other than exactly perpendicular to the camera axis. For example, if the model were tipped 1 degree away from the sun, then the background would have a tau angle of +1°. The calculated cone elevation would then exactly match the model at the peak and would be within 0.2-foot at the end of the trace.

If the process gamma were actually 1.2 instead of 1.4, the cone angle on the sun side of the model would be 26.8°, exactly matching the slope of the model.

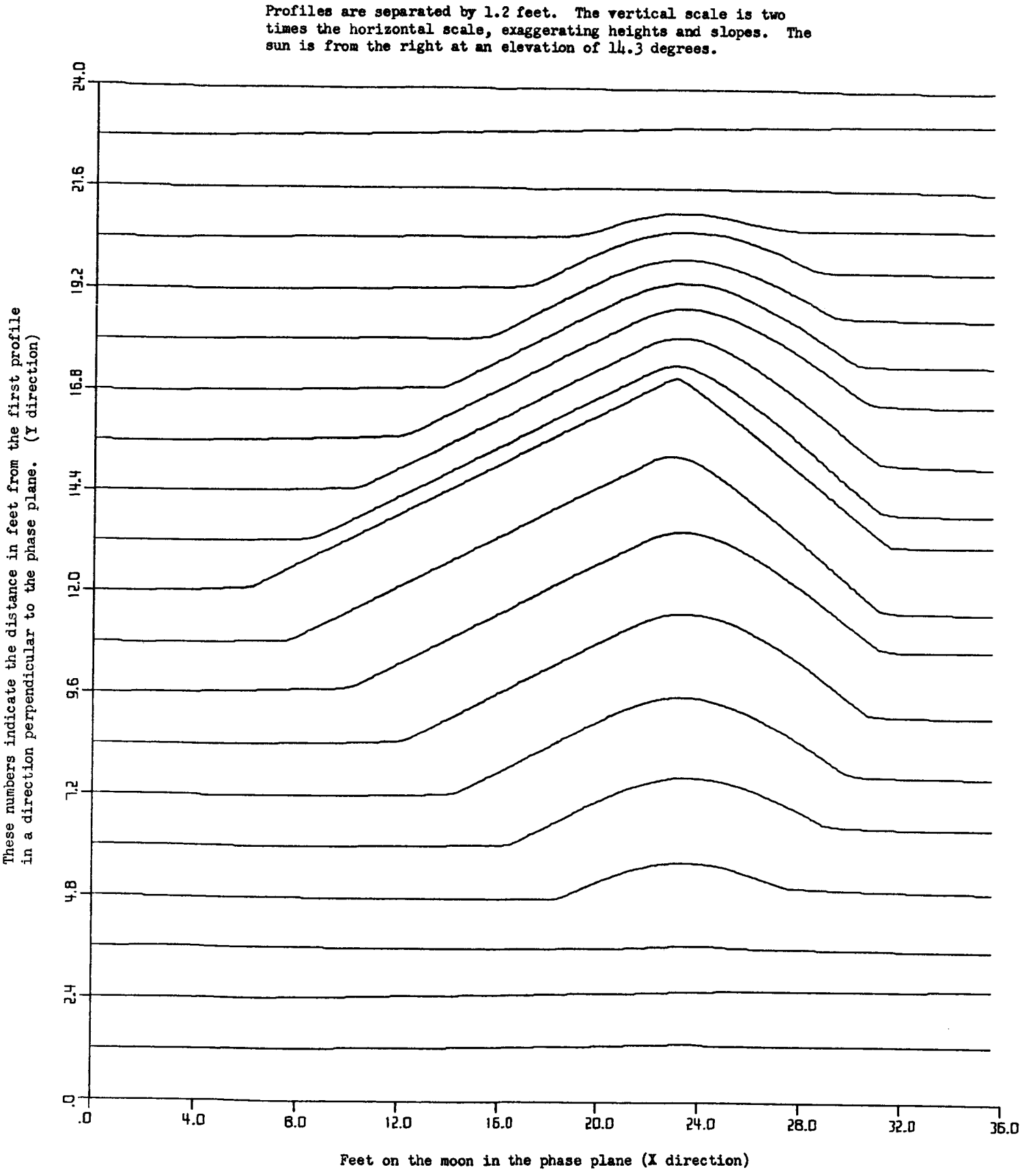

Figure A1-20. LM-4 PROFILES COMPUTED FROM MICRODENSITOMETER SCANS MADE WITH IMPROVED COMPUTER PROGRAM.

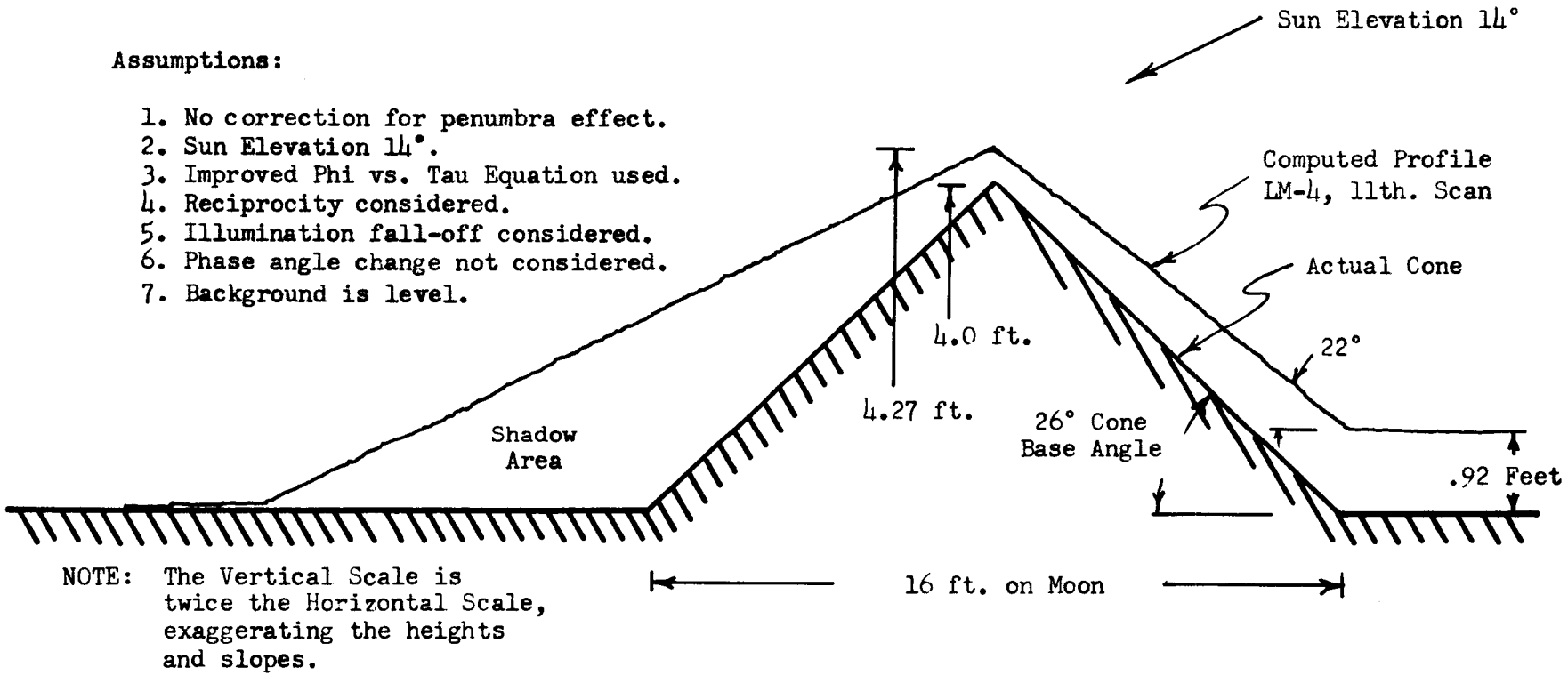

Figure A1-21. LM-4 COMPUTED PROFILE FOR THE CENTRAL SCAN MADE WITH IMPROVED COMPUTER PROGRAM AND COMPARED WITH ACTUAL PROFILE.

The following adjustments were used to derive the profiles in Figure A1-20:

1. No correction was made for the penumbra effect.
2. Sun elevation was 14°
3. Refined phi-tau equation was used.
4. A change of 0.19 volt in microdensitometer output was distributed uniformly throughout each trace to compensate for fall-off in illumination across the model.
5. No compensation made for change in phase angle except that in item (4). Based on the profiles in Figure A1-20, the elevation map shown in Figure A1-22 was generated.

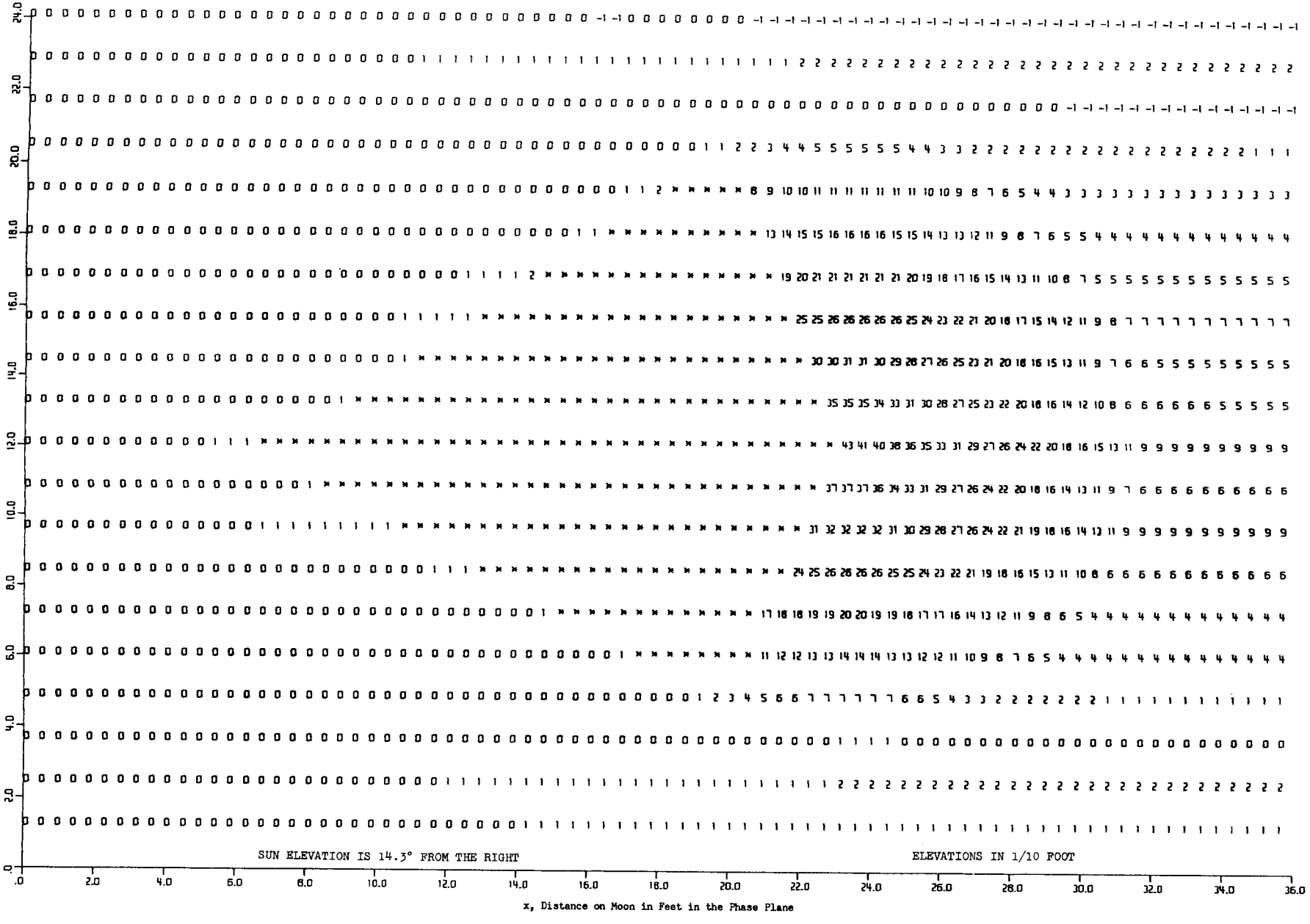

Figure A1-22. ELEVATION MAP MADE FROM PROFILES SHOWN IN FIGURE A1-20

Numbers plotted give elevations in tenths of a foot. Sun elevation is 14.3° from the right.

Calculated Value For A

In the previous analysis A has been calculated from:

$$A = \frac{\Phi}{E}$$

Since there is a flat area in the target, tau is known for a value of microdensitometer voltage, and therefore, E and Φ are known. A values obtained by the computer from this equation during analysis of LM-4 were between 0.132 and 0.0954

A can be computed from the known constants as follows:

$$A = \frac{4N^2}{10.76\ I\rho Tt}$$

For LM-4 these constants have been measured as follows:

I = 44 foot-candles, illuminance

ρ = 0.0565, albedo

T = .89, transmission at center of lens in white light

t = 20 seconds, exposure time

N = f/3.8 measured at a marked f/4.0, lens aperture

$$A = \frac{4 \times 3.8^2}{10.76 \times 44 \times 0.0565 \times .89 \times 20}$$

A = 0.121

If we assume all the terms remain constant except the illumination (I), then the observed variation in A represents the following variation in I:

Computed value of A	0.132	0.121	0.0954
Corresponding value of I (foot-candles)	40.5	44	55

Part of this change, ± 2 foot-candles, can be accounted for by the illumination fall-off mentioned previously. The remainder is due to the other items discussed under Error Investigation.

Experiments No. 5 through No. 12

The odd numbered experiments in this series are traces across the peak of a 26° cone. The even numbered experiments are traces across the level surface beside the cone.

The purpose of these experiments was as follows:

1. Compare the profiles made by the odd numbered experiments that have different spot sizes and spot spacing

2. Compare the microdensitometer traces of the level surfaces made by the even numbered experiments that have different spot sizes and spot spacing and obtain an empirical measure of the light fall-off across the model

3. Compare the microdensitometer traces made of the level surfaces in the paired experiments number 5 & 6, 7 & 8, 9 & 10, 11 & 12, that have the same spot size and spot spacing

4. Determine a procedure for adjusting the profiles for shadow areas and steep slopes

5. Obtain a measure of the calculated tau angle variability with various spot sizes and spot spacing.

All of the traces were made on a single photograph of LM-4 at a lunar scale of 1:2448 (assume the model is 1/48 size, 1 inch on the model = 4 feet on the moon). The cone is 4 inches in diameter representing a 16-foot diameter cone, 4-feet high. Appendix I lists the parameters and associated microdensitometer tracing parameters for these experiments.

The following sections detail the studies from Experiments No. 5 through No. 12.

Tracing Parameters

Table A1-III lists some of the tracing parameters projected on to the lunar surface.

TABLE A1- III

MICRODENSITOMETER TRACING PARAMETERS FOR

EXPERIMENTS No. 5 THROUGH No. 12 PROJECTED TO THE LUNAR SURFACE

Experiment Number	Pitch P feet	Spot Size d feet	Spot Spacing x feet	d/p	x/p	O/x	$(2d/p)^2$
5	0.073	0.0514	0.0445	0.70	0.61	360	1.41
6	0.073	0.0514	0.0445	0.70	0.61	-	1.41
7	0.073	0.132	0.134	1.81	1.84	119	13.1
8	0.073	0.132	0.134	1.81	1.84	-	13.1
9	0.073	0.425	0.445	5.8	6.1	36	116
10	0.073	0.425	0.445	5.8	6.1	-	116
11	0.073	1.04	0.445	14.3	6.1	36	812
12	0.073	1.04	0.445	14.3	6.1	-	812

P = Pitch of the limiting high contrast tri-bar
d = Spot diameter
x = Spot spacing
O = Object size - 16 feet in diameter

The ratio d/p in these experiments varies from 0.70 to 14.3. Very little information concering the object can be obtained by searching the film with

spot sizes smaller than 1/2 pitch of the limiting high contrast tri-bar; therefore, d/p should not be smaller than 1/2. The larger the ratio of d/p the smaller is the influence of film grain on the variation of density measurement, and therefore, the smaller the variation we should expect in the calculation of tau.

Except for experiments No. 11 and No. 12, the ratio of d/p and x/p are about the same, since the spot diameter and the spot spacing are nearly the same. Experiments No. 11 and No. 12 have a spot size considerably larger than the spot spacing. The area covered by each scanning spot therefore overlaps nearly one half of the area of the previous spot.

The ratio of object size to spot spacing (O/x) can be compared to the D/P ratio described in previous work under this study, where D is the diameter of an 8:1 crater and P is the pitch of the limiting high contrast tri-bar. Note that this ratio needs to be at least 10* to visually indentify 95 percent of the craters at a sun elevation of 15°. Extrapolating from the visual data, we might assume that at least 10 independent measurements are needed across the diameter of a lunar object for 95 percent identification. In the odd numbered experiments of this photoclinometry study O/x is at least 36, giving 36 independent measurements across the diameter of the 26° cone. This number is adequate to describe this cone in considerable detail.

The last column of Table A1-III is a ratio of the area of the microdensitometer spot to the area of the smallest useful spot. (The smallest useful spot is defined as one having a diameter of P/2.) These ratios have been selected to be nearly 1, 10, 100, 1000. The larger this ratio becomes, the smaller the influence that grain will have on the density measurements and the larger the lunar object must become before it will be adequately described by the microdensitometer trace.

*Figure D3-8, Page 120, Final Report Lunar Photo Study, NAS9-3826.

To Summarize the Tracing Parameters: These experiments have d/P larger than 1/2 and O/x larger than 36. In the first six experiments the spot size is nearly the same as the spot spacing, the last two experiments have a spot size twice as large as the spot spacing.

General Procedure

The data from the microdensitometer was analyzed and the following input given to the computer:

1. Experiment Number
2. Run Number
3. Number of Scans
4. Number of spots per scan
5. Sun direction
6. Sun elevation
7. Shadow - Microdensitometer volts representing film base plus fog
8. Spot spacing in feet on the moon in the phase plane (x)
9. Initial value of X, where X is feet on the moon in the phase plane
10. Scan spacing in feet on the moon at right angles to the phase plane (y)
11. Initial value of Y
12. Initial height of each trace
13. Microdensitometer voltage vs exposure table
14. Equation for light fall-off across the model
15. The number of points to be considered at the end of the trace that will be used to determine the mean height (Experiments No. 5 through No. 12 only).

While most of these items are self explanatory, items 2 and 5 require some explanation. In these experiments an empirical approach was used to adjust the profiles to fit the model. Profiles were computed a number of times with small changes in one or more of the parameters. A new run number was assigned for each computation and the computer input data recorded under that run number.

Item 5 is a record of the direction of the sun with respect to the trace. All traces must be made in the phase plane, so the trace is made either toward or away from the sun. The computer program was made for traces running into the sun. If the trace is made away from the sun the data points must be reversed for correct height calculation across shadow areas.

The computer calculates a lunar profile according to the following procedure from the input data:

1. Compute a profile from the observed parameters
2. Observe the errors
3. Determine adjustments necessary
4. Make the adjustments or changes in the parameters
5. Recompute a new profile (new run)
6. Repeat item 2 through 5 until a satisfactory fit is obtained.

The correction or adjustments and their effect on the profile are described in the following paragraphs.

Correction For Light Fall-Off Across Model

Figure A1-23 shows an ideal microdensitometer trace across the peak of a 26° cone with a sun elevation of 15°. In the lower part of the figure a profile of the cone is shown along with an ideal computed profile. No

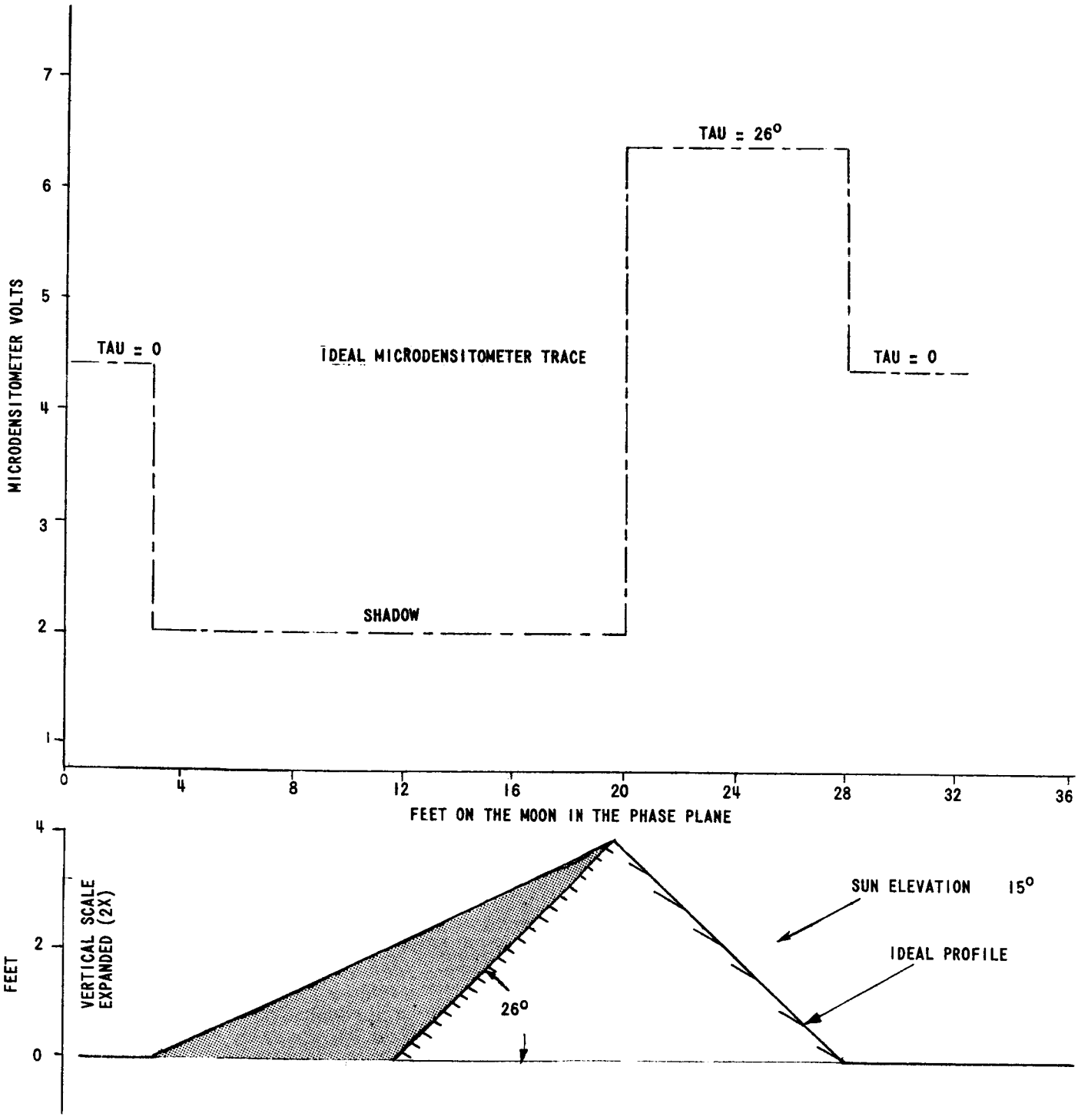

Figure A1-23. IDEAL MICRODENSITOMETER TRACE ACROSS THE PEAK OF A 26° CONE AND LUNAR PROFILE

light fall-off across the model is present in this ideal trace.

Figure A1-24 shows the microdensitometer scan across the peak of the 26° cone for experiment 5. It will be noticed that the background has a higher voltage (density) at the end of the trace than at the beginning because of the change in distance of that part of the model from the light source. Compensation for this change has been accomplished by setting the value of microdensitometer volts for zero degrees tau according to the equation:

$$V = 5.5 + 0.4\ X/35.6$$
$$= 5.5 + 0.0112\ X$$

where V = microdensitometer volts

X = feet on the moon in the phase plane

This equation, which was written from inspection of the trace, has been drawn in Figure A1-24 to show the relative position of zero tau angle. It is used by the computer to find A, the ratio of phi to exposure. If A is too large, the background as well as the slopes near zero will be tipped toward the sun (more negative slopes). If A is correct, then the slopes near zero will be calculated correctly.

Along the left side of Figure A1-24 is a scale of tau values obtained from the adjusted sensitometry used for experiment No. 5, run 3. The profile in the lower portion of Figure A1-24 was made from the run 3 data.

It is interesting to draw lines of constant tau values on a plot of microdensitometer voltage vs feet on the moon. This has been done in Figure A1-25 for this experiment using the sensitometric data of experiment No. 5, run 3. The lines of constant tau are nearly straight and parallel, but

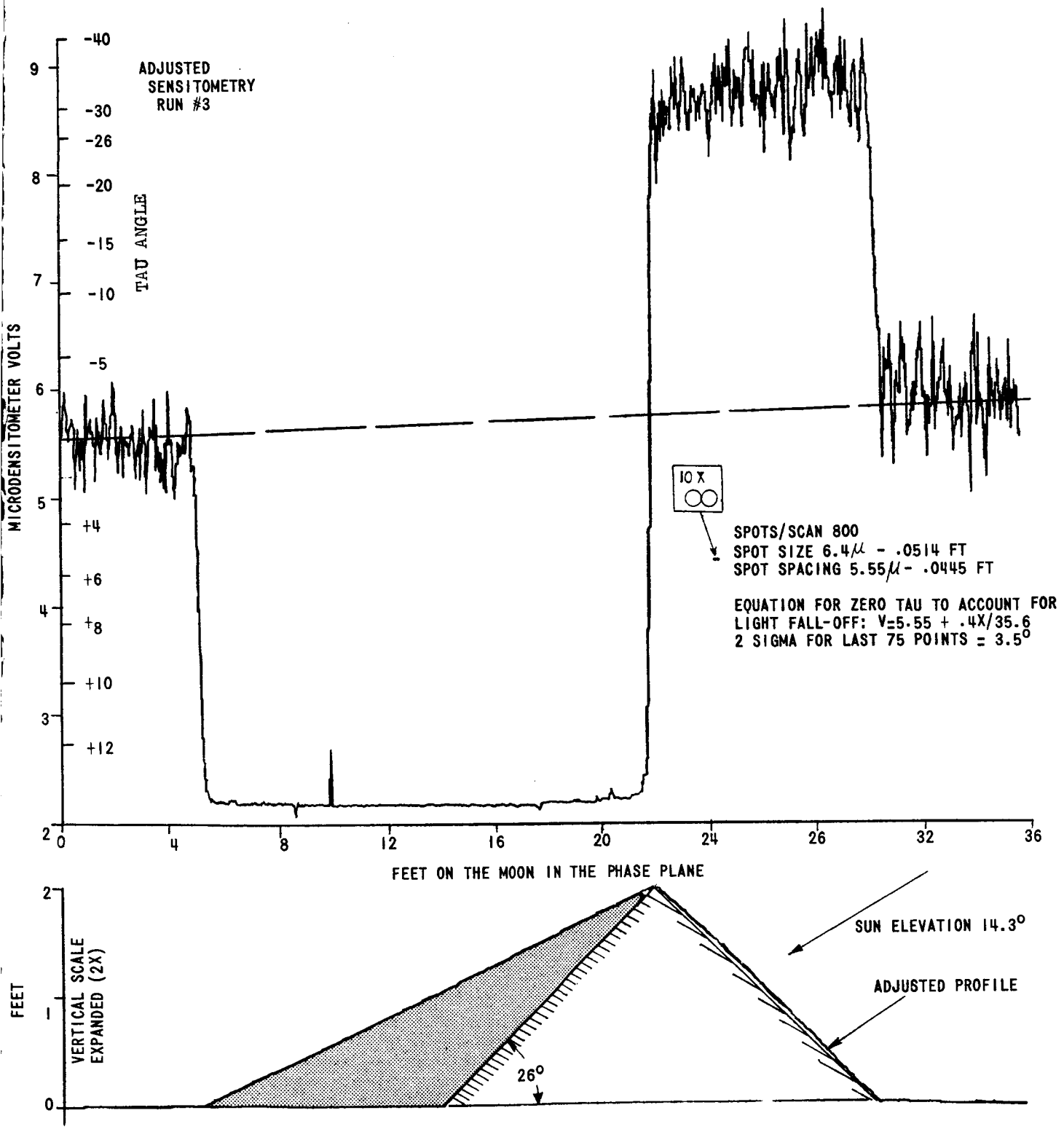

Figure A1-24. EXPERIMENT 5, RUN 3, MICRODENSITOMETER TRACE AND LUNAR PROFILE - 26° CONE

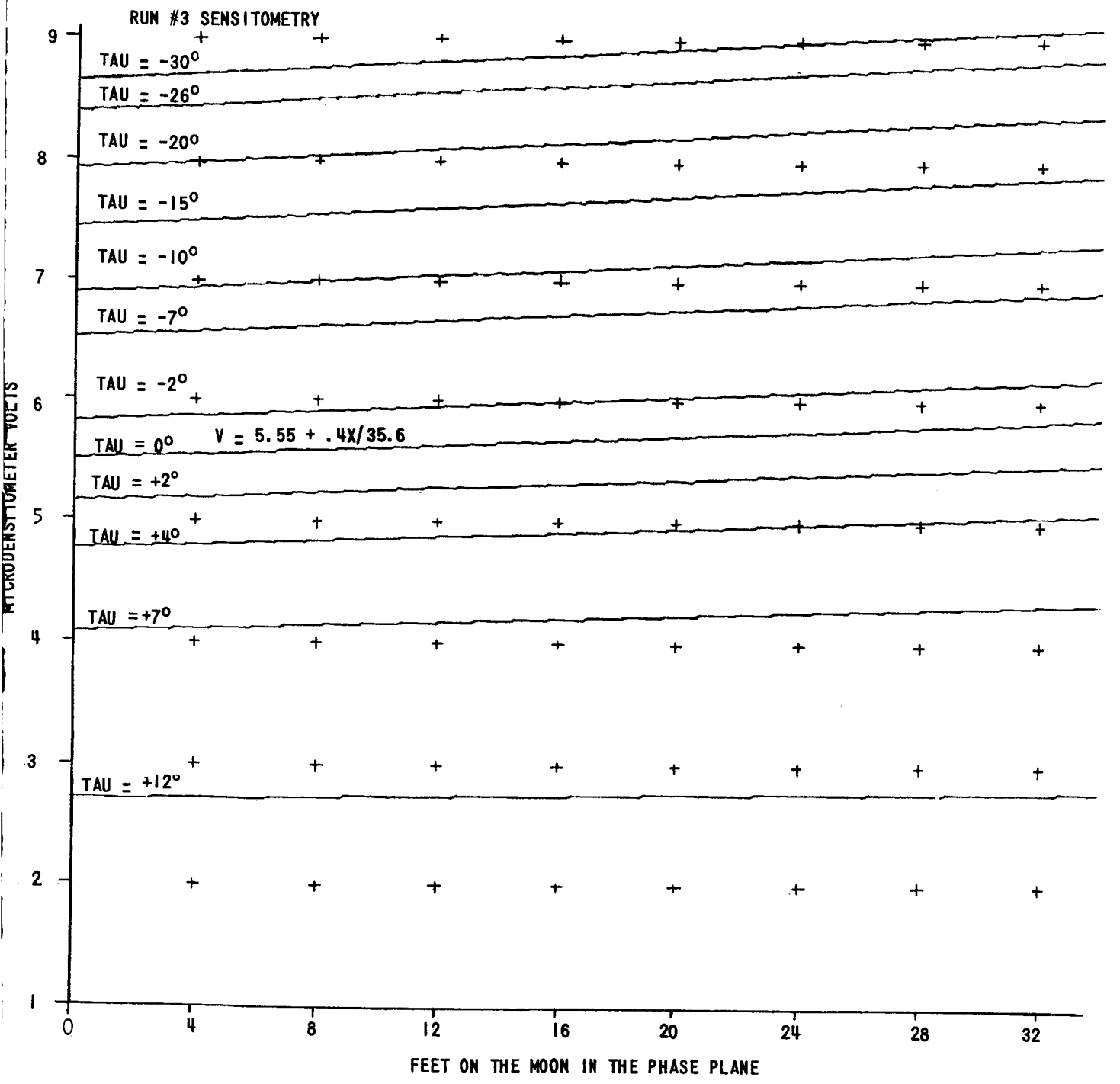

Figure A1-25. CALCULATED TAU VALUES PLOTTED ON THE MICRODENSITOMETER VOLTAGE VS. LUNAR DISTANCES COORDINATES WITH EXPERIMENT 5, RUN 3 SENSITOMETRY

they do spread apart as the X distance increases. This expansion between lines of constant tau values shows the effect of change in illumination across the model because of the finite distance of the light source. The equation for light fall-off across the model for each experiment has been included in the figure with the corresponding microdensitometer trace. A knowledge of this distortion will help to understand the photoclinometry of our simulated lunar models. Photoclinometry of actual lunar photographs will not have this distortion.

Correction For Penumbra And Shadow

The profile transition from the level surface to the shadow area is shown in Table A1-IV with the experiment No. 5, run 3 data.

In this experiment, nine measurements were made in the penumbra area compared to the theoretical 13 (See Table A1-IV). This difference means that there was insufficient light at the last four points to give a density above the fog level. The other experiments show a similar gradual change through the penumbra area.

TABLE A1-IV

COMPUTED TAU ANGLES AND ADJUSTED HEIGHT*

VALUES IN THE PENUMBRA AREA

Horizontal Distance, X Feet	Computed Tau Angle Degrees	Computed Adjusted Heights* Feet	Values for Theoretical Point Source Sun at 13.6° Altitude	
			Tau Angle Degrees	Height Feet
4.98	1.9	0.024	0	0
5.03	3.6	0.026	0	0
5.07	7.1	0.032	0	0
5.12	8.3	0.038	0	0
5.16	9.9	0.046	0	0
5.21	11.4	0.054	0	0
5.25	12.4	0.064	0	0
5.30	12.7	0.074	0	0
5.34	13.5	0.085	13.6	0.011
5.38	13.4	0.095	13.6	0.022
5.42	13.6**	0.106	13.6	0.033

* Adjusted Heights for these experiments are described in the following sections.

** After the density reaches the low value of base plus fog, the computer is instructed to use the given sun elevation for computing the profile. This point was reached at X = 5.42 feet.

Empirically it was found that if the computer used a sun elevation of 13.6° to trace the profile in the shadow area, the correct elevation change was obtained from the start of the penumbra to the peak of the cone. These data are shown in Table A1-V for photography under a 15° sun elevation.

TABLE A1-V

COMPUTED PEAK OF THE PROFILE FOR

EXPERIMENTS 5, 7, 9 and 11: ACTUAL HEIGHT = 4 FEET

Experiment Number	Run Number	Computed Peak height - feet	Profile height*	A
5	3	4.00	0.0094	13
7	4	4.04	0.0007	4.3
9	7	3.95	0.0028	1.3
11	5	3.97	0.0046	1.3

*At start of penumbra X = 3.8 feet

A = Theoretical number of microdensitometer measurements made in the penumbra. The penumbra of a point 4 feet high with 15° sun elevation is about 0.583 foot when projected onto the level surface; therefore:

$$A = \frac{0.583}{\text{Spot Spacing}}$$

The height of the peak will depend not only upon the sun elevation but upon the profile height calculated by the program up to the penumbra and on how well the program handles the penumbra area. Column 4 in Table A1-V shows that the profile is near zero at X = 3.8 feet just before the penumbra.

The value of 13.6° for the sun elevation was used to make the profiles in Figures A1-24, A1-26, A1-27 and A1-28 even though it is 0.7° less than the measured sun elevation of 14.3°.

Height Adjustment For Steep Slopes

In the odd numbered experiments it was soon discovered that the computer profile for the steep 26° slope with the original sensitometry was in error by about -7°. This gave a change in height from the peak to the base of the cone of about 2.6 feet where the correct value is 4 feet. (See Table A1-VI, Column 3.) This profile is a simple geometric shape with a uniform slope that should be a straight line, nearly independent of the rest of the parameters. It therefore offers an opportunity to study the effects of small changes in the parameters given to the computer to correct or adjust the profile to give the correct slope. A program that will compute slopes correctly for level surfaces and steep slopes will be likely to compute the shallow slopes quite accurately. The following paragraph describes the methods that were investigated to reduce the errors in slope and change in height.

The two methods used for this investigation are: (a) adjust the curve of microdensitometer voltage vs exposure to reduce the final elevation of the profile to a value near zero and (b) make a proportional adjustment in height to each measurement of the profile to bring the remaining elevation error to zero. This last method is a standard procedure in Civil Engineering as it distributes the error of closure proportionately throughout the profile. Table A1-VI lists the computed heights of the last points for the odd numbered experiments No. 5 through No. 11. The third column shows the final height of the profile at the last point of the trace before any adjustment has been made.

Since the profile in these experiments should return to zero for the last several feet, a slight adjustment was made to the microdensitometer vs exposure

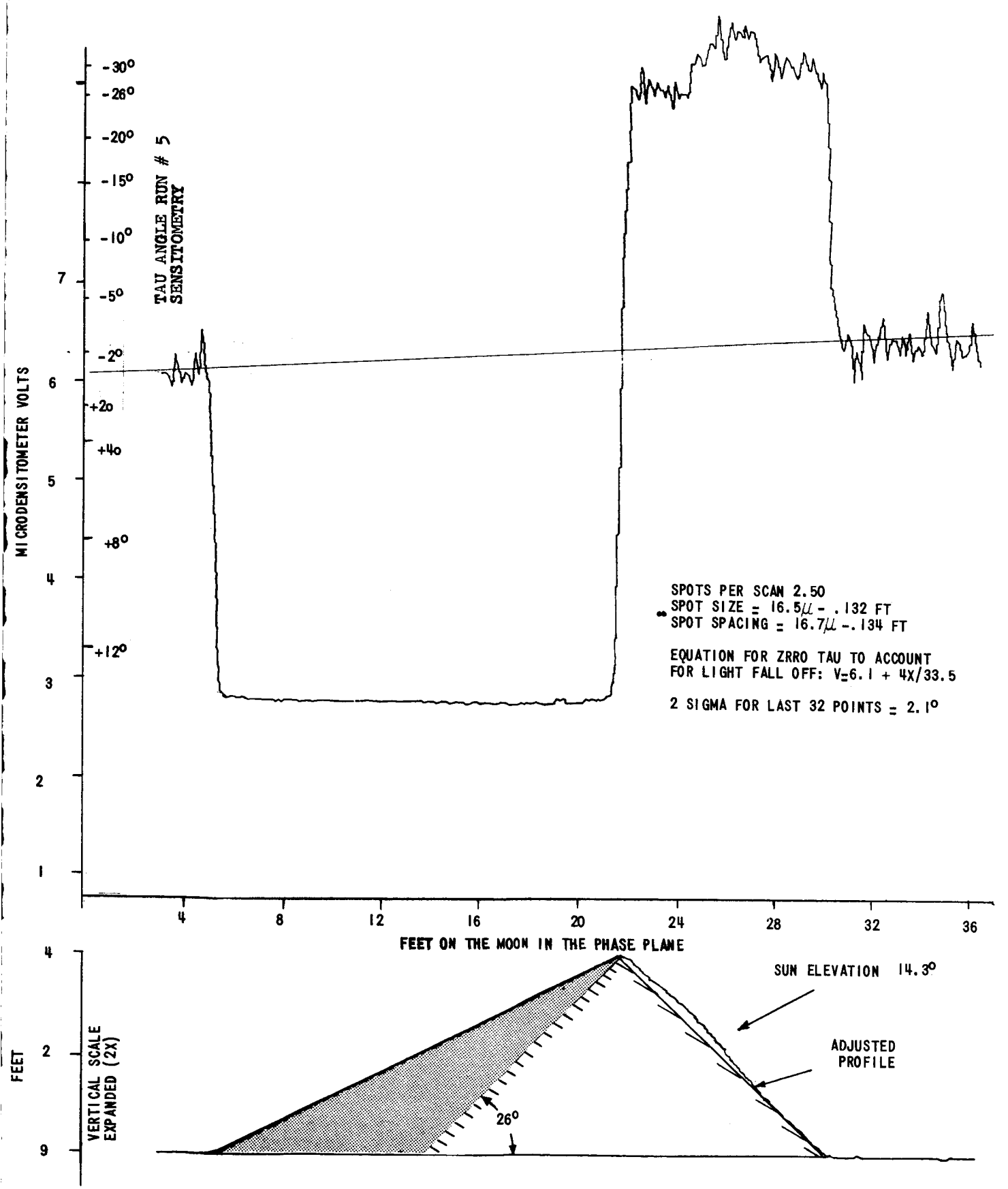

Figure A1-26. EXPERIMENT 7, RUN 4 MICRODENSITOMETER TRACE AND LUNAR PROFILE - 26° CONE

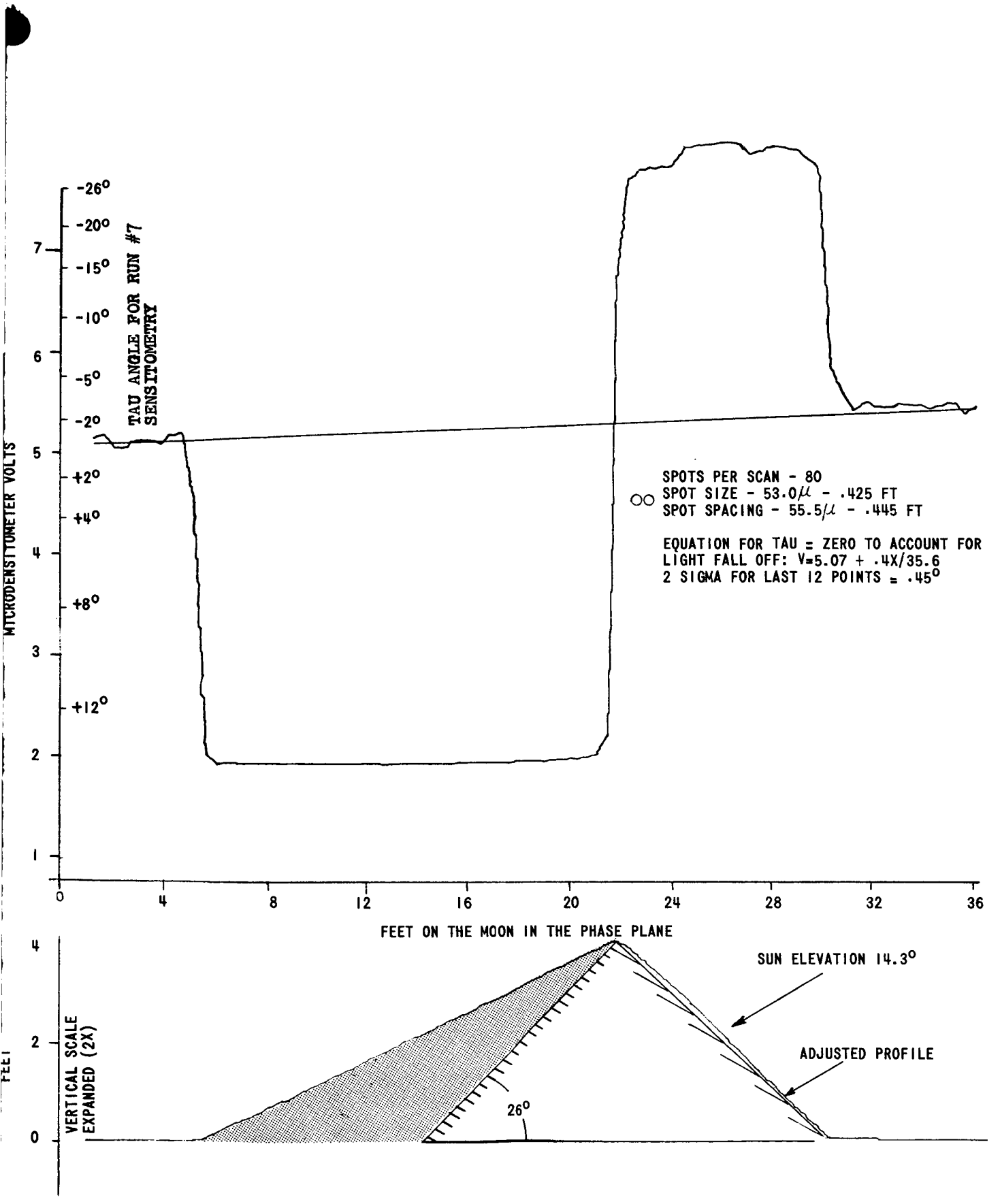

Figure A1-27. EXPERIMENT 9, RUN 7, MICRODENSITOMETER TRACE AND LUNAR PROFILE - 26° CONE

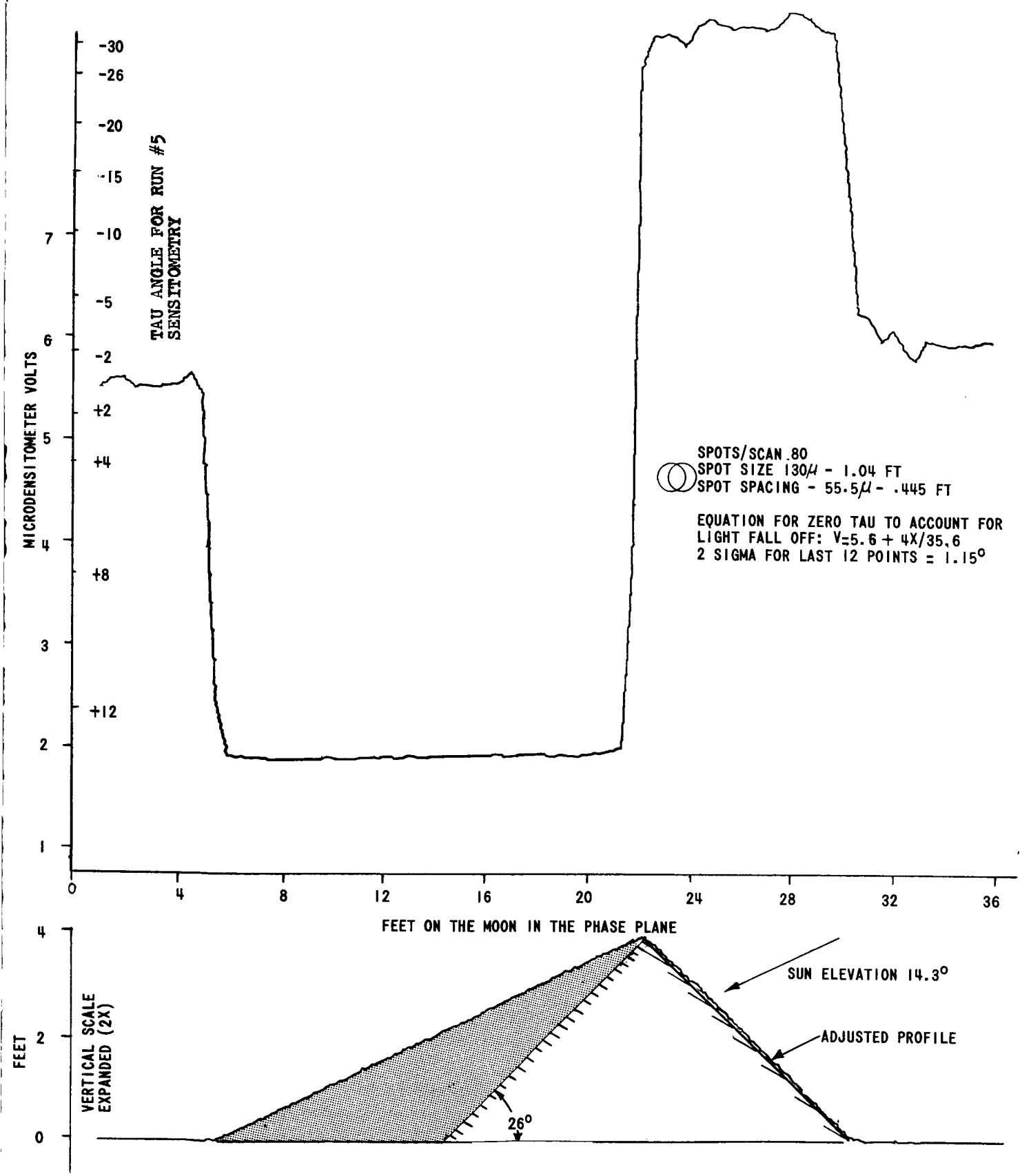

Figure A1-28. EXPERIMENT 11, RUN 5, MICRODENSITOMETER TRACE AND LUNAR PROFILE - 26° CONE

curve and the profile re-computed to bring the last several feet to zero. This adjustment was made empirically by moving the curve of microdensitometer volts vs exposure a slight amount in the high density area to increase the calculated slope, and force the change in profile height at the steep slope position to be nearly 4 feet.

TABLE A1-VI

COMPUTED HEIGHTS OF THE LAST POINTS FROM EXPERIMENTS 5, 7, 9 and 11

VALUES WITH ADJUSTED SENSITOMETRY

Experiment Number	n Points per Scan	Unadjusted* Height of the Last Point, feet	Run Number	** Δlog E	Hn Height of Last Point, feet	$\bar{H}$ Mean Height, feet	Number of points considered***	Ha_n Final**** Residual Height of Last Point feet
5	800	+1.36	3	+.024	.117	.114	75	.004
7	250	+1.39	4	+.041	-.033	-.026	32	-.006
9	80	No data	7	+.040	.103	.096	12	.007
11	80	+1.19	5	+.034	.154	.114	12	.010

Equation for adjusting the height by the error of closure method (all data in feet):

$$Ha_i = H_i \pm \left| \bar{H} \ (x_i/x_n) \right| \quad \text{where } i = 1, 2, 3....n$$

Ha_i = adjusted height with error of closure included

H_i = computed height with sensitometry adjustment included

$\bar{H}$ = mean of H_i over level lunar surface for the points considered

x_i = horizontal position on the moon in the phase plane

x_n = last horizontal position of the trace.

---

* From original sensitometry before any adjustment

** Δlog E required in the sensitometry curve, in the region of high density, to reduce H_n to a low value

*** In determining the plane near the end of the trace

****With error of closure adjustment included

For example: The Δ log phi between 0° tau and 26° tau with an alpha of 75.7 is 0.1263. Therefore the Δ log E between the exposure of the background and that for the 26° slope will also be 0.1263. The difference in microdensitometer voltage in experiment No. 5 between the background and the 26° slope is about 3.2 volts or a Δ log E of 0.1023 with the original sensitometry curve (run 1). By bending the curve for the higher microdensitometer voltages by an amount Δ log E = 0.024, the derived profile will very nearly match the 26° cone (run 3). The lower portion of the curve remains unchanged. Table A-VII gives the values for exposure used in run 1 and run 3 and the Δ log E changes.

TABLE A1-VII

MICRODENSITOMETER VOLTS VS EXPOSURE FOR EXPERIMENT No. 5

Micro-D Volts	Run 1 Exposure	Run 3 Exposure	Δ log E
2.15	.05	.05	0
2.46	.15	.15	0
4	.53	.53	0
5	.79	.79	0
6	1.07	1.07	0
7	1.40	1.40	0
8	1.74	1.79	.012
9	2.13	2.25	.024
10	2.59	2.80	.034

Run 1 gives an average slope of about 18 1/2 degrees and a change in height from peak to base of 2.6 feet. Run 3 gives an average slope of nearly 26° and a change in height from peak to slope of about 4 feet.

These tests emphasize the reduction in sensitivity to change in slope at large negative tau angles compared to the sensitivity in the region of zero tau. For example:

Data from Experiment No. 5, run 3 show -

Near tau values of:	ΔTau/ΔV
+13°	3.4°/Volt
0°	5.9°/Volt
-28°	14.8°/Volt

This is also evident by inspection of the tau scales at the left of Figures A1-24, A1-26, A1-27 and A1-28.

This experiment shows that determination of steep slopes will be very sensitive to the shape of the sensitometric curve. Changes similar to those shown in Table A1-VI were made in the microdensitometer curves in experiments Nos. 7, 9 and 11 to investigate the amount of Δlog E required to match the 26° cone profile. These values are shown in Table A1-VI column 5, and the final height, H_n, obtained by this adjustment is shown in column 6. A comparison of column 6 with column 3 shows the improvements made by this technique.

$\bar{H}$ in Table A1-VI, column 7 is the mean height of the adjusted profile over the final number of points listed in column 8. The mean height was used in the final height adjustment made by the error of closure method by proportioning the mean height error throughout the profile according to the equation under Table A1-VI.

Ha_n in column 9 is the final residual height of the last point of the trace with adjustment in sensitometry and in error of closure. The values for Ha_i have been used to plot the profiles in Figures A1-24, A1-26, A1-27 A1-28.

A comment should be made concerning the theoretical accuracy of the measurements near the peak of the cone with various size scanning spots. A very small spot will measure only one small narrow element of the cone.

As the spot becomes larger it will include more of the elements around the side of the cone that have either higher or lower values of the photometric function depending upon the position of the measuring spot with respect to the sun.

Integration of these elements within the measuring spot on the element of the cone toward the sun will cause a low density to be recorded and a low slope to be calculated. As the spot moves away from the peak it will tend to measure a single element with a slope equal to the base angle of the cone. The effect of this error on the 26° cone profile is to make the profile rounded near the peak and to calculate a smaller change in height than the true change in height.

Profile Comparison

Figures A1-24, A1-26, A1-27 and A1-28 show the microdensitometer trace and lunar profile for experiments Nos. 5, 7, 9 and 11. Noted on each figure are the following data:

1. The microdensitometer trace made with the tracing parameters listed
2. A scale of tau angle values made from the adjusted sensitometry at X = zero
3. A calculated profile made from the adjusted sensitometry with the error of closure included in the calculations
4. The size of the scanning spot and spot spacing
5. The number of spots per scan
6. The equation for zero tau angle to account for light fall-off across the model
7. Sun direction and elevation angle
8. A measure of the variability in tau angle in the level areas.

In Figure A1-29 the profiles for all the odd numbered experiments are shown together. These profiles were made on the Calcomp Plotter using the adjusted heights data. These profiles are essentially four straight lines that are determined by only three parameters - the level surface near the cone, the sun elevation, and the 26° slope. These parameters are shown in Table A1-VIII along with the effect they have on the profile and the most sensitive correction or adjustment used to bring the profile into its correct shape.

Each straight section of the profile is nearly independent of the others making it possible to establish the base line, then establish the height to the peak, and finally to bring the 26° slope into its proper position by the adjustment techniques described.

With small corrections to the computer input data, a profile can be generated that is a very close match to the 26° cone at a sun elevation of 14.3° for a wide range of spot sizes and spot spacings within the bounds of the parameters of these experiments.

It should be noted that this experiment is concerned with an object that is large with respect to the spot sizes and spaces considered, and that the elements measured are straight lines with surface normals in the phase plane. Later experiments will consider more complicated surfaces with elements that have normals out of the phase plane and with object sizes approaching the size of the scanning spot.

Comparison Of Traces Over A Level Surface

Figure A1-30 shows the microdensitometer trace across the level surface made in the even numbered experiments Nos. 6, 8, 10 and 12. Under each trace is a table that shows the number of spots per scan, the spot size and spot spacing, the equation for light fall-off across the model, the sensitivity to change in tau angle with change in voltage, and a 2-sigma value for tau angle.

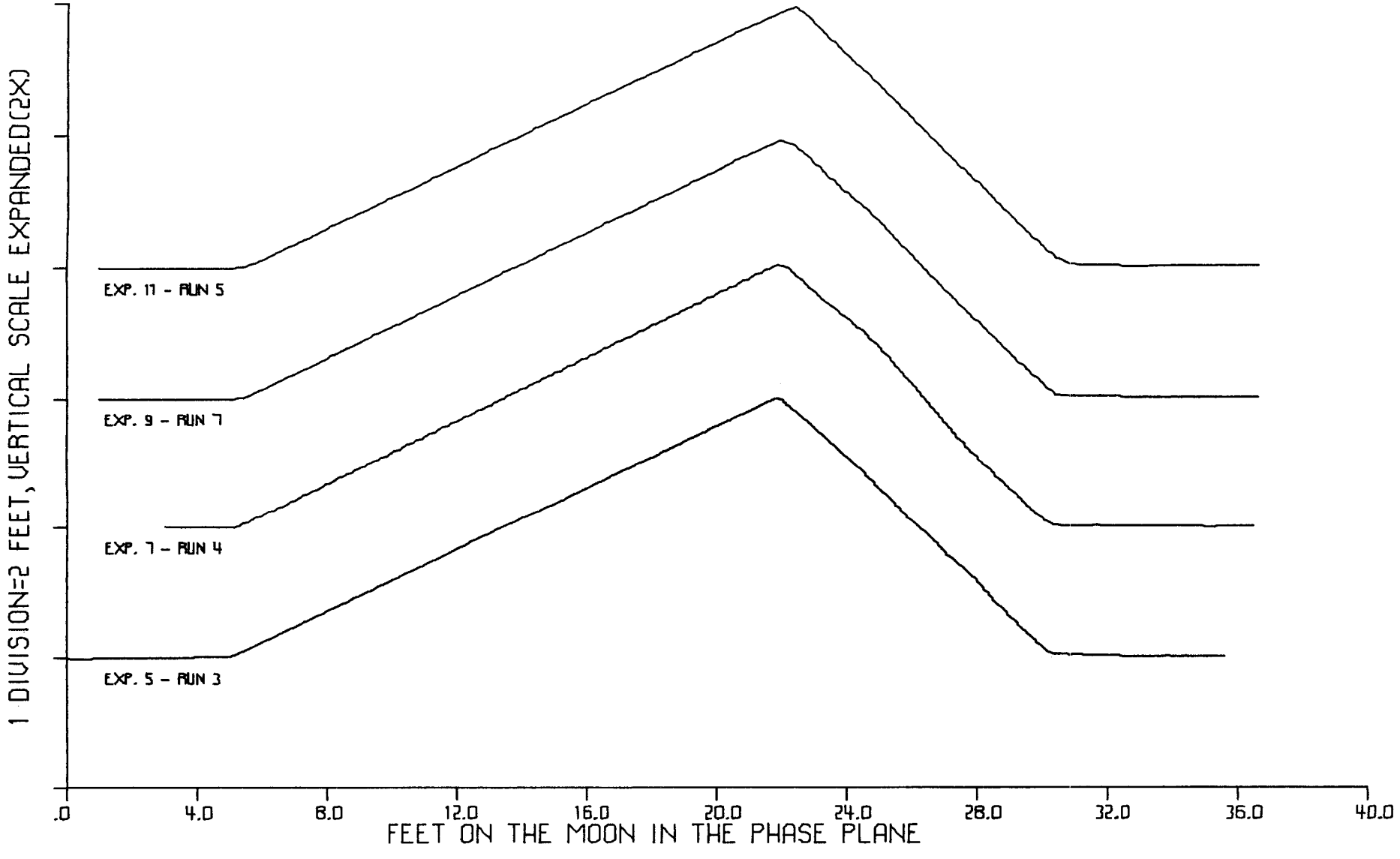

Figure A1-29. PROFILES MADE WITH CALCOMP PLOTTER FROM EXPERIMENTS 5, 7, 9 AND 11.

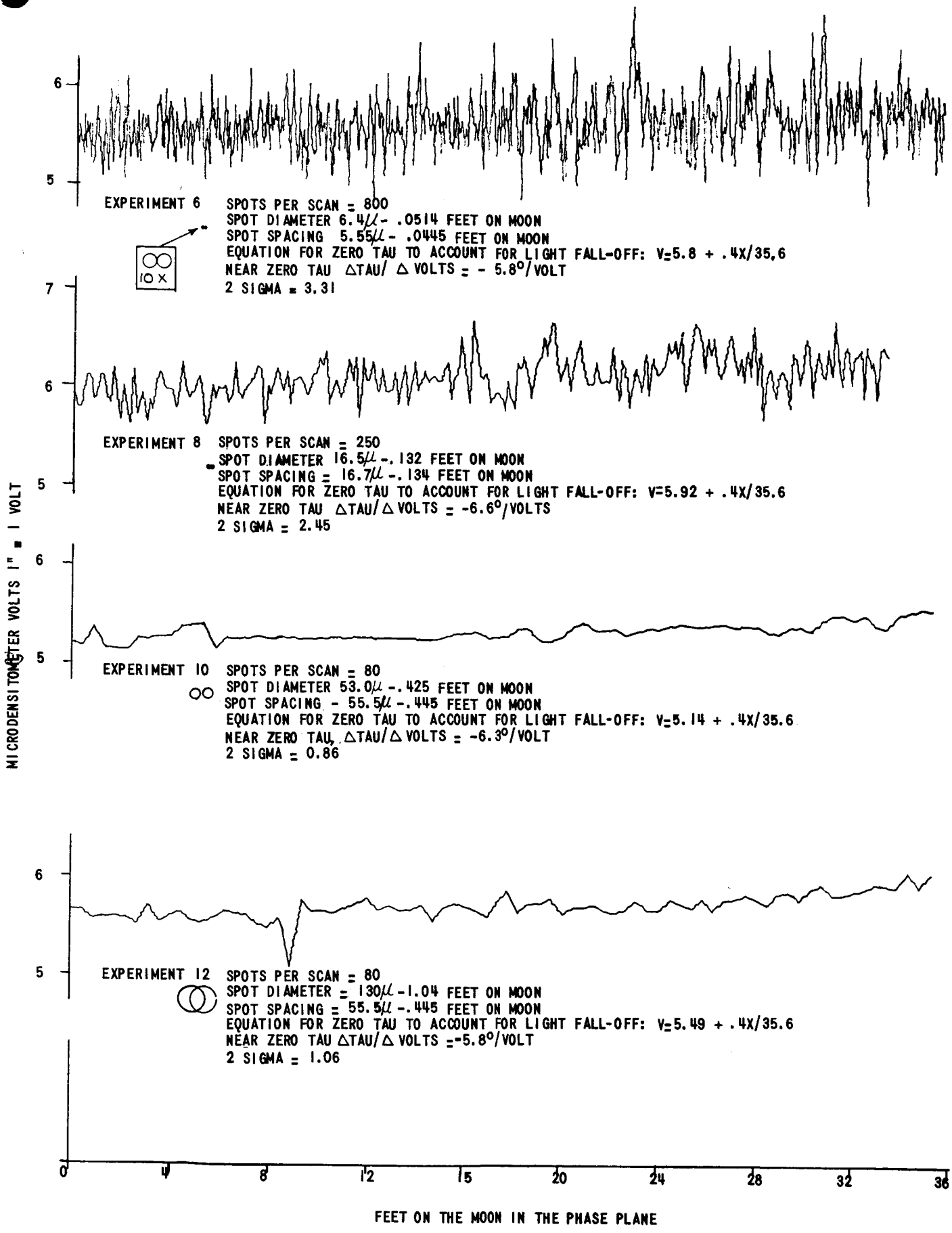

Figure A1-30. EXPERIMENTS 6, 8, 10, 12 MICRODENSITOMETER TRACES FOR FLAT SURFACES WITH TRACING PARAMETERS AND CALCULATED STATISTICAL DATA

TABLE A1-VIII

FACTORS EFFECTING THE PROFILE ACROSS

THE PEAK OF A 26° CONE

Factor	Use in Making Profile	Method of Adjustment
1. Level surface near the cone	Needed to establish zero tau Corrects for light fall-off across model. Measure variability in tau angle.	Write equation for zero tau + light fall-off by inspection of microdensitometer trace or by computer.
2. Sun elevation	Determines height from penumbra to peak of cone.	Empirically varying sun elevation provided to computer.
3. 26° slope	Determines height from peak to base of cone.	Empirically varying the sensitometry for high density

The equations for light fall-off were made by inspection of the trace, but they compare favorably with computed values obtained from a least squares curve fit for a first degree equation. For example, in experiment No. 6:

Curve obtained by inspection

(1) $V = 5.48 + .0112\ X$

Curve obtained by computer using a least squares curve fit

(2) $V = 5.52 + .009\ X$

The curve obtained by inspection starts a little lower (5.48 rather than 5.52 at X = 0) but has a steeper slope. The effect on the profile of using this equation is to make a level surface slightly concave if the computed equation (2) describes a level surface; in this case the error is about 0.2° in tau and less than 0.05 foot in height. The curve obtained by inspection is of adequate accuracy for this experiment.

Table Al-IX shows the 2-sigma values for tau angles for experiments Nos. 5 through 12. The last several points of the odd numbered experiments have been included in this table for completeness. Column 8 and 9 list the minimum and maximum unadjusted heights and column 10, (E), is the sum of these values. E shows the excursion of the profile, i.e., in experiment No. 6 the height of profile is within a range of 0.086 foot for its entire length. From a comparison of E for the four experiments it is evident that the 2-sigma values for tau do not have a direct correlation with the profile errors.

Variations in density using the small spot in experiment 6 produce a large variation in calculated tau angle. The larger spot used in experiment No. 10 is not influenced by grains in the film and shows much smaller variation in calculated tau angle but no improvement in total variation of the profile. In experiment No. 6 the spot spacing is 1/10 that of experiment No. 10; even though the variation in tau is greater, the computed profiles are very nearly the same.

TABLE A1-IX

VARIATION IN CALCULATED TAU ANGLE AND

PROFILE LIMITS FOR EXPERIMENTS 5 THROUGH 12

Experiment Number	Run Number	Spot Size feet	Spot Spacing feet	Number of Points Considered	± 2 Sigma Variation in Tau °	d/P	Unadjusted Height		
							Min. feet	Max. feet	E feet
5	3	0.051	0.0445	75	3.54	0.70			
6	1	0.051	0.0445	800	3.31	0.70	-0.082	+0.004	0.086
7	4	0.132	0.1339	32	2.09	1.80			
8	1	0.132	0.1339	250	2.45	1.80	-0.003	+0.076	0.079
9	7	0.425	0.445	12	0.46	5.8			
10	1	0.425	0.445	80	0.86	5.8	-0.047	+0.056	0.103
11	5	1.04	0.445	12	1.15	14.3			
12	1	1.04	0.445	80	1.06	14.3	-0.028	+0.022	0.050

E = Sum of the maximum and minimum values of height, or the total excursion of the profile in feet.

When mapping a known uniform surface, a small spot with small spot spacing, even though it has a large 2-sigma value, can produce a surface profile very much like that from a large spot with larger spot spacing that integrates the density better and has a smaller 2-sigma value.

Conclusion From Experiments No. 5 Through No. 12

1. Corrections and adjustments must be made to the original data to obtain accurate lunar profiles of a 26° cone when the sun elevation is 15°.

2. The base line (tau = 0) of the profile of a 26° cone is sensitive to the ratio (A) of the photometric function (phi) to the exposure (E). If A is too large, the background as well as all of the slopes near zero will be tipped toward the sun.

3. The shadow line of the profile is best calculated by giving the computer a sun elevation 0.7° less than the measured sun elevation. This correction is a function of shadow length, slope of the surrounding plane, sun elevation, shadow edge texture etc., and will require more investigation before a good empirical formula can be derived.

4. When using the original sensitometry, the sunlit slope of a conical profile calculated nearly 7° less than the model slope. The sensitivity to slope change is lower at large negative tau angles than it is in the region of zero tau angle.

5. With small corrections to the computer input data, a profile can be generated that is very close match to the 26° cone at a sun elevation of 14.3° for a wide range of spot sizes and spot spacing within the bounds of the parameters of these experiments.

6. Mapping a uniform surface using a small spot with small spot spacing can produce a surface profile very much like that from a large spot with a large spot spacing. The small spot, however, has a large 2-sigma value, while the large spot integrates the density better and has a smaller 2-sigma value.

Experiments No. 13 and No. 14

Purpose

Experiment No. 13 was the first attempt in this study to make a lunar map with photo system A, the simulated LOP photo system. The model was LM-3, a 4-inch diameter 7° cone representing a 16-foot 7° cone on the lunar surface. The scale, resolution, and contrast simulate a positive record from the GRE for a high resolution picture from Lunar Orbiter.

The purpose of experiment No. 14 was to make a lunar map of the model used in experiment No. 13 but from pictures taken by photo system B. These images have slightly better original resolution, larger original film scale and slightly lower contrast. In system B the original negative was analyzed. Values for these parameters and those for experiments No. 15 and No. 16 are listed in Appendix I. The latter experiments are described on pages 99 to 111.

Photography and Scanning Experiment No. 13

The original photography for experiment No. 13 was taken on Kodak Special High Definition Aerial Film Type SO-243 film at a scale of 1:74,450. The film was processed in D19-D76 for eight minutes at 68°F. From this negative a positive 7.2x enlargement was made on Kodak Aerographic Duplicating Film Type 5427 processed in D-76 for six minutes at 68°F. The over-all measured gamma in the area of interest is 2.1. This value compares favorably with

the over-all gamma of 2.3 for LOP.

The film was scanned with the microdensitometer and the voltage values punched into IBM cards. Each card holds 18 readings, a scan number, and a card number. At the completion of the scanning operation the deck of IBM cards was sent to the computer programmer along with the necessary calibration data.

The positive photo record made in experiment No. 13 showed considerable flare since it is an enlargement of a very small image with clear surround. To minimize the effect of this flare, the first six spots and the last nine spots of each scan were rejected. Only 25 spots were analyzed by creating a new deck of cards with the 7th through the 31st spot of each scan retained. This reduced the profile to 27 feet from the original 43 feet.

Analysis and Computer Input Experiment No. 13

The instructions to the programmer included the following:

1. All items in Appendix I marked with an asterisk
2. Deck of IBM cards with microdensitometer voltage readings for experiment No. 13
3. Data from Table A1-X

TABLE A1-X

MICRODENSITOMETER VS EXPOSURE DATA FOR EXPERIMENT No. 13, POSITIVE PHOTO RECORD

μD Volts	Density 5427	Density SO-243	Step No. on 5427	Log E SO-243	E SO-243
9.90	2.02	0.45	10	$\bar{1}$.91	0.8128
7.65	1.71	0.58	9	0.15	1.413
5.60	1.38	0.73	8	0.30	1.995
3.57	1.07	0.88	7	0.45	2.818
1.91	0.78	1.04	6	0.59	3.890
0.50	0.54	1.19	5	0.72	5.248

Using a modified least squares curve fit for the data of Table A1-IX a fourth degree equation was found relating microdensitometer voltage to exposure on the SO-243 film. This curve, used in the computer program to calculate profiles, expresses the photometry of the two-stage photographic process.

The graphical solution for obtaining tau angle from microdensitometer volts from a positive record is shown in Figure A1-31. The computer can easily multiply the required input values for the fundamental equations without using logarithmic forms.

4. Phi-tau equation for the photometric function of copper oxide dust with a phase angle of 75.7° (sun elevation 14.3°)
5. Equation for zero tau angle to account for the light fall-off across the model. $V = 4.4 - 0.0259\ X$
   where V is microdensitometer volts and X is the distance in feet on the moon in the phase plane from the start of the trace. Since the first and last spot are on a level surface, this equation is a straight line connecting the mean of the 1st spot and the mean of the last spot for all 28 scans.
6. Position of the scans - Scan separation is 1.07 feet measured at right angles to the phase plane.
7. Procedure for obtaining profiles from a positive photo record.

Traces and Profiles Experiment No. 13

Figure A1-32 shows three of the 28 microdensitometer scans and the profiles made from these three scans. Scan 19 was made across the peak of the 7°

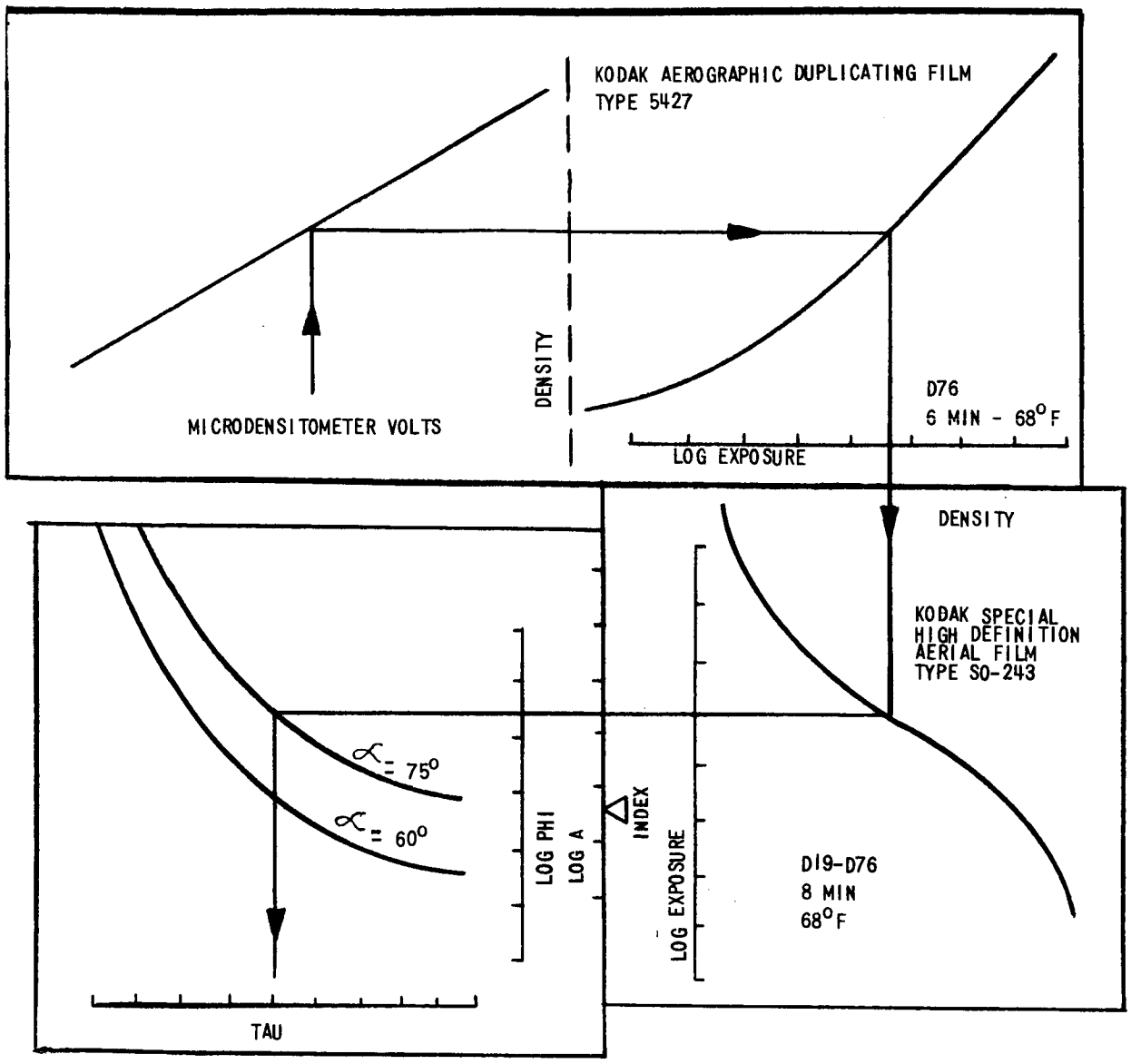

PROCEDURE:

1. Obtain value for Log $\frac{4\ N^2}{10.76\ I\rho\ Tt}$ = Log A = Log $\frac{\Phi}{E}$
2. Align value of Log A with index on the characteristic curve for SO-243.
3. Align characteristic curve for SO-243 with the characteristic curve for Type 5427 at proper densities and the microdensitometer calibration curve with proper densities as indicated above.
4. Enter the curve of microdensitometer voltage vs density and obtain density of Type 5427.
5. From density of Type 5427 find corresponding density of SO-243 and the Log E of SO-243.
6. From Log E of SO-243 find Log Phi.
7. From Log Phi find Tau corresponding to the correct phase angle alpha.

Figure A1-31. GRAPHICAL SOLUTION FOR OBTAINING TAU FROM MICRODENSITOMETER VOLTAGE FROM A POSITIVE MADE FROM THE ORIGINAL NEGATIVE MATERIAL, SYSTEM A

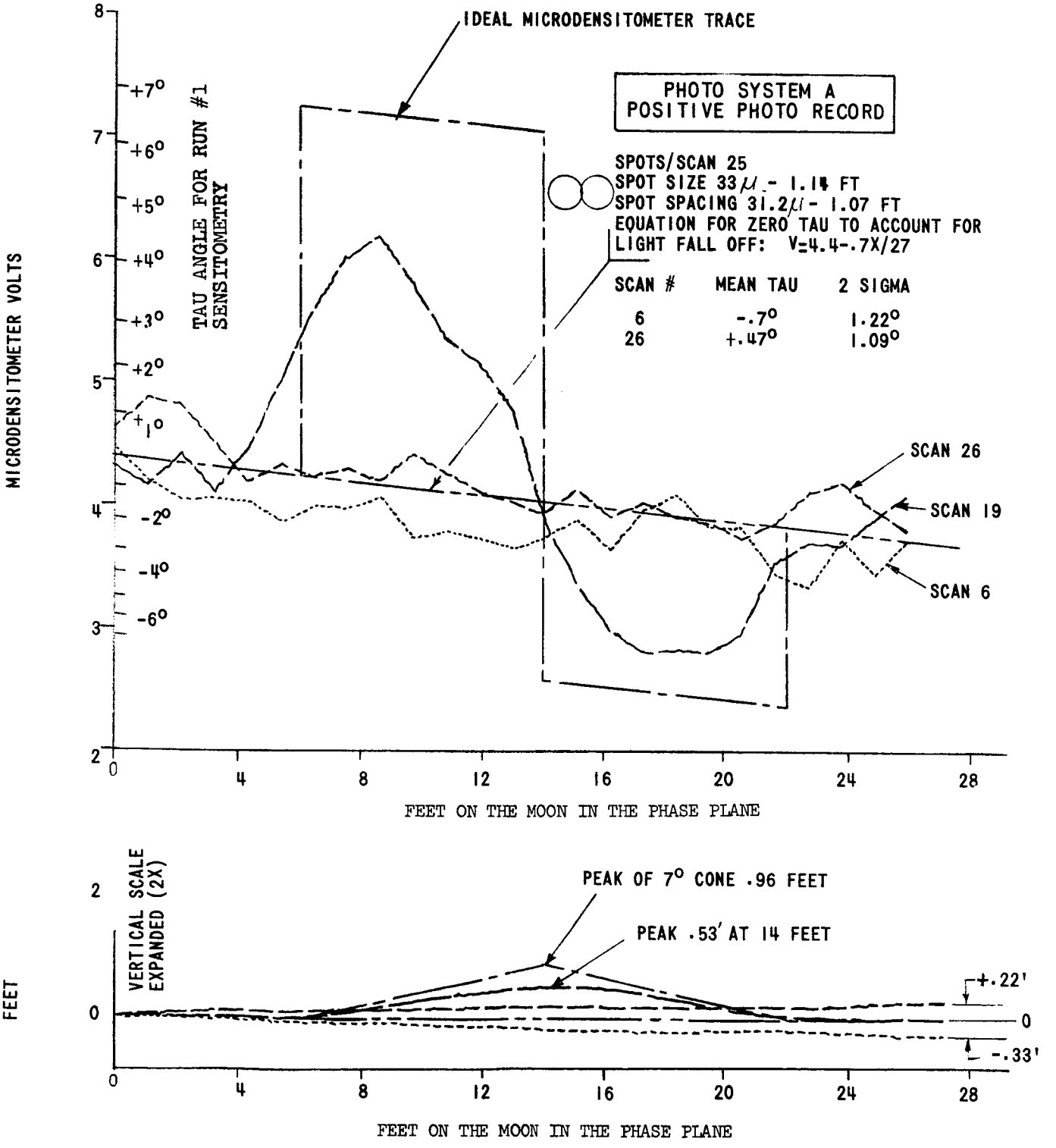

Figure A1-32. EXPERIMENT 13, MICRODENSITOMETER TRACE AND LUNAR PROFILE, 7° CONE, PHOTO SYSTEM A

cone while scan 6 and 26 are typical traces across the level areas at either side of the cone. The photo record is a positive and has the negative tau angles (slopes towards the sun) in the low densities or low microdensitometer voltage region. The line representing the equation for zero tau slopes down to the right for a positive photo record with the sun coming from the right. This line is actually a short section of a second degree equation, but it is considered a straight line for this experiment.

In the table on the upper right of Figure A1-32, two circles have been drawn to scale to illustrate the spot diameter and spot spacing. The diameter and spacing of these spots are given in microns on the film and in feet on the moon.

The ideal microdensitometer trace shown in the figure is a theoretical one made across the peak of the cone assuming an infinitely small spot, perfect optics, and a film with no grain, but does include light fall-off across the model. Scan 19 in Figure A1-32 approaches this trace as a limit.

The profile made from scan 19 shows that the peak reaches 0.53 feet rather than 0.96, the actual height. Scan 6 has a mean tau angle and 2-sigma value for tau of $-0.7° \pm 1.22°$. The profile slopes down with a residual of -0.33 feet at the end of the 27 foot profile. Scan 26 has a mean tau angle and 2-sigma value for tau of $+0.47° \pm 1.09°$ with a residual of +0.22 feet at the end of the 27-foot profile.

The profiles listed in Table A1-XI were made on a Calcomp Plotter for all 28 scans. In general they show the 7° cone with the traces each side of number 19 having a hyperbolic shape. The flat sections are nearly flat. The profiles have residual errors at the end of 27 feet varying from -0.54 to +0.66 feet. Since the low scan numbers generally have negative residuals and the high scan numbers show positive residuals, it is possible that the illumination was slightly uneven in the Y direction across the model. The low scan numbers are similar to scan 6 that is nearly all below the average

microdensitometer voltage and the high scan numbers have microdensitometer voltages above the average, similar to scan 26.

No attempt was made to adjust the profiles by bending the curve of microdensitometer voltage vs exposure or by utilizing the error-of-closure technique, described earlier in this report.

TABLE A1-XI

LIST OF PROFILES AND MAPS - EXPERIMENTS 13 THROUGH 16

Experiment 13

1. Profiles (28 scans) scale 1" = 4 ft.
2. Map - scale 1" = 2 ft.

Experiment 14

1. Profiles (7 scans) scale 1" = 4 ft.
2. Map, scale 1" = 2 ft.
3. Profile of scan 4, run 2, scale 1" = 4 ft.

Experiment 15

1. Profiles (3 scans) scale 1" = 4 ft.
2. Map, scale 1" = 2 ft.

Experiment 16

1. Profiles (25 scans) scale 1" = 4 ft.
2. Map, scale 1" = 2 ft.

Because of the size of these profiles and maps they have not been included in this report but a copy of each has been sent to Mr. Robert L. Jones, MSC-NASA, Houston, Texas for use by persons in NASA who wish to study them further. Duplicates remain at Kodak.

Lunar Map Experiment No. 13

The computed heights for all 28 scans were assembled by the Calcomp Plotter into a map. The map shows the cone and the flat area around the cone with the accuracy noted previously. The central scan does not reach the maximum peak of 0.96 feet because the large scanning spot integrates many elements of the cone causing the slope to appear lower than the element in the phase plane that passes over the peak. The large scanning spot rounds off the peak.

The edges of the cone have a location uncertainity about the size of the scanning spot.

Photography and Scanning Experiment No. 14

The original photography for experiment 14 was taken on Kodak Special High Definition Aerial Film Type SO-243 film at a scale of 1:30,000. The film was processed in D19-D76 for eight minutes at 68°F. giving a gamma in the area of interest of 1.2. This value is lower than normal because of the reciprocity failure of SO-243 film when the camera exposure is several hundred seconds.

Seven scans were made across the model as shown in Figure A1-33. These samples were considered adequate for a comparison with the profiles from system A photography. One scan crosses the peak of the cone, one scan falls on each side of the peak and close to it, one scan is half way down the side of the cone on each side of the peak, and one scan crosses the flat area on each side of the cone. The scanning parameters are listed in Appendix 1.

Analysis and Computer Input Experiment No. 14

The instructions to the programmer include the following:

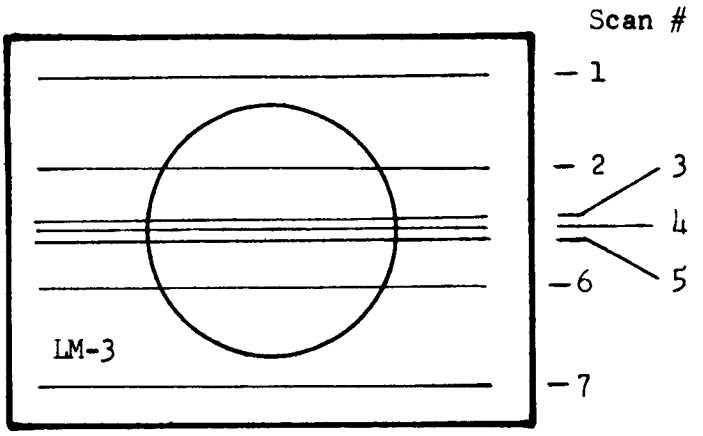

Figure A1-33. PLACEMENT OF SCAN LINES IN EXPERIMENT NO. 14

1. All items in Appendix I marked with an asterisk.
2. Deck of IBM cards with microdensitometer voltage readings for experiment 14.
3. Data from Table A1-XII

TABLE A1-XII

MICRODENSITOMETER AND EXPOSURE DATA FOR EXPERIMENT No. 14, NEGATIVE PHOTO RECORD

μD Volts	Density	Step	Log E	E
9.00	1.32	10	0.88	7.586
6.75	1.08	9	0.68	4.786
4.90	0.86	8	0.48	3.020
3.60	0.76	7	0.28	1.905
2.50	0.52	6	0.08	1.202

A second-degree equation connecting microdensitometer volts with exposure was obtained by the computer by a modified least square curve fit and was used in the computer program to calculate profiles.

4. Phi-tau equation for the photometric function for copper oxide dust at a phase angle of 75.7° (sun elevation 14.3°)
5. Equation for zero tau angle to account for light fall-off

$$V = 5.3 + .0122\ X$$

where V = microdensitometer volts

X = feet on the moon in the phase plane from the start of the trace.

This equation was obtained by inspection of Scans 1 and 7.

6. Position of the seven scans in the Y direction at right angles to the phase plane.

TABLE A1-XIII

SCAN POSITIONS EXPERIMENT No. 14

	Y Dimension	
Scan No.	On Film Microns	On Moon Feet
7	300	29.5
6	190	18.7
5	160	15.8
4	150	14.8
3	140	13.8
2	110	10.8
1	0	0

7. Procedure for obtaining profiles from a negative photo record.
8. For Run No. 1 make no adjustments to the sensitometry.

Traces and Profiles Experiment No. 14

The upper part of Figure A1-34 shows the microdensitometer trace of the central scan. Because of the larger scale of experiment No. 14, this trace closely matches the ideal microdensitometer trace and reproduces the correct profile fairly well. There are 135 spots per scan compared to the 27 spots of experiment No. 13. Only 27 feet of this trace are shown in Figure A1-24, making the scale comparable to that of Figure A1-33. The small circles at the

upper right in Figure A1-34 show the spot spacing and spot size. The size and spacing are given in microns on the film and in feet on the moon.

The equation for zero tau to account for light fall-off across the model is a line sloping up to the right for a negative photo record exposed with the sun on the right. The line is a short section of a second-degree equation, but it is considered a straight line for this experiment.

The table located in the center of Figure A1-34 and repeated here for convience (Table A1-XIV), shows the mean tau angle and the 2-sigma values for four sections of the central trace.

TABLE A1-XIV

MEAN TAU ANGLE AND 2-SIGMA VALUE FOR THE CENTRAL SCAN OVER A 7° CONE, EXPERIMENT No. 14

Run #1

X - Dimensions - feet From	To	Mean Tau, Degrees	2-Sigma, Degrees	Number of points considered
0.0	14.0	- 0.25	± 3.5	46
16.5	23.0	+ 6.7	± 1.7	22
24.5	31.5	- 8.1	± 6.3	23
32.5	41.4	- 0.58	± 3.2	30

The profile made from this trace is shown in the lower half of Figure A1-34 and is in very close agreement with the actual dimensions of the cone. The change in height for the positive slope is 0.86 foot and is 1.1 foot for the negative slope. The actual height of the cone is 0.96 foot.

Inspection of Table A1-XIV indicates that a better equation is possible to

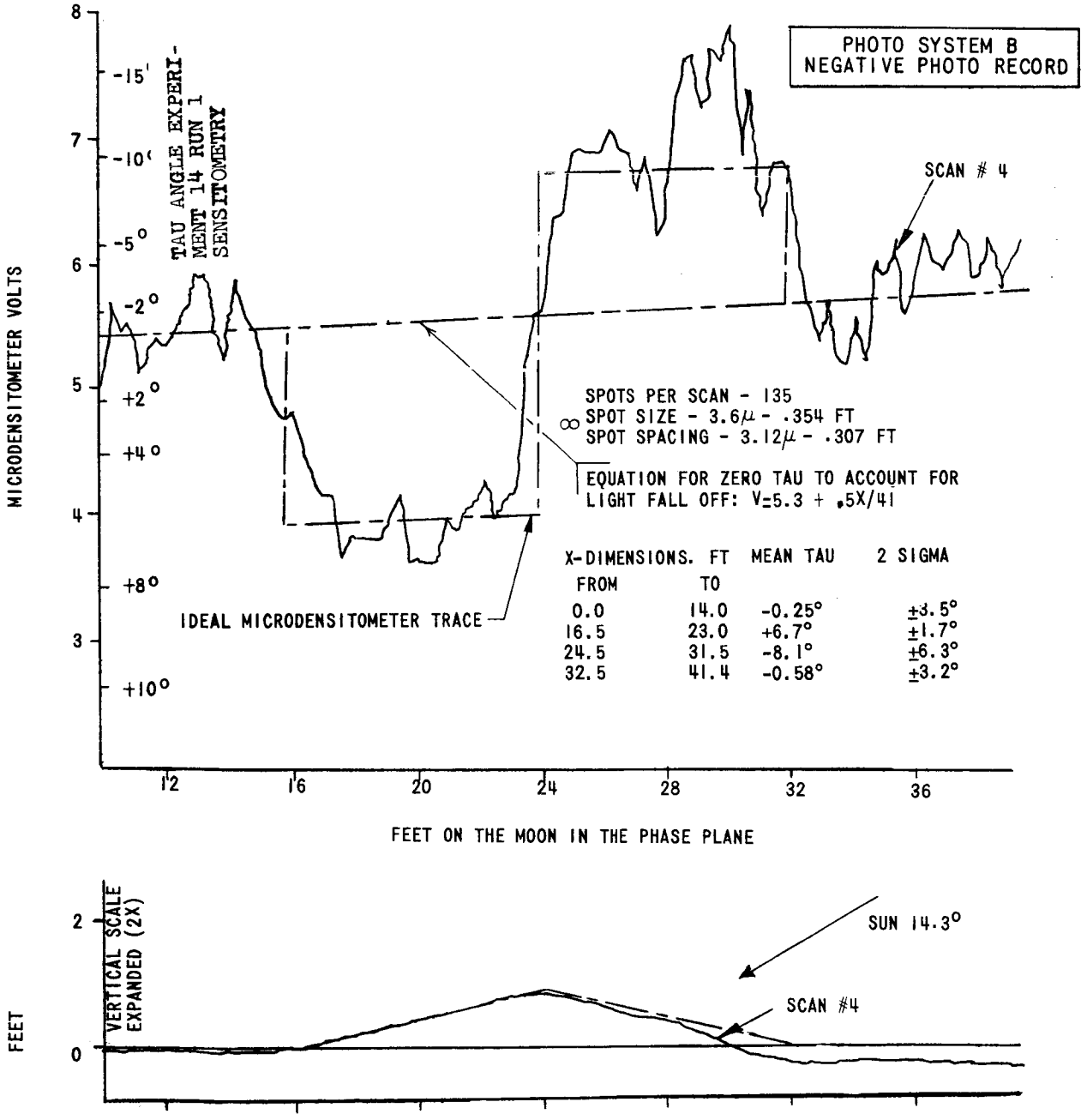

Figure A-34. EXPERIMENT 14, SCAN 4 MICRODENSITOMETER TRACE AND LUNAR PROFILE 7° CONE, PHOTO SYSTEM B

account for light fall-off across the model. An improved equation was obtained by requesting the computer to find, by a modified least squares curve fit, the first degree equation between the microdensitometer voltages and the distance X for the points in scan 4 that are measuring the level background. (0 to 14 feet and 32.5 to 41.5 feet.)

This equation, V = 5.3228 + .581 X/41 is very little different than the equation used in Run 1, V = 5.3 + .5 X/41 but it improves the slopes and height values as follows:

TABLE A1-XV

MEAN TAU ANGLE AND 2-SIGMA VALUE FOR THE CENTRAL SCAN OVER A 7° CONE, EXPERIMENT No. 14

Run #2

X - Dimensions - feet From	To	Mean Tau, Degrees	2-Sigma, Degrees	Number of points considered
0.0	14.0	-0.031	± 3.4	46
16.5	23.0	+6.9	± 1.7	22
24.5	31.5	-7.3	± 6.2	23
32.5	41.4	-0.18	± 3.3	30

The level surfaces have been improved so that very little residual angle remains. The positive slope has been improved from + 6.7° to + 6.9° and the negative slope from - 8.1° to - 7.3°. All of the elements are now within .3° of their actual slope. The change in height is now 0.89 foot for the positive slope and is 0.90 foot for the negative slope. (Measured value 0.96) The improved equation for zero tau causes the profile to end with a residual of only -0.03 foot.

The 2-sigma values for tau angle have been included in the above tables to show a measure of tau angle variability caused by film grain. This variability is a function of density and has been plotted in Figure A1-35 for the parameters of photo system B, Experiment No. 14. These parameters are SO-243 film processed in D19-D76 for 8 min. at 68°F, scale 1:30,000, Fisher copper oxide dust, scanning spot diameter 1/2 the pitch of the limiting tri-bar (3.6 microns), and spot spacing 3.1 microns. Notice that the 2-sigma values in Table A1-XIII and Table A1-XIV are very nearly the same since these values are a measure of film grain and the sensitivity to tau angle change with change in microdensitometer volts.

Scan 1 and 7 were made across the flat surface on either side of the 7° cone. An equation for zero tau was obtained from these scans to get an idea of the variability in similar measurements.

TABLE A1-XVI

COEFFICIENTS FOR ZERO TAU EQUATION, EXPERIMENT No. 14

Scan #	Run #	1st Coefficient	2nd Coefficient	No. of points considered
1	2	5.193	0.01569	135
4	2	5.323	0.01419	76
7	2	5.387	0.01024	135
4	1	5.3	0.012	visual inspection

Scan 4, Run 1 coefficients are included here for reference.

These variations can be attributed to variations in the illumination, processing, density measurements, and the photometric functions of the copper

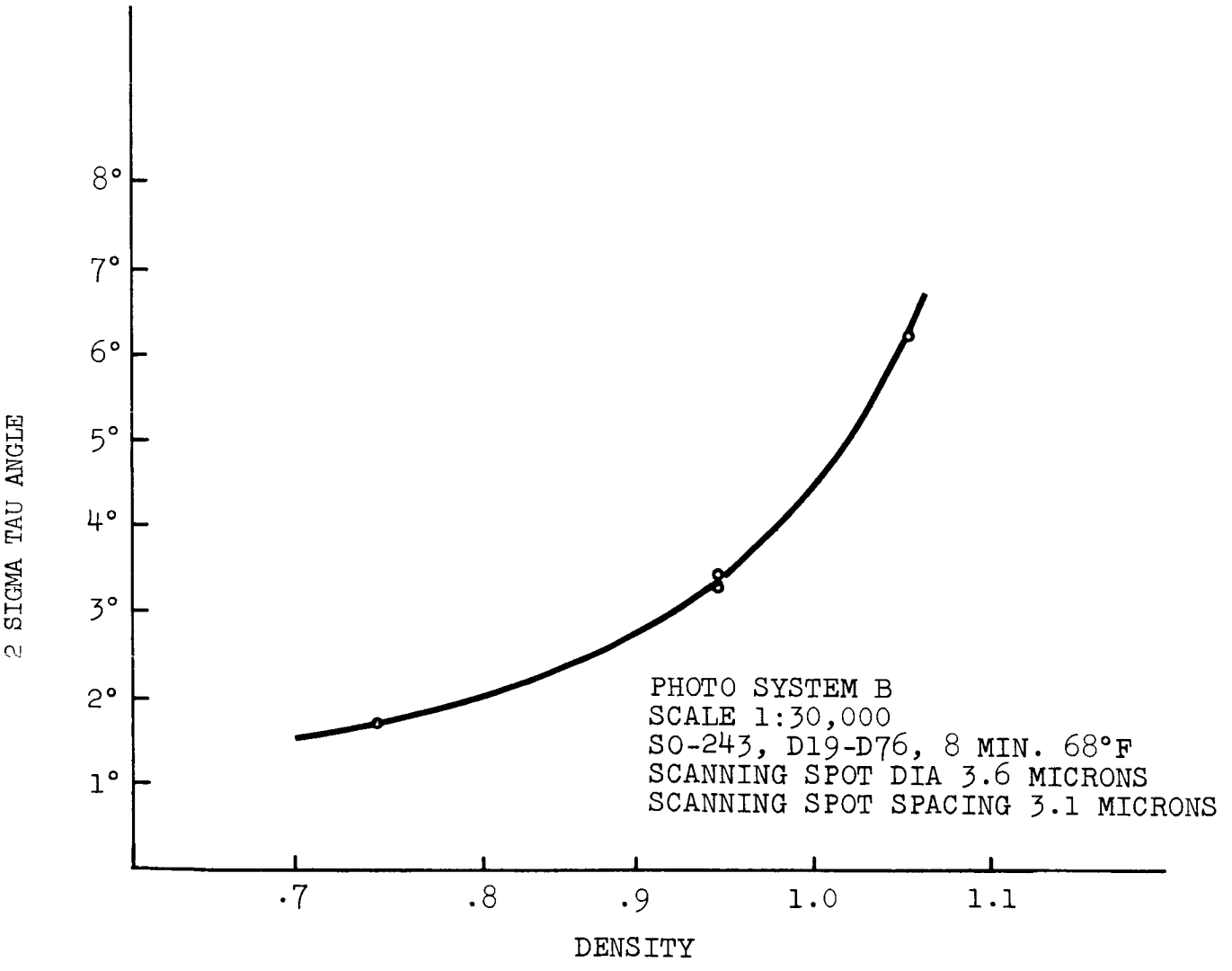

Figure A1-35. RELATIONSHIP BETWEEN 2-SIGMA FOR TAU ANGLE AND DENSITY FOR EXPERIMENT 14

oxide dust.

Copies of the profiles and maps of experiment No. 14 are at NASA and Kodak.

Conclusions from Experiments No. 13 and No. 14

1. The profile of the 16-foot diameter, 7° cone made with photo system A looks very much like a low convex spherical surface with diameter to height ratio about 30 to 1. The actual ratio is 17 to 1 for the model.
2. The profile of the 16-foot diameter, 7° cone made with photo system B is more like a cone with diameter to height about 18 or 19 to 1.
3. The improved profile obtained in experiment No. 14 (photo system B) over that obtained in experiment 13 (photo system A) is primarily because of the increased scale of the original photography.
4. Profiles of objects with low slopes and profiles of level background can be computed from the densities obtained with photo system A and photo system B provided the objects are large compared to the scanning spot.

	Photo System A	Photo System B
Ratio object Dia/Spot Dia	14	45
Actual Dia/height	17:1	17:1
Mapped Dia/height	30:1	19:1

5. No shadow areas were present on LM-3 with a 14.3° sun elevation; therefore, these experiments were only concerned with illuminated areas and slopes of less than 7°.

Experiments No. 15 and No. 16

Purpose

The purpose of experiment No. 15 is to make a lunar map of LM-9 using photo system A, a positive photo record, simulating LOP scale, resolution, and contrast. A photograph and description of LM-9 are shown in Figure A1-36. It has 26° cones, slopes of 3 1/2°, and craters with diameter-to-depth ratios of 8:1. These objects will have shadow areas at a sun elevation of 14.3°.

Experiment No. 16 will also map LM-9 but using photo system B, a negative photo record with improved scale, resolution, and lower contrast.

Values for the photographic and tracing parameters for these experiments are shown in Appendix I.

Photography and Scanning for Experiment No. 15

The original photograph for experiment No. 15 was taken on Kodak Special High Definition Aerial Film, Type SO-243 at a scale of 1:74,450. The film was processed in D19-D76 for eight minutes at 68°F. A positive 7.2 X enlargement was made from this negative, on Kodak Aerographic Duplicating Film Type 5427 processed in D76 for six minutes at 68°F. The over-all gamma in the area of interest is 2.1, and the positive enlargement has a resolution of 16 lines per millimeter.

The details of the scanning parameters are given in Appendix I. The film was scanned with a microdensitometer and a deck of IBM cards were created with microdensitometer volts recorded for each spot position. Calibration data for the microdensitometer were sent to the computer programmer with the IBM cards.

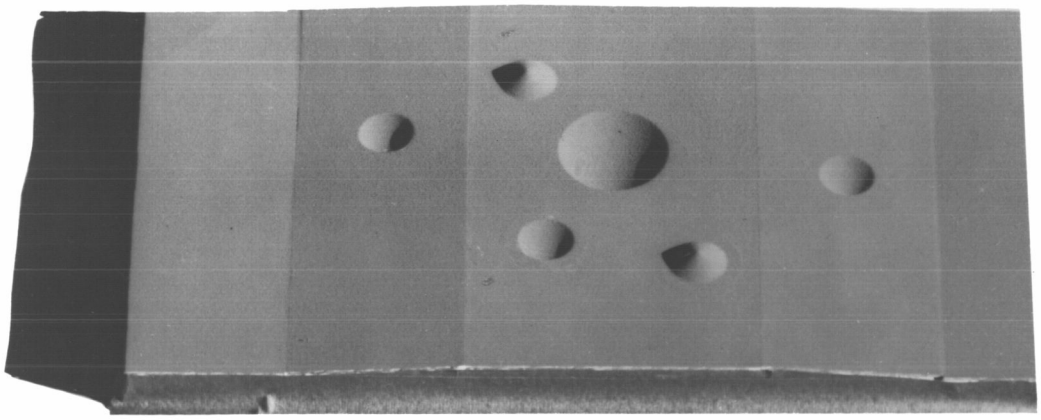

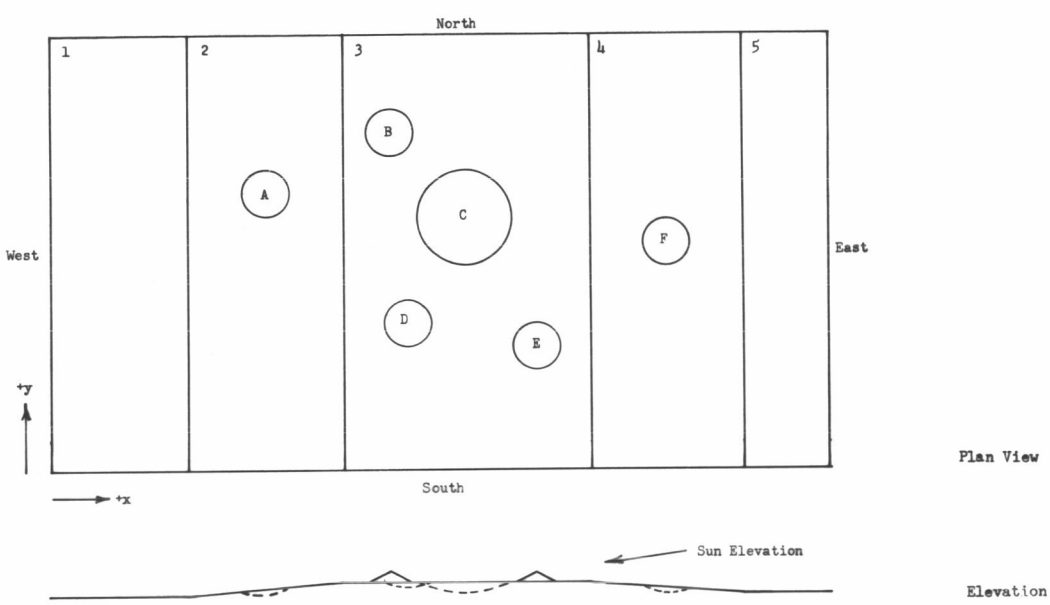

Geometric Shape	D/d	Base Angle	Symbol	Model Dimensions Inches: Coordinates X, Y	Model Dimensions Inches: Measured Depth or Height	Lunar Dimensions Feet: Coordinates X, Y	Lunar Dimensions Feet: Diameter	Lunar Dimensions Feet: Depth or Height
1" Dia.Sph.Concave	8:1		A	4.43, 5.77	-	17.72, 23.08	4	-
1" Dia.Con.Convex		26°	B	6.95, 7.00	.229	27.80, 28.00	4	.92
2" Dia.Sph.Concave	8:1		C	8.50, 5.20	.247	34.00, 20.80	8	.99
1" Dia.Sph.Concave	8:1		D	7.30, 3.02	.119	29.20, 12.08	4	.48
1" Dia.Con.Convex		26°	E	9.95, 2.52	.230	39.80, 10.08	4	.92
1" Dia.Sph.Concave	8:1		F	12.67, 4.71	-	50.68, 18.84	4	-

Panel #	E-West Dimension: Model Inches	E-West Dimension: Lunar Feet	Slope Tau in Degrees	Height Feet
1	2.8	11.2	0	0
2	3.2	12.8	+3½°	-
3	5.1	20.4	0	.75
4	3.1	12.4	-3½°	-
5	1.8	8.2	0	0

Figure A1-36. PHOTOGRAPH AND DESCRIPTION OF LM-9

Analysis and Computer Input, Experiment No. 15

The instructions to the programmer included the following:

1. All items in Appendix I marked with an asterisk
2. Deck of IBM cards with microdensitometer voltage readings for experiment No. 15
3. Data of Table A1-XVII

TABLE A1-XVII

MICRODENSITOMETER AND EXPOSURE DATA FOR EXPERIMENT No. 15

POSITIVE PHOTO RECORD

μD Volts	Density 5427	Density SO-243	Step # 5427	Log E SO-243	E SO-243
8.2	1.59	.58	9	0.13	0.1349
5.4	1.27	.73	8	0.31	0.2042
2.8	0.98	.89	7	0.46	0.2884
0.6	0.70	1.02	6	0.58	0.3802

A third-degree equation found by a modified least squares curve fit related microdensitometer volts to exposure on the SO-243 film. This equation was used in the computer program to calculate profiles. The equation obtained from Table A1-XVI takes into account the two photographic steps in the LOP system.

4. Phi-tau equation for the photometric function of copper oxide at a phase angle of 75.7° (sun elevation 14.3°)

5. Equation for zero tau angle to account for the light fall-off across the model.

$$V = 5.15 - 0.0175\ X$$

This equation describes the straight line connecting the mean of spot 1 and the mean of spot 53 for all 30 scans.

6. Scan separation is 1.14 feet for 30 scans
7. Procedure for obtaining profiles from a positive photo record.

Traces and Profiles Experiment No. 15

Figure A1-37 shows the microdensitometer trace of scan 22 and a lunar profile of LM-9 made from this scan. Scan 22 crosses the center of the 4-foot diameter crater on the positive slope and crosses the 8-foot crater 2 feet from its center. The table at the right in Figure A1-37 shows the spot size and spot spacing with film dimensions in microns and lunar dimensions in feet. The equation for zero tau is also in the table. The level for zero tau angle slopes down to the right for a simulated sun coming from the right. The ideal microdensitometry shows the level areas and sloping surfaces of LM-9 but does not show the expected deflection of the trace across the craters. The profile made from the trace has been corrected by the error of closure method to end the trace at zero height. The residual height before adjustment (-2.19 feet) shows that for this scan a better equation for zero tau should have been used.

In general, the level areas and slopes are a good match to the model. The details of the craters are nearly lost, with the small 4-foot crater just showing in the profile and the large 8-foot crater evident but distorted into a much shallower and larger depression. Examination of the trace shows that at no time did any measurement show a full shadow reading i.e., the spot size is larger than any of the shadow areas encountered by the spot.

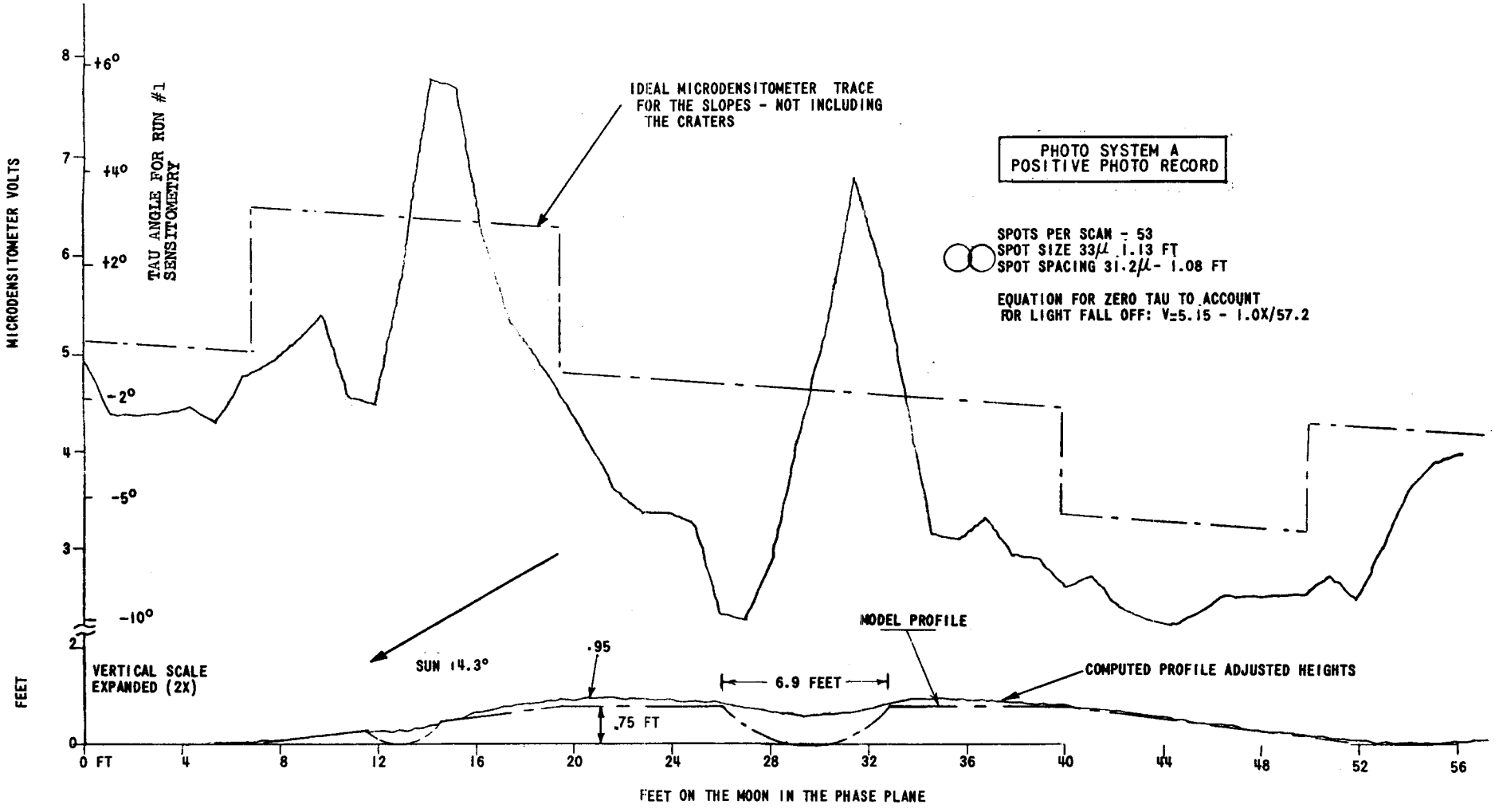

Figure A1-37. EXPERIMENT 15, SCAN 22 MICRODENSITOMETER TRACE AND LUNAR PROFILE OF LM-9 PHOTO SYSTEM A

Scan 22 is typical of the other 30 scans. All profiles made from these scans show the 3 1/2° slopes and show some change in slope where craters and cones are encountered.

All of the traces would be improved with a better equation for zero tau angle.

Map, Experiment No. 15

A map was made from the 30 traces of experiment No. 15 using the profiles with the adjusted heights. In general this map shows:

1. The level areas are nearly level.
2. The central level area, panel 3, is from 0.9 to 1.3 feet high compared to the actual height of 0.75 feet.
3. The 3 1/2° slopes are about 5°.
4. The 8-foot diameter crater is about 10 or 12 feet in diameter and has a depression about 0.7 feet compared to the actual depth of 0.99 feet.
5. The 4-foot craters within the sloping surfaces are just detectable as a depression.
6. The 4-foot diameter 26° cones are mapped as 6 to 8 feet in diameter, spherical-like surfaces, 0.3 foot high compared to the actual height of 0.92 foot.
   If a better zero tau curve for light fall-off across the model were used, the slopes and height of the middle level area would be improved but there would be no improvement in resolution of the craters and cones.

   Copies of the profiles and maps made from experiment 15 data are at NASA and Kodak. See Table A1-X.

Photography and Scanning Experiment No. 16

The original photography for experiment No. 16 was taken on Kodak Special High Definition Aerial Film Type SO-243 at a scale of 1:30,000. The film was processed in D19-D76 for eight minutes at 68°F giving a gamma in the area of interest of 1.2; 25 scans were made across the model as shown in Figure A1-38. The scanning parameters are listed in Appendix I.

Analysis and Computer Input, Experiment No. 16

The instructions to the programmer included the following:

1. All items in Appendix I marked with an asterisk
2. Deck of IBM cards with microdensitometer vs exposure data for experiment 16
3. Table A1-XVIII

TABLE A1-XVIII

MICRODENSITOMETER VS EXPOSURE DATA FOR EXPERIMENT 16

NEGATIVE PHOTO RECORD

μD Volts	Density	Step #	Log E	E
9.80	1.59	11	1.08	12.02
7.80	1.32	10	0.88	7.586
6.25	1.08	9	0.68	4.786
4.90	0.86	8	0.48	3.020
3.80	0.67	7	0.28	1.905
3.05	0.52	6	0.08	1.202
2.35	0.40	5	1.88	0.7586

A sixth-degree equation connecting the microdensitometer volts with the exposure was obtained by a modified least

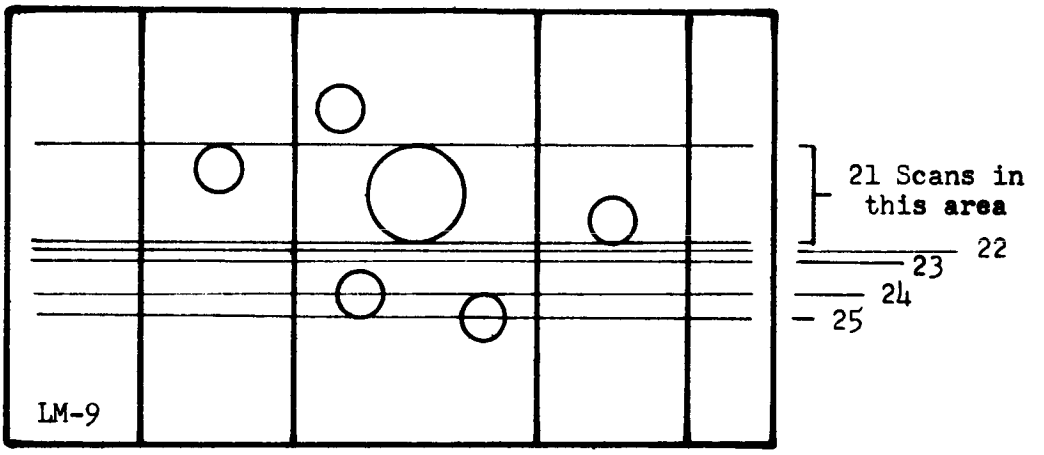

Figure A1-38. PLACEMENT OF SCAN LINES IN EXPERIMENT NO. 16

squares curve fit and used by the computer program to calculate profiles.

4. Phi-tau equation for the photometric function for copper oxide dust at a phase angle of 75.6° (sun elevation 14.3°)
5. Equation for zero tau angle to account for light fall-off

$$V = 4.95 + 0.00685\,X$$

where V = microdensitometer volts

X = feet on the moon in the phase plane from the start of the scan

This equation was obtained by drawing a straight line between the mean of the first spot and the mean of the last spot for all 25 scans.

6. Position of the scans - Scan separation in the Y direction at right angles to the phase plane for 21 scans is 3.6 microns on the film or 0.354 feet on the moon. The first scan is 24.08 feet from the origin, and the scans through scan 21 cover the area from 24.08 feet to 16.63 feet. The remaining scans are located as follows:

TABLE A1-XIX

Y POSITION OF MICRODENSITOMETER SCANS FOR SCANS 22 - 25, EXPERIMENT 16

Scan #	Y Dimension, feet
22	16.1
23	15.5
24	12.8
24	10.8

7. Procedure for obtaining profiles from a negative photo record

8. Use the last 20 spots to establish zero elevation and adjust the profiles by the error of closure techniques for each scan.

Traces and Profiles, Experiment No. 16

Figure A1-39 shows scan 7 microdensitometer trace and lunar profile of LM-9 made during experiment No. 16. The table at the right shows the number of spots per scan (190), the spot size and spot spacing drawn to scale, the dimension on the film in microns and on the moon in feet, and the equation for zero tau to account for light fall-off across the model. The equation for light fall-off is a line sloping up to the right for a negative photo record with the simulated sun coming from the right. It is a short section of a second-degree equation but is considered a straight line for this experiment. A scale at the left shows the tau angles for the sensitometry of Run 1.

Scan 7 passes across the center of the 4-foot crater on the positive slope and across the 8-foot crater, 2 feet from the center. The ideal trace includes the expected trace across the craters as well as the level areas and slopes.

The profile made from this trace has been corrected by the error of closure method using the mean of the last 20 spots to determine the final height of the computed trace. The 3 1/2° slopes are mapped at about 5°, making the central height about 1 foot high compared to 0.75 foot the actual height. The 4-foot crater on the positive slope shows a good resemblance to a crater with a diameter-to-depth ratio of 8:1 and is in the correct position on the trace.

The 8-foot crater on the model has a diameter to depth of 8:1 but the cord cut by scan 7 is 6.9 feet long and the depth at the center of this cord is 0.79 feet. The profile made from the trace has rounded these dimensions to a diameter of about 8 feet and a depth of about 0.72 foot. Scan 7 is typical of the other 25 scans.

The profile made from scan 22 that traces across the slopes but not the craters and cones shows the slopes steeper than the 3 1/2° of the model by about 1 1/2°. This makes the level area in the center reach a height of 1.0 to 1.1 feet compared to 0.75 feet, the actual height.

The profile made from scan 25 that crosses the peak of the 26° cone (E)[Figure A1-36] reaches a height of 0.5 foot above the level area of panel 3 compared to the actual height of 0.92 foot.

Map, Experiment No. 16

The data from the profiles were plotted by the Calcomp Plotter to form a map. Each 4th spot was plotted at a scale of 1 inch equals 2 feet. In general this map shows:

1. The level areas as nearly level
2. The central area panel 3 is from 1.0 to 1.3 feet high (actual height 0.75 ft.)
3. The 3 1/2-degree slopes are nearly 5°
4. The diameter of the large crater is about 8 feet (actual diameter 8 feet)
5. The depth of the 8-foot crater is about 1.0 feet (actual depth 0.99 foot)
6. The 4-foot diameter craters are hard to eveluate on the slope, but they are in the correct position in the x and y dimension and appear to have about the correct depths.
7. The 4-foot diameter cone is located in its correct position. It is 0.5 foot high (actual height 0.92 foot)
8 From the sensitometry, the shadow should correspond to base plus fog density that was measured as 1.6 micro-

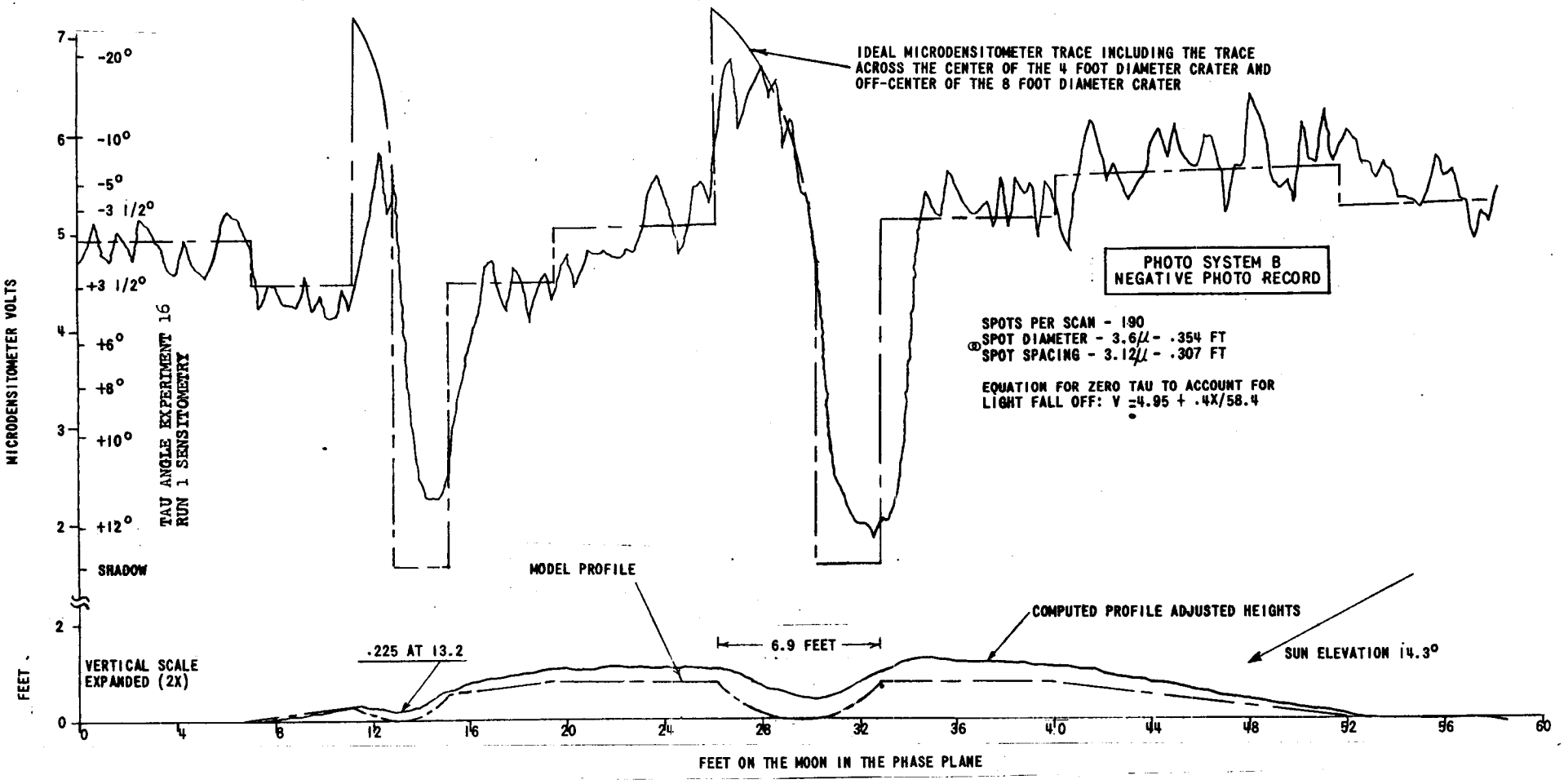

Figure A1-39. EXPERIMENT 16 SCAN 7 MICRODENSITOMETER TRACE AND LUNAR PROFILE OF LM-9 PHOTO SYSTEM B

densitometer volts. There were no voltage readings less than 1.9 volts showing that no shadow areas were recognized by the computer program.

Conclusions from Experiment No. 15 and No. 16

1. The 3 1/2° slope of LM-9 was mapped at about a 5° slope in both photo system A and photo system B.
2. The level areas were nearly level for both systems, with the central panel mapped 130 percent of the actual height.
3. The 4-foot crater was lost by photo system A and was well detected in photo system B.
4. The 8-foot diameter crater was shown as a large shallow depression in photo system A and was quite well defined in photo system B.
5. The 4-foot diameter, 26° cone was shown by photo system A to be rounded over with about 30 percent of its actual height and 50 percent larger in diameter. In photo system B this cone is 60 percent of its actual height and has approximately the correct diameter.
6. No shadow area was detected with either system even though the spot size was such that shadows should have been detected.
7. Photo system B has better capability for mapping detail because of the better original scale and better resolution.

EXPERIMENTS No. 17 AND No. 18

Purpose

The purpose of experiment No. 17 is to make a lunar map of model KLM6-65 using photo system A, a positive photo record simulating LOP scale, resolu-

tion, and contrast. Figure A1-40 is a record photograph of KLM6-65 showing the area to be mapped.

Experiment No. 18 will also map KLM6-65 but using photo system B, a hypothetical negative photo record with improved scale and resolution and lower contrast.

Values for the photographic and tracing parameters for these experiments are shown in Appendix I.

Photography and Scanning, Experiment No. 17

The original photograph for experiment No. 17 was taken on Kodak Special High Definition Aerial Film Type SO-243 at a scale of 1:74,450. The film was processed in D19-D76 for 8 minutes at 68°F. A positive 7.2X enlargement was made from this negative, on Kodak Aerographic Duplicating Film Tpye 5427 processed in D76 for 6 minutes at 68°F. The over-all gamma in the area of interest is 2.1, and the positive enlargement has a resolution of 16 lines per millimeter.

The details of the scanning parameters are given in Appendix I. The film was scanned with a microdensitometer and a deck of IBM cards created with microdensitometer voltage recorded for each spot position. Calibration data for the microdensitometer were sent to the computer programmer with the IBM cards.

Analysis, Computer Input, Traces, Profiles and Map Experiment No. 17

Experiment No. 17 was not completed because of the need to complete experiment No. 18. The stereo photography that was sent to NASA corresponding to experiment No. 17 (Plate No's 11 and 12, Table IV, 6th Bi-Monthly Report, Page 34) did not have adequate scale and resolution to make a stereo map, but in experiment No. 18 a stereo map was made by NASA from two plates that were enlarged 9.7 times from plates no's 15 and 16. It was decided to place the

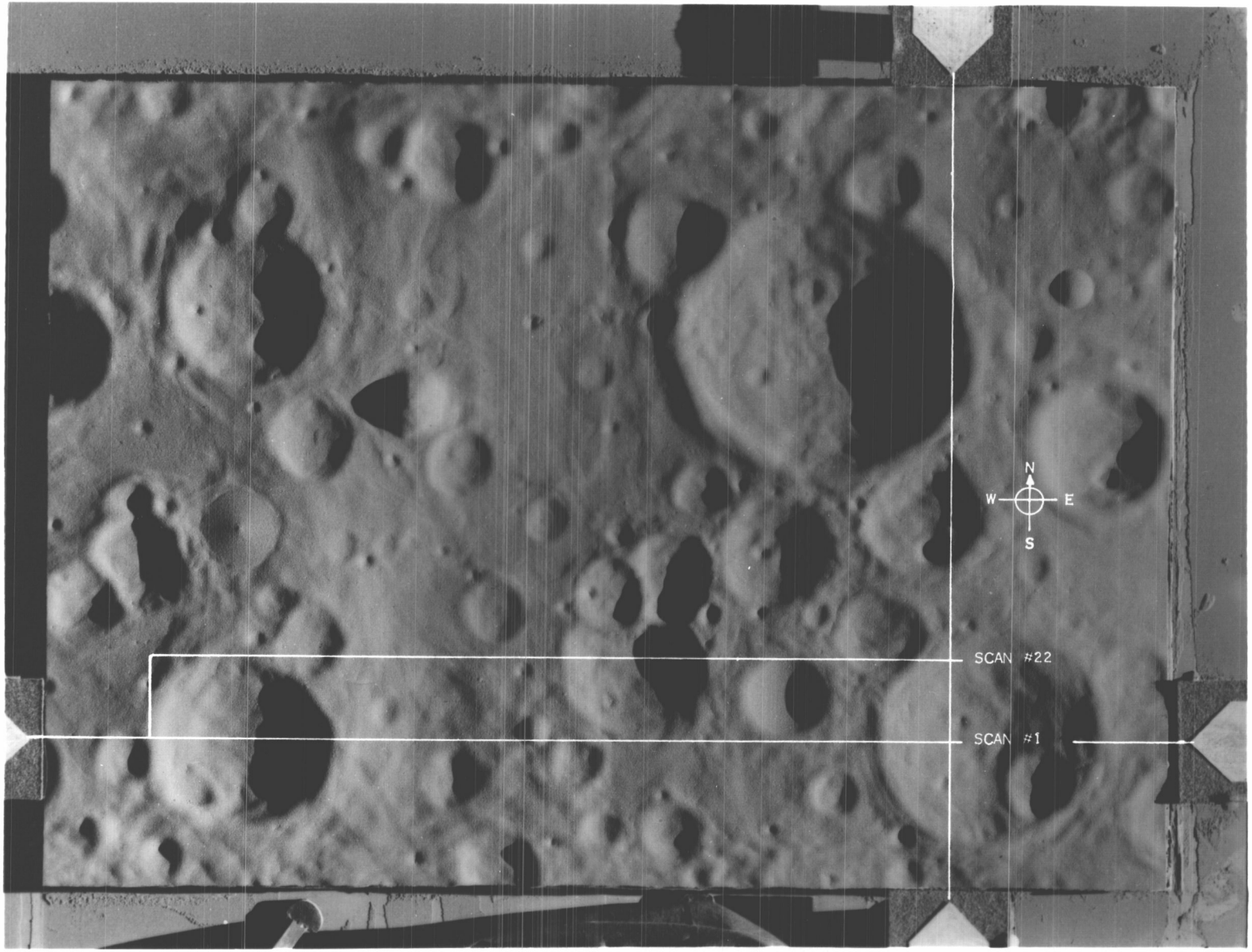

Figure A1-40. PHOTOGRAPH OF KLM 6-65 SHOWING THE 8 x 80 FOOT AREA TO BE MAPPED BY STEREO AND PHOTOCLINOMETRY METHODS

remaining mapping effort on experiment No. 18 where a comparison between photoclinometry and stereo mapping could be made.

Photography and Scanning Experiment No. 18

The original photography for experiment No. 18 was taken on Kodak Special High Definition Aerial Film Type SO-243 at a scale of 1:30,000. The film was processed in D19-D76 for 8 minutes at 68°F giving a gamma in the area of interest of 1.2.

Analysis and Computer Input, Experiment No. 18

The instructions to the programmer included the following:

1. All items in Appendix I marked with an asterisk
2. Deck of IBM cards with microdensitometer vs exposure data for experiment No. 18
3. Table A1-XX

A modified least squares curve fit was used to obtain a third degree equation connecting the microdensitometer voltage with the exposure given the film. This equation was used by the computer program in the calculation of profiles.

TABLE A1-XX

MICRODENSITOMETER VOLTAGE AND CAMERA EXPOSURE DATA FOR EXPERIMENT No. 18
NEGATIVE PHOTO RECORD

μD Volts	Step #	Log E	Camera Exposure
9.31	11	$\bar{1}.65$	0.4467
9.31	10	$\bar{1}.50$	0.3162
6.72	9	$\bar{1}.35$	0.2239
4.81	8	$\bar{1}.20$	0.1585
3.30	7	$\bar{1}.05$	0.1122
2.30	6	$\bar{2}.90$	0.07943
1.39	5	$\bar{2}.75$	0.05623
0.78	4	$\bar{2}.60$	0.03981

4. Phi-tau equation for the photometric function for copper oxide dust at a phase angle of 75.6° (sun elevation 14.3°) In the experiments from No. 5 through experiment No. 16, two phi-tau equations have been used to cover the values of phi of interest. The first equation was used for all phi values below 0.1881 and the second equation was used for all phi values above 0.1881. The 2-sigma variation from the observed points for these equations is ± 0.15° tau angle. However, in the neighborhood of phi = 0.1881, the slope of these curves had a marked discontinuity. To remove this discontinuity the computer derived a single phi-tau curve that had a 2-sigma variation from the observed points of ± 0.28° tau angle but was free from the discontinuity mentioned above. The following single equation was used in experiment 18:

$$\text{Tau} = 14.5 - 0.89 \times 10^{2}\Phi - 0.12 \times 10^{3}\Phi^{2} - 0.49 \times 10^{4}\Phi^{3}$$

$$+0.38 \times 10^{5}\Phi^{4} - 0.12 \times 10^{6}\Phi^{5} + 0.14 \times 10^{6}\Phi^{6}$$

5. Equation for zero tau angle to account for light fall-off

$$V = 4.66 + 0.00926X$$

where V = Microdensitometer voltage

X = Feet on the moon in the phase plane from the start of the scan.

This equation was obtained as follows:

(a) A flat plane surface coated with copper oxide dust was substituted for the KLM6-65 model.

(b) This dusted surface was photographed on SO-243 film at the same scale as KLM6-65 and with the same sun elevation.

(c) The photograph was processed along with the photographs of experiment No. 18.

(d) Twenty-two microdensitometer traces were made across this flat surface in the identical area as the area to be mapped and using the same spot size, spot spacing, and scan spacing as those in experiment No. 18.

(e) A mean density was obtained for each X position in the 22 scans and a first degree equation obtained through these means.

(f) This equation was adjusted to account for the change in gain settings of the microdensitometer between measurements of the flat surface and scanning of experiment No. 18.

6. Position of the scans. Experiment No. 18 maps an area 8 feet x 80 feet as shown in Figure A1-40. Twenty-two scans were made with a separation between scans of 4.07 microns on the film, representing 0.40 feet on the moon.

In addition to these 22 traces, three traces were made across the cone and one trace across the large boulder for a total of 26 traces in the experiment.

7. Procedure for obtaining profiles from a negative photo record.

Traces and Profiles, Experiment No. 18

The analogue microdensitometer traces made during the 26 scans were not analyzed but are on file for future study. Figure A1-41 is a sample page of computer output. The column marked 'VOLTS' lists the microdensitometer voltage read into the IBM cards. The column marked 'E' is exposure in meter-candle-seconds obtained from the microdensitometer voltage through the sensitometry for that experiment. 'A' is the ratio phi/E obtained by the light fall-off equation for each value of X. 'Phi' is obtained by multiplying E x A. 'Tau' is obtained through the phi vs. tau curve. 'X' is the position of the microdensitometer spot in feet measured from the start of the scan and is in the phase plane. 'Y' is the distance of the scan in feet from an arbitrary zero perpendicular to the phase plane. The 'HEIGHT' is the computed height and the 'ADJ HEIGHT' is the height of the point with the error of closure increment included. The asterisks mark the heights that are in shadow.

VOLTS	E	A	PHI	TAU	X	Y	HEIGHT	ADJ HEIGHT
0.41400000E 01	0.22199544E 01	0.34024520E-01	0.75532879E 01	0.59237245E 01	30.69999	22.68000	0.40381	0.32258
0.30400000E 01	0.12086466E 01	0.33999176E-01	0.41092987E 01	0.10346049E 02	31.00699	22.68000	0.45986	0.37781
0.25200000E 01	0.84722665E 00	0.33973864E-01	0.28783564E 01	0.11740060E 02	31.31399	22.68000	0.52366	0.44080
0.23500000E 01	0.75490814E 00	0.33948579E-01	0.25628059E 01	0.12079806E 02	31.62099	22.68000	0.59793	0.51426*
0.21500000E 01	0.66677383E 00	0.33923325E-01	0.22619185E 01	0.12396319E 02	31.92799	22.68000	0.67220	0.58772*
0.20700000E 01	0.63843903E 00	0.33898097E-01	0.21641868E 01	0.12497482E 02	32.23499	22.68000	0.74647	0.66118*
0.20600000E 01	0.63519484E 00	0.33872896E-01	0.21515889E 01	0.12510461E 02	32.54199	22.68000	0.82074	0.73463*
0.19100000E 01	0.59492022E 00	0.33847726E-01	0.20136696E 01	0.12651640E 02	32.84899	22.68000	0.89501	0.80809*
0.21200000E 01	0.65565914E 00	0.33822583E-01	0.22176086E 01	0.12442287E 02	33.15599	22.68000	0.96928	0.88155*
0.21000000E 01	0.64857322E 00	0.33797471E-01	0.21920134E 01	0.12468762E 02	33.46299	22.68000	1.04356	0.95501*
0.23200000E 01	0.74020600E 00	0.33772386E-01	0.24998523E 01	0.12146646E 02	33.76999	22.68000	1.11783	1.02847*
0.28200000E 01	0.10429871E 01	0.33747327E-01	0.35198028E 01	0.11026636E 02	34.07699	22.68000	1.17765	1.08748
0.41400000E 01	0.22199544E 01	0.33722298E-01	0.74861961E 01	0.60175121E 01	34.38399	22.68000	1.21001	1.11903
0.50900000E 01	0.32561518E 01	0.33697297E-01	0.10972351E 02	0.66121709E 00	34.69099	22.68000	1.21355	1.12176
0.54600000E 01	0.37030833E 01	0.33672322E-01	0.12469141E 02	-0.19634303E 01	34.99799	22.68000	1.20303	1.11042
0.52700000E 01	0.34698965E 01	0.33647377E-01	0.11675292E 02	-0.54709017E 00	35.30499	22.68000	1.20010	1.10668
0.52100000E 01	0.33979129E 01	0.33622460E-01	0.11424619E 02	-0.11116600E 00	35.61199	22.68000	1.19950	1.10527
0.56699999E 01	0.39709992E 01	0.33597570E-01	0.13341592E 02	-0.35787033E 01	35.91899	22.68000	1.18030	1.08526
0.54799999E 01	0.37281189E 01	0.33572708E-01	0.12516305E 02	-0.20492372E 01	36.22599	22.68000	1.16932	1.07346
0.53399999E 01	0.35548562E 01	0.33547875E-01	0.11925787E 02	-0.98820031E 00	36.53299	22.68000	1.16402	1.06735
0.52299999E 01	0.34218234E 01	0.33523070E-01	0.11471002E 02	-0.19140959E 00	36.83999	22.68000	1.16300	1.06552
0.52600000E 01	0.34578464E 01	0.33498289E-01	0.11583194E 02	-0.38628698E 00	37.14699	22.68000	1.16093	1.06263
0.53699999E 01	0.35916008E 01	0.33473537E-01	0.12022358E 02	-0.11597066E 01	37.45399	22.68000	1.15471	1.05561
0.51000000E 01	0.32678567E 01	0.33448815E-01	0.10930593E 02	0.73160934E 00	37.76099	22.68000	1.15863	1.05872
0.55900000E 01	0.38675924E 01	0.33424120E-01	0.12927087E 02	-0.28040787E 01	38.06799	22.68000	1.14360	1.04287
0.50900000E 01	0.32561518E 01	0.33399453E-01	0.10875369E 02	0.82446170E 00	38.37499	22.68000	1.14801	1.04647
0.55999999E 01	0.38804253E 01	0.33374813E-01	0.12950847E 02	-0.28481387E 01	38.68199	22.68000	1.13274	1.03039
0.54200000E 01	0.36533005E 01	0.33350198E-01	0.12183829E 02	-0.14482489E 01	38.98899	22.68000	1.12498	1.02181
0.55499999E 01	0.38165200E 01	0.33325613E-01	0.12718787E 02	-0.24196557E 01	39.29599	22.68000	1.11201	1.00803
0.49900000E 01	0.31401420E 01	0.33301055E-01	0.10457004E 02	0.15189996E 01	39.60299	22.68000	1.12015	1.01536
0.55700000E 01	0.38420046E 01	0.33276521E-01	0.12784855E 02	-0.25412222E 01	39.90999	22.68000	1.10652	1.00092
0.53800000E 01	0.36038948E 01	0.33252017E-01	0.11983677E 02	-0.10909150E 01	40.21699	22.68000	1.10068	0.99426
0.50600000E 01	0.32211518E 01	0.33227539E-01	0.10703095E 02	0.11123590E 01	40.52398	22.68000	1.10664	0.99941
0.48600000E 01	0.29920279E 01	0.33203088E-01	0.99344565E 01	0.23645265E 01	40.83098	22.68000	1.11931	1.01127
0.55200000E 01	0.37784841E 01	0.33178665E-01	0.12536506E 02	-0.20860456E 01	41.13798	22.68000	1.10813	0.99928
0.59600000E 01	0.43611201E 01	0.33154267E-01	0.14458974E 02	-0.57218219E 01	41.44498	22.68000	1.07737	0.96771
0.62000000E 01	0.47041585E 01	0.33129898E-01	0.15584829E 02	-0.79340798E 01	41.75198	22.68000	1.03458	0.92411
0.59199999E 01	0.43057991E 01	0.33105555E-01	0.14254587E 02	-0.53247174E 01	42.05898	22.68000	1.00597	0.89468
0.55499999E 01	0.38165200E 01	0.33081239E-01	0.12625521E 02	-0.22486304E 01	42.36598	22.68000	0.99392	0.88181
0.57600000E 01	0.40894284E 01	0.33056953E-01	0.13518404E 02	-0.39128124E 01	42.67298	22.68000	0.97292	0.86000
0.55300000E 01	0.37911377E 01	0.33032689E-01	0.12523147E 02	-0.20617015E 01	42.97998	22.68000	0.96187	0.84814
0.53600000E 01	0.35793301E 01	0.33008451E-01	0.11814814E 02	-0.79210997E 00	43.28698	22.68000	0.95762	0.84308
0.55100000E 01	0.37658555E 01	0.32984244E-01	0.12421389E 02	-0.18767377E 01	43.59398	22.68000	0.94756	0.83221
0.56100000E 01	0.38932843E 01	0.32960060E-01	0.12832288E 02	-0.26287102E 01	43.90098	22.68000	0.93347	0.81730
0.60000000E 01	0.44169534E 01	0.32935905E-01	0.14547635E 02	-0.58946572E 01	44.20798	22.68000	0.90177	0.78480
0.61000000E 01	0.45588442E 01	0.32911774E-01	0.15003965E 02	-0.67887739E 01	44.51498	22.68000	0.86522	0.74744
0.58099999E 01	0.41562219E 01	0.32887668E-01	0.13668845E 02	-0.41987146E 01	44.82198	22.68000	0.84269	0.72409
0.61400000E 01	0.46165498E 01	0.32863593E-01	0.15171641E 02	-0.71188217E 01	45.12898	22.68000	0.80435	0.68493
0.58499999E 01	0.42101882E 01	0.32839542E-01	0.13826065E 02	-0.44990193E 01	45.43598	22.68000	0.78019	0.65996
0.57300000E 01	0.40496987E 01	0.32815518E-01	0.13289296E 02	-0.34802920E 01	45.74298	22.68000	0.76152	0.64048

Figure A1-41. SAMPLE PAGE OF IBM COMPUTED OUTPUT. EXPERIMENT 18 DATA

A complete set of 26 profiles were made from the microdensitometer traces. Figure A1-42 shows three of the 26 profiles compared to actual profiles made from measurements on KLM6-65. The original horizontal scale was 1 inch = 4 feet; the vertical scale was exagerated by making it 1 inch = 1 foot to better show the differences in elevation. While the profiles made by photoclinometry are very much like the actual profiles of KLM6-65, most photo-derived slopes are lower. Consequently, the heights and depths of the photo profiles are less than the actual heights and depths of the model.

Elevation Map, Experiment No. 18

The following procedure was used to create the map of KLM6-65 (Figure A1-43) from Experiment No. 18 data:

1. Each profile was drawn on a separate sheet of tracing paper.
2. These twenty-two profiles were assembled on an illuminator and adjusted by inspection, comparing this profile set with a vertical photograph of KLM6-65 made with photo system B.
3. Once the profiles were adjusted to depict the area as interpreted in the photograph, a line was arbitrarily drawn under the 22 assembled profiles. This line was considered zero elevation.
4. The elevation above the arbitrary zero was measured for the first and last point of each trace.
5. Profiles at right angles to the phase plane (Y profiles) were constructed for all first points and for all last points. Minor adjustments were made to smooth the data and make these Y profiles look like the photograph of KLM6-65.

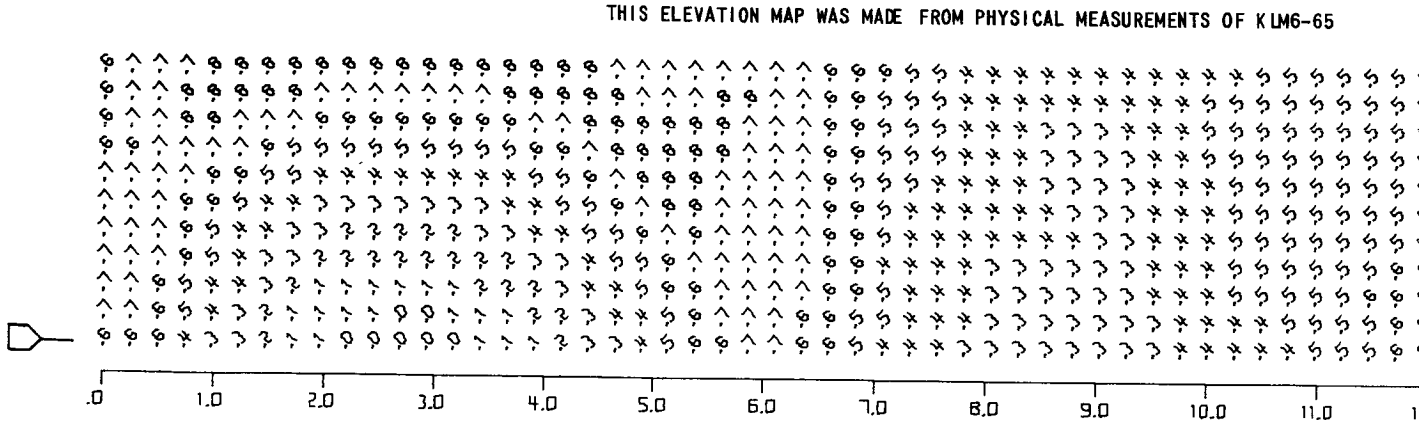

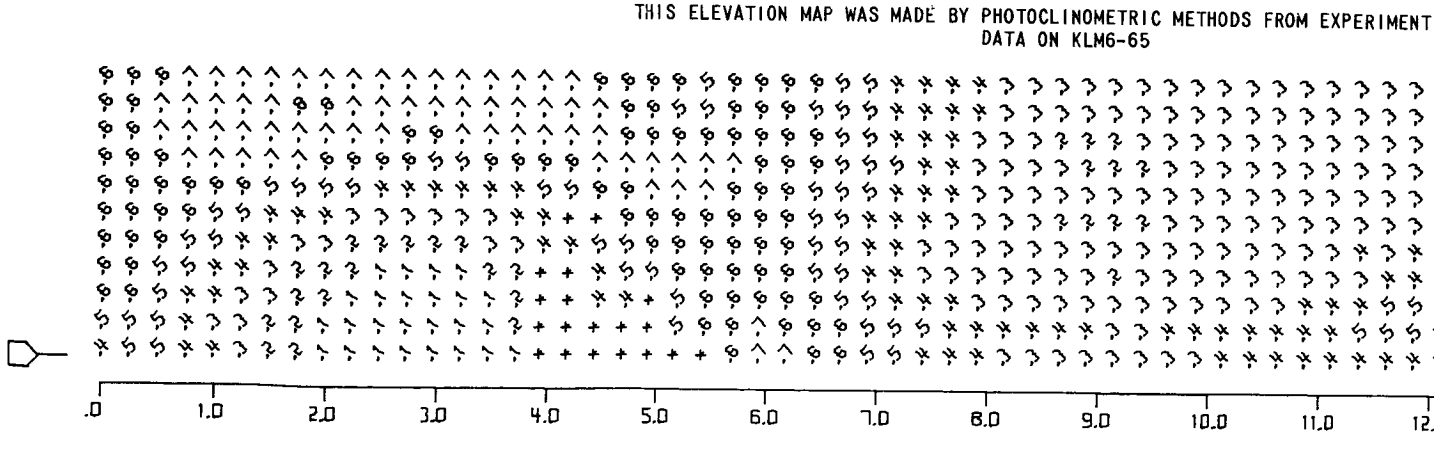

Figure A1-43. ELEVATION MAPS (I) MADE FROM PHYSICAL
OBTAINED BY PHOTOCLINOMETRY IN EXPERMI

FOLDOUT FRAME

MODEL

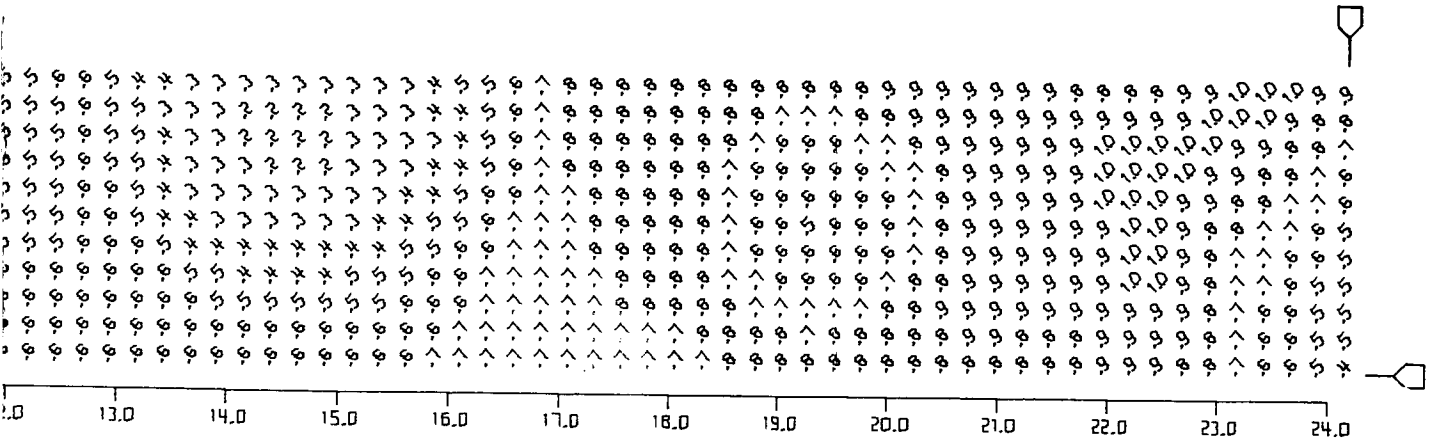

ERS ON THE MOON

TION ROUNDED TO THE NEAREST .1 METER
OW AREAS
IAL SCALE 1:48

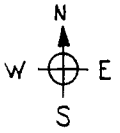

PHOTOCLINOMETRY

18

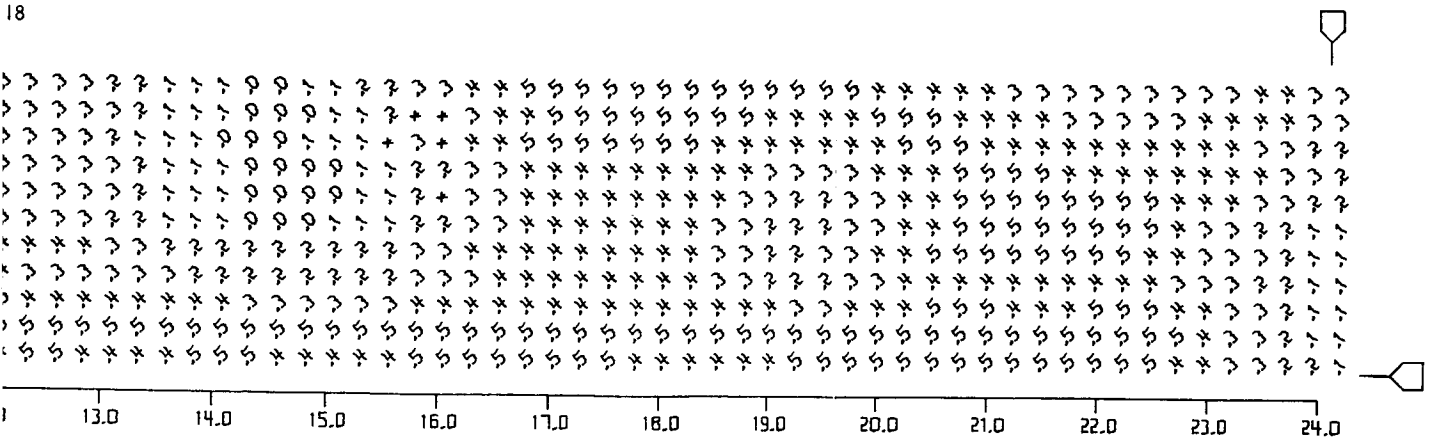

THE MOON IN THE PHASE PLANE

MEASUREMENTS OF KLM6-65 AND (2) MADE FROM DATA
NT 18

FOLDOUT FRAME 2

1 1

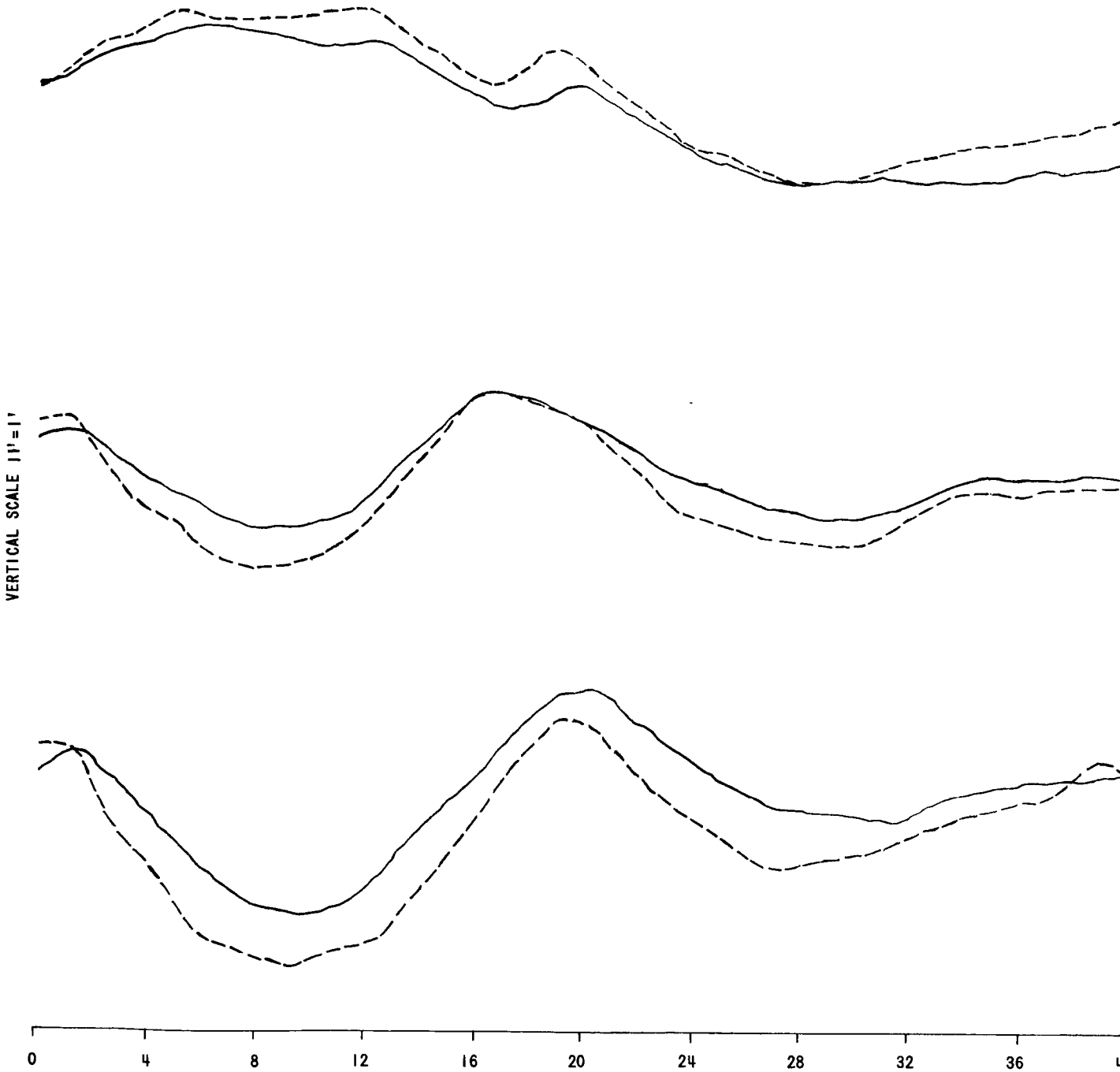

Figure A1-42. COMPARISON OF SELECTED PROFILES MADE BY PHO

FOLDOUT FRAME 1

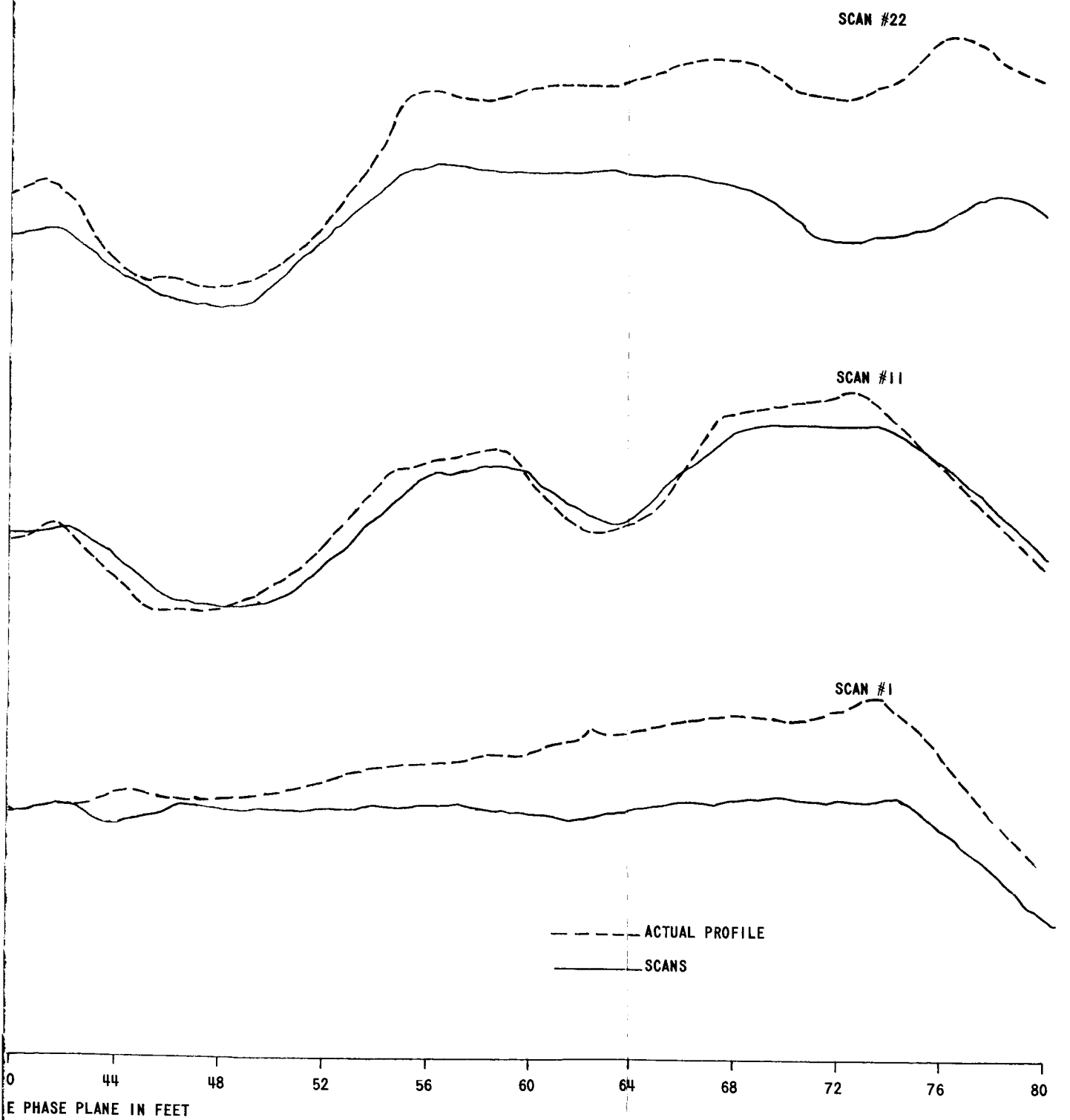

E PHASE PLANE IN FEET

TOCLIOMETRY WITH THE ACTUAL MEASURED PROFILES OF KLM6-65

FOLDOUT FRAME 2

1

6. The computer was given an elevation for the beginning and end of each scan that fit these adjusted Y profiles.
7. The computer created a second set of profiles (run 2) with adjusted heights. The lowest point in any profile in experiment No. 18, run 2 occurs at 9.02 feet in the first scan and amounts to 0.169 feet. i.e., All elevation values are positive.
8. The heights were converted into meters and rounded to the nearest 0.1 meter by adding 0.05 meter to the calculated adjusted height and printing only the first figure.
9. Figure A1-43 shows the elevation map obtained by this method using the Calcomp Plotter. The data are plotted for every other point in alternate scans. In this way larger size numbers could be used in the 2-x 20-inch map. The numbers were turned 45° from the vertical in order to eliminate confusion between adjacent numbers.
10. In Figure A1-43, the horizontal scale was printed in meters in order to compare this map with the stereo map of the same area made by NASA.

Figure A1-43 also shows an elevation map obtained from physical measurements made on the KLM6-65 model. The model was mounted on the table of a Ferranti Coordinate Measuring Machine and a probe brought down to contact the undusted model. X, Y, and Z dimensions were measured and recorded to an accuracy of

0.001 inch. Twenty one scans separated by 0.1 inch on the model were made in a direction that become the phase plane. Each scan included 201 points separated by 0.1 inch. This covered the 2 x 20-inch area of interest, with 4,221 elevations. These elevations were rounded in 0.1-meter intervals by adding 0.05 to the meter conversion and printing only the first figure (for elevations above 0.9 the first 2 figures were printed). In order to accommodate large size figures in the 2 x 20-inch map every other point and every other scan were plotted in Figure A1-43. The X and Y scale of the original map is 1:48 and the horizontal scale at the bottom has been printed in meters.

Shadow areas have been marked with an asterisk by the computer for each point where the microdensitometer voltage indicated that the instrument was reading base plus fog on the film. It will be noticed that only two areas are so marked on the map. Several additional areas should have been found, in particular, the 8:1 concave spherical surface near 19 meters has a shadow on the east side as shown in Figure A1-40.

Contour Map Comparison - KLM6-65

Figure A1-44 shows a comparison of three contour maps; one made from measurements of the model KLM6-65, one made by stereo methods from stereo plates enlarged 9.7 X from photo system B parameters, and one made by photo-clinometry with photo system B parameters. Both mapping methods show the primary features, the craters at 3, 15, 19 and 24 meters. Table A1-XX lists these craters with comments. The stereo map shows a gradual rise in terrain toward the east. It is remarkably close to the model, however, in view of the fact that both the model builder and the stereo plotter arbitrarily selected a zero elevation. The same comment can be made about the map made by photo-

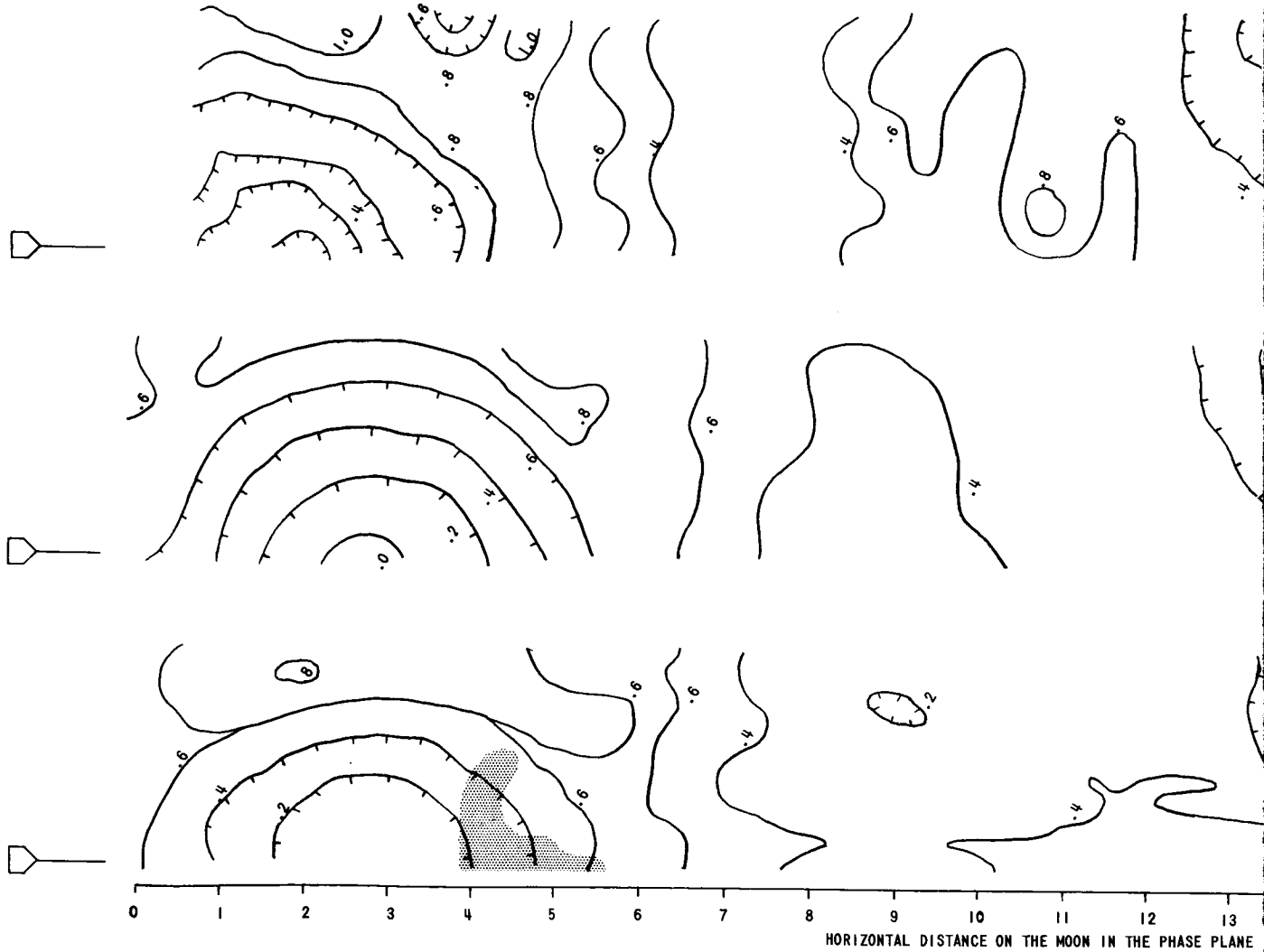

ORIGINAL SCALE 4:48

Figure A1-44. COMPARISON OF CONTOUR MAPS MADE BY STEREO
WITH A CONTOUR MAP MADE FROM MEASUREMENTS

FOLDOUT FRAME 1

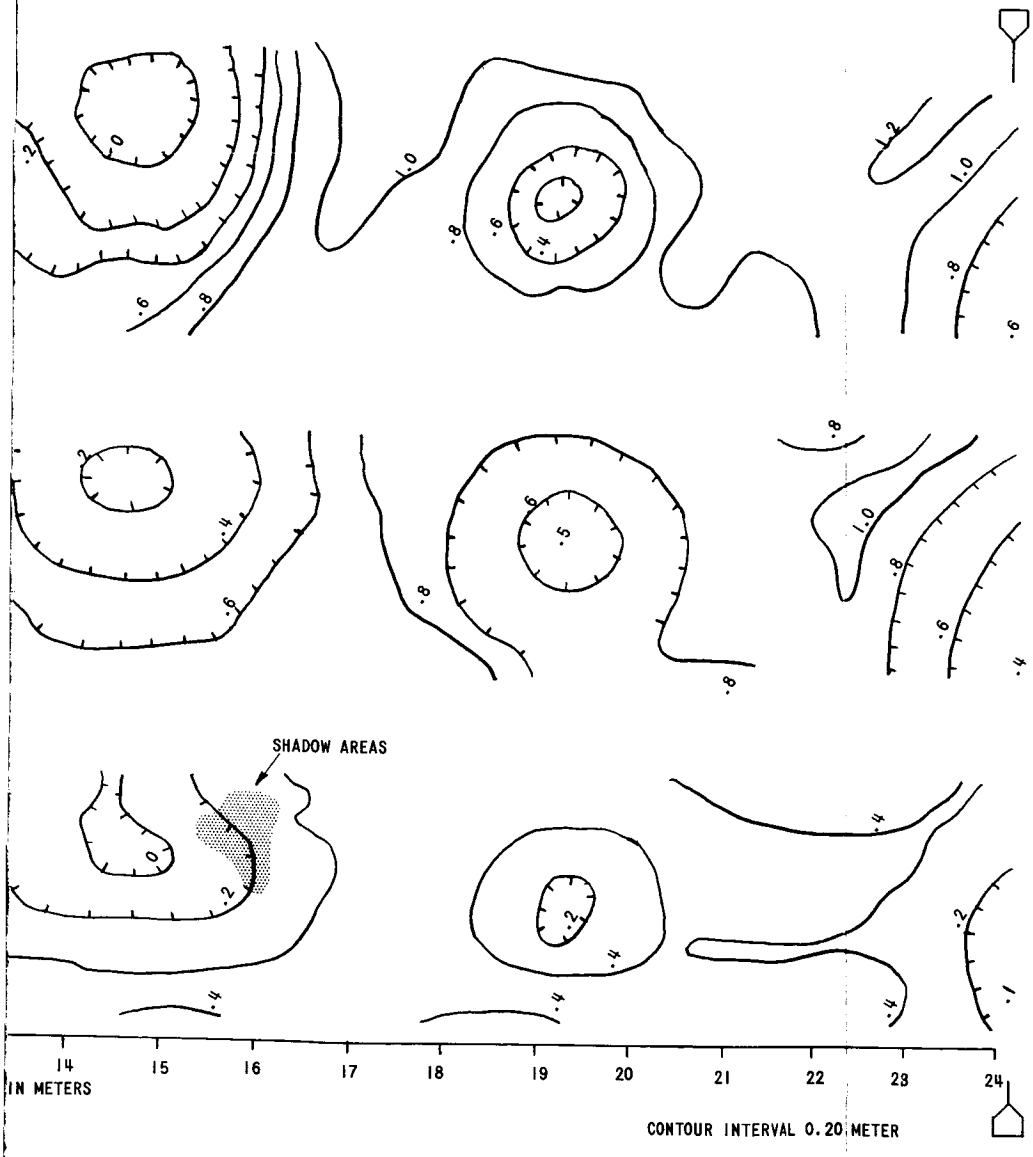

STEREO

CONTOUR MAP TO THE LEFT WAS MADE BY STEREO METHODS AT NASA FROM STEREO PHOTOGRAPHS OF KLM6-65 SUPPLIED BY EASTMAN KODAK CO. THESE PLATES WERE POSITIVES ENLARGED 9.7 TIMES FROM PHOTO SYSTEM B, PLATES 17 AND 18 SUN ELEVATION 14.3°

MODEL

CONTOUR MAP TO THE LEFT WAS MADE FROM PHYSICAL MEASUREMENTS ON KLM6-65

N
W E
S

PHOTOCLINOMETRY

CONTOUR MAP TO THE LEFT WAS MADE BY PHOTOCLINOMETERY. PHOTO SYSTEM B, SUN ELEVATION 14.3° EXPERIMENT 18 DATA.

METHODS AND BY PHOTOCLINOMETRY
ON KLM6-65.

FOLDOUT FRAME 2

1

clinometry that arbitrarily selected as level a surface that sloped the terrain downward to the east. Further adjustments in either method could easily correct for this effect when additional knowledge of the elevations is available. In general, stereo tended to plot the slopes steeper than actual and photoclinometry tended to plot the slopes less steep than the actual model.

Adjustment can easily be made to the photoclinometry calculation to make the slopes steeper, provided it can be shown that the slopes as plotted are indeed too shallow. This can be accomplished by making the curve of microdensitometer voltage versus exposure have a steeper slope.

TABLE A1-XXI

COMMENTS ON CONTOUR MAPS MADE BY STEREO AND PHOTOCLINOMETRY METHODS

Feature	Stereo Map	Photoclinometry Map
Crater at 3 meters	Correct elevation	Correct elevation
	Correct depth	Shallow crater
	Correct slopes	Nearly correct slope
Crater at 15 meters	Elevation correct	Elevation low
	Low bottom to crater	Nearly correct slope
	High rim to east	
	Steep slope to east	
Crater at 19 meters*	Diameter to depth about	Elevation low
	4 to 1	Nearly correct slope
	Steep and deep crater	
Crater at 25 meters	Elevation 0.2 meter high	Elevation low
	Correct slope	Shallow slope

*This is a concave spherical surface with diameter to depth 8:1

Experiment No. 18, Run 3

To properly compare the photoclinometry map with the model it was decided to adjust the photoclinometry heights to the same zero elevation as the model.

This was accomplished as follows:

1. The calculated heights of the first scan were subtracted from their corresponding heights on the model. It was necessary to interpolate between calculated heights and measured heights since the spot spacings were different between the calculated heights (0.41 foot on moon) and the measured heights (0.40 foot on the moon). From this data an error curve was created for this scan.

2. From the above difference points the computer found a first degree difference equation for scan 1.

3. The value of this first degree equation at X = 0 and at X = 24.36 meters is the amount of height required to be algebraicaly added to the ends of the photoclinometry derived profile by the error of closure method to bring scan 1 profile into a best fit with the model surface.

4. The photoclinometry calculated heights for scan 1 were adjusted according to this best fit equation.

5. Similarly, all heights on all scans were adjusted to bring them into a best fit with their corresponding profiles of the model. This was Experiment No. 18 Run 3.

All of these adjusted heights were then subtracted from their corresponding heights on the model. Again it was necessary to interpolate between points because of the different spot spacing. A plot of these differences between the model and the photoclinometrically derived map is shown in Figure A1-45.

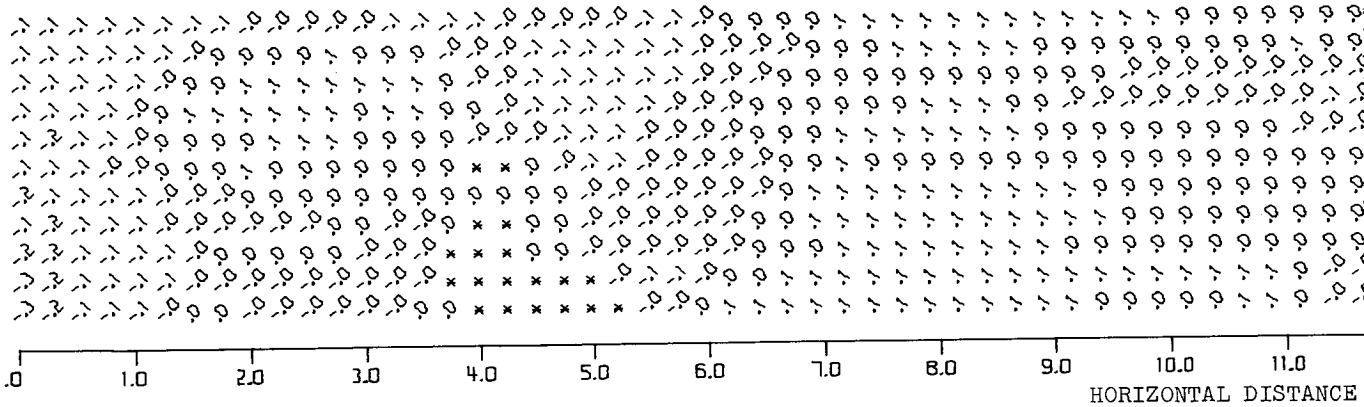

POSITIVE VALUES SHOW WHERE THE MAP INDICATES HEIGHTS ABOVE THE MODEL

Figure A1-45. DIFFERENCE IN HEIG
EXPERIMENT 18 RUN

FOLDOUT FRAME 1

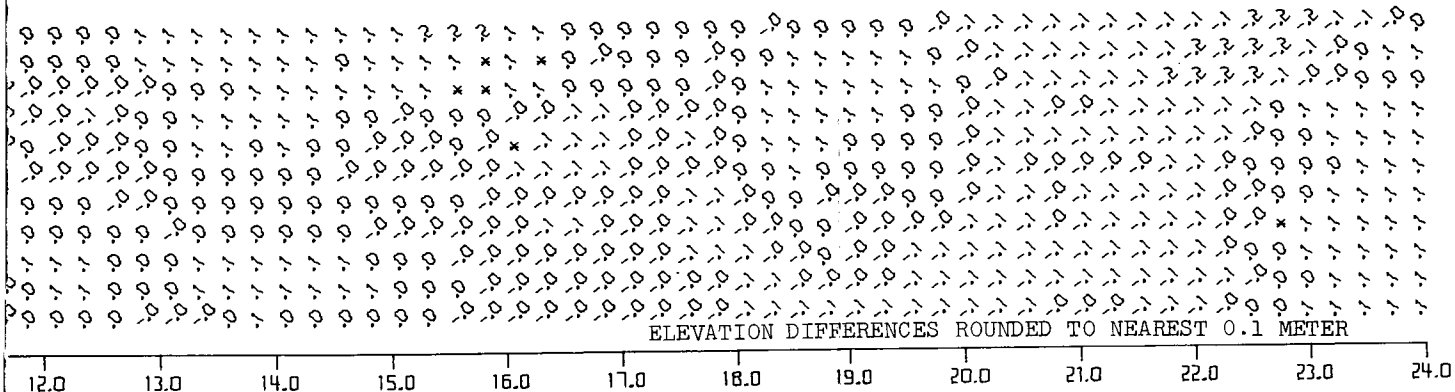

IN THE PHASE PLANE IN METERS

NEGATIVE VALUES SHOW WHERE THE MAP INDICATES HEIGHTS BELOW THE MODEL

HT BETWEEN CALCULATED ADJUSTED HEIGHTS
3 AND THE MODEL

FOLDOUT FRAME 2

As a measure of the agreement between the surface derived by photoclinometry and the surface of the model the mean of the elevation differences between these two surfaces was obtained, neglecting any of the points in the shadow areas. This mean has a value of - 0.00136 meter (0.053 inch) which shows an extremely good forced fit.

The 2-sigma value for the differences in height between the photoclinometry elevation and the model dimensions is ± 0.13 meter (5.1 inches) over the mapped 8-x 80-foot area based upon the 4290 calculated adjusted height values obtained from the data in Run 3.

The following table shows the distribution of these differences from which the 2-sigma value was calculated:

Difference in Meters	Number of Calculated Values
-0.4	0
-0.3	6
-0.2	88
-0.1	829
0	2358
+0.1	868
+0.2	37
+0.3	0
Shadow	104

Comments on the Difference Map

An examination of this difference map shows that on the photoclinometric map the heights are everywhere within ± 0.1 meter (± 4 inches) of the correct elevation over the 8-x 80-foot area except in three small areas. The elevation

errors in two of these small areas reach + 0.2 meter (+ 8 inches) and - 0.2 meter (- 8 inches) and the third small area reaches - 0.3 meter (- 12 inches).

Profiles of the 22 traces were made on the Calcomp Plotter at a scale of 1:48. These were traced on stiff paper then cut out and assembled with a wooden spacer to make a three dimensional scale model of the mapped surface. Figure A1-46 is a photograph of this assembly showing the 22 traces in their respective positions along with a section of KLM6-65 showing the original mapped surface outlined with a narrow white tape.

Conclusions from Experiment No. 18

1. Good contour maps can be made from photo system B lunar photography by either stereo plotting or photoclinometry.
2. Photoclinometry requires only one vertical photograph but depends upon the assumption of a constant albedo. A variable albedo, unless monitored and corrected, will map slopes that are not present on the lunar surface or fail to map slopes that are present on the lunar surface.
3. Contour intervals of 0.1 meter to 0.2 meter should be possible with photo system B using either stereo plotting or photoclinometry.
4. A few bench marks of known height will increase the accuracy of the contour maps made by either the stereo or photoclinometric methods.
5. If it can be shown that photoclinometry methods are giving slopes that are either too steep or too shallow, adjustments can be made to the program to bring the slopes into agreement with expected values.

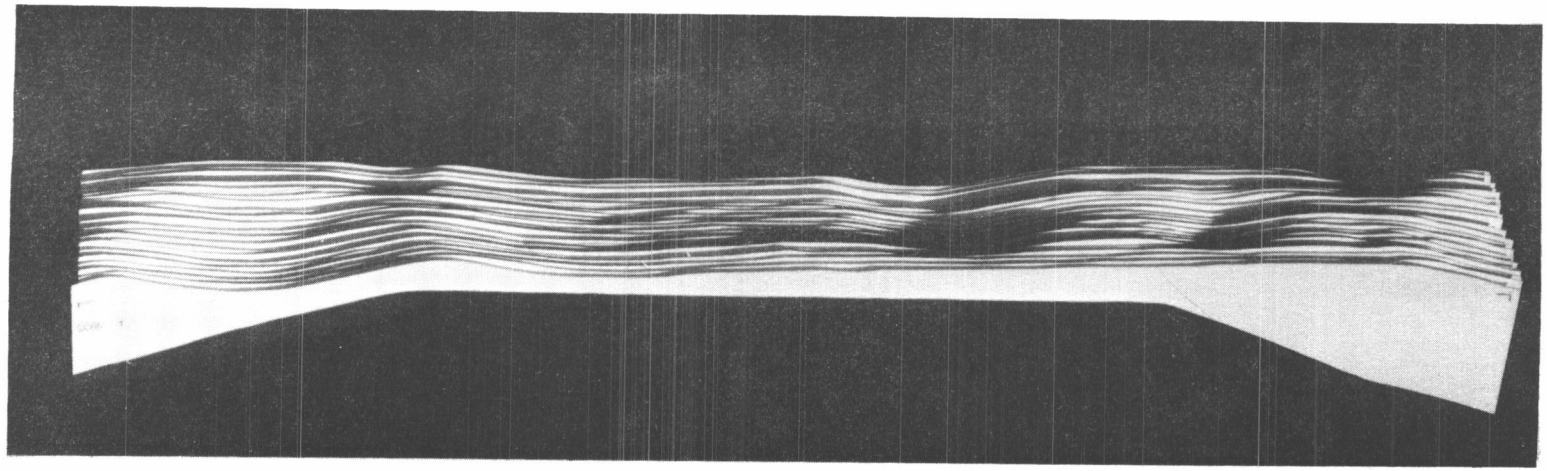

ASSEMBLED PROFILES

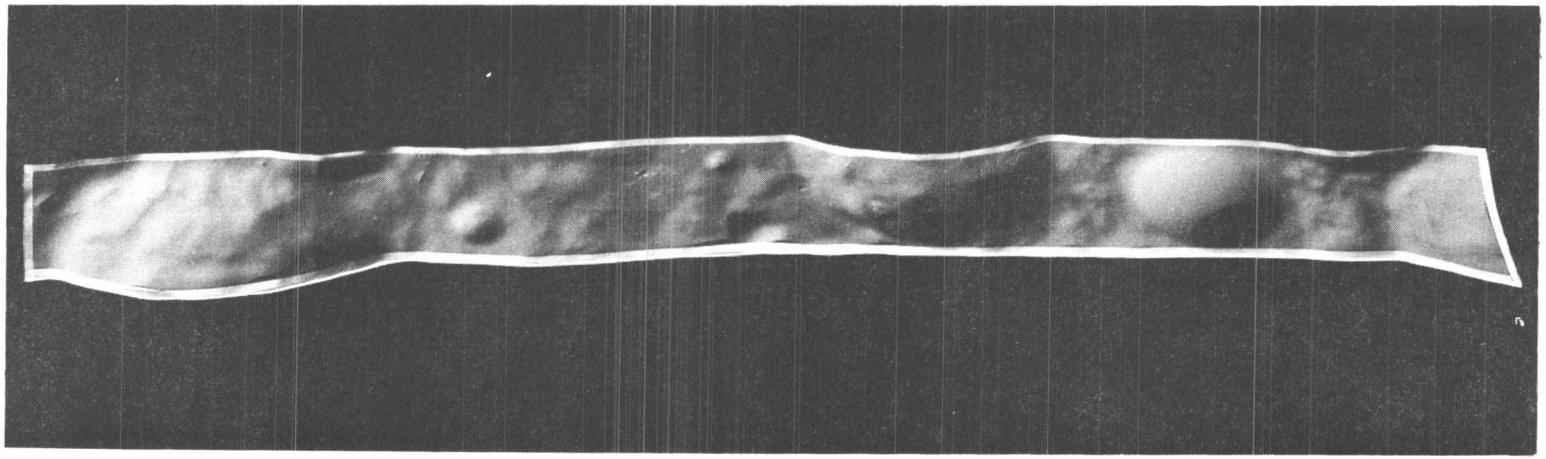

UNDUSTED SECTION OF KLM6-65

Figure A1-46. PHOTOGRAPHS OF THE ASSEMBLED PROFILES MADE FROM EXPERIMENT 18, RUN 3 DATA AND THE COMPARABLE SECTION OF KLM6-65 MODEL.

6. The error of closure method used to adjust the profile in experiment No. 18 will be useful for adjusting lunar profiles provided:
   a. the slope adjustment is not too great (less than about ±5°)
   b. good elevation data can be obtained on which to base the adjustments.

7. After adjusting experiment No. 18 data by Run 3 (photo system B) the 2-sigma value for difference in height between the model and the map made with photoclinometry was ± 0.1306 meter (± 5.1 inches) based upon 4290 data points.

A.2 STEREO MAPPING

Simulated lunar stereo photography from two systems was studied. System A simulates the photography expected from the 24-inch lens on Lunar Orbiter, while system B is a hypothetical system yielding higher resolution. Table A2-I lists the basic parameters for these systems; Table A2-II itemizes the glass plates that were sent to NASA for stereo mapping.

Photo System A

The Lunar Orbiter will take high resolution photographs over selected areas of the moon at a scale of 1:75,450 on 70mm SO-243 film using a 24-inch lens. In this Lunar Photo Study (LPS), the lunar models are at a scale of 1:48. The original LPS photography was taken on SO-243 film at a scale of 1:1572 which matches the LOP scale. (1:48 x 1:1,572 = 1:75,450). LOP will scan and transmit the exposed and processed images to a ground reconstruction station which will reconstruct sections of the 70mm film at a scale 7.2 times the vehicle scale. The scale on the ground will be 1:10,500 with the picture reproduced at an over-all gamma of about 2.3 and a limiting resolution near 16 lines/mm. To simulate the LOP ground reconstruction, the original photography from LPS is enlarged to match LOP in scale, gamma, and resolution.

Three photographs of LM-9 were made - one simulating vertical photography for the photoclinometry study (Experiment No. 15) and two at an angle of 7 1/2° from the vertical to provide for the right and left eye stereo images. Enlargements from this stereo pair were mounted on 7-inch x 7-inch glass plates and sent to NASA for stereo plotting. (Plates 5 & 6.)

Similarly, three photographs of KLM6-65 were made at this scale for study by stereo and photoclinometry. (Plates 11 and 12.)

TABLE A2-I

PHOTOGRAPHIC PARAMETERS FOR LUNAR MAPPING

Orbital System	A	B*	B (3x)**	B (9.7x)***
Original scale	74,450	30,000		
Original film, high contrast resolution, lines/mm	115.	138		
Scale of film record on earth	10,500	30,000		
Ratio, taking/earth resolution	7.2	1.0		
Laboratory Model				
Model Scale	1:48	1:48		
Size, inches, of KLM6-65	40 x 40	40 x 40		
Photographic reduction from model	1:1570	1:625		
Lens, focal length - speed	15mm-f/15	15mm-f/11		
Film	SO-243	SO-243		
Original resolution, lines/mm	115	138		
Enlargement	7.2x	none	2.9x	9.7x
Final scale for analysis (on 7" x 7" glass plate)	1:10,000	1:30,000	1:10,500	1:3,100
Final resolution, lines/mm (on 7" x 7" glass plate)	16	138	32	10
Over-all system gamma	2.34	1.21	2.42	2.42
Stereo 1/2 angle	7 1/2°	15°	15°	15°
Equivalent altitude if made by a 6" taking lens, feet	5,250	15,000	5,250	1,550
Final image size, KLM6-65, mm	4.66 sq.	1.62 sq.	4.66 sq.	15.6 sq.
Pitch of limiting tri-bar at lunar surface - inches	25.8	8.5	12.4	12.2
mm	650	216	320	310

*B is a hypothetical system with 2.5 times the scale and 20 percent more resolution than system A. The B film uses no TV transmission link.

**B (3x) is a 2.9x enlargement used to compare B photographs with system A at the same scale.

***B (9.7x) is a 9.7x enlargement to make the correct geometric simulation in the NASA stereo equipment.

TABLE A2-II

7-INCH x 7-INCH GLASS PLATES FOR STEREO PLOTTING

Plate No.	System	Eye	Model	Pos-Neg
1	A	Left	LM-3	Pos.
2	A	Right	LM-3	Pos.
3	B (3x)	Left	LM-3	Pos.
4	B (3x)	Right	LM-3	Pos.
5	A	Left	LM-9	Pos.
6	A	Right	LM-9	Pos.
7	B (3x)	Left	LM-9	Pos.
8	B (3x)	Right	LM-9	Pos.
9	B orig.	Left	LM-9	Neg.
10	B orig.	Right	LM-9	Neg.
11	A	Left	KLM6-65	Pos.
12	A	Right	KLM6-65	Pos.
13	B (3x)	Left	KLM6-65	Pos.
14	B (3x)	Right	KLM6-65	Pos.
15	B orig.	Left	KLM6-65	Neg.
16	B orig.	Right	KLM6-65	Neg.
17*	B (9.6x)	Left	KLM6-65	Pos.
18*	B (9.6x)	Right	KLM6-65	Pos.

*These glass plates were 9 1/2 inches x 9 1/2 inches in order to fit the Wild B-8 Stereo Plotter.

LOP also uses a 3-inch lens for stereo photography, but these small scale views will not show the detail recorded by the 24-inch lens. Since the LPS program is directed at detailed mapping of landing sites, no attempt will be made to simulate this low scale photography. The Lunar Orbiter does not intend to photograph in stereo at high resolution, but a small strip of overlap between frames will yield stereo views at a half angle of 7 1/2°. This is the area of interest simulated above.

Photo System B

Photo system B is a hypothetical system producing 20 percent better resolution (in lines/mm) at a scale 2 1/2 times larger than LOP and without TV transmission to earth. The simulated original photography is on SO-243 film at a scale of 1:625 giving a lunar scale of 1:30,000 (model is 1:48) and a resolution of 134 lines/mm. Stereo half angles of 15° are used in this study.

Stereo Measurements

The stereo plates of photo system A and photo system B listed in Table A2-II were sent to NASA for evaluation. On these plates only spot height readings at selected points in model LM-9 on plates number 7 and number 8, photo system B, were possible. The LM-3 model showed insufficient detail for stereo measurement and the LM-9 model in photo system A did not have sufficient resolution for the size of the model to make height determinations. Figure A2-1 shows some of these spot readings from photo system B drawn to scale on a profile of LM-9. To establish the base from which to draw these height measurements, the eight readings at the ends of the profile were averaged. The height values of the observations are the difference between the height readings and this average.

The photography of the KLM6-65 model was provided to NASA with the incorrect geometric simulation for evaluation on the Wild B-8 Stereo Plotter. Consequently, plates number 17 and 18 were made with photo system B at an enlargement of 9.7 times to give the correct geometric simulation and were sent to NASA for evaluation. The results of this evaluation are compared with the results of photoclinometry from experiment number 18 in Figure A1-44.

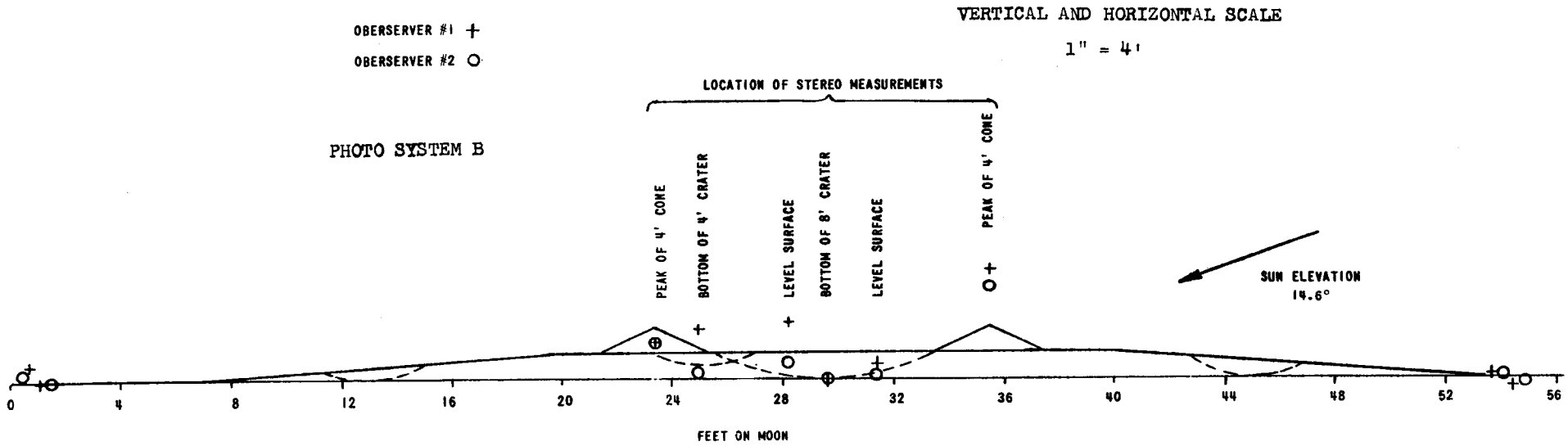

Figure A2-1. STEREO MEASUREMENT L-M 9

A.3 ERROR ANALYSIS

Two methods for analyzing the uncertainties in photoclinometry have been used in this study. The first method is summarized in Table A3-I which shows the estimated 2-sigma error values of the parameters that influence the measurement of the tau angle for both the laboratory study and an LOP mission. These errors are expressed as their equivalent error in log exposure to provide a common basis for summing the errors. It is more likely that the errors would accumulate in a random manner with some errors positive and some negative. Perhaps a better approach would be to use a Monte Carlo or similar summing technique for obtaining the tau angle uncertainty which would give a lower tau angle uncertainty for these amounts of component uncertainties. In the interest of simplicity the errors in this analysis have been root sum squared and the corresponding change in tau angle for each system has then been calculated.

TABLE A3-I

LOP PHOTOCLINOMETRY

2 - Sigma Error Analysis

Laboratory Log E	Factor	Mission Log E
0.018	Illumination	0.009
0.027	Albedo	0.04
0.004	Lens Transmission	0.006
0.002	Shutter Time	0.02
-	Shutter Uniformity	0.013
-	Flare	0.008
0.004	f/Number	0.0006
0.04	Processing	-
-	LOP to GRE Photometry	0.06
0.006 (Copper oxide)	Photometric Function (Lunar)	0.20
0.004	Scanning and Microdensitometer	0.004
±0.052	Root Sum Square, Log E	±.226
±2.5°	Equivalent Tau Uncertainty	-15°, +7°

The following paragraphs discuss these estimates.

Illumination

Laboratory

The illumination on the models was measured with a Weston Model 756 Illumination Meter. The precision of this meter in the range of 44 foot-candles is about 4 percent, which gives a variation of ± 2 foot-candles in this measurement and a Δ log E of ± 0.018.

Lunar Mission

The illumination of the moon by the sun is quoted by several authorities as 12,000 to 12,500 foot-candles. This range of 500 foot-candles is a variation of about ± 2 percent and is equivalent to a Δ log E of ± 0.009. Maximum earth shine is less than 3 foot-candles and will not influence photographs exposed for sunlight.

Albedo

Laboratory

The albedo of the dusted copper oxide was calculated from measurements made with a Spectra Prichard Photometer #119. Several measurements were made with a clean surface of magnesium oxide as a standard. The mean, standard deviation, 2-sigma value, percentage error, and the 2-sigma value Δ log E were calculated as shown in the following table.

Lunar Mission

The albedo of the lunar surface have been measured by astronomers to be between 0.05 and 0.18. It is estimated that the albedo can be determined within 10 percent. This value is used in the table below.

	Albedo Value	Standard Deviation	2-Sigma	% Error (2-Sigma)	Δ Log E (2-Sigma)
Laboratory	0.0565	0.0018	0.0036	6.4	0.027
Lunar Mission	0.05 to 0.18			10.0	0.04

Lens Transmission

Laboratory

The 15mm f/2.8 Ektar lens used in the laboratory has a measured axial transmission in white light of 0.89. Our measurements show that the 2-sigma error in this value is about 1 percent of a Δ log E variation of 0.004.

Lunar Mission

The 24-inch lens used in the LOP has an obstruction in the center which required a slight modification in the technique for measurement of transmission. The 2-sigma error is estimated as 1.3 percent. This gives a Δ log E = 0.006.

Shutter Time and Shutter Uniformity

Laboratory

Exposures longer than one second were made with a Microflex timer that is accurate to about 1/2 percent when measuring a time interval of 20 seconds. This error is equivalent to a Δ log E of 0.002.

Lunar Mission

The LOP 24-inch camera uses a focal plane shutter that is calibrated during acceptance testing for both exposure time and relative exposure within the frame. It is estimated that variation from the calibration will not exceed 5 percent in exposure time and 3 percent in relative exposure within the frame. These errors become Δ log E values of 0.02 and 0.013 respectively.

Flare

Laboratory

The Lunar Photo Study photographs were made in a dark room with a very small illuminated target near the center of the field. Since nearly all of the film plane was unexposed the amount of flare in the image is considered insignificant.

Lunar Mission

It is estimated that there will be less than 2 percent flare light in the LOP camera. This amount is equivalent to 0.008 Δ log E.

F-Aperture

The measurement of aperture involves knowledge of the focal length and lens diameter.

Laboratory

These two dimensions for the 15mm lens are known to about 0.6 percent which combine to make the root sum square about 0.85 percent giving a Δ log E of 0.004.

Lunar Mission

The two dimensions for the 24-inch lens are known to 0.03 percent for focal lengths and 0.15 percent for diameter. Those combine with a root sum square to 0.153 percent and give a Δ log E = 0.0006.

Processing - LOP To GRE

Laboratory

The densities of the photographs made in the laboratory have small errors in processing, sensitometry, and densitometry that for this study have been lumped together. The estimated error for these factors is nearly 10 percent which gives a Δ log E of 0.04.

Lunar Mission

The errors in calibration curves for all steps from the LOP vehicle film to the GRE film densities amount to 15 percent. This has a value of Δ log E of 0.06. These include the effects of BIMAT processing, readout scanning, electrical signal transmission, GRE reconstruction, sensitometry, and densitometry of the 35mm record.

Photometric Function

Laboratory

There is an error associated with measurement of the photometric function of the laboratory model. Factors of importance are the measurement of phase angle, the instrument and reading errors of the Spectra Prichard Spot Brightness Meter, and the knowledge of tau angle. The 2-sigma variation of the observed points from the equation derived by the computer amounts to 0.28° in tau angle. This value will be used in the laboratory calculations and is equivalent to a Δ log E = 0.006.

Lunar Mission

The errors for the photometric function for the lunar mission are made up of at least two components. The first - the estimated aiming error of about 0.2° is very small compared to the estimated 10° error* associated with the scattered observations used to create the curve for the lunar photometric function. The change in the lunar photometric function from a phase angle (alpha) of 70° to 80° at zero tau angle is

$$\Delta\Phi = \Phi_{70°} - \Phi_{80°}$$

$$= 0.1375 - 0.0695 = 0.0680$$

This error in phi amounts to a fractional error in tau of

$$\frac{0.0680}{0.1137} = 0.60$$

(phi at tau = 0° and alpha = 75° is 0.1137)

or an uncertainty in log E of

$$\log 1.60 = 0.20$$

---

*JPL Technical Report No. 32-664, Figure 10, Page 10, g = 74.5°. "The Lunar Reflectivity Model for Ranger Block 111 Analysis," D. Willingham.

Microdensitometer Tracing

The uncertainty in a density determined by the microdensitometer is estimated to be about 1 percent for both the laboratory study and the lunar mission. This error gives a Δlog E of 0.004.

Comment on the Error Analysis

The log E errors were root sum squared to combine the 2-sigma errors into an equivalent log E error for all the components. These values of ± 0.054 for the laboratory study and ± 0.226 for the lunar mission are converted to equivalent uncertainty in the tau angle as follows:

For small changes in Δ log E which will be equally small changes in Δ log Φ, the uncertainty in tau =

$$\left[\text{antilog } (\Delta \log \Phi) - 1\right] \times \left(\Phi_T = 0\right) \times \left(\frac{\Delta T}{\Delta \Phi}\right)$$

For the Laboratory Study:

$\Delta T = (1.13\text{-}1) \times (0.1137) \times (172) = \pm 2.6°$

For the Lunar Mission:

The relatively large value of 0.226 log E can best be evaluated by an inspection of the phi-tau curve. Such a change in Δ log E will be an equal change in Δ log phi and is computed as an error in tau angle of -15° to + 7°.

Obviously the major contributor to this large error in photoclinometry from the LOP mission is the uncertainty in the lunar photometric function. These measurements are taken from the earth where the knowledge of the lunar slopes has been limited to large areas of the lunar surface and where measurements must be made through the earth's unsteady atmosphere. In the

laboratory, the observed points of the phi-tau-alpha curve differ from the computed curve by a 2-sigma error of 0.28° tau angle. With better data from the lunar surface it is possible that this large error can be reduced to a much smaller value. If the photometric function can be determined for the moon as well as it is known for the laboratory materials, then the Λ log E root sum square becomes 0.08 for the lunar mission and the 2-sigma uncertainty in tau becomes ± 3.9°.

Second Method of Error Analysis

The second method of analyzing the uncertainties in the tau angle is to derive an expression for the effect on the tau angle of a small change in any one of the mapping parameters. Such an expression is derived in the next paragraph, and its use demonstrated in Table A3-III where the root-sum-square of the uncertainities in tau are found to agree with the values obtained earlier by other less direct methods.

The four fundamental equations that determine the lunar profile from vertical lunar photography are:

$$V = f(d) = f(E) \qquad (1)$$

$$E = \frac{10.76\, I_{\rho} \Phi T t}{4\, N2} \qquad (2)$$

$$\Phi = f(\alpha, \text{tau}) \qquad (3)$$

$$h_{x_n} = \sum_{i=o}^{n} (\tan \text{tau}_i \cdot \Delta x_i) \qquad (4)$$

Definition of Terms

D = Density

E = Exposure (meter-candle-seconds)

V = Microdensitometer volts

I = Illuminance on the scene, (foot-candles)

ρ = Albedo

Φ = Photometric function (a function of alpha and tau)

T = Transmission of the lens

t = Exposure time (seconds)

N = f/aperture

h_{x_o} = Initial height of trace

h_{x_n} = Height of the profile at x_n position

x = Spot spacing projected to the lunar surface

tau = Component of the angular slope of the lunar surface in the phase plane.

$$A = \Phi/E = \frac{4N^2}{10.76\ I_o T t}$$

In experiment No. 5 the following parameters were measured:

N = f/3.8 measured at a marked f/4.0 lens aperture

I = 44 foot-candles illuminance

ρ = 0.0565, albedo

T = 0.89 Transmission at center of lens in white light

t = 20 seconds, exposure time

E = 0.94 meter-candle-seconds

A therefore becomes:

$$A = \frac{4 \times 3.8^2}{10.76 \times 44 \times 0.0565 \times 0.89 \times 20}$$

$$= 0.121$$

For slopes near zero tau angle, these equations can be simplified to calculate the effect on the tau angle of small changes in the variables. By differentiating the first equation relating microdensitometer voltage to exposure, a coefficient is obtained that describes the effect on exposure for small changes in microdensitometer voltage:

$$\frac{\Delta E}{\Delta V} = C_1 \qquad (5)$$

$$\Delta E = C_1 \Delta V$$

where ΔE = small change in exposure

ΔV = small change in voltage

C_1 = slope of the curve of microdensitometer volts vs exposures at a specific point

In experiment No. 5, $C_1 = 0.28$ meter-candle-seconds/microdensitometer volt at 6 volts near the region where tau equals zero.

Equation 3 can be simplified for small changes in phi near zero tau angle and for a constant sun elevation $(90 - \alpha)$ by differentiating the tau - phi curve.

$$\frac{\Delta \text{ tau}}{\Delta \text{ phi}} = C_2 \qquad (6)$$

$$\Delta \text{ tau} = C_2 \, \Delta \text{ phi}$$

where Δ tau = a small change in tau angle

Δ phi = a small change in phi, the lunar photometric function

C_2 = slope of the phi-tau curve at a specific point

In experiment No. 5, $C_2 = 172°$ near zero tau angle.

Equation (2) can be written -

$$\Phi = \frac{4\ EN^2}{10.76\ I_{\rho} Tt} = A\ E \qquad (7)$$

A coefficient can be obtained from equations 7 and 6 that expresses the relation between an uncertainty in the parameter and its effect on the angle tau by obtaining the partial derivitive of tau with respect to each parameter.

For example, the effect on the tau angle of an uncertainty in the measurement of N can be obtained as follows:

$$\Delta\tau = C_2\ \Delta\Phi$$

$$\frac{\Delta\tau}{\Delta N} = C_2\ \frac{\Delta\Phi}{\Delta N} = \frac{C_2\ 8\ E\ N}{10.76\ I\ \rho\ Tt}$$

For experiment No. 5

$$\frac{\Delta\tau}{\Delta N} = \frac{(-172)\ 8 \times 0.94 \times 3.8}{10.76 \times 44 \times 0.0565 \times 0.89 \times 20}$$

$$= -10.3°/\text{aperture unit}$$

Similarily coefficients for each of the other parameters can be obtained for any specific system. Table A3-II lists these equations and the coefficients for the parameters in experiment No. 5. These coefficients will change when

any one of the values in the equation change, but it should be easy to arrive at new values if the magnitude of the parameters are known.

Equation 14 can be used where the parameters in "A" remain constant, as in a single photograph of the lunar surface with constant albedo. The only variable would then be a change in density (microdensitometer volts). In experiment No. 5 for example:

$$\frac{\Delta\tau}{\Delta V} = (-172) \times 28 \times 0.121$$

$$= -5.85°/\text{volt}$$

The equations in Table A3-II are very useful in determining the effect of a small change in any one of the parameters on the tau angle. They should be easier to use and understand than the method of finding the change in Log E for a small change in a parameter and from this determining the change in tau angle.

Table A3-III has been prepared to show the error analysis by photoclinometry and covers the identical items listed in Table A3-I. The root sum square of the tau angle uncertainties is ±2.4°

The uncertainties in tau, shown in Table A3-III, are useful in showing the parameters that have the most influence on the total uncertainty. For instance, variations in albedo and processing are the largest contributors to the total uncertainty, and shutter time and microdensitometer scanning are nearly insignificant factors.

TABLE A3-II

EQUATIONS FOR OBTAINING THE COEFFICIENTS CONNECTING SMALL CHANGES IN TAU WITH SMALL CHANGES IN THE PARAMETERS.

Parameter	Equation	Units	Coefficient for Experiment No. 5	Equation Number
f/Aperture	$\frac{\Delta\tau}{\Delta N} = \frac{8C_2\ EN}{10.76\ I_\rho Tt}$	deg/Aperture Unit	-10.3	(8)
Illumination	$\frac{\Delta\tau}{\Delta I} = \frac{4C_2\ EN^2(-1)}{10.76\ {}_oTtI^2}$	deg/Foot-Candle	0.445	(9)
Albedo	$\frac{\Delta\tau}{\Delta\rho} = \frac{4C_2EN^2(-1)}{10.76\ ITt_o{}^2}$	deg/Albedo Unit	348	(10)
Transmission	$\frac{\Delta\tau}{\Delta T} = \frac{4C_2\ EN^2(-1)}{10.76\ I_\rho tT^2}$	deg/Transmission Unit	22.1	(11)
Exposure Time	$\frac{\Delta\tau}{\Delta t} = \frac{4C_2\ EN^2(-1)}{10.76\ I_\rho Tt^2}$	deg/second	0.98	(12)
Exposure	$\frac{\Delta\tau}{\Delta E} = \frac{4C_2\ N^2}{10.76\ I_\rho Tt}$	deg/m-c-s	-20.9	(13)
Microdensitometer Volts	$\frac{\Delta\tau}{\Delta V} = \frac{4\ C_1\ C_2\ N^2}{10.76\ I_oTt}$	deg/volt	-5.85	(14)
	$= C_1\ C_2\ A$	deg/volt	-5.85	(14)
Alpha (Phase Angle)	$\frac{\Delta\tau}{\Delta\alpha} = \frac{11.8°}{10°}$	deg/deg.	1.18	(15)

TABLE A3-III

PHOTOCLINOMETRY ERROR ANALYSIS

LABORATORY DATA FROM EXPERIMENT NO. 5.

Parameter	Symbol	Estimated error in Experiment No. 5	Coefficient Experiment No. 5	Uncertainties in Tau degrees.	$(tau)^2$
Illumination	I	2 foot-candles	0.445°/foot-candles	0.89°	0.79
Albedo	ρ	0.0036 albedo unit	348°/albedo unit	1.25°	1.56
Lens Transmission	T	0.009 Transmission unit	22.1°/Transmission unit	0.198°	0.0392
Shutter Time	t	0.1 second	0.98°/second	0.089°	0.0079
f/Number	N	0.03 aperture unit	-10.3°/aperture unit	-0.3°	0.096
Processing	-	0.094 m-c-s	-20.9°/ m-c-s	-1.8°	3.25
Photometric Function	Φ	*		0.28°	0.079
Scanning Microdensitometer	V	0.02 volt	-5.85°/volt	-0.12°	0.0144
	Sum of Squares				5.84

Root Sum Squares of the Tau Angle (Uncertainty in Tau) ± 2.4°

* The uncertainty in the Photometric function was obtained by computing the 2-sigma values from the single phi-tau curve obtained by a modified least squares curve fit from the observed phi-tau data.

A word of caution concerning the use of these coefficients. Both C_1 and C_2 are not constants but are the slopes of the curves between two parameters at a specific point. These will change in value for small changes in the parameters involved and must be re-evaluated each time they are used. C_2 is part of every one of the equations (except $\frac{\Delta\tau}{\Delta\alpha}$) and will change with change in alpha and change in phi. However, with constant alpha at zero tau angle the value will remain constant at -172° for a small change in phi. The absolute value of the coefficients cannot be compared directly because their influence upon the tau uncertainty depends upon the magnitude of the parameter uncertainty; only after that uncertainty has been multiplied by the coefficient can the effect of that parameter on the uncertainty in tau angle be determined.

The preceding analysis of error in tau angle ignores the variations caused by image grain. A measure of this effect was given in Figure A1-30 where scanning spots of 6.4, 16.5, and 53 microns gave for a level surface 2-sigma errors in tau angle of 3.31°, 2.45°, and 0.86°, respectively. For a realistic spot size of about 6 microns, it appears that the tau error from film grain is about equal to that shown in Table A1-XIV for the LOP laboratory study, i.e., ± 2.4°. Assuming that these two contributors can be root sum squared, the error values in Table A3-IV were calculated.

TABLE A3-IV

CALCULATED ERROR IN HEIGHT AFTER 100 FEET OF SCAN

Photo System	2-Sigma Error in Tau Angle Parameters*	Grain**	2-Sigma R-S-S Total Tau Error in Degrees	Spot Spacing Feet	2-Sigma Error in Height after 100 Feet of Scan
A. Lab	± 2.4°	± 1.2°	± 2.7	1.07	± 0.48
A. Mission	+ 7°	± 1.2°	+ 7.8	1.07	± 1.3
	- 15°	± 1.2°	- 15.4	1.07	± 2.8
B. Lab	± 2.4°	± 3.3°	± 4.08	0.307	± 0.39

* From Table A3-III or Table A3-I

** From Table A1-XIV or Figure A1-32

Since both height and tau angle are of concern, it is useful to calculate the error in height after 100 feet along a scan line. From a zero reference height at the start of a scan, the height after n readings is

$$h_n = \sum_{i=o}^{n} X_i (\tan \tau)_i$$

The variance, $\sigma_n^2 = \Sigma (X_i)^2 \ (\sigma_{\tan\tau})^2$

where x_i is the increment in distance along the scan and $(\sigma_{\tan\tau})^2$ is the variance in a single value of the tangent of the tau angle. The 2-sigma error values shown in column 6 of Table A3-IV were calculated for 100 equal increments as listed in column 5 and using the 2-sigma errors in the target of the tau angle equavalent to the R-S-S errors shown in column 4. These height errors are the uncertainty expected in the calculated height at the end of a scan covering 100 feet. The values are strictly for a scan across a uniform area where tau is zero, but they may have application to any scan across a potential landing area.

A.4 A SECOND METHOD OF PHOTOCLINOMETRY Φ_1/Φ_2

If two photographs of the same lunar area from two camera positions are made, many of the variables in the photometric function equation will cancel out and in particular it will not be necessary to have a knowledge of the albedo. Assuming the situation with two photographs taken as shown in Figure A4-1 from camera stations 1 and 2

where $\Phi = \dfrac{4N^2 E}{10.76 I \rho T t} = f(\alpha, \tau)$

the ratio $\dfrac{\Phi_1}{\Phi_2}$ becomes $\dfrac{T_2 t_2 E_1}{T_1 t_1 E_2}$

I, ρ, N^2 and the constants are common therefore canceling out in the ratio equation.

The transmission can be measured for any zone in the lens so the value of transmission ration T_2/T_1 can be easily found and will in many places in the photographic field be unity.

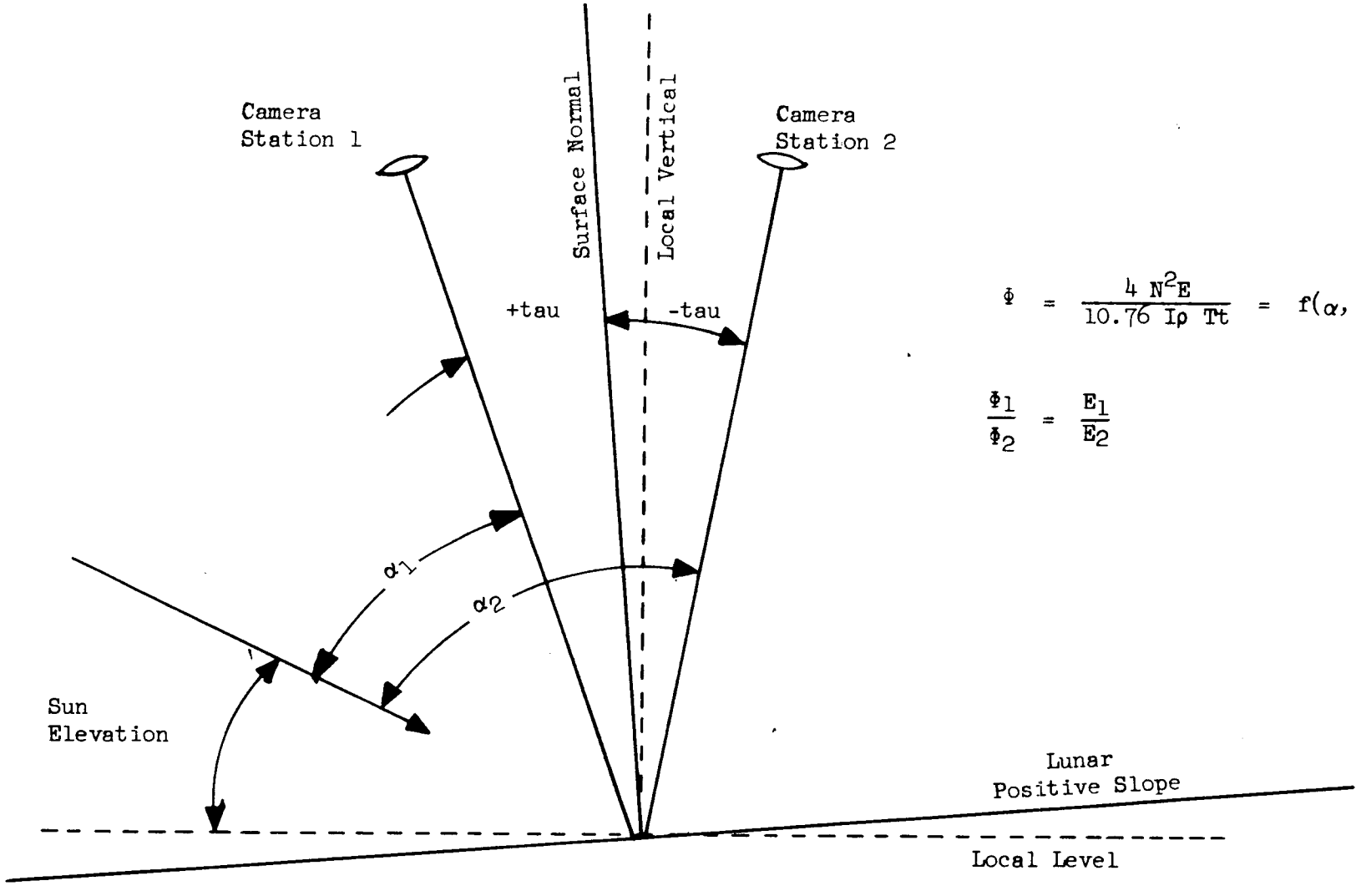

Figure A4-1. A SECOND METHOD OF PHOTOCLINOMETRY Φ_1/Φ_2, DEFINITIONS

If the exposure time is highly repeatable, the ratio t_2/t_1 will be equal to unity. The ratio of the photometric function, most of the time therefore, will become:

$$\frac{\Phi_1}{\Phi_2} = \frac{E_1}{E_2}$$

where E, the exposure, can be determined from a measurement of the density and the use of careful sensitometry.

Figure A4-2 shows the lunar slope plotted against the log of the ratio Φ_1/Φ_2 assuming knowledge of the photometric function and the angle alpha. In general, as the camera stations are separated, the magnitude of the ratio increases but soon turns back upon itself giving a double valued function. As the sun elevation becomes lower, the ratio curve becomes less steep which will help to improve the accuracy of the slope determination.

This system of photoclinometry looks promising for areas where not much detail is present in a lunar scene and where it would be difficult to analyze the photographs with stereo techniques. It can also be an additional technique to spot check the stereo slopes by photoclinometry. It will be necessary to obtain accurate measures of the alpha angles for the system to be useful.

This method is presented in the hope that it may become a useful tool for lunar mapping. An error analysis will be required before a good evaluation of its usefulness can be made.

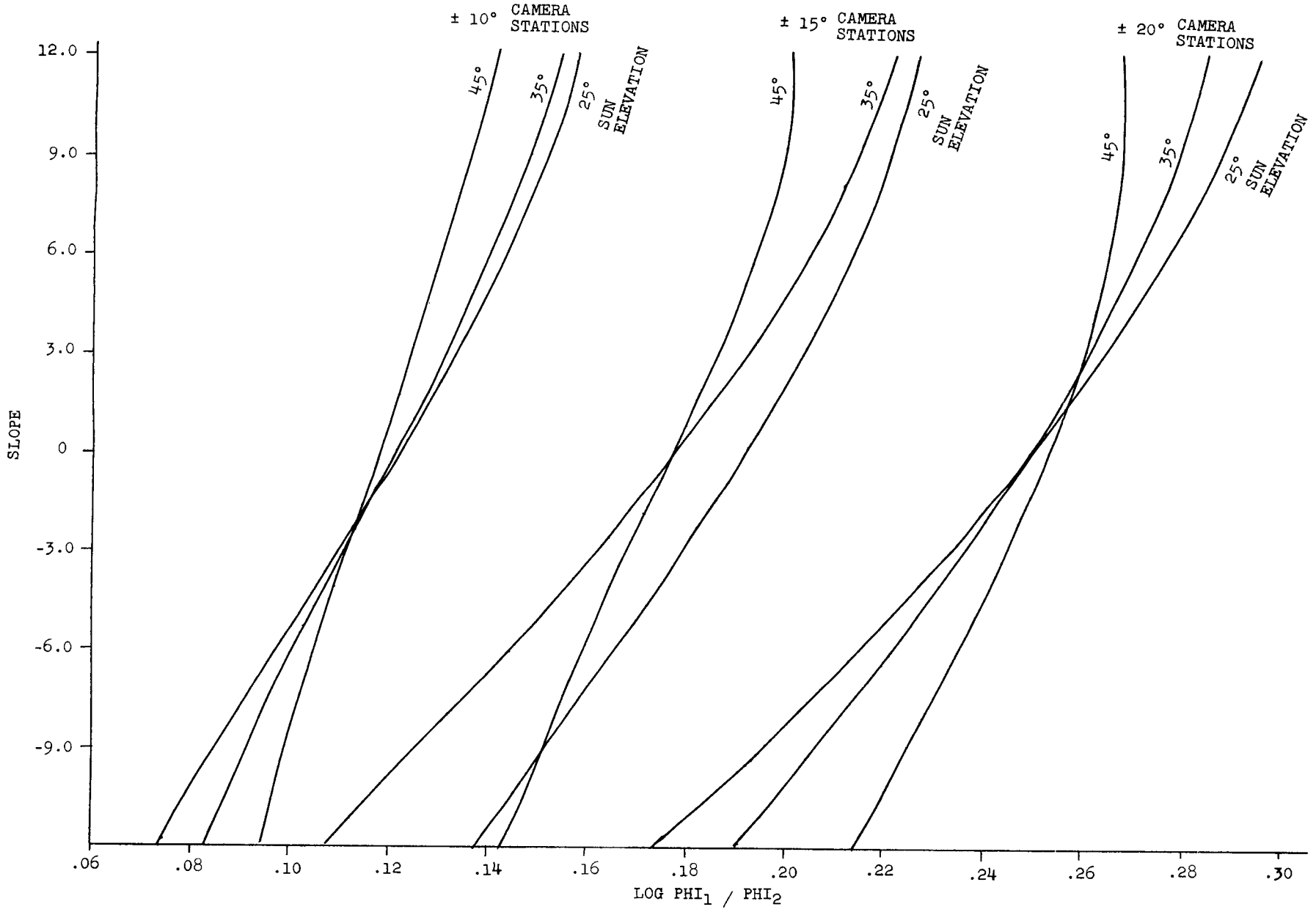

Figure A4-2. LUNAR SLOPE VS LOG Φ_1/Φ_2

SECTION B

DETECTION AND ENHANCEMENT OF LUNAR PHOTO DETAILS

B.1 DETAIL ENHANCEMENT IN IMAGES BY MULTIPLE PHOTOGRAPHY

Investigators have shown that image detail obtained with a given lens-film system is increased by a multiple printing technique.* Enhancement by multiple photography is especially noticeable in low contrast detail. The theory of the technique is that in two separately exposed images of the same scene, the grain pattern hindering recognition of fine detail will not be the same in the two images By superimposing the images and printing them onto a finer-grained film, the two random-grain patterns combine to produce a higher contrast, less grainy, sharper picture.

To illustrate how this technique can be applied to enhance the low contrast detail in lunar photography a number of separate exposures of a simulated lunar scene were made on Royal X Pan Recording Film, Type 5475 and processed to a gamma of 0.47 Three of these images were enlarged approximately 40X onto SO-153, Kodak Special Fine Grain Aerial Duplicating Film (Estar Base) processed to a gamma of 1.0. Concurrently a number of separate exposures of the simulated lunar scene made on Royal X Pan Recording Film, Type 5475 were processed to a gamma of 0.80. One of these images was enlarged approximately 40X onto SO-153, Kodak Special Fine Grain Aerial Duplicating Film (Estar Base) and processed to a gamma of 1.0.

Negative A was made by carefully superimposing in register three positive images made from the lower gamma (0.47) negatives and contact printing these positives onto Kodak Commercial Film (Estar Base) which was then processed to a gamma of 0.88.

Negative B was made from the positive which had been enlarged from the higher gamma (0.80) negative by contact printing it onto Kodak Commercial Film (Estar Base) which was processed to a gamma of 0.88.

---

*See "Photographic Image Enhancement by Superimpositions of Multiple Images", by R. J. Kohler and H. K. Howell, Photographic Science and Engineering, Vol. 7, No 4, July, 1963.

Negative A and negative B were contact printed simultaneously onto Polycontrast Paper to make Figure B1-1. The original scene had a 6-step gray scale which was monitored through the various steps to show the gamma of negative A and negative B to be identical.

Since the over-all gammas of the two photographs printed in Figure B1-1 are the same, it is possible to make a comparison based on noise suppression alone. The photographs show that much of the low contrast, fine detail covered by the grain pattern in the single image photograph is brought out in the superimposed image photograph. Furthermore, false "details" caused by random grain patterns in the single negative are eliminated in the multiple print.

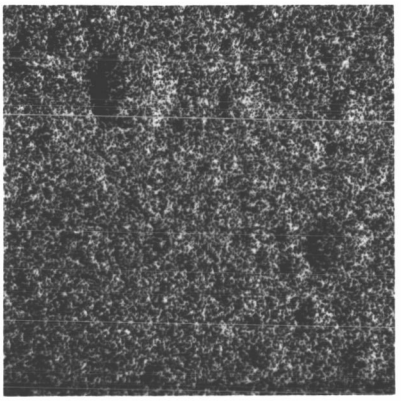

PHOTOGRAPH OF SCENE FROM A SINGLE NEGATIVE

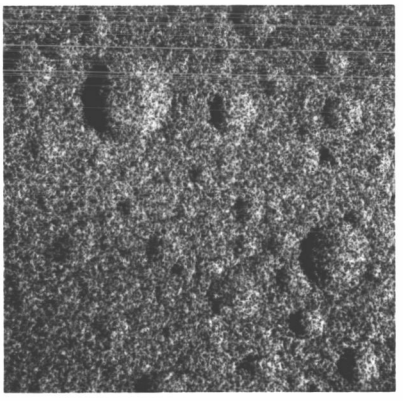

PHOTOGRAPH OF SCENE BY SUPERIMPOSITION
OF THREE SEPARATELY EXPOSED NEGATIVES

Figure B1-1. ENHANCED DETAIL OF A LUNAR SCENE BY SUPERIMPOSED PRINTING OF THREE SEPARATELY EXPOSED NEGATIVES

B.2 HIGH CONTRAST PRINTING

A lunar scene taken at high sun elevations will have a very low contrast. A photograph with such a low scene luminance range can be improved by high contrast printing to bring out details that would normally be lost. Figure B2-1 shows such a photograph taken of KLM6-65 at a sun elevation of 75°. The gamma of the scene as shown at the top of Figure B2-1 is 0.93, a value derived from a negative with gamma 0.60 and a paper print with gamma 1.55. This print should therefore look very much like the scene as observed by a human observer.

The high contrast print in Figure B2-1 was made by printing the same negative used in the low contrast scene onto Kodalith Ortho Film Type 3 making a higher contrast positive. This high contrast positive was printed onto Kodalith Ortho Film Type 3 again making a high contrast negative. This negative was then printed onto a polycontrast paper at high contrast. A neutral density step wedge was carried along during these operations in order to evaluate the steps as they were made. The final over-all gamma from the original scene including the paper print is 8.55.

For a scene with a very low brightness range, an improvement like that in Figure B2-1 is possible, but note that all the detail in the light albedo areas is completely gone. These areas are outside of the density range of the print. The high contrast photograph, however, shows nearly as much detail as a photograph taken at low sun elevation without loosing the details normally covered by shadow. If this effect is sought by using high contrast negative materials, very careful exposure control is required.

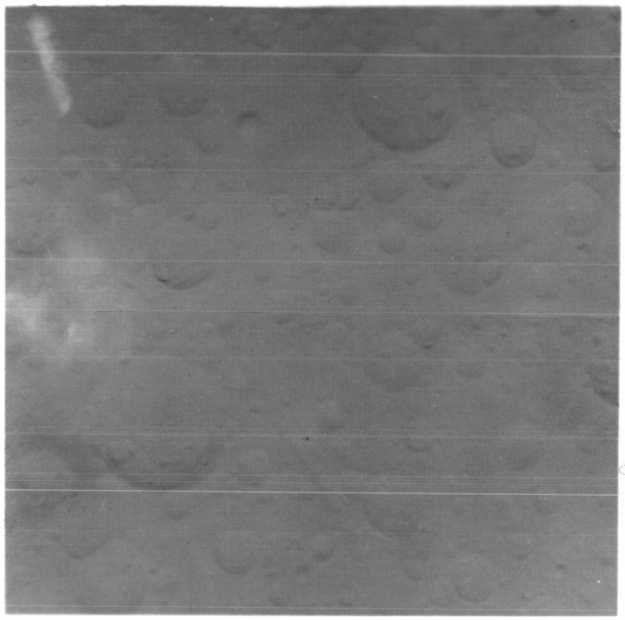

KLM6-65 at 75° Sun Elevation

Overall Gamma = 0.95

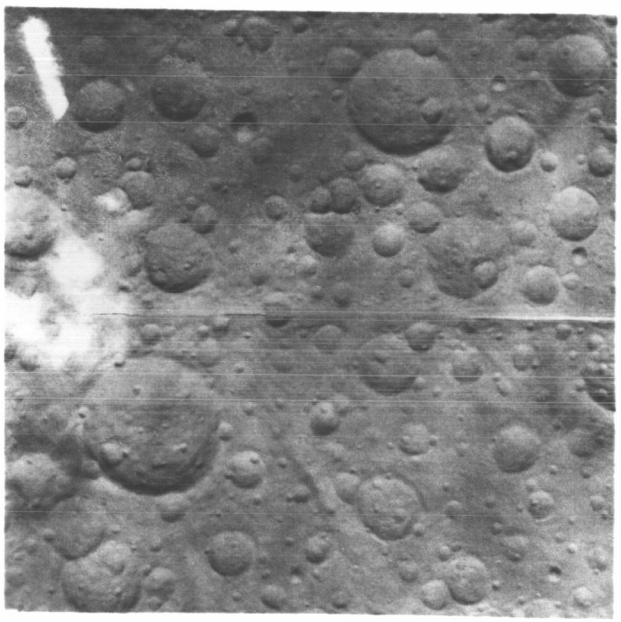

KLM6-65 at 75° Sun Elevation

Overall Gamma = 8.55

Figure B2-1. EXAMPLE OF HIGH CONTRAST PRINTING SHOWING THE IMPROVEMENT THAT CAN BE MADE IN CERTAIN LUNAR SCENES BY HIGH CONTRAST PRINTING TECHNIQUES

B.3 MOTION PICTURE SIMULATIONS

Four motion picture simulations of the view from the window of the landing Lunar Excursion Module (LEM) were produced under Phase II of this contract. These four simulations follow the same lunar descent trajectory, each with different sun conditions as follows:

Simulation	Sun Conditions
#1	5° Sun Elevation, 5° Sun Azimuth*
#2	10° Sun Elevation, 5° Sun Azimuth*
#3	60° Sun Elevation, 0° Azimuth (sun in the trajectory plane)
#4	170° Sun Elevation, 0° Azimuth (sun in the trajectory plane)

Making these new motion pictures continued an earlier effort under Phase I of this study in which a simulation at 37° sun elevation was made for a different trajectory.** Because of experience gained in making the first simulation and improvements in film and techniques, the new simulations are smoother and show less grain than the earlier pictures.

These motion pictures show the effect of varying sun elevation on a typical lunar scene; individually, they show the change in contrast of the scene under fixed sun conditions as the LEM trajectory is traversed. The real-time sequence of events allows planners to judge whether or not enough time is available to assess the landing sites for this trajectory. Five copies of the four motion picture simulations were sent to NASA for evaluation

Several characteristics of these simulations are shown in Figure B 3-1.

---

*Measured to the left of the trajectory plane.

**See "Final Report, Lunar Photo Study", Contract NAS9-3826, October 1965, pages 123-133 for a description of this first simulation.

Motion Picture Simulations - Top Views
Eastman Kodak Company - NAS-9-3826

5°, 10°, 60°, 170° Sun Elevations

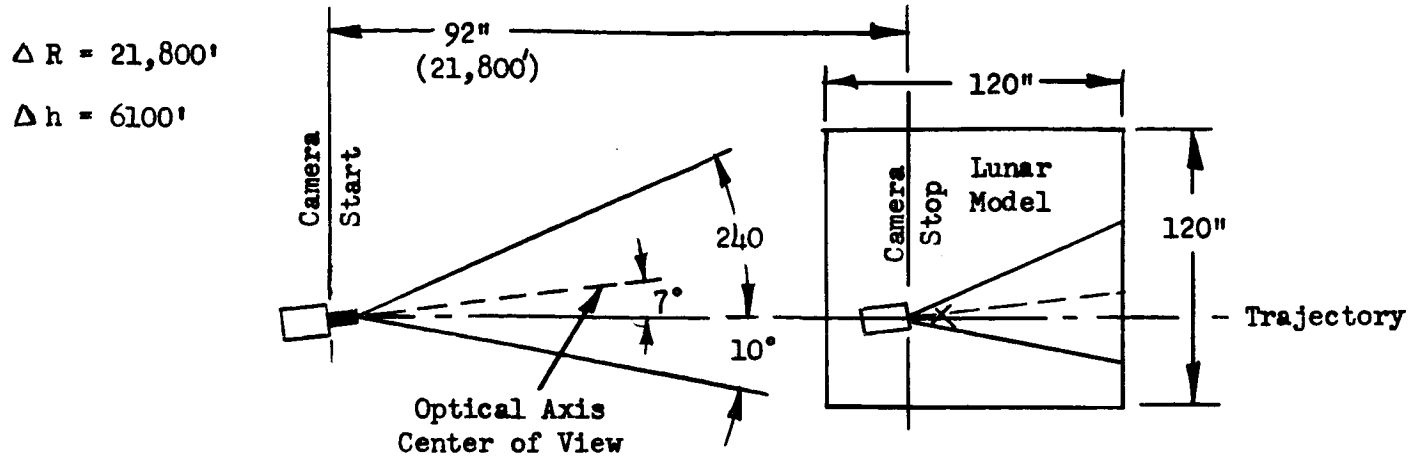

Final Approach Phase - Scale 1:3000

X = Landing Site

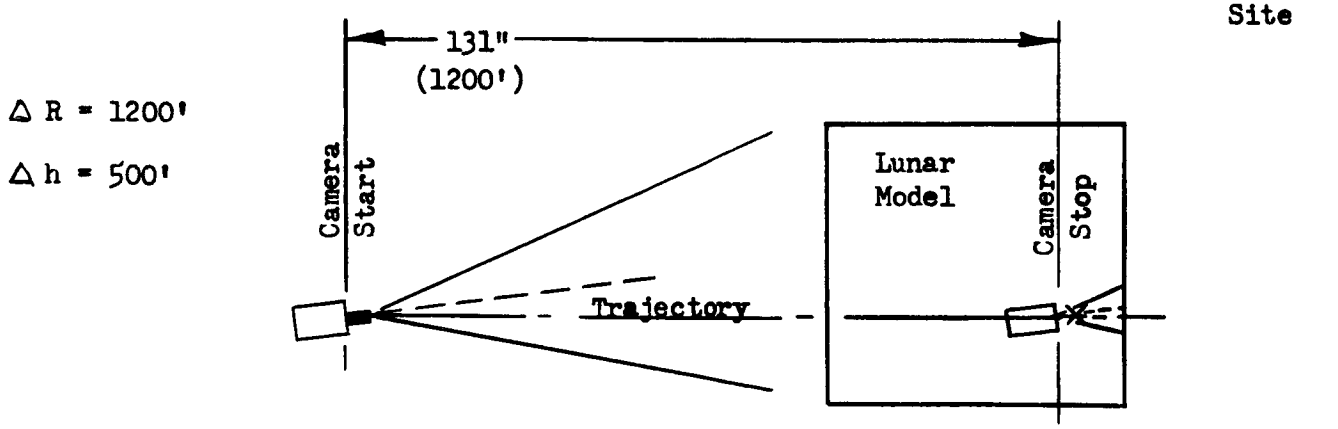

Landing Phase - Scale 1:110

Lens = 15mm Cine Ektar
F/# used = f/16
Exposure = 3 seconds

Films: Neg. - Double-X Neg., Type 7222;
Pos. - Fine Grain Dupe Pos. Type 7366

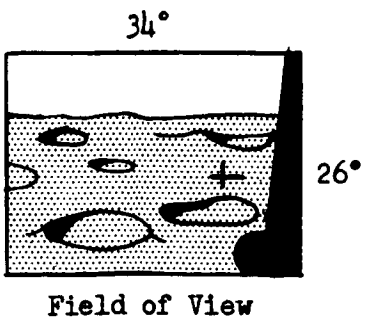

Field of View

Figure B3-1. PLAN VIEW OF THE FINAL APPROACH PHASE AND LANDING PHASE FOR THE MOTION PICTURES.

Descent Trajectory

The new descent trajectory supplied by NASA is described in MSC Internal Note No. 66-EG-10, March 18, 1966. This note outlines for Project Apollo the preliminary LEM powdered descent trajectory for flight AS-504-A. The description includes three phases, (1) Braking phase, (2) Final Approach phase, and (3) Landing phase.

Braking Phase

The Braking phase is not included in this simulation as the lunar surface is not in view. The Final Approach phase and the Landing phase are the portions of the descent covered by the motion picture simulations.

Final Approach Phase

The Final Approach phase covers an altitude change of 5,600 feet and a range change of 21,800 feet. At the start, LEM altitude is 6,100 feet and the range to the landing site is 23,000 feet; at the end, altitude is 500 feet and range is 1,200 feet. Forward velocity is 500 feet per second at the start and 60 feet per second at the end of the phase. This phase lasts 78 seconds during which time the flight path angle gradually increases from 15° to 20°.

The Final Approach phase starts in the middle of the pitch maneuver that brings the lunar surface into view. Part of this maneuver is in the Braking phase at a rate of six degrees per second, changing the pitch angle from 63° to 45°; the other part is in the Final Approach phase at 3.5 degrees per second, reducing the pitch to 37°. After pitchover, the landing site is seen in the LEM window at 37° look angle, i.e., 37° from the downward vehicle vertical and maintains this position in the window to the end of the phase. The start of a second pitch maneuver ends the Final Approach phase and initiates the Landing phase.

Landing Phase

The Landing phase covers the LEM descent from 500 feet to the surface. The range covered is 1,200 feet and the flight path angle is constant at 17°. The flight path velocity decreases to 0, at which time the vehicle is hovering at 100 feet over the landing site, and then resumes at 5 feet per second for the vertical descent to the surface. This phase takes 76 seconds.

A pitchover at 6 degrees per second initiates this phase, decreasing the pitch angle from 30 degrees to 11 degrees. The landing site is then seen at 56° look angle. The pitch angle does not change until the vehicle is over the landing site 50 seconds later. This second pitchover reduces the pitch angle to zero. The vehicle can hover over the landing site for up to 30 seconds to assess alternate landing sites; it then makes a vertical descent to the surface at 5 feet per second.

Camera View and Mask

Camera View

Figure B3-2 shows the angular coverage of the left window of the LEM from the design eye point. The rectangular area shows the angular coverage of the 16mm frame in the simulation. The camera holds this view fixed throughout the simulation and may be thought of as rigidly attached to the LEM vehicle. This camera view was selected to satisfy two conditions set by NASA-MSC and one fixed by the lens used:

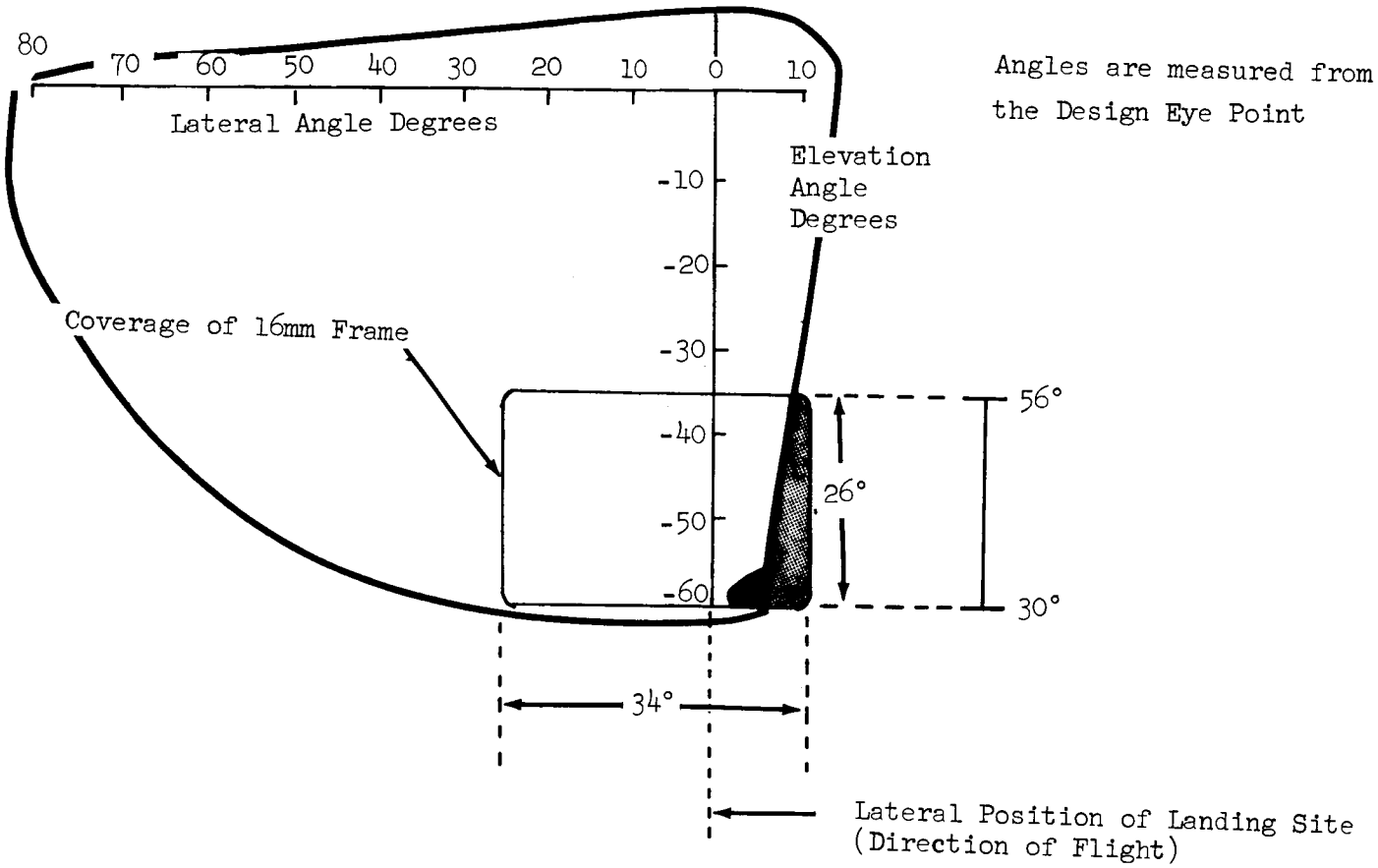

Figure B3-2. ANGULAR COVERAGE OF 16MM FRAME RELATIVE TO THE VIEW FROM LEM WINDOW

1. The LEM landing gear pad shall be visible in the scene.
2. The landing site shall always be visible in the scene.
3. The angular field of view of a projected 16mm frame recorded with a 15mm lens is 34° horizontally by 26° vertically.

The position of the landing site in the LEM window is described by the look angle. The look angle of an object is the angle between the downward LEM vertical axis (-X axis) and the line drawn from the design eye point to the object. The bottom edge of the LEM window has a look angle of 25°, so that objects with a look angle less than this cannot be seen in the window. The greatest look angle of the landing site for the trajectory simulated is 56°, so that the vertical angular coverage required to have the landing site in view at all times is 31°. By placing the bottom of the camera view at 30° look angle, the top of the camera view falls at 56° look angle. Therefore in these simulations, objects with look angles less than 30° are not seen. The landing site falls below 30° only at the end of the trajectory as the vehicle approaches zero range.

Mask

To show the portion of the LEM landing gear pad included in the camera view, a special mask was made and placed in the image plane of the Kodak Cine Special Motion Picture camera. The mask blacks out those areas in the camera view that are beyond the edge of the LEM window or that are within the LEM window view but that obstruct the view of the lunar surface, i.e. the landing gear pad. The lateral positioning of the camera view was set with the edge of the LEM window coming into view in the top right hand corner. This makes the center of the camera view point 7° to the left of the landing site. The mask intrudes from the right an increasing amount down the right side of the window with the landing gear pad showing at the bottom right corner.

Two masks were made; the first was used in the 5° simulation and the second was used in the other three simulations. The second mask allows for the fact that the projected image is slightly smaller than the recorded image.

Making the New Simulations

The trajectory for the new motion pictures was simulated in two parts corresponding to the Final Approach phase and the Landing phase and were run at different scale factors. Producing the new simulations in two parts is a major improvement over the Phase I simulation which was made in four parts at four different scale factors. Other improvements resulted from gaining better control of the camera's motions, improving the shutter release mechanism, and using a film with finer grain.

Lunar Surface Model

Enlarging the size of the existing lunar surface model from 80 x 80 inches to 120 x 120 inches was the first step to a two part simulation. The new model consists of a foreground section 40 x 120 inches built to a scale of 1:960 and seen mostly in the first part of the simulation. Attached to this is a background section 80 x 120 inches built to a scale of 1:48 which is primarily in view during the Landing phase part of the simulation. A larger model than this could not be covered by the illuminant. The model was dusted with Fisher Cupric Oxide to give it the light reflecting properties of the lunar surface.

Illuminant

A Kodak Master Model 1000-watt projector with a 5-inch f/2.3 projection lens illuminated the model for the new simulations. This light source has several desirable characteristics: (1) large angular coverage, (2) high light output, and (3) portability and low weight. The angular coverage is 25 degrees, which compares with 20 degrees for the light source used in the Phase I simulation. The illumination intensity at 21 feet is 70 foot-candles, almost twice the 44 foot-candles for the old source at the same distance.

At twenty one feet the lens diameter matches the sun's one-half degree angular subtense at the moon's surface. This short distance and the low weight of the projector permitted simulating the 60° sun elevation.

Scales

The Final Approach phase was simulated at a model-to-moon scale of 1:3,000; the Landing phase was simulated at a model-to-moon scale of 1:110. These scales were selected by considering the camera orientation, the angular coverage of the camera view, and the size of the lunar model. Some scaled values for the descent parameters are listed with the actual values in Table B3-I. Table B3-II lists the surface characteristics of the foreground and background sections of the model at model-to-moon scales of 1:3,000 and 1:110, respectively. The change of 5,600 feet in altitude and 21,800 feet in range during the Final Approach phase become 25 and 92 inches, respectively in the lab. At a scale of 1:110, the Landing phase change of 500 feet in altitude and 1,200 feet in range becomes 54 inches and 131 inches, respectively. Special equipment was designed and constructed to maintain accurate control of the camera over these distances.

Camera Movement

With the scales of the simulation established and knowing that the final motion picture will be projected at sound speed (24 frames per second), it is possible to schedule the interframe changes in camera position. For each record of trajectory, the flight path distance traveled is multiplied by the appropriate scale factor. This gives the distance that the camera must be moved for each second of simulation (24 frames); dividing these scaled distances by 24 gives the distance that the camera must be moved for each frame. For pitch angle changes, the angular pitch rate is converted to degrees of camera rotation per frame.

TABLE B3-I

PARAMETERS OF LEM DESCENT FOR USE IN MOTION PICTURE

Phase	Preliminary LEM Descent, Flight As-504A				Simulated LEM Descent				
	Time to go (sec.)	Altitude (feet)	Range (feet)	Pitch Angle* (deg.)	Frame Number	Altitude (inches)	Angle Between Camera Axis and Horizontal		Model to Moon Scale
Final Approach	154	6100	23000	45	0	25	92	-3°	1/3000
	152	5900	22200	37	48	24	89	-11°	
	79	625	1700	31	1800	2.5	7	-18°	
	76	500	1200	11	1872	2	5	-37°	
Landing	76	500	1200	11	1873	54	131	-37°	1/110
	28	-	-	11	3024	-	-	-37°	
	26	100	0	0	3072	11	0	-48°	
	9	46	0	0	3480	5	0	-48°	
	0	15	0	0	3696	1.6	0	-48°	

*Pitch Angle = Angle between LEM vertical axis (X axis) and local vertical.

TABLE B3-II

SURFACE CHARACTERISTICS OF LUNAR MODEL USED IN THE MOTION PICTURE SIMULATIONS

Trajectory Phase	Model-To-Moon Scale	Section of Model	Crater Diameter Range, inches on Model	Crater Diameter Range, Meters on Moon	Crater Density on Moon (# per Km^2)	Boulder Diameter Range, Meters on Moon	Boulder Density on Moon (# per Km^2)
Final Approach	1:3000	Foreground	0.063 - 0.187	4.4 - 13	590		
			0.187 - 0.312	13 - 22	108		
			0.312 - 0.437	22 - 31	38		
			0.437 - 0.56	31 - 40	24		
			0.56 - 0.81	40 - 57	9.4		
			0.81 - 1.06	57 - 79	3.8		
			1.06 - 1.31	79 - 92	2.24		
			1.31 - 1.94	92 - 136	0.86		
			1.94 - 3.19	136 - 224	0.32		
			3.19 - 5.7	224 - 400	0.22		
			5.7 - 9.5	400 - 664	0.22		
			9.5 - 12.0	664 - 840	0.22		

Table Cont'd. on Next Page

TABLE B3-II (Continued)

Trajectory Phase	Model-To-Moon Scale	Section of Model	Crater Diameter Range, inches on Model	Crater Diameter Range, Meters On Moon	Crater Density on Moon (# per Km^2)	Boulder Diameter Range, Meters on Moon	Boulder Density on Moon (# per Km^2)
Landing	1:110	Background	0.125 - 0.25	0.35- 0.70	3.66×10^5	0.35 - 1.05	160
			0.25 - 1.25	0.70- 3.5	7950	1.05 - 1.75	0
			1.25 - 2.5	3.5 - 7.0	3980	1.75 - 2.44	160
			2.5 - 5.0	7.0 - 14.0	716	2.44 - 3.14	80
			5.0 - 6.25	14.0 - 17.5	398	3.14 - 3.84	0
			6.25 - 7.5	17.5 - 21.0	200	3.84 - 4.54	80
			7.5 - 10.0	21.0 - 28.0	103		
			10.0 - 12.5	28.0 - 35.0	80		

Boulder Height Range, Meter on Moon	Density on Moon (# per Km^2)
0.14 - 0.35	240
0.35 - 1.05	160
1.05 - 1.75	80

Two schedules of camera movements were derived from the above calculations, one for simulating the Final Approach phase, reproduced in Table B3-III, and the other for simulating the Landing phase, reproduced in Table B3-IV. Note that in these tables focus settings are changed to insure that the sharpest images of the simulated lunar scene are recorded. Note also that section 23 of the Landing phase schedule (Table B3-IV) allows 6 seconds of hover time at 100 feet for assessment of alternate landing areas.

A slight simplification of the Final Approach phase trajectory was made for calculating camera advance. The time average of the flight path angle, which ranges from 15° at the start to 20° at the end of the phase, was used. Since all but the last 12 seconds of flight in this phase is at 15 to 17 degrees, little error has been introduced. The camera advances per frame for the Final Approach phase were made along the average slope of 16 degrees. For the Landing phase, the flight path angle is constant at 17 degrees.

TABLE B3-III

SCHEDULE OF CAMERA MOVEMENTS FOR FINAL APPROACH PHASE

Section #	No. of Frames in Section	Cumulative Count of Frames	Inches Advance Per Frame	Camera Angle*	Degrees Change In Pitch	Focus
Intro	80	-	0.088	+17°	0.25°/frame	7'
1	56	56	0.088	-3°	1°/7 frames	7'
2	88	144	0.082	-11°	-	7'
3	96	240	0.077	-11°	-	7'
4	144	384	0.071	-11°	-	7'
5	144	528	0.066	-11°	-	7'
6	144	672	0.060	-11°	-	7'
7	144	816	0.055	-11°	-	7'
8	144	960	0.049	-11°	-	7'
9	144	1104	0.044	-11°	0.5° Total this section	5'
10	192	1296	0.038	-11.5°	0.5° Total this section	5'
11	144	1440	0.033	-12°	0.5° Total this section	4'
12	144	1584	0.027	12.5°	1° Total this section	3'
13	144	1728	0.022	-13.5°	2° Total this section	18"
14	64	1792	0.016	-15.5°	1.5° Total this section	12"
15	32	1824	0.016	-17°	0.25°/frame	9"
16	48	1872	0.011	-25°	0.25°/frame	8"

*With respect to the horizontal

TABLE B3-IV

SCHEDULE OF CAMERA MOVEMENTS FOR LANDING PHASE

Section #	No. of Frames in Section	Cummulative Count of Frames	Inches* Advance Per Frame	Inches Drop per Frame	Camera** Angle	Degrees Change In Pitch	Focus
Intro.	76	-	0.246	0	-18°	.25°/frame	9'
1	50	50	0.246	0	-37°	0°/frame	9'
2	50	100	0.213	0	-37°	0°/frame	9'
3	50	150	0.197	0	-37°	0°/frame	9'
4	50	200	0.186	0	-37°	0°/frame	6'
5	100	300	0.181	0	-37°	0°/frame	6'
6	100	400	0.175	0	-37°	0°/frame	4'
7	50	450	0.164	0	-37°	0°/frame	4'
8	50	500	0.148	0	-37°	0°/frame	4'
9	50	550	0.131	0	-37°	0°/frame	4'
10	50	600	0.123	0	-37°	0°/frame	3'
11	50	650	0.115	0	-37°	0°/frame	3'
12	50	700	0.098	0	-37°	0°/frame	3'
13	50	750	0.082	0	-37°	0°/frame	3'
14	50	800	0.066	0	-37°	0°/frame	3'
15	100	900	0.060	0	-37°	0°/frame	2'
16	50	950	0.049	0	-37°	0°/frame	2'
17	50	1000	0.038	0	-37°	0°/frame	2'

*Along Trajectory Path

**With respect to the horizontal

Table Cont'd. on Next Page

TABLE B3-IV (Continued)

Section #	No. of Frames in Section	Cumulative Count of Frames	Inches* Advance Per Frame	Inches Drop per Frame	Camera** Angle	Degrees Change In Pitch	Focus
18	50	1050	0.027	0	-37°	0°/frame	2'
19	50	1100	0.016	0	-37°	0°/frame	18"
20	50	1150	0.011	0	-37°	0°/frame	18"
21	6	1156	0.005	0	-37°	0°/frame	15"
22	44	1200	0.005	0	-37°	0.25°/frame	15"
23	144	1344	0	0	-48°	0°/frame	15"
24	480	1824	0	0.022	-48°	0°/frame	13"-7"

*Along Trajectory Path

**With respect to the horizontal

The camera was moved smoothly and accurately along the flight path so that none of the apparatus supporting the camera would cast a shadow on the scene. The camera was supported on a cart riding down a ramp placed to one side of the model. The camera overhangs the ramp by 34 inches, enough to keep the ramp out of the field of view. Three wheels on the cart were guided by three ways on the ramp insuring smooth motion and constant alignment. Control of the cart on the ramp was provided by a rack with a worm gear drive. The accuracy of the interframe adjustments was about ±0.003 inch.

Camera, Lens, and Film

A Cine-Kodak Special camera combined with its Electronic Release Control Outfit provided the film advance and shutter control for these simulations. The camera was mounted on a special bracket that places the nodal point of the lens on the axis of rotation used for changing the pitch angle. This special mounting allows pure rotational motion to be simulated; i.e., without a translational component included. A 15mm f/2.8 Cine Ektar lens was used to form the images.

The photographic materials used in these simulations were selected to give low graininess and an over-all gamma of 1.0 in the final prints while providing a high speed camera film. Eastman Double-X Negative Film, Type 7222, was selected for use in the camera. This film has a tungsten exposure index of 200 and an RMS Granularity of 15, higher in speed and lower in grain than Tri-X Reversal, index 160 and granularity 24, used in the first simulation.

The 1.0 gamma was produced by processing the negative film to a gamma of 0.70, printing it onto Eastman Fine Grain Duplicating Positive Film Type 7366 and processing the positive to a gamma of 1.4. The resulting print produces the contrast of the dusted lunar model as it is seen by the human eye.

The Four Motion Picture Simulations

Each simulation begins with the pitch maneuver that brings the lunar surface into view. Simulations No. 2, No. 3, and No. 4 follow exactly the schedules of camera movements given in Tables B3-III and B3-IV. Simulation No. 1 was the first attempt at using the new trajectory and follows closely but not exactly the given schedules. Each simulation ends at an altitude of 46 feet or 6 seconds from touchdown. Contact of the camera body with the model prevented completing the descent to touchdown. The scheduled final height of the lens above the model, 1.6 inches, corresponds to the height that the eye point will be above the surface when the LEM is on the surface.

It is necessary to depart from a desired 0° sun azimuth angle by 5° on simulation No. 1 and No. 2 to prevent the shadow of the camera from entering objectionably into the field of view.

Some additional information on each of the four simulations is given below. When these simulations are projected at 24 frames per second events occur in a real time sequence.

Simulation No. 1

In the first motion picture simulation the sun is 5° above the horizon, behind the vehicle and with a 5° azimuth angle to the left of the trajectory plane. Exposure was 6 seconds at f/22 for the Final Approach phase and 3 seconds at f/16 for the Landing phase, i.e., the same exposure was given for both phases.

Simulation No. 2

For the second motion picture simulation the sun is 10° above the horizon, behind the vehicle, and with a 5° azimuth angle to the left of the trajectory plane. This simulation differs from simulation No. 1 only in that the sun elevation has been increased 5°. The 5° azimuth angle was included in this

simulation to reduce equipment shadows in the scene and to keep simulation No. 2 identical to simulation No. 1 except for the 5° change in sun elevation. A 3-second exposure at f/16 was used for both parts of the simulation.

Simulation No. 3

For the third motion picture simulation the sun is 60° above the horizon in the vertical plane that includes the trajectory. The LEM is moving away from the sun. Exposure for each frame was 3 seconds at f/16 for both the Final Approach phase and for the Landing phase. Calculations in Table B3-V shows that this simulation has the lowest contrast that agrees with the visual impression of the motion picture.

Simulation No. 4

For the fourth motion picture simulation the sun is 170° above the horizon in a vertical plane which includes the trajectory. The LEM is moving toward the sun. The exposure for each frame was 8 seconds at f/11 for both the Final Approach phase and the Landing phase.

Scene Contrast

The values of the parameters describing the photometric function at the landing site are important to keep in mind when comparing these simulations. The parameters, called alpha and tau, are defined and related to the LEM position in the Final Approach phase in Figure B3-3.

Two sets of values are given for each simulation in Table B3-V. One set describes the conditions for the Final Approach phase, in which a 15-degree angle between the line-of-sight direction to the landing area and the horizontal at the landing area has been assumed. The other set describes the conditions for the Landing phase, in which a 23-degree angle between the line-of-sight direction to the landing area and the horizontal at the landing area has been assumed. Included in each set are the values for

ALPHA = PHASE ANGLE, ANGLE BETWEEN LINE-OF-SIGHT DIRECTION AND SUN'S DIRECTION

TAU = AUXILIARY ANGLE, ANGLE BETWEEN LINE-OF-SIGHT AND SURFACE NORMAL PROJECTED INTO THE PHASE PLANE

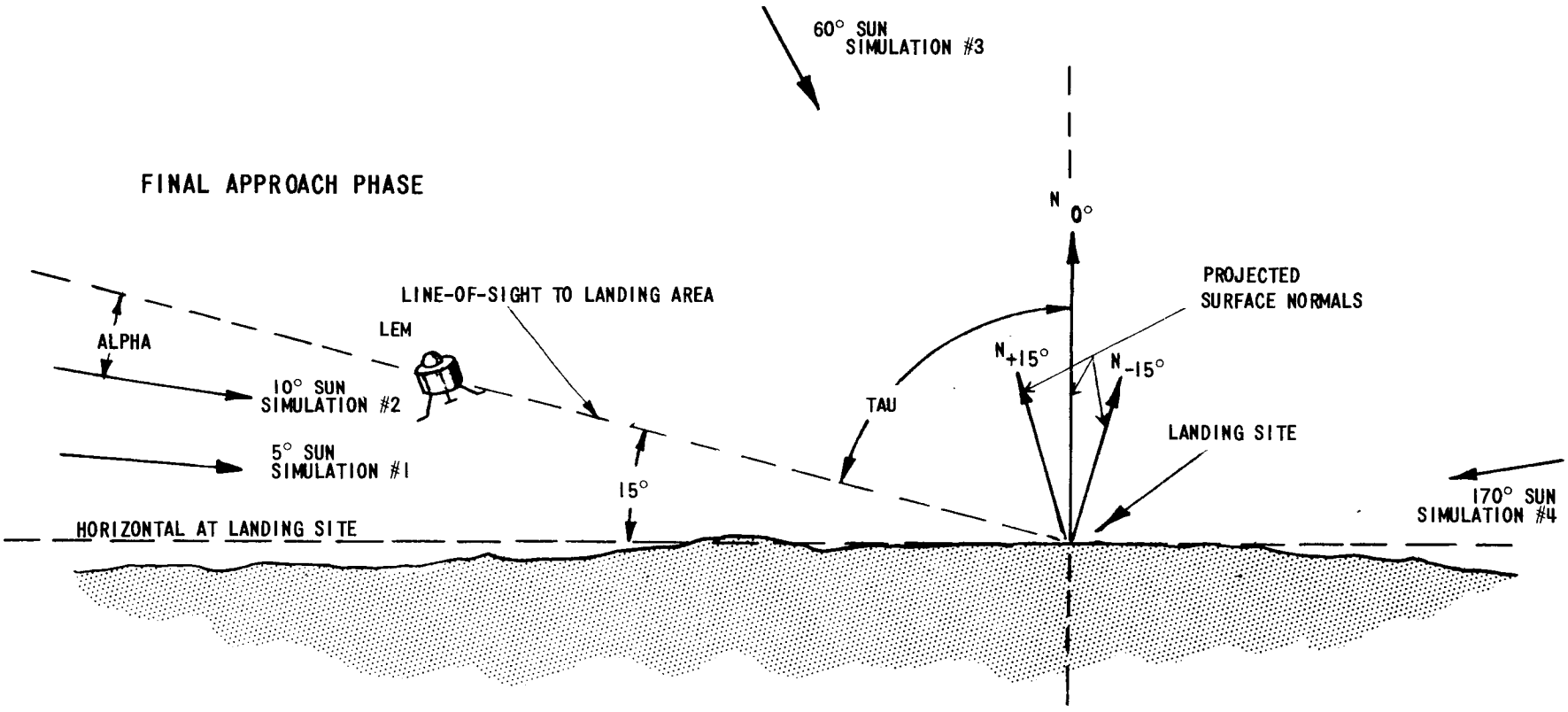

Figure B3-3. PARAMETERS DESCRIBING THE PHOTOMETRIC FUNCTION AT THE LANDING SITE FOR THE FINAL APPROACH PHASE OF THE DESCENT TRAJECTORY

TABLE B3-V

PHOTOMETRIC FUNCTION AND CONTRAST VALUES OF FIVE SLOPES AT THE LANDING AREA IN THE MOTION PICTURE SIMULATION

		FINAL APPROACH PHASE				LANDING PHASE			
Simulation Number		1	2	3	4	1	2	3	4
Sun Elevation		5°	10°	60°	170°	5°	10°	60°	170°
Phase Angle Alpha		10°	5°	45°	155°*	19°	13°	37°	147°*
Zero Slope:	Tau	+75°	+75°	-75°	-75°	+67°	+67°	-67°	-67°
	Phi Lunar	0.108	0.525	0.451	0.0189	0.054	0.138	0.507	0.0216
	Phi CuO	0.336	0.608	0.592	0.0603	0.2145	0.386	0.658	0.0649
-15° Slope:	Tau	+90°	+90°	-90°	-90°	+82°	+82°	-82°	-82°
	Phi Lunar	N	N	N	N	S	S	0.525	0.0481
	Phi CuO	N	N	N	N	S	S	0.712	0.145
	Contrast Lunar	N	N	N	N	S	S	1.04	2.23
	Contrast CuO	N	N	N	N	S	S	1.09	2.23
-7° Slope:	Tau	+82°	+82°	-82°	-82°	+74°	+74°	-74°	-74°
	Phi Lunar	S	0.180	0.461	0.0319	S	0.038	0.516	0.0349
	Phi CuO	S	0.407	0.625	0.102	S	0.117	0.681	0.108
	Contrast Lunar	S	2.92	1.02	1.69	S	3.63	1.02	1.62
	Contrast CuO	S	1.49	1.06	1.69	S	3.30	1.04	1.66

S = Slope is in shadow
N = Slope is out of sight
Contrast = As Defined in the Text
* = Extrapolated Phi Values of copper oxide dust

Table Cont'd. on Next Page

TABLE B3-V (Continued)

PHOTOMETRIC FUNCTION AND CONTRAST VALUES OF FIVE SLOPES
AT THE LANDING AREA IN THE MOTION PICTURE SIMULATION

	Final Approach Phase				Landing Phase			
	1	2	3	4	1	2	3	4
+7° Slope: Tau	+68°	+68°	-68°	-68°	+60°	+60°	-60°	-60°
Phi Lunar	0.250	0.706	0.442	0.00474	0.138	0.259	0.497	0.00681
Phi CuO	0.476	0.702	0.526	0.0137	0.326	0.476	0.631	0.0217
Contrast Lunar	2.31	1.34	1.02	3.99	2.74	1.88	1.02	3.17
Contrast CuO	1.42	1.15	1.05	4.40	1.52	1.23	1.04	2.90
+15° Slope: Tau	+60°	+60°	-60°	-60°	+52°	+52°	-52°	-52°
Phi Lunar	0.392	0.753	0.434	S	0.235	0.361	0.487	S
Phi CuO	0.574	0.757	0.532	S	0.421	0.544	0.603	S
Contrast Lunar	3.63	1.43	1.04	S	4.66	2.62	1.04	S
Contrast CuO	1.71	1.25	1.11	S	1.96	1.41	1.08	S

S = Slope is in shadow
N = Slope is out of sight
Contrast = As Defined in the Text
* = Extrapolated Phi Values of copper oxide dust

surfaces at the landing site of: (1) 0° slope, (2) + 7° and + 15° slopes, that increase in elevation in the direction that the LEM vehicle is moving and (3) - 7° and - 15° slopes, that decrease in elevation in the direction that the LEM vehicle is traveling.

For each set of parameters considered, two photometric function values are given in Table B3-V. One value represents the lunar photometric function and the other value represents the photometric function for dusted Fisher Cupric Oxide. Fisher Cupric Oxide is the material that was dusted onto the lunar model to simulate the lunar photometric function for the motion picture simulations.

The brightness of each of the sloping areas mentioned above has been compared with the brightness of the level area by taking the ratio of the value for the brighter area to the value for the darker area. This ratio is called the contrast and is shown in Table B3-V for values from the lunar photometric function and for values from the cupric oxide photometric function.

For the conditions of simulations No. 1 and No. 2 a slope of positive value, as defined above, will be brighter than a 0° slope and a slope of negative value, as defined above, will be less bright than a 0° slope. However, for the conditions of simulations No. 3 and No. 4 a slope of positive value will be darker than a 0° slope while a slope of negative value will be brighter than a 0° slope. The contrast in a given lunar scene depends on the rate of change in brightness with change in slope. This rate is a function of the viewing and illumination geometry. The conditions in simulation No. 3 produce low contrast in the scene, while the conditions for simulations No. 1, 2, and 4 produce relatively high contrast.

A look at the contrast values in Table B3-V shows that the contrast in the scene for a particular simulation is different at different points in the trajectory. For instance, the lunar contrast between the +7° slope and the 0° slope in simulation No. 1, 5° sun elevation, is 2.31 at the beginning of the Final Approach phase and 2.74 at the beginning of the Landing phase. This indicates that the contrast is increasing as the landing site is approached along this trajectory under these illumination conditions. A similar comparison shows that contrast increases along the trajectory for simulation No. 2, remains constant for simulation No. 3 and decreases for simulation No. 4. Although the contrast is decreasing for simulation No. 4, it does not fall below the contrast values of the other simulations.

Under ideal conditions a contrast of 1.02 or a 2-percent change in luminance should be detectable by the human eye. If the areas under consideration are small or the areas are not adjacent to each other or separated by a gradual change in luminance (change in slope at the lunar surface) a luminance change greater than 2 percent will be required to detect the change in slope. In the case of 60° sun elevation a lunar slope of ± 7° is required before a 2-percent change in luminance is reached. In other words a slope change of at least ± 7° must occur at the landing site before it would be possible to detect any change from a level surface and then it must be adjacent to the level area.

The photometric function of dusted Fisher cupric oxide is given in Figure B 3-4. The phi value for a 0° slope at the landing site at the start of each of the trajectory phases is indicated on the figure. The curves of the lunar photometric function are flatter for large negative tau angles than are the curves of the cupric oxide photometric function, so that in the 60-degree simulation the simulated scene will have more contrast than a Fedoret's lunar scene.

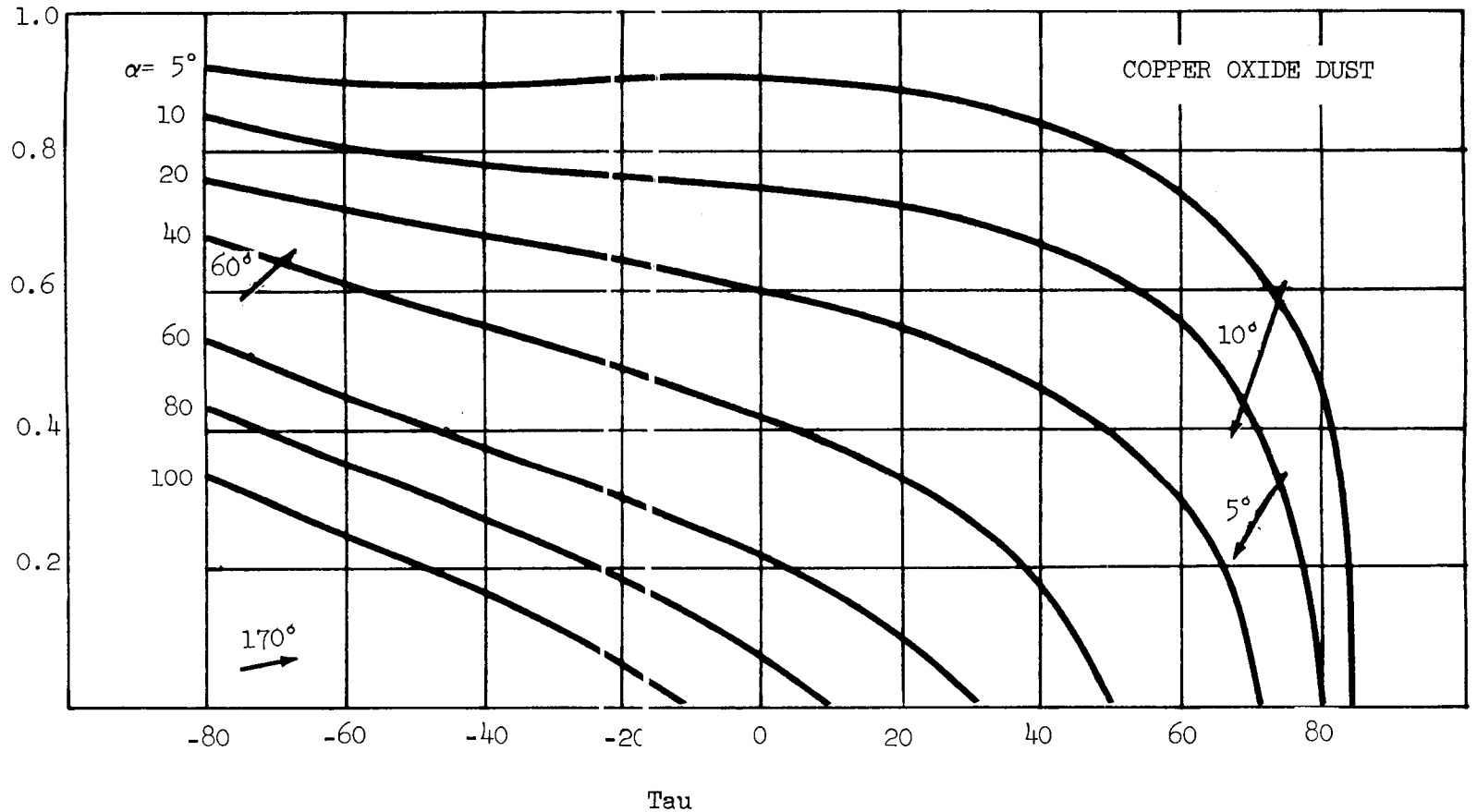

Figure B3-4. LOCATION OF THE BACKGROUND VALUES OF THE PHOTOMETRIC FUNCTION FOR COPPER OXIDE FOR THE FOUR MOTION PICTURES AT SUN ELEVATIONS OF 5°, 10°, 60°, AND 170°

Conclusions - Motion Pictures

1. For a lunar landing area of constant albedo that has a photometric function similar to dusted copper oxide and under the sun conditions considered, these simulations are a good representation of the anticipated view from the window of the LEM during the lunar landing.

2. The 5° or 10° sun elevation simulation with sunlight coming from the rear of the LEM will give a high contrast scene showing good brightness differences between the slopes under consideration for the landing LEM with no flare problem caused by the LEM window.

3. The simulation at 60° sun elevation with the sunlight coming from nearly overhead shows the least contrast of the four simulations and is not recommended for the landing LEM.

4. The 170° sun elevation simulation with the sunlight coming from in front of the landing LEM demonstrates the flare problem that will be present with sunlight falling on the windows. If a way can be found to shade the window the flare problem will be eliminated and the lunar scene will be of sufficient contrast to make decisions concerning a landing in the LEM.

5. The calculated contrasts shown in Table B3-V agree with the visual impressions given to the viewer during the projection of the motion picture simulations.

B.4 PHOTOGRAPHY OF SURVEYOR MODEL

Test Plan

This experiment was done from 18 March to 1 April 1966 at the request of Mr. T. Young of the NASA Langley Research Center. The photography simulated the appearance of a Surveyor spacecraft on the lunar surface as recorded with the Lunar Orbiter 24-inch lens at altitudes of 25, 50, 100, and 135 kilometers. The scale of the Kodak KLM6-65 lunar model was relabeled 1:64 to match that of the Surveyor model supplied by Mr. Young. This is believed to be a justifiable extrapolation from the original KLM6-65 scale of 1:48. The spacecraft model was painted with white enamel but with a few surfaces covered with silver paint and with one of the two panels on top painted black.

Since the intent of the test was to demonstrate the ease of detecting Surveyor from LOP photography, pictures were taken vertically at sun altitudes of 10°, 20°, 30°, and 40° and with Surveyor in four positions on the lunar surface. Each position offered a different degree of difficulty in detecting the spacecraft.

Procedure for Test

The KLM6-65 model is 40 inches on a side and represents an area 210 feet on a side of the moon. The crater and boulder distributions represented by this model at a scale of 1:64 are given in Table B4-I. The model was dusted with Fisher Cupric Oxide to closely match the lunar photometric function.

Photographic Setup

An open corridor 185 feet long served as the work area for photographing the models. A surveyor's transit was used to position the sun simulator

TABLE B4-I

DENSITY OF CRATERS AND BOULDERS ON LUNAR MODEL

LOP - SURVEYOR SIMULATION

Crater Diameter Range, Meters	Number of Craters on Model	Crater Density per km^2 on Moon	Boulder Diameter Range, Meters	Number of Boulders on Model	Boulder Density per km^2 on Moon
0.20 - 0.41	4600	1.08×10^6	0.20 - 0.61	2	470
0.41 - 2.0	100	23,600	0.61 - 1.0	0	0
2.0 - 4.1	50	11,800	1.0 - 1.4	2	470
4.1 - 6.1	9	2,120	1.4 - 1.8	1	240
6.1 - 8.1	5	1,180	1.8 - 2.2	0	0
8.1 - 10.2	2.5	590	2.2 - 2.6	1	240
10.2 - 12.2	1.3	300			
12.2 - 16.2	1	240			

and the camera. Angles of 10°, 20°, 30°, and 40° were measured out at the center of the model from a zero degree line lying in the plane of the lunar model. Eighteen feet from the center of the model in these directions was placed a 500-watt slide projector to simulate the sun. The 1.9-inch lens diameter subtends 1/2° at the center of the model, as does the sun as seen from the moon. See Figure B4-1.

Using a Cine Ektar lens with a measured focal length of 15.7mm, it was possible to simulate altitudes of 25, 50, 100, and 135 kilometers within the available corridor. Four camera distances were marked off on a line centered on the lunar model and perpendicular to the zero degree line. It was necessary to shift the camera position parallel to the surface at each distance so as to be directly over the Surveyor model in every position. It was felt that by having the Surveyor vertical axis and the camera axis coincide, it was possible to eliminate a bias on detection caused by the angle of view from the spacecraft.

It is necessary to have the plane of the target surface perpendicular to the camera axis for vertical photography. The board to which the surface model is clamped was brought to a vertical position without the model to align the surface. A bubble level was used for this. Next, a mirror was attached to the board so that its front silvered surface was parallel to the surface of the board. Perpendicularity of the board was assured by reflecting light from a source located on the camera line established above back to the source. The lunar surface model was then clamped to the board with the assumption that the model surface would be parallel to the board.

Surveyor Positions

Figure B4-2 records the lunar surface model with Surveyor located for Position III photography. N, S, E, and W indicate directions on the model. The southwest corner is the origin of a coordinate system used to describe Surveyor locations; X is to the east and Y is to the north. The sun in this picture is 20° above the western horizon.

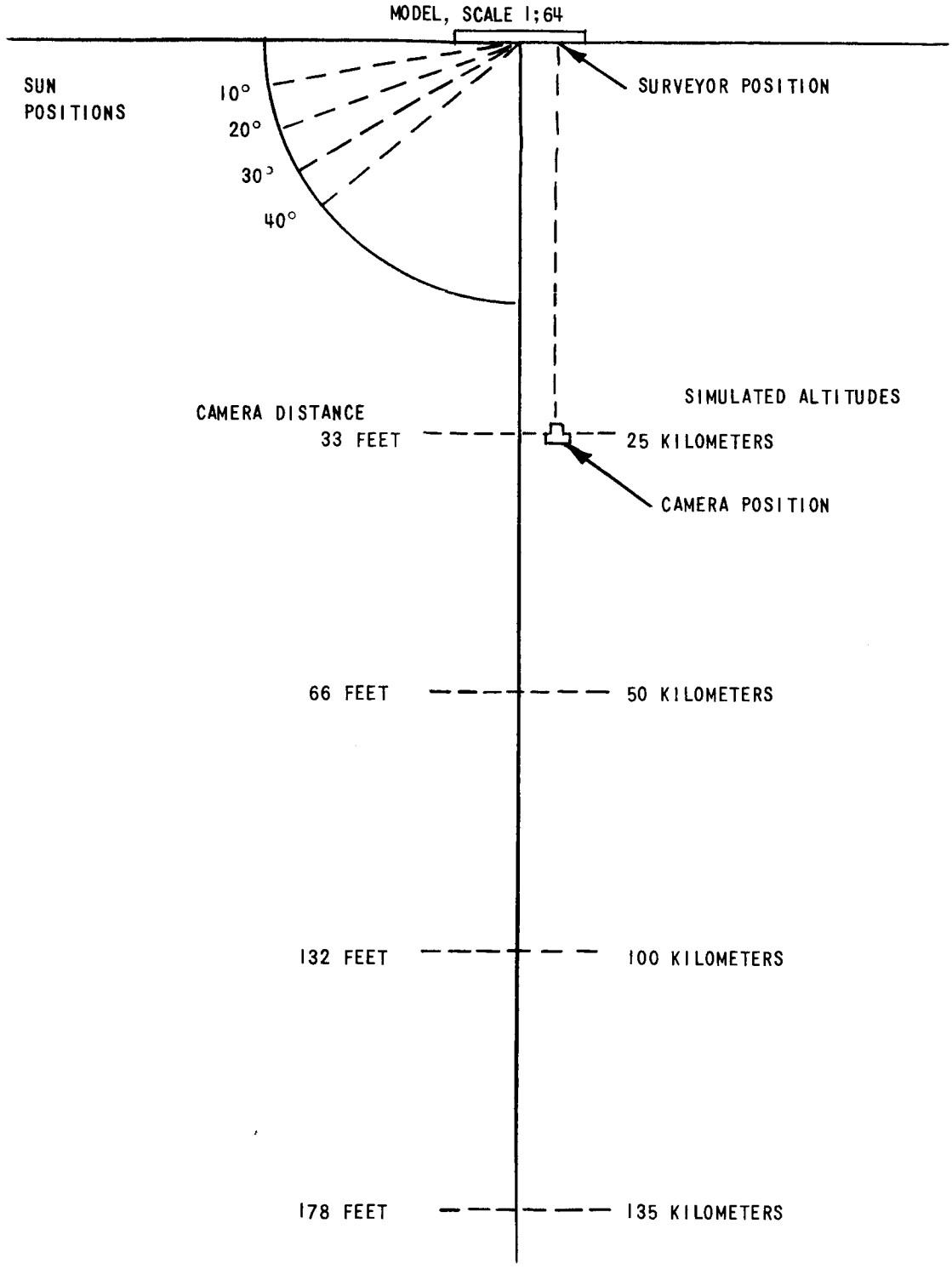

Figure B4-1. POSITIONS OF CAMERA, MODEL, AND SUN FOR SURVEYOR PHOTOGRAPHY

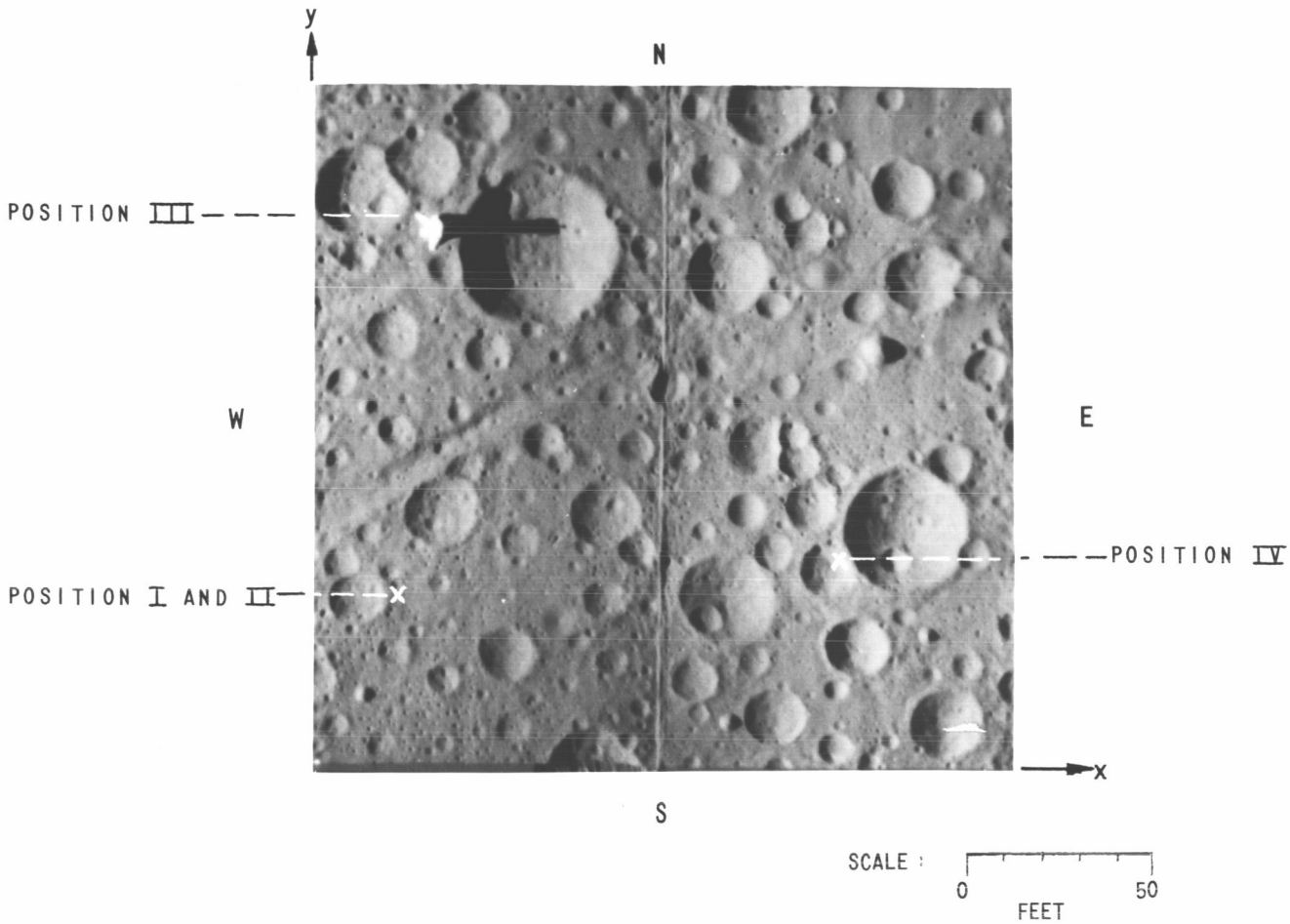

FIGURE 10

Figure B4-2. LUNAR MODEL USED IN SIMULATION POSITIONS I, II, III, AND IV OF SURVEYOR MODEL ON THE SURFACE

Position I

Coordinates: X = 32 feet, Y = 53 feet.
Orientation: Solar panel (black panel) towards the sun.

Position I represents a situation that offers very good detection possibilities. The coordinates locate the spacecraft in an area that is level and relatively smooth. The spacecraft orientation with solar panels toward the sun gives the greatest shadow area on the surface. The nearest crater to the east, i.e., in the shadow direction, is a 10-foot crater 56 feet away. Directly west of the spacecraft is a 16-foot crater, and to the NNE is a 20-foot crater.

Position II

Coordinates: X = 32 feet, Y = 53 feet.
Orientation: Solar panel 90° from the sun direction.

Position II is identical to Position I, except that the spacecraft has been rotated 90°. The orientation is less favorable, as the solar panel and high gain antenna cast a minimum shadow.

Position III

Coordinates: X = 37 feet, Y = 163 feet.
Orientation: Solar panel towards the sun.

Position III coordinates place the Surveyor spacecraft on a level area at the edge of a large crater. Although the spacecraft orientation is identical to that in Position I, this position is less favorable for detection because of the interference of the shadow in the large crater. This crater is 45 feet in diameter and 4.5 feet deep. To the south, on the lip of the large crater, is a small 9-foot crater. To the north is a 20-foot crater with an intersecting 27-foot crater to the west. The center of the spacecraft is 9 feet from the crater lip.

Position IV

Coordinates: X = 155 feet, Y = 68 feet.

Orientation: 15° tilt on vertical axis, solar panel towards the sun.

Position IV was planned to give a rather poor chance to detect the Surveyor. The coordinates locate the spacecraft in a heavily cratered area and on the edge of a 37-foot crater. One leg of the spacecraft rests in the bottom of a 15-foot crater with the other two legs resting on the rim, giving a 15° tilt of the vertical axis towards the southeast corner. Some nearby craters are as follows:

Direction	Diameter
SE	17 feet
N	13 feet
NW	11 feet
SW	27 feet

Shadow Lengths

Shadow lengths cast by the Surveyor spacecraft under the four sun conditions were calculated and are given below. Surveyor height to top of solar panel was measured to be 8.4 feet at a scale of 64:1.

Sun Elevation	Shadow Length on Moon
10°	48 feet
20°	23 feet
30°	14.5 feet
40°	10 feet

Photography

Negative Images. The camera was positioned at each of four distances from the target for each position of the Surveyor on the lunar model. Exposures made at each of the sun altitudes generated 64 original negatives. As in the LOP camera, SO-243 film was used to record these original images. The Cine Ektar 15 mm f/2.5 lens set at a measured aperture of f/7.85 imaged the models onto the film producing a high contrast resolution of 157 lines per millimeter in the negatives. This resolution is higher than the expected 116 lines per millimeter high contrast resolution for LOP photography. However, the 157 lines per millimeter was carefully selected to compensate for the loss in resolution that subsequently occurs in making the positive enlargements. This step reduces 157 lines per millimeter to an equivalent 116 lines per millimeter in the original negative image.

Exposure times are as follows:

Sun Elevation	Exposure Time
10°	732 seconds
20°	309 seconds
30°	183 seconds
40°	119 seconds

These exposure times are calculated to give a constant background density of 1.0. This density is slightly higher than the 0.8 density expected from the LOP payload.

Gamma of the negative images is 1.2, or a little lower than the BIMAT processed LOP film that has a gamma of 1.5. The 64 original negatives closely match LOP payload negatives for scale, grain structure, density, and gamma, but not for resolution.

Positive Images. Each of the 64 original negatives was enlarged 7.2 times onto Type 5427 Aerial Duplicating Film and processed to a gamma of 2.0. The high contrast resolution of the resulting positive images is 16 lines per millimeter and the over-all gamma is 2.4. These positive images closely match the LOP reconstructed images from the GRE in scale, grain pattern, resolution and contrast.

The conditions simulated in each of the 64 positive images are listed in Table B4-II. These images were arranged on an illuminator and analyzed using a 7X hand magnifier. The change in rendition of the vehicle and its shadow is noted in Table B4-III along with comments on the ease of detection and identification of details for each test condition. Figure B4-3 shows several test frames enlarged to yield a constant size for the lunar scene.

Conclusions from Visual Analysis

In general, the Surveyor model was surprisingly easy to see against the KLM6-65 scene. The white and silver paint on the vehicle contrasted sharply with the 6-percent reflectance of the copper oxide dust on the lunar surface model. At high sun altitudes the white vehicle was easily seen, even in the view from 135 kilometers.

However, the viewer should remember that detection of Surveyor in these tests was substantially easier than it will be in actual LOP photography for several reasons:

1. The model was localized precisely in an area only 210 feet on a side. In practice, the location of Surveyor will be uncertain by 5 or 10 kilometers, necessitating search over many framelets of LOP record.
2. The KLM6-65 model was uniform albedo that gives it a very smooth appearance, especially at high sun altitudes.

TABLE B4-II

LIST OF POSITIVE IMAGES SIMULATING LOP HIGH RESOLUTION PHOTOGRAPHY OF SURVEYOR ON LUNAR SURFACE

Altitude in Kilometers	Scale of Positives	Sun Elevation Degrees	Position Number I Negative Number	II Negative Number	III Negative Number	IV Negative Number
25	1:5,700	10	27-1	32-1	29-1	31-2
25	1:5,700	20	27-3	32-2	29-2	31-3
25	1:5,700	30	27-6	32-4	29-4	31-4
25	1:5,700	40	27-7	32-5	29-7	31-5
50	1:11,400	10	27-18	32-10	29-14	31-9
50	1:11,400	20	27-16	32-9	29-12	31-8
50	1:11,400	30	27-14	32-8	29-11	31-7
50	1:11,400	40	27-10	32-7	29-8	31-6
100	1:22,800	10	28-11	32-11	30-1	31-10
100	1:22,800	20	28-15	32-12	30-3	31-11
100	1:22,800	30	28-16	32-13	30-5	31-12
100	1:22,800	40	28-19	32-14	30-7	31-13
135	1:30,700	10	28-9	32-18	30-14	31-17
135	1:30,700	20	28-8	32-17	30-13	31-16
135	1:30,700	30	28-4	32-16	30-11	31-15
135	1:30,700	40	28-2	32-15	30-8	31-14

Positives have been enlarged 7.2 times from the vehicle film.

TABLE B4-III

ANALYSIS OF SURVEYOR SIMULATION PICTURES

AT LOP - GRE SCALE (7.2X)

Position	Alt., km	Sun Altitude in Degrees: For Best Information	Sun Altitude in Degrees: Vehicle Shape Seen	Sun Altitude in Degrees: Shadow Details Seen	COMMENTS
I	25	10	All	All	Easy to see details even at 40°
Most favorable; level area	50	10-20	40	10-20	Easy to see at 40°, uniform background helps
	100	10	--	10	Shapeless image at 40°
	135	10	--	--	Image difficult to see at 40°, background too light, uniform
II	25	10	All	All	Very clear
Same as I, but Surveyor turned 90° to make less shadow	50	10	All	10	----------
	100	20	40	--	----------
	135	10-20	--	--	Very difficult. No shadow at 30° and 40°
III	25	10-20	All	20	Shadow in large crater hides details
Model on sunward side of large crater	50	20-30	40	20-30	Difficult to see at 10°
	100	20	40	--	Difficult to see at 10° and 30°
	135	20	--	--	Very difficult to see at 10° and 30°

Table Cont'd. on Next Page

TABLE B4-III (Continued)

Position	Alt., Km	Sun Altitude in Degrees: For Best Information	Sun Altitude in Degrees: Vehicle Shape Seen	Sun Altitude in Degrees: Shadow Details Seen	COMMENTS
IV	25	20	All	All	Clearly identifiable at all sun altitudes
Surveyor	50	20	All	40	----------
has 15° tilt in heavily cratered area	100	20	40	--	Very difficult at 10°; crater shadows confusing
	135	40	--	--	Very difficult at 20°; doubtful detection at 10°

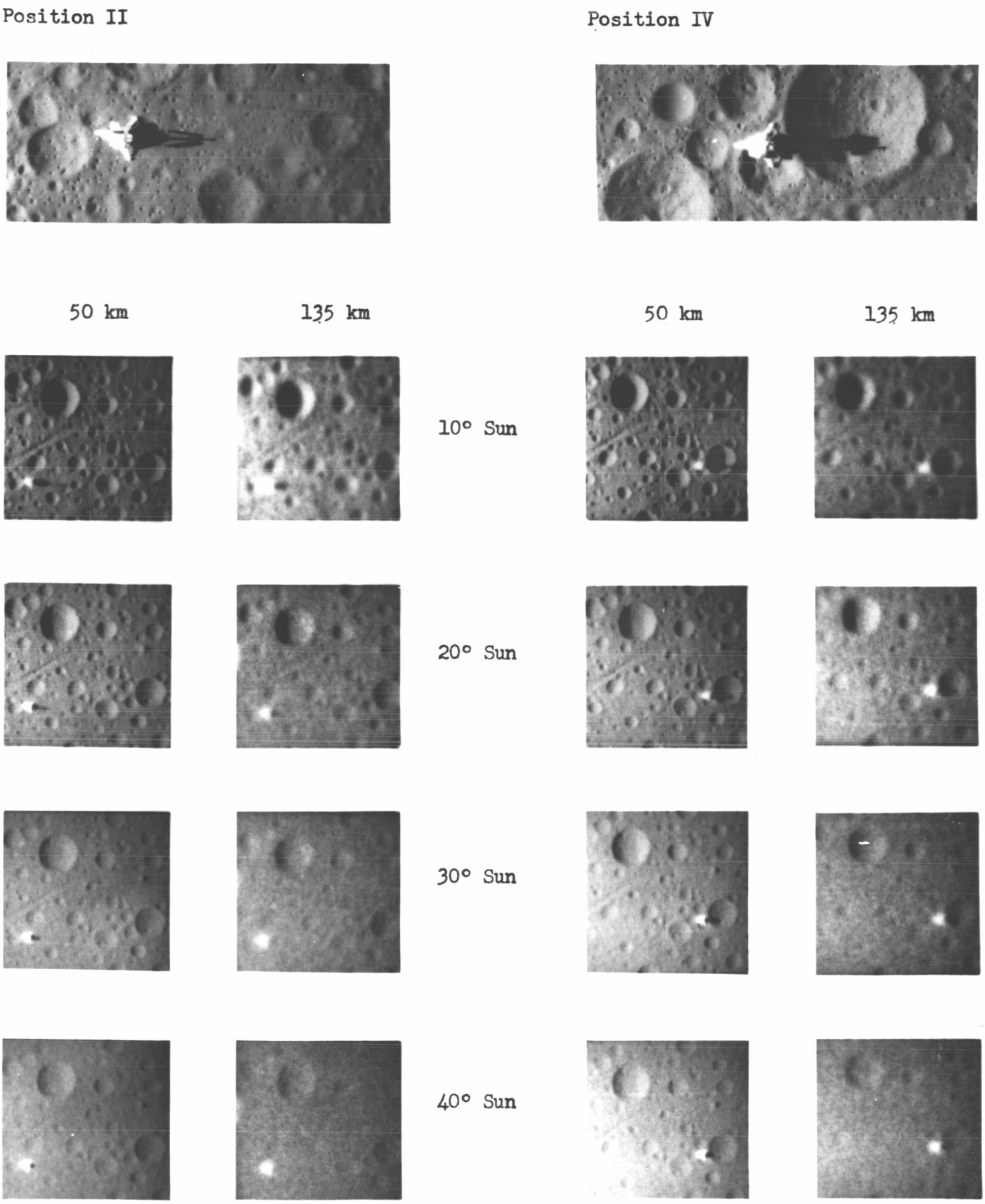

Figure B4-3. SIMULATED LOP HIGH RESOLUTION PHOTOGRAPHY OF SURVEYOR SPACECRAFT ON LUNAR SURFACE FOR TWO SURVEYOR POSITIONS, WITH TWO CAMERA ALTITUDES AND WITH FOUR SUN ELEVATIONS

3. In these tests, the spacecraft model was carefully placed on the scene without disturbing the surroundings and in a manner to show the full height of the vehicle.

4. Since the Surveyor model was probably more "solid" than a real vehicle, it was easier to see and may have reflected more light than would an actual spacecraft.

If the Surveyor lands upright on a fairly uniform area, say 40 to 80 feet in diameter, it will most easily be detected by photography taken at 10° sun altitude. If, however, the vehicle lands in rough terrain or so that its shadow falls on the shadow of a large crater, then it will be easier to see on pictures taken at 20° sun altitude. If this rough area has a uniform albedo, the best detection may even be at 40° sun altitude, particularly if LOP is in a rather high orbit. In any case, detection and identification are substantially easier from 50 kilometers than from higher orbits, and details on the vehicle are always seen in pictures taken from 25 kilometers.

SECTION C

METHODS OF RATING PICTURE QUALITY

C.1 EDGE TRACE ANALYSIS

It has been shown in aerial photography that a fair correlation exists between the resolution of tri-bar targets and the resolution obtained by the analysis of edges in a scene utilizing microdensitometer traces and a computer program. This part of the Lunar Photo Study extends this correlation to lunar photography where it could be employed to evaluate the quality of lunar photographs in which no tri-bar targets appear.

If a microdensitometer trace of an edge is Fourier analyzed for the frequency components in the trace a measure of the frequency response of the photo system can be obtained. In general, the more rapid the trace changes from minimum to maximum density the more high frequencies are present in the image. Utilization of a high speed computer makes this analysis simple and practical.

Prediction of Resolution from MTF and AIM Curves

Fourier analysis of a trace across a shadow edge in a lunar scene will yield the Modulation Transfer Function (MTF) of the photographic system. This MTF curve can be plotted on the same graph as the Aerial Image Modulation (AIM) curve for the film-process combination used to record the edge. Such a plot is shown in Figure C1-1. Since the AIM curve represents the aerial image modulation required by the film to yield a just resolvable image of a tri-bar pattern, the MTF of the film is divided out of the system MTF curve before Figure C1-1 is plotted. This procedure "divides" the photographic system at the aerial image - the MTF curve specifying the quality of the aerial image formed as a result of lens quality, image motion, and defocus, and the AIM curve specifying the image quality required by the film in order for qualified observers to just detect tri-bar resolution. The intersection of these two curves is the predicted system resolution.

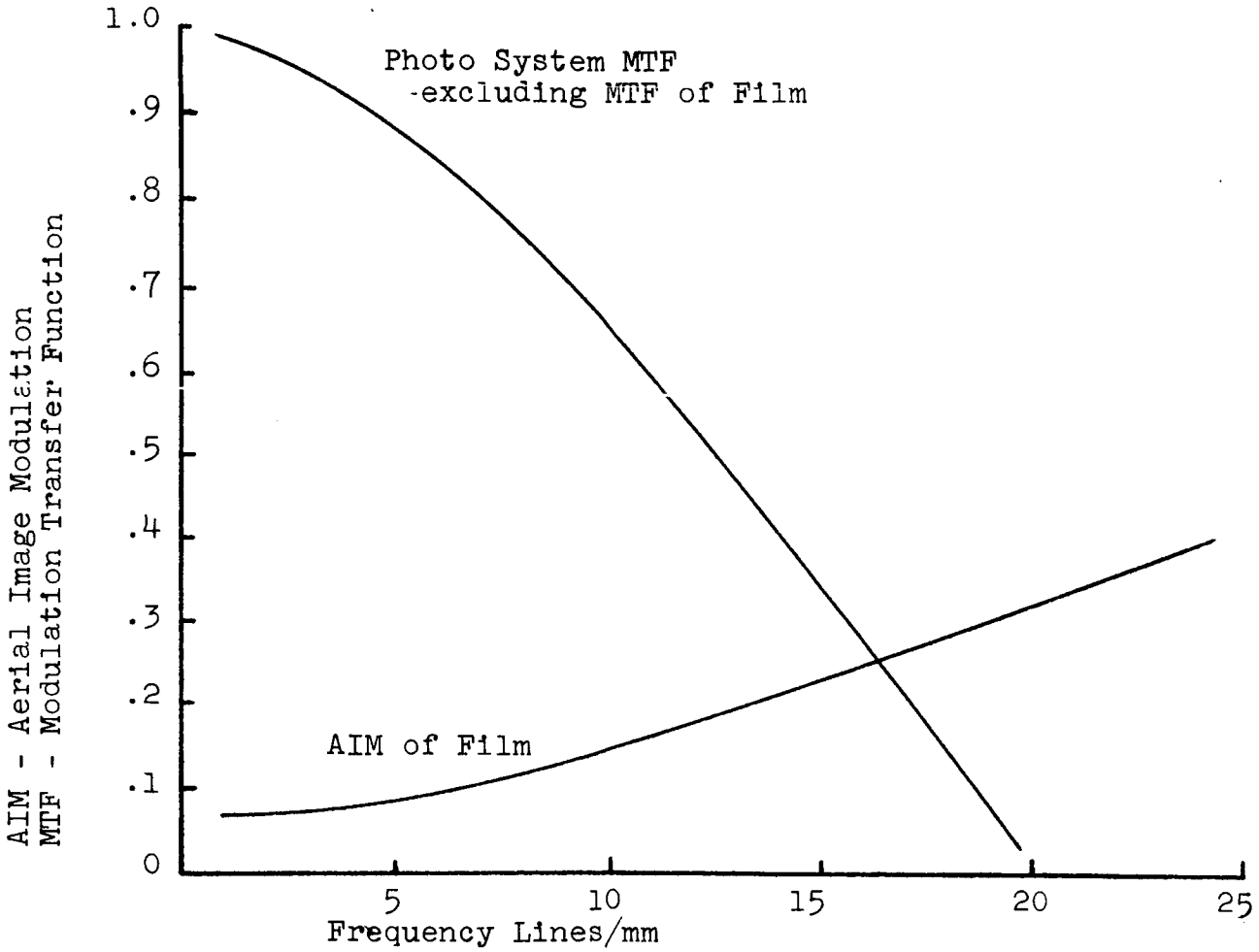

Figure C1-1. MODULATION TRANSFER FUNCTION AND AERIAL IMAGE MODULATION CURVES FOR A PHOTO SYSTEM

Traceable Edges in Lunar Scenes

In order for the edge-trace method to work with lunar photography, we need to explore the frequency with which suitable edges are found in lunar pictures.

In aerial photography of man-made objects there are usually a number of straight, high contrast edges that can be used for analysis. These edges should be at least 100-microns long on the SO-243 film to minimize the effects of film grain. The scanning slit in the microdensitometer is a compromise between a narrow slit that allows very little light to reach the measuring phototube but will include the higher frequencies of the trace, and a wider slit that passes more light but cannot measure the higher frequencies. A slit width of 10 microns would eliminate all frequencies above 100 lines per millimeter and seriously attenuate frequencies as low as 20 lines/mm or 10 lines/mm. In Lunar Orbiter photography, frequencies of 15 to 20 lines/mm might be recorded on the GRE film. Proposed slit dimensions for edge tracing are in the neighborhood of 1μ x 100μ or 3μ x 30μ, these slits giving about the same amount of illumination to the measuring phototube. Three microns is 1/17 of the pitch of the highest frequency of interest (20 lines/mm) and is considered adequate for this study. The straightness of the edge and the alignment of the measuring slit are important if reliable results are to be obtained.

Figure C1-2 shows the result of a count of edges that are 30μ and 100μ long and that are considered adequate for edge tracing on a photograph of KLM6-65 at several sun elevations. Figure C1-2 shows that below a sun elevation of 30° the number of traceable edges increases rapidly. In order to use these shadow areas successfully, the up-sun side of a crater should have a smooth texture with rapid curvature away from the sun, and the downside should not cause a shadow long enough to make the penumbra resolvable. The slope of the surface upon which the penumbra falls will effect the lengths of the

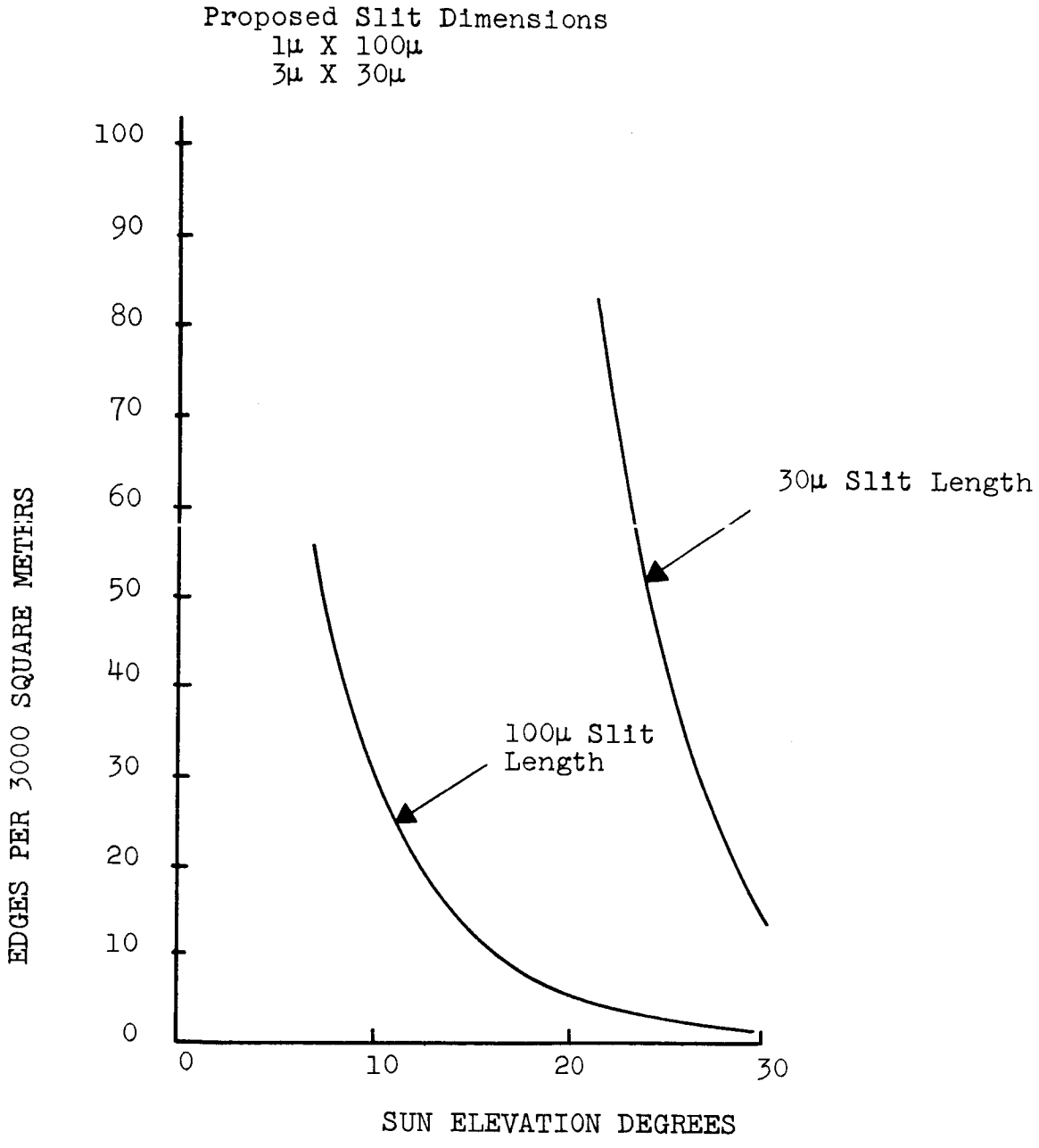

Figure C1-2. ESTIMATED NUMBER OF TRACEABLE EDGES PER 3000 SQUARE METERS ON THE LUNAR SURFACE SUITABLE FOR EDGE TRACE ANALYSIS VS SUN ELEVATION

penumbra and the suitability of the shadow for edge tracing. A slope away from the sun will lengthen the horizontal projected length of the penumbra and may make the edge unsuitable; a slope toward the sun will shorten the horizontal projected length of the penumbra and improve its suitability for edge tracing.

First Edge Trace Experiment

In a separate program Eastman Kodak has derived an AIM curve for SO-243 film. This curve was used in the following experiment to verify the edge trace method using a lunar scene photographed by system B, the hypothetical system of high resolution in which the spacecraft camera film is returned for analysis.

A preliminary experiment was made tracing an edge on a negative of KLM6-65 taken at a sun elevation of 14.3°. Photo system B was used with Kodak High Definition Aerial Film Type SO-243 film at a scale of 1:30,000. The film was processed in D19-D76 for eight minutes at 68°F giving a gamma of 1.2 and a resolution of 134 lines/mm.

The tracing slit was 1μ x 20μ and the edge was traced three times. The data were recorded on IBM cards and given to a computer along with the Edge Trace program for obtaining an MTF curve. These three MTF curves were then averaged and the MTF of the film divided out, thereby obtaining an MTF curve for the simulated photo system B excluding the MTF of the film. This curve was plotted on the same coordinates as an AIM curve for the SO-243 film. The intersection of these curves occurred at 138 lines/mm, a value in good agreement with the observed resolution of 134 lines/mm.

Edge Trace Using LOP Readout Film

A second test was run by tracing edges on SO-349 film, the GRE readout from

SO-243 images simulating a lunar scene recorded by the LOP 24-inch lens. The limiting resolution of tri-bar charts photographed simultaneously with the lunar edges was plotted on the MTF curves derived from the edge trace analysis. A line drawn through these resolution points on the MTF curves from systems of three quality levels is a first approximation to an AIM curve for the LOP system.

The purpose of the edge trace experiment is to evaluate the possibility of measuring the LOP system performance by making microdensitometric traces of sharp edges in lunar scenes as they are found on the primary earth record (35mm GRE positive). The experiment consists of placing images of a lunar scene at several quality levels (resolution) on a strip of 70mm film, Type SO-243. The film is placed in an LOP readout gate, the image is read out and reconstructed via GRE equipment onto 35mm film. An edge (shadow edge) in the lunar scene is traced for each of the three quality levels. The MTF curve derived from each edge trace will be compared with the observed tri-bar resolution to see if a correlation exists between the observed resolution and the required modulation at that resolution.

Basic Elements

Figure C1-3 shows the following target elements:

1. Lunar scene with edges (shadows)
2. Artificial edges ("perfect edge") as a control
3. Gray scale from which to derive relative D log E curve
4. Tri-bar charts to establish limiting high contrast resolution.

Lunar Scene

The lunar scene is a section of KLM6-65 dusted with Fisher CuO. The assumed scale of model-to-moon is 1:48. The sun, at an elevation of 18°, is simulated

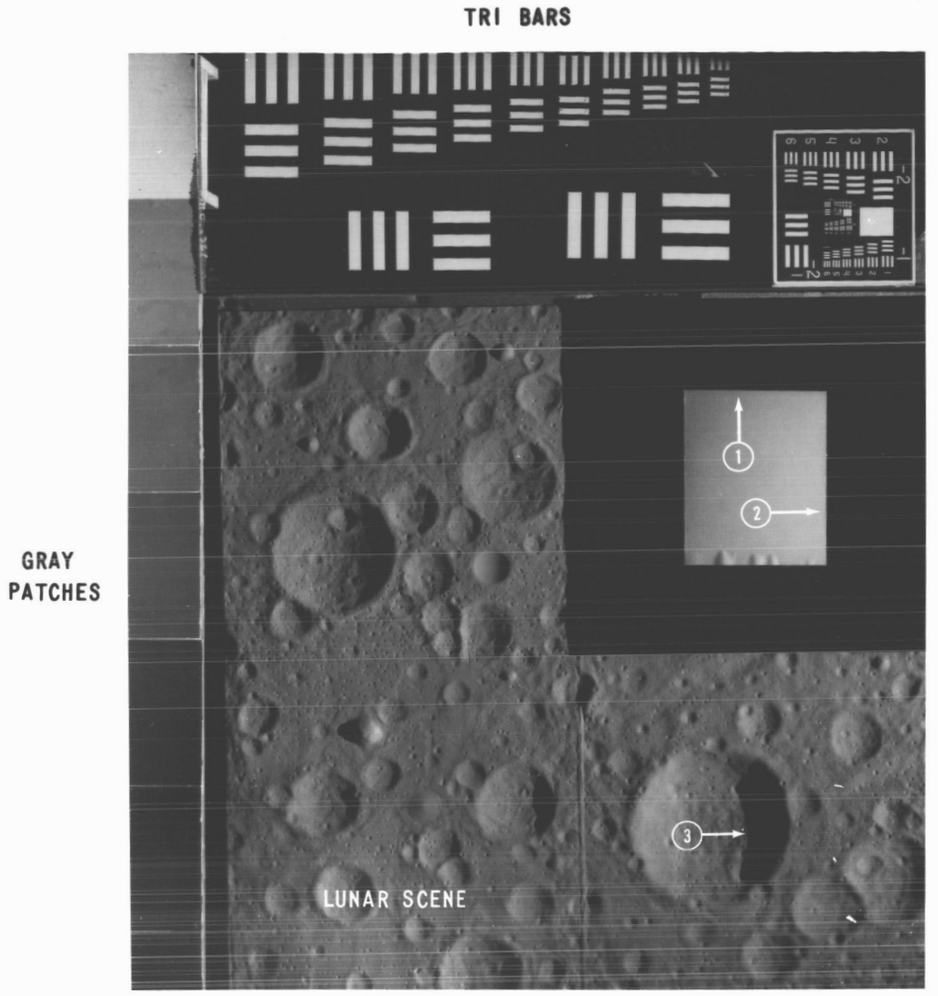

1 PERFECT EDGE AT RIGHT ANGLES TO THE CRATER SHADOW EDGE

2 PERFECT EDGE PARALLEL TO THE CRATER SHADOW EDGE

3 EDGE OF SHADOW IN LUNAR CRATER

Figure C1-3. PHOTOGRAPH OF THE TARGET USED IN EDGE TRACE ANALYSIS SHOWING THE ARRANGEMENT OF THE BASIC ELEMENTS

by a Kodak 500-watt projector placed 14.3 feet away from the center of the scene. A 1.5-inch diameter aperture over the lens simulates the 1/2° angular subtense of the sun.

Photo Scale

The nominal scale of photography with the LOP 24-inch lens is 1:75,450. This was simulated by assuming a 1:48 model-to-moon scale and photographing with a 15mm lens #R0105 (15.7mm focal length) at a film-to-target distance of 81 feet. The scene-to-film reduction (1572) when multiplied by the model scale (48) gives an over-all scale of 1:75,450.

Resolution

Nominal LOP high contrast resolution is 116 lines/mm. It was decided to run the first experiment at quality levels of 46 lines/mm, 92 lines/mm, 152 lines/mm high contrast. These quality levels were reached by setting the 15mm lens at f/8 and defocusing until the desired quality level was reached. The 152 lines/mm level occurred 0.002 inch from the plane of best focus, the 92 lines/mm level at 0.004 inch, and the 46 lines/mm level at 0.007 inch. Table C1-I lists these values along with the measured resolution on both the 70mm camera film and the 35mm GRE film.

Film and Contrast

The LOP camera uses Kodak Special High Definition Aerial Film Type SO-243 that is BIMAT processed to a nominal gamma of 1.40. The images to be read out by the LOP equipment were exposed on Type SO-243 film and BIMAT processed at a temperature of 80°F. The normal sensitometric exposure (1/100 sec) produced a gamma of 1.45 for this process; however, a sensitometric exposure made with the exposure time used to record the scene images (40 seconds) included reciprocity effects and produced a gamma of 1.26.

TABLE C1-I

EDGE TRACE ANALYSIS FILM PARAMETERS

70mm Film Number	Focus Setting from Optimum	Resolution on 70mm Film lines/mm	GRE Number	Resolution on 35mm Film lines/mm
17	0.002 inch	152	17A	15.1
18	0.004 inch	92	18A	13.6
19	0.007 inch	46	19A	7.1

The GRE 35mm positive record is made on Eastman Special Television Recording Film SO-349. As a control on the change in contrast from the scene to the image on the reconstructed record, the brightnesses of the gray patches were recorded at the time of photography. It is possible to construct a relative D-Log E curve from the densities of the gray patches on the reconstructed record. This curve was used in the analysis of performance by edge tracing. Table C1-II lists these measurements and calculations.

Density

The LOP system was designed to transmit densities in the range 0.3 to 1.0 NH Blue or 0.2 to 1.25 visual density. The exposure time used to record the scene was adjusted to produce a density for the lunar scene background of 0.6 NH Blue. Other elements of the scene, i.e., the artificial edge and gray scale, were kept in the range of 0.3 to 1.0 NH Blue density.

Orientation

Since the readout is a line-scan system, it is possible that the resolution in the direction of the line scan could be different than the resolution at right angles to these scans. Consequently, the targets were exposed onto the 70mm film in two orientations, one with the scan lines at right angles to the shadow edge and one 90° from that with the scan lines parallel to the shadow edge. Three images of each quality were placed on the film in two orientations for a total of six targets across the 70mm film. These six images were repeated a short distance away to insure that a complete readout of all the targets would be included in one 35mm framelet.

Figure C1-4 shows enlarged sections of the 35mm GRE film of the target area at the three quality levels.

TABLE C1-II

MEASURED PATCH BRIGHTNESS IN EDGE TRACE TARGET AND CALCULATED Δ Log E's

Patch #	Brightness in* Foot-Lamberts	Brightness Difference	Δ Log E	Relative Log E	Micro Densitometer Volts
1	1.77			000	1.65
		-0.81	0.266		
2	0.96			0.266	2.65
		-0.27	0.143		
3	0.69			0.409	3.70
		-0.20	0.148		
4	0.49			0.557	5.00
		-0.205	0.235		
5	0.285			0.792	7.48
		-0.062	0.107		
6	0.223			0.899	8.18
		-0.043	0.093		
7	0.180			0.992	8.70
		-1.36	0.6[illegible]		
8	0.044			1.633	--
Center Patch	1.20				
		-1.05	0.903		
Felt Background	0.15				

*Measured with Pritchard Spot Brightness Meter, Serial #356

ORIGINAL QUALITY OF PHOTOGRAPHY ON SO243 FILM IN LINES PER MM

FINAL QUALITY AFTER ENLARGING 7.2× THROUGH THE READ-OUT AND GROUND RECONSTRUCTION EQUIPMENT IN LINES PER MM

152

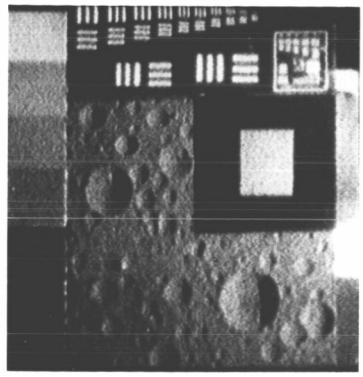

15.1

92

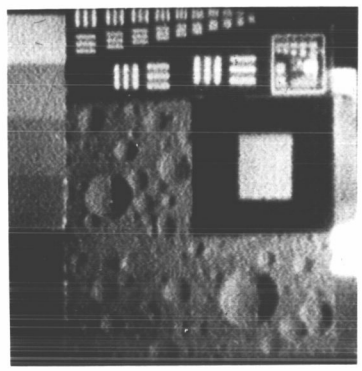

13.6

46

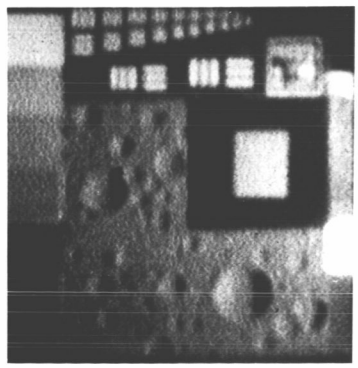

7.1

Figure C1-4. ENLARGED SECTIONS OF THE 35MM FILM MADE BY THE LOP GROUND RECONSTRUCTION EQUIPMENT FOR THE EDGE TRACE ANALYSIS

Microdensitometer Scanning

The 35mm GRE films were scanned in a microdensitometer using a 5- x 160 - micron slit. Referred to Figure C1-3, the slit was moved across the artificial edge both perpendicular (1) and parallel (2) to the scan lines and across the selected lunar edge parallel (3) to the scan lines. Each edge was traced three times and the traces smoothed by a hand to remove the effects of grain noise. Figure C1-5 and C1-6 show typical edge traces made across the artificial edge. The three traces were then superimposed and translated to obtain an average curve for each edge. A curve follower then traced the smoothed curve and measured the ordinate for each 0.1-inch on the curve. This is equivalent to measuring the density every 2.5 microns on the film. These ordinate values are punched into IBM cards.

These punch cards, the sensitometry information and a computer program are given to the computer. The output from the computer is the MTF curves, Figures C1-7, C1-8 and C1-9, for the three quality systems.

Forced AIM Curve

These points in Figure C1-10 are obtained from the three previous figures. The points from the artificial edge and the lunar edge that are perpendicular to the scan lines appear to be enough alike to use these data to derive a "Forced" AIM curve for the complete LOP system. Based upon this limited data, the mean AIM of the six points considered is 0.22 with a 2-sigma value of ± 0.15. If a horizontal AIM curve is drawn at 0.22 with limits of ± 0.15 and crossed with the three MTF curves derived from the lunar crater edge, the following values of resolution are predicted:

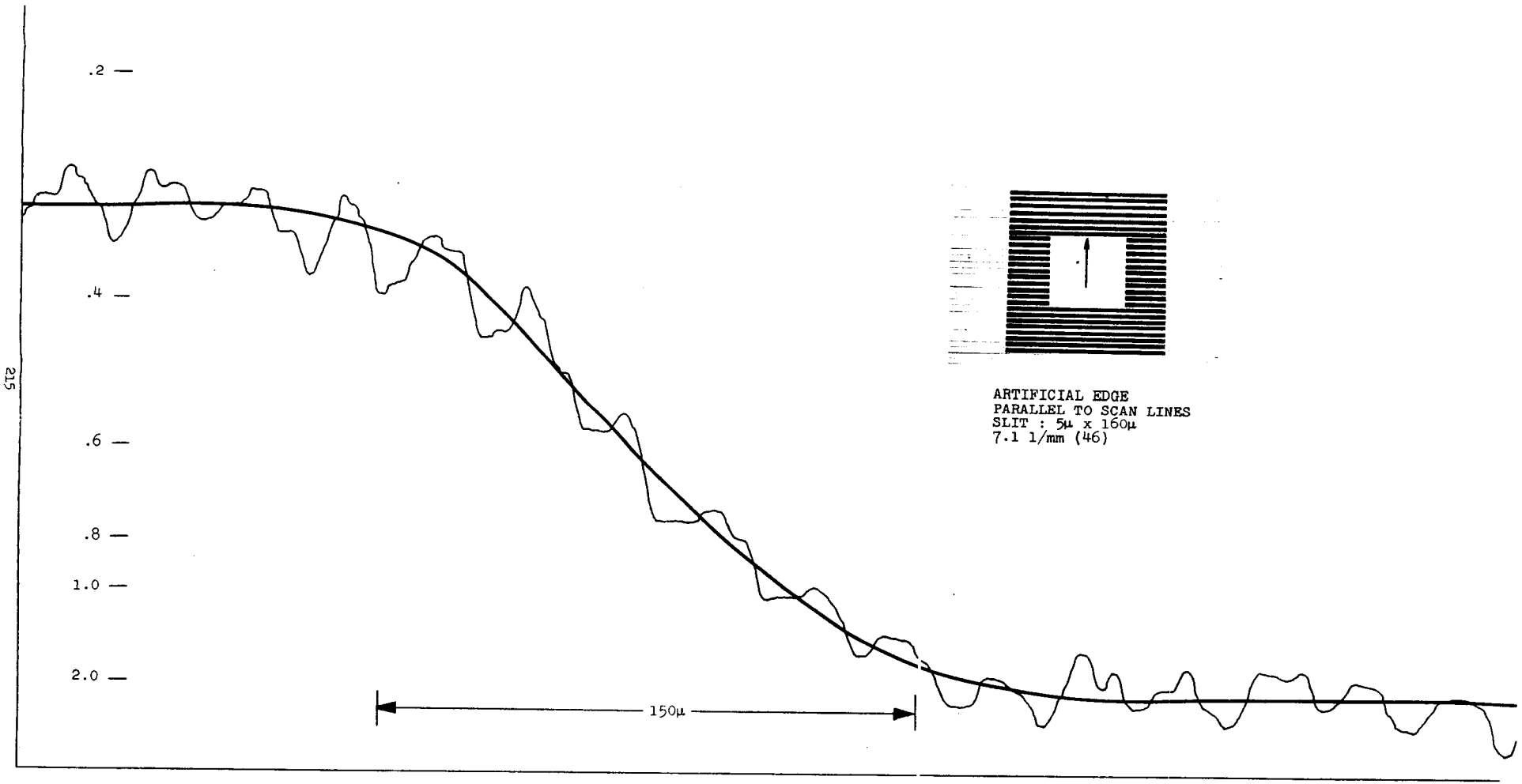

Figure C1-5. TYPICAL MICRODENSITOMETER TRACE ACROSS AN ARTIFICIAL EDGE PERPENDICULAR TO THE SCAN LINES SHOWING THE HAND SMOOTHED CURVE

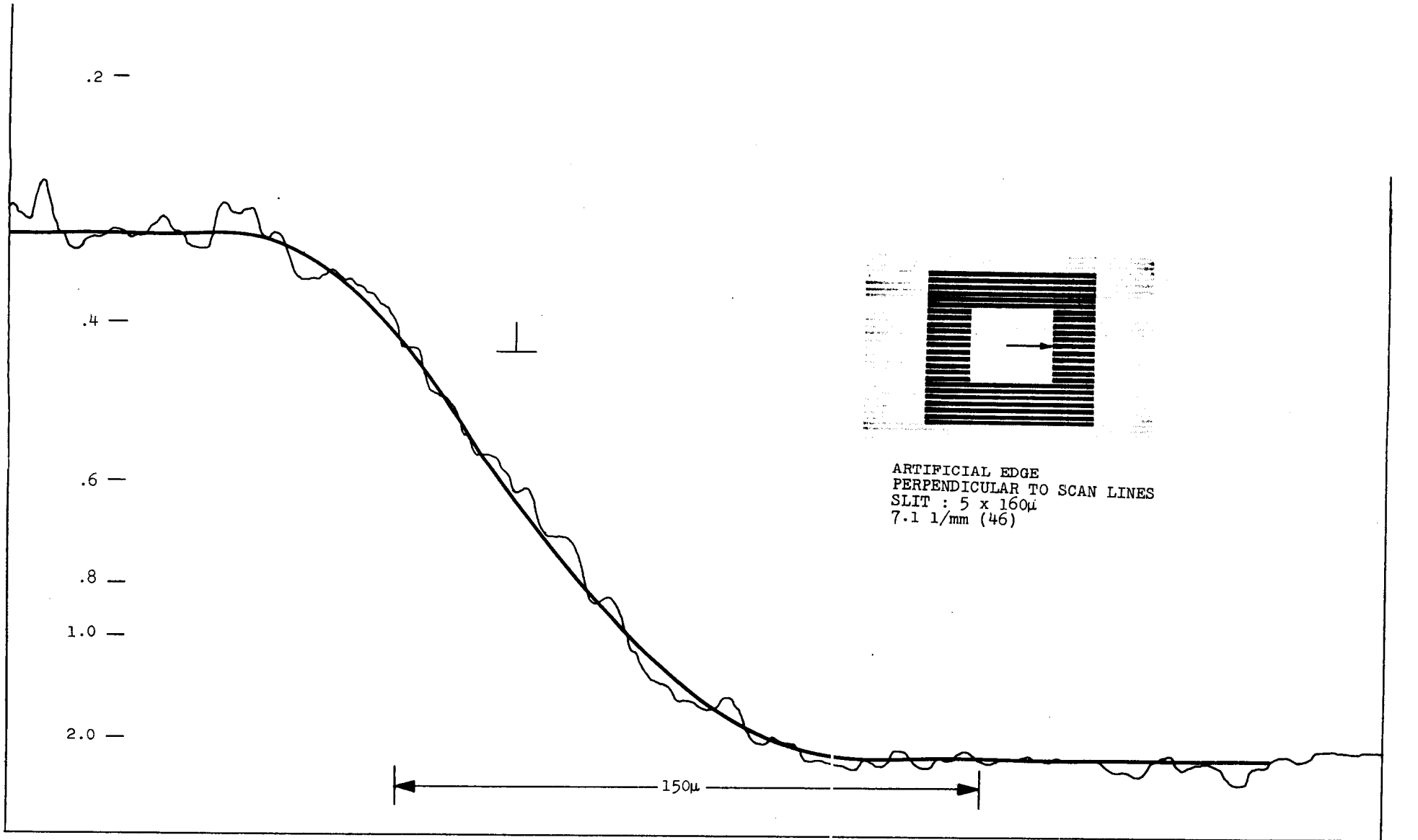

Figure C1 6. TYPICAL MICRODENSITOMETER TRACE ACROSS AN ARTIFICIAL EDGE THAT IS PERPENDICULAR TO THE SCAN LINES SHOWING THE HAND SMOOTHED CURVE

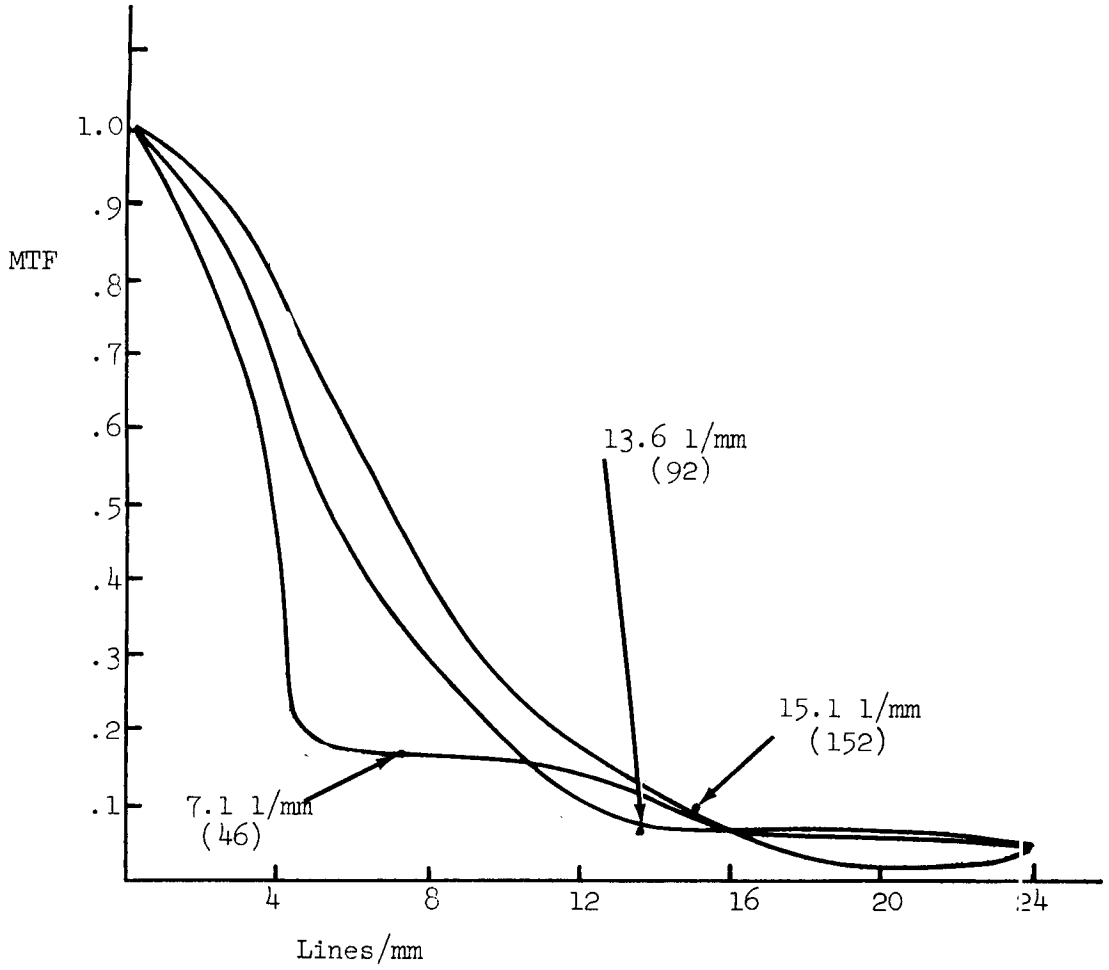

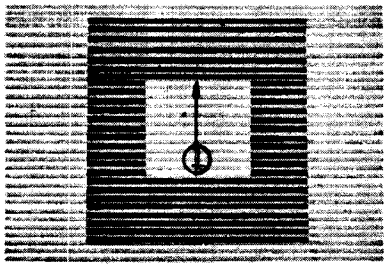

Figure C1-7. MTF DERIVED FROM TRACE OF ARTIFICIAL EDGE PARALLEL TO SCAN LINES (1)

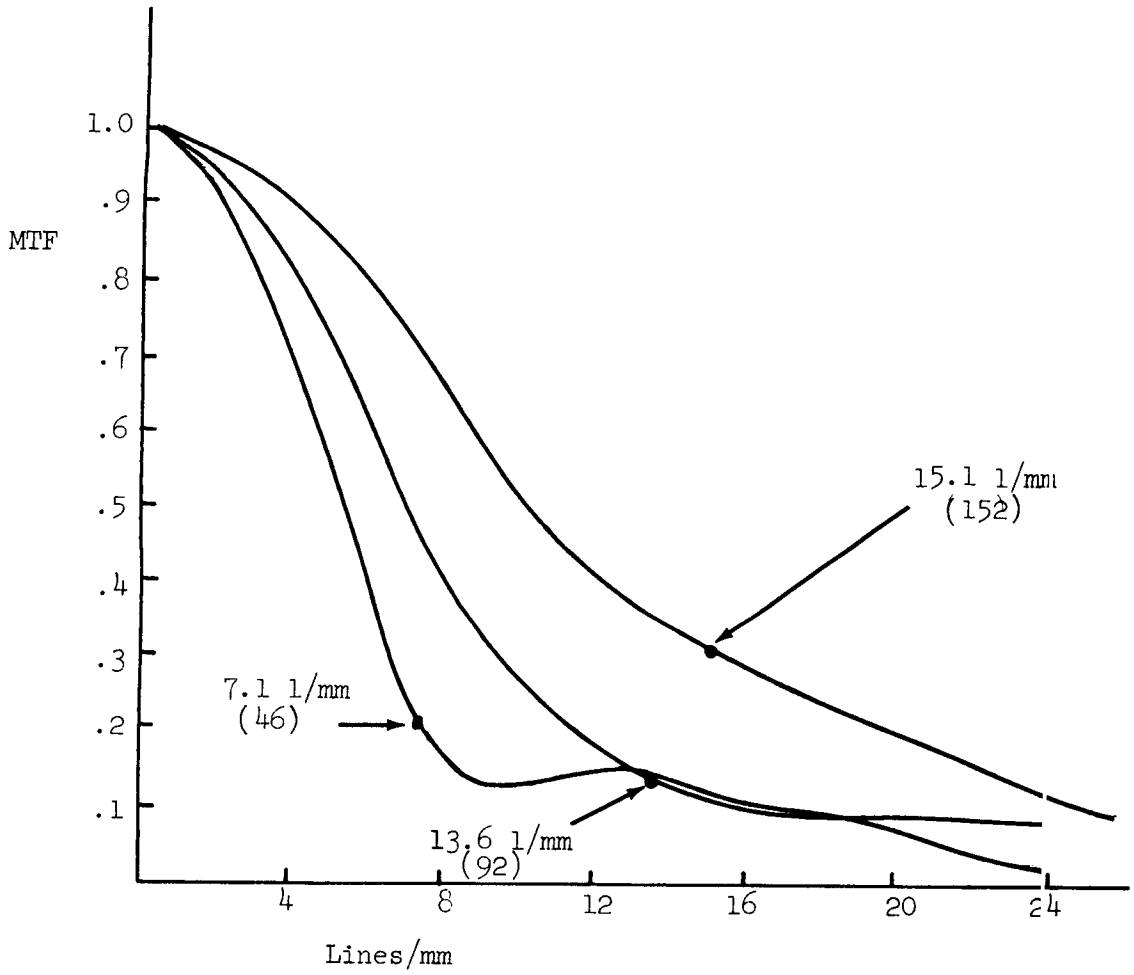

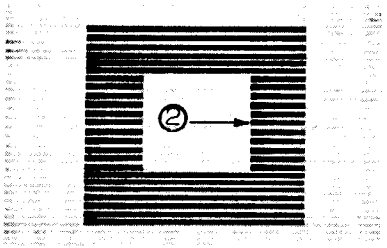

Figure C1-8. MTF DERIVED FROM TRACE OF ARTIFICAL EDGE PERPENDICULAR TO SCAN LINES ②

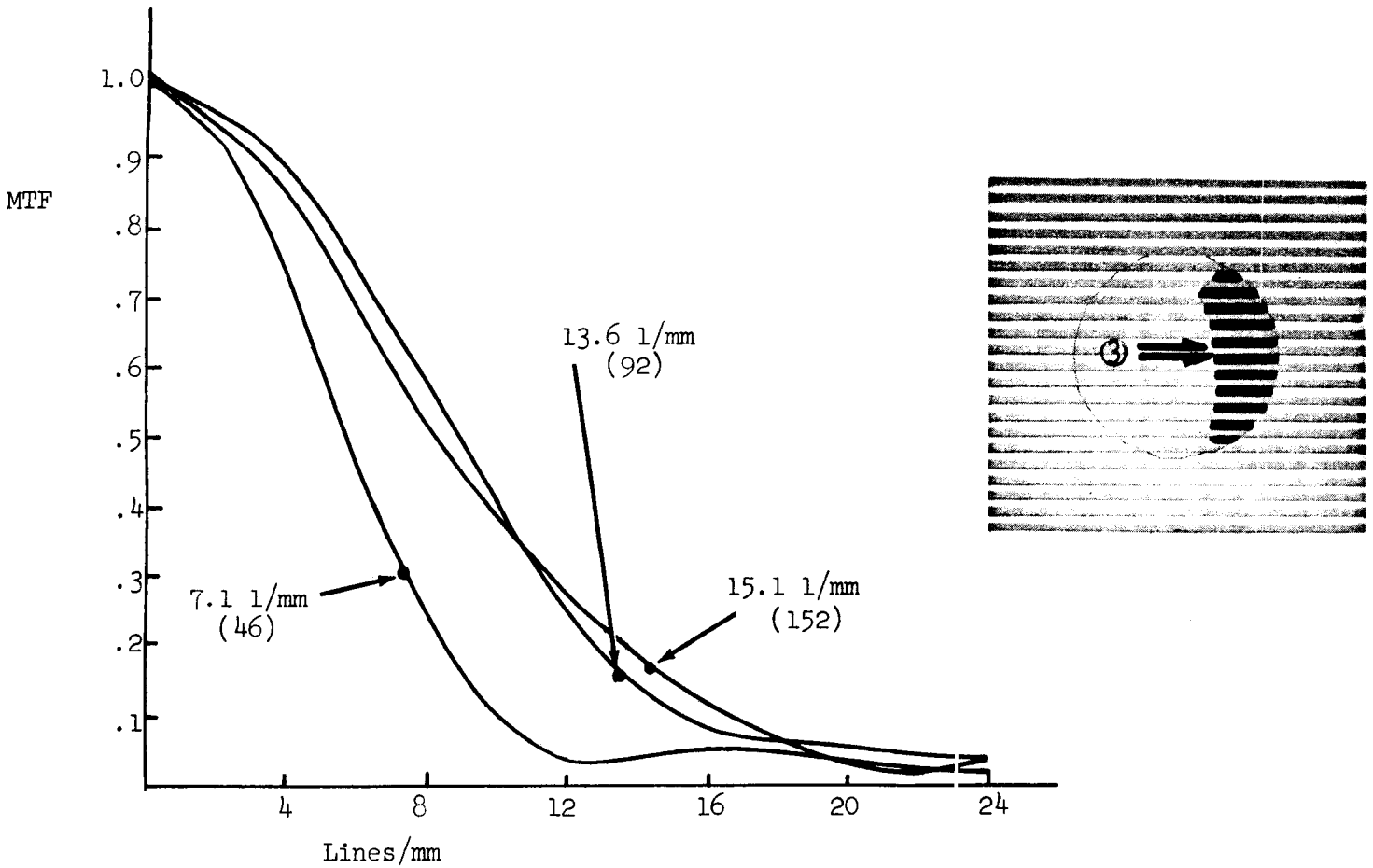

Figure C1-9. MTF DERIVED FROM TRACE OF LUNAR SHADOW EDGE PERPENDICULAR TO SCAN LINES ③

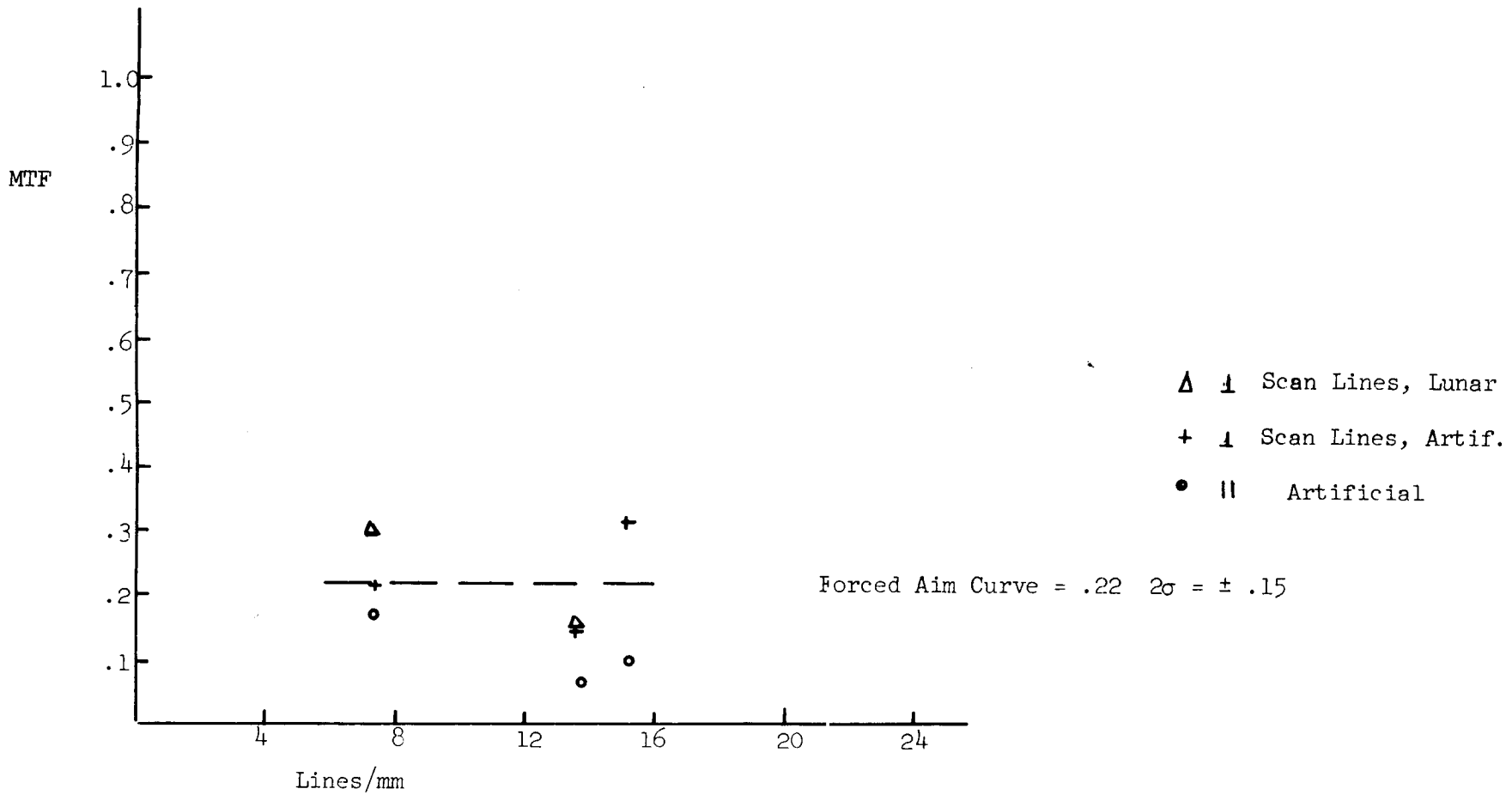

Figure C1-10. FORCED PHOTO SYSTEM AIM CURVE FOR EDGES PERPENDICULAR TO THE SCAN LINES

GRE Image Number	Original Resolution on SO-243 Film	Final Resolution on GRE Film	Predicted Resolution from Forced AIM		
			-2σ	Mean	+2σ
17A	152	15.1	10.0	12.6	19.4
18A	92	13.6	10.2	12.4	16.4
19A	46	7.1	6.3	8.3	10.6

While the 2-sigma limits are rather broad, they agree with past experience using edge trace analysis on pictures of aerial scenes. The agreement between observation and prediction at 7.1 and 13.6 lines/mm is good, while there is a larger discrepancy at 15.1 lines/mm. These data are very limited, and we may expect improved accuracy and precision when more edges have been analyzed.

C.2 COMPARISON IMAGE FILE FOR LOP QUALITY EVALUATION

One method of evaluating system performance is to compare an operational photograph with a file of photographs having known image degradations. A file of 65 images was prepared for use in rating the quality of LOP lunar photography by this technique. These images show the effect of variations in one or more of the following parameters:

1. Image Scale
2. Sun Elevation
3. Radiation Fog
4. Exposure
5. Image Smear
6. Resolution (Defocus)

Table C2-I lists the images in the file along with the values of the parameters characterizing each image.

A comparison of an operational LOP image, i.e., a 35mm reconstructed framelet, with the images in this file should help determine which, if any, of these

TABLE C2-I

COMPARISON IMAGE FILE

Image File Number	Altitude (km)	Scale, Original Negative	Scale, Reconstructed Positive	Sun Elevation Degrees	Total Gamma	Radiation Fog Density	Radiation Fog Roentgens	Exposure	Vehicle Linear Image Smear μ	Vehicle High Contrast Static Resolution l/mm
1	25	41,000	5,700	15	1.2	0	0	Nominal	0	100
2	25	41,000	5,700	25	1.2	0	0	Nominal	0	50
3	25	41,000	5,700	25	1.2	0	0	Nominal	0	100
4	25	41,000	5,700	40	1.2	0	0	Nominal	0	100
5	38	62,300	8,660	15	1.2	0	0	Nominal	0	100
6	38	62,300	8,660	25	1.2	0	0	Nominal	0	50
7	38	62,300	8,660	25	1.2	0	0	Nominal	0	100
8	38	62,300	8,660	40	1.2	0	0	Nominal	0	100
9	46	75,450	10,500	15	1.2	0	0	Nominal	0	100
9S	46	75,450	10,500	15	2.4	0	0	Nominal	Static	100
10S	46	75,450	10,500	15	2.4	0	0	Nominal	Static	75
11	46	75,450	10,500	15	2.4	0	0	Nominal	10	75
12	46	75,450	10,500	15	2.4	0	0	Nominal	10	100
13	46	75,450	10,500	15	2.4	0	0	Nominal	20	50
14	46	75,450	10,500	15	2.4	0	0	Nominal	20	75
15	46	75,450	10,500	15	2.4	0	0	Nominal	20	100
16	46	75,450	10,500	15	1.2	0	0	- 2	0	100
17	46	75,450	10,500	15	1.2	0	0	- 1	0	100
18	46	75,450	10,500	15	1.2	0	0	+ 1	0	100
19	46	75,450	10,500	15	1.2	0	0	+ 2	0	100
20	46	75,450	10,500	15	1.2	0.53	50	Nominal	0	100

Table Cont'd on Next Page

TABLE C2-I (Continued)

Image File Number	Altitude (km)	Scale, Original Negative	Scale, Reconstructed Positive	Sun Elevation Degrees	Total Gamma	Radiation Fog Density	Radiation Fog Roentgens	Exposure	Vehicle Linear Image Smear μ	Vehicle High Contrast Static Resolution l/mm
21	46	75,450	10,500	15	1.2	1.02	230	Nominal	0	100
22	46	75,450	10,500	25	1.2	0	0	Nominal	0	50
22S	46	75,450	10,500	25	2.4	0	0	Nominal	Static	50
23	46	75,450	10,500	25	1.2	0	0	Nominal	0	75
23S	46	75,450	10,500	25	2.4	0	0	Nominal	Static	75
24	46	75,450	10,500	25	1.2	0	0	Nominal	0	100
24S	46	75,450	10,500	25	2.4	0	0	Nominal	Static	100
25	46	75,450	10,500	25	2.4	0	0	Nominal	5	100
26	46	75,450	10,500	25	2.4	0	0	Nominal	10	75
27	46	75,450	10,500	25	2.4	0	0	Nominal	10	100
28	46	75,450	10,500	25	2.4	0	0	Nominal	20	50
29	46	75,450	10,500	25	2.4	0	0	Nominal	20	75
30	46	75,450	10,500	25	2.4	0	0	Nominal	20	100
31	46	75,450	10,500	25	1.2	0	0	- 2	0	100
32	46	75,450	10,500	25	1.2	0	0	- 1	0	100
33	46	75,450	10,500	25	1.2	0	0	+ 1	0	100
34	46	75,450	10,500	25	1.2	0	0	+ 2	0	100
35	46	75,450	10,500	25	1.2	0.53	50	Nominal	0	100
36	46	75,450	10,500	25	1.2	0.53	50	- 2	0	100
37	46	75,450	10,500	25	1.2	0.53	50	- 1	0	100
38	46	75,450	10,500	25	1.2	0.53	50	+ 1	0	100
39	46	75,450	10,500	25	1.2	0.53	50	+ 2	0	100

Table Cont'd. on Next Page

TABLE C2-I (Continued-2)

Image File Number	Altitude (km)	Scale, Original Negative	Scale, Reconstructed Positive	Sun Elevation Degrees	Total Gamma	Radiation Fog Density	Radiation Fog Roentgens	Exposure	Vehicle Linear Image Smear μ	Vehicle High Contrast Static Resolution l/mm
40	46	75,450	10,500	25	1.2	1.02	230	Nominal	0	100
41	46	75,450	10,500	25	1.2	1.02	230	- 2	0	100
42	46	75,450	10,500	25	1.2	1.02	230	- 1	0	100
43	46	75,450	10,500	25	1.2	1.02	230	+ 1	0	100
44	46	75,450	10,500	25	1.2	1.02	230	+ 2	0	100
45	46	75,450	10,500	40	1.2	0	0	Nominal	0	100
45S	46	75,450	10,500	40	2.4	0	0	Nominal	Static	100
46S	46	75,450	10,500	40	2.4	0	0	Nominal	Static	75
47	46	75,450	10,500	40	2.4	0	0	Nominal	10	75
48	46	75,450	10,500	40	2.4	0	0	Nominal	10	100
49	46	75,450	10,500	40	2.4	0	0	Nominal	20	75
50	46	75,450	10,500	40	2.4	0	0	Nominal	20	100
51	46	75,450	10,500	40	1.2	0	0	- 2	0	100
52	46	75,450	10,500	40	1.2	0	0	- 1	0	100
53	46	75,450	10,500	40	1.2	0	0	+ 1	0	100
54	46	75,450	10,500	40	1.2	0	0	+ 2	0	100
55	46	75,450	10,500	40	1.2	0.53	50	Nominal	0	100
56	46	75,450	10,500	40	1.2	1.02	230	Nominal	0	100
57	90	147,600	20,500	15	1.2	0	0	Nominal	0	100
58	90	147,600	20,500	25	1.2	0	0	Nominal	0	100
59	90	147,600	20,500	25	1.2	0	0	Nominal	0	50
60	90	147,600	20,500	40	1.2	0	0	Nominal	0	100

parameters are effecting picture quality. To assist in making comparisons a viewer was purchased and sent along with ten duplicate sets of this file to NASA.

Model Selection and Photography

Kodak Lunar Model 2-66 (KLM2-66) has surface characteristics listed in Table C2-II. It differs from KLM6-65 by the addition of small craters extrapolated from Ranger data. The model consists of two vacuum formed plastic sections joined together smoothly and dusted with Fisher cupric oxide. The light reflecting properties of dusted cupric oxide closely match those of the moon. A model-to-moon scale of 1:210 was assumed for all scene file photography. Included in the scene for all photography were high contrast tri-bars and a series of gray patches. The tri-bars were used to measure image quality, while the gray patches were a check on over-all contrast.

Each image in the scene file was originally exposed on edge printed, 70mm, Kodak Special High Definition Aerial Film SO-243. Two methods were followed in exposing these images: 1) the dusted model was imaged directly on the film and exposed, 2) a positive photograph of the model was imaged on the film and exposed. The first method was used for all images except those with linear image smear. The edge print served two purposes; 1) to locate and identify images on the reconstructed film, and 2) to check the performance of the readout and reconstruction equipment.

The original images were arrayed on the 70mm film to maximize the number of images on each readout framelet and to minimize the number of framelets required to read out the images. This procedure reduces both the time to read out the images and the possibility that the readout or reconstruction equipment will influence the quality of the images through drift in calibration. Seven separate pieces of film were required to record all the images in the scene

TABLE C2-II

SURFACE CHARACTERISTICS OF LUNAR MODEL USED IN SCENE FILE PHOTOGRAPHY

Crater Diameter Range, Meters on Moon	Number of Craters on Model	Crater Density on Moon (# per Km^2)
0.67 - 1.37	4600	10^5
1.37 - 6.7	100	2200
6.7 - 13.7	50	1100
13.7 - 26.7	9	200
26.7 - 33.4	5	110
33.4 - 40.0	2.5	55
40.0 - 53.4	1.3	29
53.4 - 66.8	1	22

Boulder Diameter Range, Meters on Moon	Number of Boulder on Model	Boulder Density on Moon (# per Km^2)
0.67 - 2.0	2	44
2.0 - 3.3	0	0
3.3 - 4.7	2	44
4.7 - 6.0	1	22
6.0 - 7.3	0	0
7.3 - 8.7	1	22

Boulder Height Range, Meter on Moon	Number on Model	Boulder Density on Moon (# per Km^2)
0.27 - 0.67	3	66
0.67 - 2.0	2	44
2.0 - 3.3	1	22

file; four of the pieces correspond to the four simulated altitudes, two correspond to the two levels of radiation fog, and the seventh piece held the images with image smear.

Each section of SO-243 was processed under conditions simulating LOP camera processing by lamination with Kodak BIMAT Film (Estar Base) Type SO-111 presoaked in PS 485K. The sections were taped together, placed in an engineering model read-out section and read out to LOP ground reconstruction equipment (GRE). The readout reconstruction process enlarges the SO-243 image 7.2 times. The GRE recorded the signals on Eastman Special Television Recording Film Type SO-349.

A negative of the SO-349, 35mm record was made on Eastman Fine Grain Duplicating Panchromatic Negative Film Type 5234, and ten duplicate positives were printed from this negative on the same film. The process gamma was adjusted close to 1.0 to preserve the contrast of the original SO-349 record.

The images on the 35mm record were identified from the edge print numbers and the best ones selected for the image file. Ten sets of these images were cut out, mounted in standard 2-inch x 2-inch slide mounts and numbered according to the listing in Table C2-I.

An Example Illustrating Use of the Scene File

Assume an image is returned from a high resolution picture taken at 25° sun elevation from a nominal 46-kilometer altitude. Assume further that this image is somewhat light in density and the craters appear elongated in a direction along the length of the 35mm record. Since this is a positive record and the record is light, we suspect that the original SO-243 was overexposed. We go to the file and pick out images #24, #33 and #34 for 46-kilometer, 25°

sun elevation photography which correspond to nominal exposure, one stop over exposure, and two stops over exposure on the vehicle film respectively. The direction of distortion in the craters points to insufficient image compensation, however, nonlinearities in the mechanical scan in the vehicle or in the GRE film drive may also be contributing factors. Inspecting several framelets of the picture, we find the same distortions are uniformly present in all. This supports the theory of image smear, and a check of dimensions on the 35mm framelet including the edge print eliminates the possibility of non-linearities in scan. We go to the image file and again for 46-kilometer and 25° sun elevation pick out images #24, 25, 27 and 30. These images all have a static resolution of 100 lines/mm high contrast but #24 has no image smear, #25 has 5 microns of image smear, #27 has 10 microns of image smear and #30 has 20 microns of image smear.

Placing the sample GRE framelet under the viewer, a comparison is first made with file images #24, #33 and #34. It is found that the overexposure falls between #24 (nominal) and #33 (1 stop over exposure). File image #34, 2 stops over exposure, is much lighter than the framelet. A one-stop reduction in exposure is therefore recommended.

Next the file images with smear are successively compared with the GRE framelet. Similarities in crater shape are found between the framelet and file images #27 and #30. More revealing, however might be an inspection of the just resolvable detail in each of the images.

Several points to keep in mind during the comparison are the distance separating scan lines, the probable direction of image smear, the effect of image smear on micro contrast, and the interaction of static resolution and image smear. The image on 35mm SO-349 is formed by the reconstruction equipment at a rate of 800 lines/second while the film is traveling 0.816 inch

per second. This produces a scan line separation of 26 microns on the film, a distance representing 39 lines/mm on the film. The scan lines can therefore be used to measure the size of small objects in the scene. Below is a helpful table for this purpose.

No. of Scan Lines	Distance Across on Film	Associated Resolution
1	26 microns	39 lines/mm
2	52	19
3	78	13
4	104	9.7
5	130	7.8
6	156	6.5
7	182	5.6

The motion of the image across the vehicle film plane is in a direction perpendicular to the length of the 70mm film. The sun direction, or the direction that the sun casts a shadow is also perpendicular to the long direction of the vehicle film. This direction is along the length of the 35mm record. Since the scan lines are across the 35mm record, we see that uncompensated image motion will produce smear across the scan lines.

Smear lowers the contrast of small objects in the image. Suppose, for example, the image of a crater half filled with shadow were moved across the film a distance equal to half the width of the crater. Then the highlight exposure is spread over twice the area on the film with none of the area getting the full highlight exposure. Similarily the shadow exposure is increased by the highlight moving into this area. Thus the highlight receives less exposure and the shadow receives more exposure causing a reduction in contrast in the processed image.

Separating the effects of small amounts of linear image smear from lens defocus may be a difficult job. Linear image smear will reduce resolution in one direction, while defocus will generally reduce resolution in all directions. The loss in resolution for linear image smear will affect the dimensions of objects in the direction of smear but not in the direction perpendicular to the direction of smear. A sharp edge parallel to the direction of smear will remain sharp, while sharp edges perpendicular to the direction of smear will lose their sharpness.

If in addition to a difference in sharpness of perpendicular edges the edges appear less sharp than they should, defocus may be contributing to image degradation. Finally, if all edges are equally sharp or unsharp, then defocus for some other characteristic of the imaging system is at fault.

Returning to the LOP 35mm framelet, we look for the smallest resolvable details. Shadow edges parallel to the scan lines in this image are less sharp than shadow edges perpendicular to the scan lines. Uncompenseated linear image motion has degraded the quality of this image. Comparing edges in file images #24 and #24S with edges in the framelet oriented perpendicular to the scan lines, we find that the framelet images are not as sharp as they should be. This effect indicates that defocus may also be a factor in degrading the picture.

We return to the image file and select numbers 23S, 26 and 29. These all have high contrast static resolution of 75 lines/mm, where 23S has no smear, 26 has 10 microns of smear and 29 has 20 microns of smear. Comparing the framelet with these images shows that the framelet images perpendicular to the scan lines are similar to the edges in #23S and that by over-all appearance the framelet best matches #26*. Number 26 has 10 microns of smear in an image of 75 lines/mm static high contrast resolution. These values may be combined by the formula:

$$1/R^{1.3} = 1/Ro^{1.3} + M^{1.3} \text{ **}$$

where R = Combined resolution 1/mm

R_O= Static resolution 1/mm

M = Linear Displacement millimeters

yielding

R = 50 lines/mm

---

*Present equipment used in simulating linear image motion did not allow proper orientation of the image on the SO-243 70mm record. Consequently, in the file images, the sun direction and the direction of smear are parallel to the scan lines on the 35mm record.

**See "Influence of Image Motion on the Resolution of a Photographic System" by Dieter P. Paris, Photographic Science and Engineering, Volume 6, Number 1, January-February 1962.

APPENDIX I

LIST OF PHOTOCLINOMETRY EXPERIMENTS AND MICRODENSITOMETER TRACING PARAMETERS

Experiment No.	Units	1	2	3	4	5 & 6	7 & 8	9 & 10	11 & 12	13	14	15	16	17	18
Model		LM-2	LM-2	LM-3	LM-4	LM-4	LM-4	LM-4	LM-4	LM-3	LM-3	LM-9	LM-9	KLM6-65	KLM6-65
Object		sphere	sphere	7°cone	26°cone	26°cone	26°cone	26°cone	26°cone	7°cone	7°cone	6 shapes	6 shapes	Lunar Surf	Lunar Surf
Sun Elevation*		29.5°	14.3°	14.3°	14.3°	14.3°	14.3°	14.3°	14.3°	14.3°	14.3°	14.3°	14.3°	14.3°	14.3°
Lunar Scale		1:2448	1:2448	1:2448	1:2448	1:2448	1:2448	1:2448	1:2448	1:10,500	1:30,000	1:10,500	1:30,000	1:10,500	1:30,000
Photo System										A	B	A	B	A	B
Resolution	lines/mm	110	110	110	110	110	110	110	110	16	134	16	134	16	141
Gamma, over all										2.1	1.2	2.1	1.2	2.1	2.1
Pitch Limiting Tri-Bar Chart	microns	9.1	9.1	9.1	9.1	9.1	9.1	9.1	9.1	62	7.45	62	7.45	62	7.1
	feet			0.073	0.073	0.073	0.073	0.073	0.073	2.13	0.73	2.13	0.73	2.13	0.70
Pitch/2	microns	4.5	4.5	4.5	4.5	4.5	4.5	4.5	4.5	31	3.7	31	3.7	31	3.5
	feet			0.036	0.036	0.036	0.036	0.036	0.036	1.07	0.36	1.07	0.36	1.07	0.35
Area To Be Traced															
Length*	mm	4.4	4.4	4.4	4.4	4.4	4.4	4.4	4.4	0.78	0.42	1.63	0.593	2.31	0.814
	feet			35.3	35.3	35.3	35.3	35.3	35.3	27	41.3	56	58.2	80	80
Width*	mm	2.9	2.9	2.9	2.9	0.0004	0.0165	0.053	0.130	0.9	0.3*	0.99	0.076*	0.254	0.090
	feet			23.3	23.3					31	29.4	34	5.46	8.8	8.9
Spot Diameter	microns	53.0	53.0	53.0	53.0	6.4	16.5	53.0	130	33.0	3.6	33.0	3.6	33.0	3.6
	feet			0.425	0.425	0.0514	0.132	0.425	1.04	1.14	0.354	1.14	0.354	1.14	0.354
Spot Spacing*	microns	55.5	55.5	55.5	55.5	55.5	16.7	55.5	55.5	31.2	3.12	31.2	3.12	12.5	4.16
	feet			0.445	0.445	0.0445	0.134	0.445	0.445	1.07	0.307	1.07	0.307	0.43	0.41
Spots/Scan*		80	80	80	80	800	250	80	80	25	135	53	190	185	196
Scan Spacing*	microns	150	150	150	150	**	**	**	**	33.0	10.0	33.0	3.6	11.6	4.07
	feet			1.2	1.2					1.14	0.984	1.14	0.354	0.40	0.40
Total Scans*		20	20	20	20	2	2	2	2	28	7	30	25	26	26
Data Points		1600	1600	1600	1600	1600	500	160	160	700	945	1590	4750	4810	5096
Ratio Spot Dia/Pitch		5.8	5.8	5.8	5.8	0.70	1.8	5.8	14.3	0.53	0.48	0.53	0.48	0.53	0.51
Ratio Object Size/ Spot Spacing				36	36	360	112	36	36	14	45.4	7 Δ 3 1/2†	22.6Δ 11.3†		
Equation for Light Fall off Across Model*															
First Term Constant						+5.8	+5.92	+5.14	+5.49	+4.4	+5.3	+5.15	+4.95		+4.66
Coefficient for X						+0.0112	+0.0112	+0.0112	+0.0112	-0.0259	+0.0122	-0.0175	+0.00685		+0.00926

Remarks: * See Figure in Text

* Items required for computer input

** 1 trace across peak of cone
1 trace across background

Δ Largest crater LM-9, 8 feet in dia.

† Second largest crater LM-9, 4 feet in dia.

Date of latest Revision 1 November 1966